ADOPTIVE IMMUNOTHERAPY

FOR

EPSTEIN-BARR VIRUS-ASSOCIATED

POST-TRANSPLANT LYMPHOPROLIFERATIVE DISEASE

Ingólfur Johannessen
The Centre For Infectious Diseases (The University Of Edinburgh)
Edinburgh - United Kingdom

A Thesis Submitted To The University Of Edinburgh For The Degree Of
Doctor Of Medicine
- 2007 -

DECLARATION OF AUTHORSHIP

This thesis was composed by the undersigned candidate. The work included is the candidate's own (with contributions from other researchers), and has not been submitted for other professional qualification.

- To Mum, Dad, Halli, and Olivier -

ABSTRACT

Epstein-Barr virus (EBV), a human γ-herpesvirus that persistently infects >90% of the adult population, is causally associated with post-transplant lymphoproliferative disease (PTLD). PTLD arises in up to 10% of organ transplant recipients and is aggressive, difficult to treat, and fatal in up to 50% of cases despite current treatment. Therefore, novel therapeutic strategies are urgently needed to combat the disease. One such approach involves the use of *ex vivo* expanded EBV-specific cytotoxic T lymphocytes (CTLs). The aim of this study was to establish a pre-clinical SCID mouse model of PTLD in which to test CTL immunotherapy. SCID mice, which lack functional B and T lymphocytes, readily accept human xenografts, and the animals are used extensively to model human neoplasia *in vivo.*

PTLD biopsies from 5 organ transplant recipients gave rise to PTLD-like tumours in all (100%) cases. Biopsy and SCID tumour cells from 4 (80%) patients derived from the biopsy malignant cell. One biopsy (20%) gave rise to a SCID lesion that represented a non-malignant biopsy 'bystander' B cell. Despite the successful xenograft transfer, it was not possible to establish SCID tumour-derived cell lines *in vitro* for use *in vivo.* Therefore, EBV *in vitro* infected B lymphoblastoid cell lines (BLCLs) were used to give rise to PTLD-like lesions in SCID mice.

A minimum dose of $2x10^6$ BLCL cells consistently induced subcutaneous (sc) or intraperitoneal (ip) human CD45+ve, CD20+ve B immunoblastic tumours *in vivo* within 5-7 weeks. Tumours expressed EBV-encoded small RNAs (EBERs), EBV nuclear antigen (EBNA) 2 and latent membrane protein (LMP) 1 suggestive of unrestricted viral gene expression. A minority of cells expressed the immediate early virus antigen BZLF1. The lesions mirrored PTLD and were used for testing CTL immunotherapy.

Intravenous (iv) inoculation of 2 doses of $4x10^6$-$8x10^6$ autologous CTLs a week apart significantly delayed sc tumour progression in sc BLCL-injected SCID mice ($p=0.01$). Similarly, ip transfer of 1 dose of $50x10^6$ autologous CTLs, or $3x10^6$-$50x10^6$ CD8-enriched T cells, into ip BLCL-inoculated animals significantly delayed tumour development *in vivo* ($p=0.001$ for both), and prevented tumour formation in a significant proportion (40%) of mice inoculated with CD8-enriched T cells ($p=0.001$). Immunostaining showed human T cells in the SCID tumours and that the cytotoxic mechanisms involved perforin and granzyme B cytotoxic molecules. Whilst CD4-enriched T cells significantly facilitated tumour outgrowth in sc BLCL-injected mice ($p=0.04$), they did not have any significant impact on tumour development in ip BLCL-inoculated animals. A combination of interleukin (IL) 7 and 15 conditioning of CTLs *in vitro* prior to ip transfer into SCID mice significantly delayed ip BLCL-derived tumour formation *in vivo* when compared to CTLs expanded *in vitro* using standard methods involving IL2 ($p=0.04$).

PTLD can be modelled in SCID mice. In the animals, autologous CTLs and CD8-enriched T cells have a significant capacity to hinder PTLD-like tumour development. However, further studies are needed in future to delineate the role of **(1)** cytokine conditioning and **(2)** CD4-enriched T cells.

ACKNOWLEDGEMENTS

I would like to thank Prof DH Crawford for her supervision, guidance, and enduring support. I am indebted to Dr SM Burns for her encouragement, and I am also grateful to Dr NF Hallam, Prof IR Poxton and Prof SG Macpherson for their support.

I gratefully acknowledge the excellent technical assistance of Ms L Bieleski, Ms G Urquhart, Ms SL Watson, and Ms KA McAulay with preparation and analysis of cell and tissue samples and *in vivo* procedures. My thanks also go to Mr A Timpson for his help with *in vivo* work.

I would like to thank my collaborators who carried out work on PTLD biopsy and SCID tumour material: Dr A Gallagher (Leukaemia Research Fund Virus Centre, University of Glasgow; Ig clonality), Dr PA Hopwood (Centre for Infectious Disease, University of Edinburgh; EBV clonality), and Dr SM Perera (London School of Hygiene & Tropical Medicine, London; immunophenotyping). I would also like to thank Dr T Haque (Royal Free Hospital Virus Centre, London; clinical study) for her collaboration on the 72A1 mab study. I am grateful to the CRUK Study Group (Laboratory for Clinical & Molecular Virology, University of Edinburgh) for supplying some of the cellular material used in this study.

I am indebted to the staff of Biomedical Research Resources (University of Edinburgh) for maintaining the SCID mice used in this project. In particular, I am grateful to Mr W Smith, Ms C Forrest, Ms S Rossiter, Ms H Warnock, and their staff for assistance with animal husbandry. I am also indebted to Dr MA Jansen, Dr GD Merrifield, and Dr I Marshall of the Pre-Clinical MRI Facility (University of Edinburgh) for their help with MRI imaging. My thanks go to Ms F Rae (Department of Pathology, Royal Infirmary of Edinburgh) and Ms G Grant (School of Biomedical Sciences, University of Edinburgh) for technical assistance with preparation of tissues and tissue sections. Ms Mandy Lee (Medical Statistics Unit, Public Health Sciences, University of Edinburgh) offered advice on the use of statistics for which I am thankful.

Lastly, I gratefully acknowledge my funding bodies. I was supported by a Fellowship in Medical Microbiology from the Wellcome Trust (London), and the CTL study was funded by a project grant (no CZB/4/126) from the Chief Scientist Office of the Department of Health of the Scottish Executive (Edinburgh). I am also grateful for the generosity of the Southeast of Scotland Postgraduate Deanery (NHS Lothian, Edinburgh) and the Specialist Virus Centre of the Royal Infirmary of Edinburgh whose support enabled me to complete the work contained in this thesis.

CONTENTS

LIST OF FIGURES

Figures In Appendix 1:

LIST OF TABLES

Tables In Appendix 1:

ABBREVIATIONS

aBL	AIDS-related Burkitt´s lymphoma
Abs	Antibodies
aCL	AIDS-related central nervous system lymphoma
ACV	Aciclovir
AIDS	Acquired immunodeficiency syndrome
aIL	AIDS-related immunoblastic lymphoma
ALG	Anti-lymphocyte globulin
APC	Antigen presenting cell
ARLs	AIDS-related lymphomas
ASGM1	Anti-murine asialo GM1
ATG	Anti-thymocyte globulin
Aza	Azathioprine
BART	*Bam*HI A rightward transcripts
BCR	B cell receptor
BL	Burkitt´s lymphoma
BLCL	B lymphoblastoid cell line
BLPD	B cell lymphoproliferative disease
bp	Base-pair
Bx	Biopsy
CAMs	Cell adhesion molecules
CCC	Covalently closed circular
CD	Cluster designation
cLCV	Cynomolgus lymphocryptovirus
CMV	Cytomegalovirus
CNS	Central nervous system
CR	Complement receptor
CTAR	C-terminal activating region
CTLs	Cytotoxic T lymphocytes
Cy-A	Cyclosporin-A
Da	Daltons
DC	Dendritic cell
DNA	Deoxyribonucleic acid
ds	Double-stranded
DTH	Delayed-type hypersensitivity
EA(D/R)	Early antigen (diffuse/restricted)
EBERs	EBV-encoded small RNAs
eBL	Endemic Burkitt's lymphoma
EBNA	Epstein-Barr virus nuclear antigen
EBV	Epstein-Barr virus
ELISA	Enzyme-linked immunosorbent assay
FACS	Fluorescent activated cell scanning
GC	Germinal centre
GCa	Gastric carcinoma
gp	Glycoprotein
GVHD	Graft-*versus*-host disease
GVL	Graft-*versus*-leukaemia

HHV	Human herpesvirus
HIV	Human immunodeficiency virus
HL	Hodgkin's lymphoma
HRS	Hodgkin Reed-Sternberg
HSV	Herpes Simplex virus
hu-	Human-
hu-BLCL-SCID	SCID mouse inoculated with human BLCL
hu-Bx-SCID	SCID mouse implanted with human biopsy
hu-PBL-SCID	SCID mouse inoculated with human PBLs
ICAM	Intercellular adhesion molecule
IFN	Interferon
Ig	Immunoglobulin
IgH	Ig heavy chain
IgL	Ig light chain
IL	Interleukin
im	Intramuscular
IM	Infectious mononucleosis
ip	Intraperitoneal
IR	Internal repeat
ISH	*In situ* hybridization
iv	Intravenous
IVCs	Individually ventilated cages
Kbp	Kilobase-pair
KSHV	Kaposi's sarcoma-associated herpesvirus
LAK	Lymphokine-activated killer
LCV	Lymphocryptovirus
LFA	Lymphocyte function-associated antigen
LMP	Latent membrane protein
LP	Leader protein
LPD	Lymphoproliferative disease
MA	Membrane antigen
mAbs	Monoclonal antibodies
mLCV	Marmoset lymphocryptovirus
MHC	Major histocompatibility complex
MHV68	Murine herpesvirus 68
mo-	Mouse-
MRI	Magnetic resonance imaging
NHL	Non-Hodgkin's lymphoma
NK	Natural killer
NOD	Non-obese diabetic
NPC	Nasopharyngeal carcinoma
OHL	Oral hairy leukoplakia
ORF	Open reading frame
*ori*Lyt	Lytic origin of replication (lytic cycle)
*ori*P	Plasmid origin of replication (latent cycle)
p	Promoter/Protein
PBH	Polymorphic B cell hyperplasia
PBL	Polymorphic B cell lymphoma

PBLs	Peripheral blood leukocytes
PBMCs	Peripheral blood mononuclear cells
PCR	Polymerase chain reaction
PTLs	Peripheral T cell lymphomas
rLCV	Rhesus lymphocryptovirus
RNA	Ribonucleic acid
RT	Reverse transcriptase
s-Ig	Serum-immunoglobulin
sAg	Superantigen
sBL	Sporadic Burkitt's lymphoma
sc	Subcutaneous
SCID	Severe combined immunodeficient
SIV	Simian immunodeficiency virus
SPF	Specific pathogen free
ss	Single-stranded
Tc1/2	T cytotoxic cell 1 or 2
TCR	T cell receptor
Th1/2	T helper cell 1 or 2
TGF	Transforming growth factor
TK	Thymidine kinase
TNF	Tumour necrosis factor
TP	Terminal protein
TR	Terminal repeat
UL	Unique long
US	Unique short
UV	Ultraviolet
Vβ	Variable β
VCA	Viral capsid antigen
vIL10	Viral IL10
VL	Viral load
VZV	Varicella zoster virus
XLP	X-linked lymphoproliferative disease

SYMBOLS

α	Alpha/Anti
β	Beta
γ	Gamma
ϑ	Theta
ϕ	Phi
χ	Chi
1°	Primary
2°	Secondary
3°	Tertiary
4°	Quarternary
$\sim$	Approximately
$>;\geq$	Greater than; Greater than, or equal to
$<;\leq$	Less than; Less than, or equal to
*	Statistically significant

INTRODUCTION

1. Human Herpesviruses

The architecture of the virion determines inclusion in the herpesvirus family, *herpesviridae* (reviewed in Roizman, 1996). A prototype herpesvirus contains a linear 125-230 kilobasepair (kbp) double-stranded DNA (dsDNA) molecule encoding 70-100 genes contained in a core enclosed by an icosahedral capsid of 162 capsomeres surrounded by an amorphous tegument and viral glycoprotein (gp) rich envelope. The whole virion is approximately 100 nm in diameter. Species-specific herpesviruses have been described for most animals.

The Herpesvirus Study Group devised a formal nomenclature scheme for the herpesviruses on behalf of the International Committee on Taxonomy of Viruses (ICTV). The recommendations of the study group were largely based on biological characteristics of herpesviruses (host range, length of reproductive/lytic cycle, cytopathology, characteristics of latency/persistence) and were formally reported in 1981 (Roizman *et al,* 1981). The scheme subdivided the herpesvirus family into 3 subfamilies: *alpha (α)-, beta (β)-* and *gamma (γ)-herpesvirinae.* The human herpesvirus subfamilies contain 2 genera each. Thus, *α-herpesvirinae* contain the genera *simplexvirus* and *varicellovirus, β-herpesvirinae* consist of *cytomegalovirus* and *roseolovirus* whilst the *γ-herpesvirinae* contain the *lymphocryptovirus* and *rhadinovirus* genera. Individual viruses are denoted by the taxonomic unit (family/subfamily) followed by an Arabic number [for example, human herpesvirus (HHV)-4]. However, vernacular and approved names are often still used interchangeably (for example, HHV-4 and Epstein-Barr virus, EBV).

All herpesviruses encode enzymes necessary for viral DNA replication, which occurs in the host cell nucleus with assembly of capsids followed by budding through the nuclear membrane. Lytic cycle involves the release of new progeny virus which results in host cell death. All known herpesviruses have the ability to persist in a latent form [latent cycle/latency: reversibly non-productive infection (Sinclair & Sissons, 1994)] in their hosts which is characterized by a restricted viral gene expression from covalently closed circular (ccc) viral DNA episomes.

The α-herpesviruses exhibit a relatively short lytic cycle (18-24 hours) followed by rapid host cell lysis and spread *in vitro* (reviewed in Roizman, 1996). Latency is mainly established in sensory ganglia, and the human members (see Table 1) replicate in epithelium. The β-herpesviruses have long lytic cycles (48-72 hours), slow *in vitro* spread and give rise to large infected cells (cytomegalia). Latency is established in secretory glands, kidneys and lymphoreticular cells (lymphoid cells and monocytes/macrophages). The human viruses replicate in fibroblasts (cytomegalovirus, CMV) and T cells (HHV-6,7). The γ-herpesviruses are either B or T lymphotropic and establish latency in the lymphocyte. Replication occurs in epithelium or fibroblasts as well as the lymphocyte.

To date, eight herpesviruses of a total of over 130 have been isolated from humans. Their names and some characteristics are summarized in Table 1.

TABLE 1
Human Herpesviruses

Approved Name[1]	Vernacular Name[2]	Subfamily (*-herpesvirinae*)	Genus (*-virus*)	G+C Content[3] (Mole %)	Size (Kbp)
HHV-1	HSV-1	α_1	Simplex	67	152
HHV-2	HSV-2	α_1	Simplex	69	155
HHV-3	VZV	α_2	Varicello	46	125
HHV-4	EBV	γ_1	Lymphocrypto	60	172
HHV-5	CMV	β_1	Cytomegalo	57	230
HHV-6	-	β_2	Roseolo	43	162
HHV-7	-	β_2	Roseolo	40	145
HHV-8	KSHV	γ_2	Rhadino	54	141

[1]: H(uman) H(erpes) V(irus); [2]: H(erpes) S(implex) V(irus), V(aricella) Z(oster) V(irus), E(pstein)-B(arr) V(irus), C(yto)M(egalo)V(irus), K(aposi's) S(arcoma)-associated H(erpes) V(irus);
[3]: G(uanine) + C(ytosine); Kbp: Kilo ($x10^3$) base-pair (Adapted from Roizman, 1996)

Following primary infection, the human herpesviruses establish a life-long latent infection in their hosts. The infection is controlled by the host immune system, mainly by cellular immunity. Reactivation of virus from latency to lytic infection, as may occur during inherited, acquired or iatrogenic immunosuppression, results in clinical disease. Some of the ensuing disorders may prove fatal as is the case with EBV-associated post-transplant lymphoproliferative disease (PTLD) in immunosuppressed organ transplant recipients.

2. Epstein-Barr Virus (EBV)

EBV, a member of the human γ-herpesvirus subfamily, was discovered in African lymphoma cell lines by Epstein, Barr and Achong in 1964 following the initial description by Burkitt, a British surgeon working in Africa, of an endemic malignant tumour affecting the jaw of children in Uganda (Burkitt, 1958; Epstein & Barr, 1964; Epstein *et al,* 1964). Thus, EBV was the first candidate human tumour virus. The malignancy affecting African children (Burkitt's lymphoma, BL) is now known to be of B lymphocyte origin and EBV is thought to be an essential co-factor in the outgrowth of the endemic form of the tumour. Furthermore, EBV is the causative agent of infectious mononucleosis (IM), and is aetiologically associated with a variety of epithelial and lymphoid lesions in the immunocompetent and immunosuppressed host although its role in some tumours is not yet entirely clear (Epstein & Crawford, 2005; see Table 2).

TABLE 2
EBV-Associated Malignancies

Condition	Initial Description Of EBV Association By
African (endemic) Burkitt's lymphoma (eBL)	Epstein *et al,* 1964
Sporadic Burkitt's lymphoma (sBL) (subsets)	O'Conor *et al,* 1965
Nasopharyngeal carcinoma (NPC) (subsets)	Old *et al,* 1966
Non-Hodgkin's lymphoma (NHL) in immunocompromised patients (for example, post-transplant lymphoproliferative disease, PTLD)	Crawford *et al,* 1980
Hodgkin's lymphoma (HL) (subsets)	Weiss *et al,* 1989
T/NK cell lymphoma (subsets)	Jones *et al,* 1988
Tumours with suspected EBV-association: - anaplastic gastric carcinoma - salivary gland neoplasia - smooth muscle tumours in immunosuppressed states	 Imai *et al,* 1994 Raab-Traub *et al,* 1991 Lee *et al,* 1995

Of lymphoid malignancies, EBV is found in 96% of endemic (African) BL (eBL; reviewed in Magrath, 1990). In Europe and USA, around 20% of sporadic BL (sBL) is associated with EBV (reviewed in Sixbey, 2000) as well as approximately 50% of Hodgkin's lymphoma [HL; reviewed in Herbst & Niedobitek (1994) and Jarrett (2003); Jarrett *et al,* 2005] and around 90% of non-HL (NHL) arising in organ transplant recipients (PTLD; reviewed in Macsween & Crawford, 2003). Additionally, EBV is found in subsets of T/NK cell lymphomas (reviewed in Su, 1996). Furthermore, EBV is detected in almost 100% of undifferentiated (non-keratinized) and 30-100% of differentiated (keratinized) nasopharyngeal carcinoma (NPC; reviewed in Raab-Traub, 1992), and up to 10% of gastric carcinomas (GCa; reviewed in Takada, 2000).

2.1 Biology

EBV is a large enveloped γ–herpesvirus which contains a 172 kbp linear dsDNA genome within an icosahedral capsid. The virus infects B cells *in vitro* and *in vivo* (Pattengale *et al,* 1973; Klein *et al,* 1976). *In vitro,* latent infection involves expression of latent viral genes without production of virus and is compatible with host cell growth, whereas expression of the lytic genes in productive/lytic infection results in host cell death and release of infectious virus (virions).

2.1.1 *In Vitro* EBV Infection

EBV preferentially infects B lymphocytes *in vitro* through attachment of the major viral envelope glycoprotein gp350 to the B cell surface cluster designation (CD) 21 molecule (the EBV receptor) which is the complement receptor (CR) 2 that binds the C3d component of complement (Fingeroth *et al,* 1984). Entry also involves binding to a cell surface co-receptor, the major histocompatibility complex (MHC) class 2 molecules, by a second virus envelope glycoprotein, gp42, that complexes with virus-derived gp25 and gp85 mediating fusion of virus envelope with target cell membranes (Wang & Hutt-Fletcher, 1998; Speck *et al,* 2000; Borza & Hutt-Fletcher, 2002). Whilst CD21 is the main receptor for EBV, deletion mutants lacking gp350

may still infect B cells suggesting alternative means of virus entry (for example, through cell-to-cell contact) into B (and epithelial) cells (Janz *et al,* 2000; Shannon-Lowe *et al,* 2006). Although EBV has been shown to infect epithelial cells *in vitro* and *in vivo* (Sixbey *et al,* 1983, 1984; Tugizov *et al,* 2003; Pegtel *et al,* 2004), whether a CD21 homologue is normally present on epithelial cells, and the role of epithelial cells in EBV infection, is still unclear. Alternative (CD21-independent) modes of EBV entry into epithelial cells have been proposed since oropharyngeal epithelium *in vivo* may be one source of infectious virus in saliva. Thus, in their *in vitro* model of human polarized tongue and pharyngeal cells, Tugizov *et al* (2003) showed that EBV can enter epithelial cells by **(1)** direct cell-to-cell contact of apical cell membranes with EBV-infected lymphocytes; **(2)** interaction between the (lytic) virus envelope BMRF2 gp and β1 (or α5β1) integrins at basolateral membrane sites; **(3)** direct virus spread across lateral membranes. In this model, virus egress occurred from apical and basolateral membranes.

Similar to other herpesviruses, the linear EBV DNA molecule forms a ccc episome in the nucleus of latently infected cells which is where the virus replicates. Cellular DNA polymerase amplifies the episome giving rise to multiple identical copies in the host cell. During latency, the episomes are replicated once every cell cycle in synchrony with host cell DNA. Equal partitioning to progeny cells maintains a stable number of identical viral genomes per host cell which gives rise to a virus clonal population (Kieff & Rickinson, 2007).

In vitro, 1-10% of the infected B cell pool are 'immortalized' by EBV giving rise to continually proliferating B lymphoblastoid cell lines (BLCL; Pope *et al,* 1968; Tosato *et al,* 1985). In contrast to B cells, EBV infection of epithelial cells *in vitro* is difficult and does not result in full latent gene expression or lytic infection. Therefore, BLCL serve as the main *in vitro* model of EBV infection, latency and oncogenesis. Similar to antigen-stimulated B lymphocytes, BLCL express the B cell activation markers CD23, CD30, CD39 and CD70 as well as the cell adhesion molecules (CAMs) lymphocyte function-associated antigen (LFA)-1 (or CD11a/18), LFA-3 (or CD58) and intercellular adhesion molecule (ICAM)-1 (or CD54) (Rowe *et al,* 1987; Kieff & Rickinson, 2007). In contrast, these markers are virtually absent on resting B lymphocytes.

BLCL express all EBV latent proteins which constitute only 10 of a possible 70 viral-encoded proteins (Baer *et al,* 1984): six EBV nuclear antigens [EBNA-Leader Protein (LP), 1, 2, 3a, 3b and 3c] that constitute the EBNA complex, three latent membrane proteins (LMP1, 2a and 2b), and possibly one (or more) proteins of the BARF0 open reading frame from the *Bam*HI A region of the virus genome (BART transcripts; for an overview of EBV latent transcripts, see Table 3). Additionally, two small non-polyadenylated (and, thus, non-coding) EBV-encoded RNAs (EBER1 and 2) are abundantly expressed during latency. Analysis of virus deletion mutants in the BLCL model has shown that of the latent virus proteins, only EBNA1, 2, 3a, 3c and LMP1 are essential for *in vitro* mmortalization whereas EBNA-3b, LMP2a, 2b and EBERs are not (see Table 3). Whilst EBNA-LP deletion mutants have a reduced *in vitro* immortalizing capacity in B cells compared with wild-type EBV, the role of BART transcripts in immortalization remains unclear (for a review of latent virus gene expression, see Young & Rickinson, 2004).

Latent viral infection has been defined as latency 1, 2 or 3 based on EBV promoter usage and latent gene expression. Thus, 'latency 3' (observed in BLCL and most PTLD) is characterized by transcription of all the EBNAs together with the 3 LMPs. In contrast, 'latency 1' (seen in EBV-associated BL and early passage BL cell lines) involves the transcription of EBNA1 only. 'Latency 2' (detected in EBV-associated HL and NPC) entails EBNA1 expression together with a variable expression of the LMPs. EBERs and BARTs are expressed in all forms of latency (Kieff & Rickinson, 2007). However, since viral gene expression found in clinical samples does not always conform to the above latency types, this text uses an alternative scheme that refers to persistent infection as either 'unrestricted' or 'restricted'. The former expression pattern refers to a latency 3-type infection whereas the latter refers to any other more restricted profile.

TABLE 3
EBV Latent Transcripts And Their Functions

ORF	Protein	Mol.wt (kDa)	Cellular Site	Function	Required for Immortalisation?
BKRF1	EBNA1	65-97	Nucleus	Episome maintenance; transcriptional transactivator	Yes
BWRF1	EBNA-LP	20-130	Nucleus	Promotes *in vitro* immortalization; co-operates with EBNA2 in facilitating entry into cell cycle	Uncertain
BYRF1	EBNA2	75-105	Nucleus	Viral oncogene; transactivates cellular (for example, CD21, CD23) and viral (for example, LMP1 and 2) gene expression	Yes
BLRF3/BERF1	EBNA3a	130-195	Nucleus	Remains uncertain	Yes
BERF2a/b	EBNA3b	145-160	Nucleus	Regulation of cellular gene expression (for example, CD40)	No
BERF3/4	EBNA3c	130-195	Nucleus	DNA binding protein; regulates viral (for example, LMP1) and cellular (for example, CD23) expression	Yes
BNLF1	LMP1	58-63	Membrane	Viral oncogene; acts as a constitutively expressed TNF receptor; upregulates cellular genes (for example, *bcl*-2 and IL6) and activates cellular pathways (for example, NF-κB); mimics CD40 function	Yes
BARF1/BNRF1	LMP2a	54	Membrane	Acts as a constitutively activated BCR homologue; prevents entry into lytic cycle	No
BNRF1	LMP2b	40	Membrane	Remains unclear	No
BCRF1	EBER1,2	-	Nucleus/Cytoplasm	Confer resistance to apoptosis; induce IL10 production	No
BARF0	BARTs	-	Cytoplasm	Remains unclear	Not known

BCR: B cell receptor; IL: Interleukin; kDa: Kilo ($x10^3$) Dalton; Mol.wt: Molecular weight; NF: Nuclear Factor; ORF: Open reading frame; TNF: Tumour Necrosis Factor (Adapted from Kieff & Rickinson, 2007)

Lytic EBV infection involves productive viral DNA replication, expression of most virus genes, release of infectious virus and host cell death. The majority of EBV-encoded proteins are expressed during lytic infection although only a small number of BLCL cells enter lytic cycle at any given time. Since herpesviruses do not encode an RNA polymerase, EBV utilises host cell RNA polymerase II for transcription of its viral messenger RNA (mRNA). The immediate early (IE) viral proteins BRLF1 and BZLF1 initiate lytic cycle which is characterized by the sequential expression of early antigen (EA) complex, viral capsid antigen (VCA) complex and membrane antigen (MA) complex proteins. Each complex consists of several proteins (reviewed in Kieff & Rickinson, 2007). The early (IE and EA) lytic proteins are operationally differentiated from the late (VCA and MA) lytic antigens by the persistent expression of the former, but not the latter, in the presence of viral DNA synthesis inhibitors. During lytic infection, EBV also expresses a human interleukin (IL) 10 homologue (viral IL10, vIL10). Furthermore, EBNA1, LMP1, 2a, 2b and EBERs continue to be transcribed.

Based on coding sequence differences of EBNA2, 3a, 3b, 3c and EBERs, EBV is of two types referred to as 'type 1' and 'type 2' (or 'type A' and 'type B'). Both virus types have a worldwide distribution. However, Caucasian and Oriental populations are predominantly infected with type 1 virus whereas type 2 virus is frequently found in African populations (Sixbey *et al,* 1989). In contrast, immunocompromised hosts may harbour both types simultaneously (Yao *et al,* 1996a,b).

2.1.2 *In Vivo* EBV Infection

EBV is a ubiquitous agent as demonstrated by seroepidemiological studies with >90% of adults worldwide testing positive when analyzed for past infection (Henle & Henle, 1966). Infectious virus can be found in throat washings (TW) from healthy virus carriers (and IM patients), and EBV transmission occurs horizontally via saliva (Hoagland, 1955; Gerber *et al,* 1972). However, the source of virus in saliva, whether in oropharyngeal epithelial cells or intraepithelial B cells, remains uncertain.

Seroprevalence increases with the age of the population with neonates being protected by maternal anti-EBV IgG antibodies up to the age of 6 months (Biggar *et al,* 1978). Primary infection is usually asymptomatic in children. In developing societies, primary infection occurs most commonly before 3 years of age (Henle & Henle, 1969; Lang *et al,* 1977), whereas primary infection in Western societies occurs later and may even be delayed until adolescence. Seroepidemiological studies in the UK have shown 2 peaks of EBV seroconversion, one occurring at the ages of 1-6 years and the other at 14-20 years (UHP-PHLS, 1971; Crawford & Edwards, 1990). Previous studies showed that 28-70% of adults acquiring a primary infection at 17-25 years of age suffered IM, an acute self-limiting lymphoproliferative disease (Niederman *et al,* 1970; Sawyer *et al,* 1971). However, in a recent study on 2006 university students in the UK, 510 (25%) students were found to be EBV-seronegative at the time of enrolment into university (Crawford *et al,* 2006). A second blood sample was obtained from 241 (47%) of the seronegative population after 3 years of studies. Of these, 110 (46%) had experienced EBV seroconversion during their study time, and 27 (25%) had experienced IM. Penetrative sexual intercourse was a risk factor for EBV seroconversion and IM. Furthermore, EBV type 1 was significantly over-represented in the IM group. Taken together, the results suggested that IM was caused by exposure during sexual intercourse to a large EBV type 1 load.

IM has an incubation period of 30-50 days and is characterized by the classic triad of pharyngitis, generalised lymphadenopathy and fever (Macsween & Crawford, 2003). Additional signs include splenomegaly and mild hepatomegaly as well as fatigue (which may be prolonged) and (occasionally) a maculopapular rash. The disease is manifest by an absolute lymphocytosis consisting of 'atypical' lymphocytes (Downey & McKinlay, 1923) which are found to be antigen-driven mono- or oligoclonal CD8+ve T cells when T cell receptor (TCR) Vβ chain usage is analyzed (Crawford *et al,* 1981a; Callan *et al,* 1996). These cells express the CD45RO memory marker together with low expression of *bcl*-2 that correlates with their apoptosis *in vitro* (Akbar *et al,* 1993). Evidence suggests that efficient resolution of IM symptoms is associated with a broad cytotoxic T lymphocyte (CTL) response to a wide range of EBV-derived target latent and lytic epitopes (Bharadwaj

et al, 2001). Whilst EBV DNA viral load (VL; as measured by polymerase chain reaction, PCR) in peripheral blood decreases rapidly during convalescence, salivary VL remains high (6 months post-diagnosis), and IM patients remain highly infectious during this time (Balfour *et al,* 2005; Fafi-Kremer *et al,* 2005).

Following primary infection, EBV persists *in vivo* in a latent form at a fairly constant level in approximately 1-10 per 10^6 circulating B cells (Tosato & Blaese, 1985; Miyashita *et al,* 1995; Babcock *et al,* 1998). Around 90% of seropositive virus carriers (cumulative results when assayed on several occasions) give rise to BLCLs *in vitro* when **(1)** their peripheral blood leukocytes (PBLs) are cultured in the presence of the immunosuppressant cyclosporine-A (Cy-A), or **(2)** their TW are co-cultured with susceptible EBV-negative cord blood mononuclear cells (Yao *et al,* 1985a). Circulating EBV-infected B cells are antigen-selected small, CD19+ve, CD23-ve, CD27+ve, CD80-ve, surface immunoglobulin (sIg) M+ve, sIgD-ve resting memory B cells (Pope *et al,* 1968; Tosato *et al,* 1985; Miyashita *et al,* 1995, 1997; Babcock *et al,* 1998; Hochberg *et al,* 2004a).

EBV gene expression (transcriptional) patterns displayed by PBLs from healthy virus carriers have been analyzed by reverse transcriptase (RT)-PCR amplification of whole cell, or enriched B cell, population RNA extracts. Thus, Qu and Rowe (1992) reported LMP2a transcription *in vivo,* and Tierney *et al* (1994) described EBNA1, LMP2a and EBERs expression without detectable lytic BZLF1 transcripts. Similarly, Chen *et al* (1995) reported EBNA1 and LMP2a expression whereas Gonnella *et al* (1997) amplified EBNA1 and LMP1 only. In contrast, Prang *et al* (1997) detected lytic BZLF1 and BALF2 transcripts in 72% and 16%, respectively, of enriched peripheral blood B cell extracts from virus carriers.

Taken together, the only consistently expressed latent virus gene in peripheral blood of healthy virus carriers is LMP2a ('latency programme'). Furthermore, cells showing full viral latent gene expression ('growth programme') have never been observed in peripheral blood in healthy virus carriers although such an expression profile has been detected during IM (Tierney *et al,* 1994). Thus, the LMP2a-only 'latency programme' has been proposed as the mechanism of *in vivo* latency with LMP2a providing the EBV-infected memory B cell with survival signals similar to those that maintain the long-term memory B cell pool (Babcock *et al,* 1998). In line

with this is the observation by Miller *et al* (1994) that LMP2a inhibits the switch from latency to lytic infection in EBV-infected B cells *in vitro*. According to current thinking, LMP2a and LMP1 provide infected B cells with B cell receptor (BCR: sIg) and CD40 co-stimulatory signals, respectively, and thus mimic both survival signals required to maintain the infected B cell pool (Caldwell *et al*, 1998; Thorley-Lawson & Babcock, 1999; Bechtel *et al,* 2005; Mancao *et al,* 2005).

Recently, Thorley-Lawson *et al* examined the EBV expression profile of tonsils from healthy EBV carriers. The group demonstrated latently infected naïve B cells in tonsils and their presence was associated with viral replication (Babcock *et al,* 1998). Furthermore, in contrast to the studies above on peripheral blood, they showed full latent viral gene expression (including EBNA2; 'growth programme') in purified naïve (sIgD+ve) tonsillar B cells (Joseph *et al,* 2000). These cells were activated CD80+ve (B7.1+ve) lymphocytes. Based on their findings, the group suggested that infectious virus is restricted to regions of the tonsil that harbour only naïve B cells (for example, the mantle zone). Thus, latently infected memory B cells from the periphery could extravasate in the tonsillar marginal zones and reactivate EBV in response to signals in the mantle zone. The EBV-infected naïve B cells would either be killed by virus-specific T lymphocytes, or differentiate within the tonsil to become resting memory B cells that would then leave the tonsil to circulate in peripheral blood whilst virus gene expression became restricted (Thorley-Lawson & Babcock, 1999).

Model Of EBV Persistence

Thorley-Lawson *et al* have proposed a model of EBV persistence *in vivo* based on the observation that EBV persists in resting memory B lymphocytes that do not express any viral proteins (Miyashita *et al,* 1997; Babcock *et al,* 1998; Babcock *et al*, 2000; Babcock & Thorley-Lawson, 2000; Thorley-Lawson, 2001; Hochberg *et al,* 2004b; Thorley-Lawson & Gross, 2004), and that this situation arises despite the virus's clear ability to drive proliferation of its host cells. Further support for the pivotal role of B cells in both primary and persistent infection comes from studies by Faulkner *et al* (1999) demonstrating that patients lacking Bruton's tyrosine kinase

and, thus, suffering from X-linked agammaglobulinaemia and absence of functional B cells, can not be infected by EBV.

In their model, Thorley-Lawson *et al* propose that EBV promotes formation of long-lived virus-infected memory B cells using normal pathways of B cell response to antigen (Thorley-Lawson, 2005). The oral lymphoepithelium of the tonsil (tonsillar crypts; part of Waldeyer's ring) is exposed to environmental antigens that are sampled by naïve B lymphocytes (Perry & Whyte, 1998; Brandtzaeg *et al,* 1999a). When encountering specific antigen, naïve B lymphocytes are activated via their BCR and migrate as blast cells into tonsillar follicles to produce germinal centres (GC) where B cell maturation occurs (Liu & Arpin, 1997). Differentiation [involving antigen-specific T helper (Th) cells] entails rounds of proliferation associated with isotype switching and mutation of Ig genes followed by competitive selection for B cells that bind the antigen most avidely and their release as long-lived antigen-specific memory B cells. Non-selected B cells die by apoptosis. Paralleling this scenario, EBV expresses all of its growth-promoting latent antigens ('growth programme') following primary virus infection of naïve B cells in tonsillar epithelium (Joseph *et al,* 2000). Thus, the virus promotes B cell activation, blast formation, proliferation and formation of tonsillar follicles without specific antigen-mediated BCR triggering. In the tonsillar follicle, the transcription programme changes to the more restricted 'default programme' (EBNA1, LMP1 and 2 only; Babcock *et al,* 2000). At this stage, LMP2 drives Ig isotype switching (He *et al,* 2003; Casola *et al,* 2004) whilst LMP1 promotes Ig gene mutation and down-regulates *bcl*-6 expression thus retaining memory B cells in the germinal centre (Calame *et al,* 2003; Casola *et al,* 2004; Panagopoulos *et al,* 2004). Thus, the importance of the 'default programme' may be to offer virus-infected B cells a selective advantage in the germinal centre (Thorley-Lawson, 2005). For an overview of this model of EBV persistence, see Figure 1 below.

Once they leave the germinal centre, latently infected B cells switch off virus protein expression ('latency programme') and are maintained as normal memory B cells (Hochberg *et al,* 2004b). Thus, EBV-infected memory B cells are thought to express virus proteins only rarely in the peripheral circulation (Hochberg *et al,* 2004b). Whilst the numbers of such virus-infected cells can form over half of the

memory B cell pool during the acute stages of IM (Hochberg *et al,* 2004a), a steady-state of approximately 1-10 EBV-infected cells per 10^6 circulating memory B cells is detected within a year of IM reflecting a dynamic balance between cell proliferation and cell loss through lytic infection (Khan *et al,* 1996; Hochberg *et al,* 2004b). However, the role of either EBV re-infection of B cells, or direct virus infection of memory B cells, in maintenance of the virus-infected B cell pool is unclear (Arpin *et al,* 1997). Equally, Conacher *et al* (2005) have shown short-term EBV persistence in the absence of a germinal centre reaction and a typical B cell memory pool in X-linked hyper-IgM syndrome patients who (due to a mutation in the CD40 ligand gene) do not harbour such cells.

FIGURE 1
A Model Of How EBV May Establish Persistent Infection

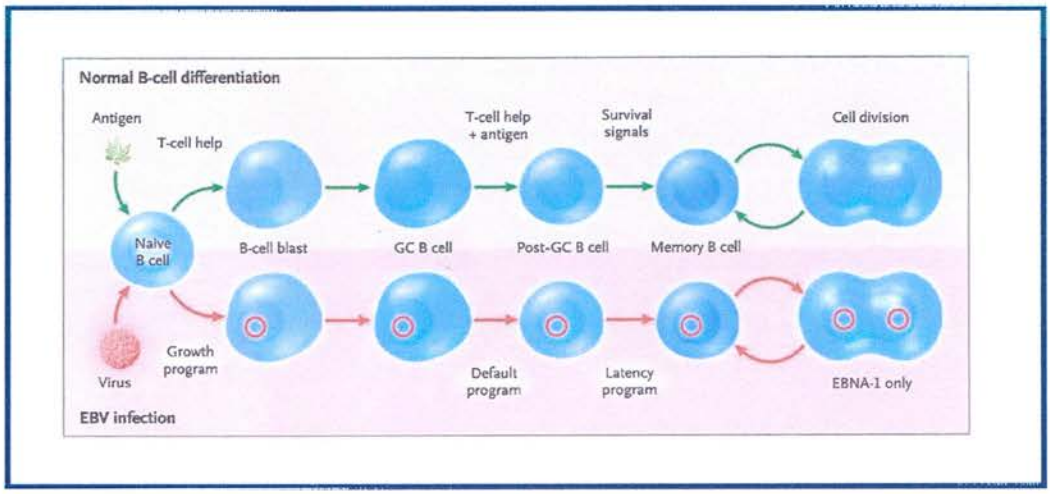

In the model, EBV infects naïve resting B cells in the lymphoid tissue of Waldeyer's ring. The 'growth programme' activates the cells to become proliferating blasts and, thus, parallels antigen-driven activation of a naïve B cell. A switch to the 'default programme' provides rescue signals akin to those delivered by antigen and antigen-specific T helper cells resulting in entry into the memory B cell pool. Upon entry into the peripheral circulation, virus-infected cells switch to the 'latency programme' which entails a shutdown of all protein-encoding genes. As part of memory B cell homeostasis, these cells divide occacionally and express EBNA1 only (if infected with virus). This permits replication of the virus genome and equal partitioning between daughter cells. Upon differentiation into plasma cells, virus-infected memory B cells reactivate EBV resulting in production of virions. EBNA: EBV nuclear antigen; GC: Germinal centre [Reprinted from Thorley-Lawson & Gross (2004) with permission from the New England Journal of Medicine. *Copyright © 2004 Massachusetts Medical Society. All rights reserved.*]

Virus reactivation in mucosal sites leads to virus transmission. Thus, as a result of antigen-mediated BCR triggering and homing of antibody-producing

memory B cells to mucosal sites, an infected memory B cell activates EBV to lytic infection (Brandtzaeg *et al,* 1999a,b; Laichalk & Thorley-Lawson, 2005). Studies *in vitro* by Crawford and Ando (1986), and *in vivo* by Laichalk and Thorley-Lawson (2005), have demonstrated such a link between B cell differentiation and lytic infection. In tonsil, this results in egress of infectious virus into saliva. The importance in transmission of reactivation of virus in genital sites is still unclear although virus is detected in samples from the male and female genito-urinary tract (Sixbey *et al,* 1986; Israele *et al,* 1991; Thomas *et al,* 2006) suggesting the possibility of sexual transmission.

The above model centres on memory B cells as site of virus persistence, but oropharyngeal epithelium may support virus replication and, thus, amplify virus in the oropharynx (Gratama *et al,* 1988; Faulkner *et al,* 1999). However, epithelial cells are not considered to support persistent EBV infection.

2.2 Immunity

2.2.1 Primary Infection

Our knowledge of the host immune response to primary EBV infection is modelled on immune responses observed during IM (the model for primary infection). IgA, IgM and IgG antibodies to VCA are usually detected by onset of IM together with anti-EA and -MA IgG (Henle & Henle, 1979). A range of (mostly IgM) heterophile and auto-antibodies also appear transiently. During convalescence, anti-EBNA1 IgG antibodies arise whilst IgA and IgM antibodies to VCA as well as the anti-EA IgG antibodies (and heterophile antibodies) decline to undetectable levels (Moss *et al,* 2001).

Cellular immunity to primary EBV infection is manifest by lymphocytosis in peripheral blood that consists mainly of 'atypical' activated CD8+ve T cells (Callan *et al,* 1996; Khanna & Burrows, 2000; Vetsika & Callan, 2004). Over 70% of lymphocytes in IM have been shown to be antigen-driven mono- or oligoclonal MHC DR+ve, CD45RO+ve, CD8+ve, CD38+ve CTLs when analyzed using PCR amplification of, and monoclonal antibodies (mab) to, the TCR Vβ-chain

(Tomkinson *et al,* 1987; Callan *et al,* 1996; Hoshino *et al,* 1999). A role for superantigen (sAg)-driven expansion has not been demonstrated despite earlier reports (Sutkowski *et al,* 1996). The transiently expanded T cell clones recognize primarily early (IE and EA) lytic EBV antigens (for example, BZLF1 and BRLF1) with up to 40% of circulating CD8+ve CTLs being directed against a single virus epitope as evidenced by tetramer analysis (Steven *et al,* 1997; Callan *et al,* 1998). In contrast, only a minor component of the CTL response in IM is directed against the latent virus antigens. As the primary infection progresses, the vastly expanded CD8+ve T cells against lytic antigens reduce in number and may even become undetectable (Callan *et al,* 2000; Hislop *et al,* 2002; Callan, 2004).

Whilst CD4+ve T lymphocytes form a minor part of the observed lymphocytosis of IM, the cells display an activated phenotype and respond to lytic and latent viral epitopes (Precopio *et al,* 2003; Williams *et al,* 2004). In particular, CD4+ve T cell responses have been described against the early lytic (BZLF1 and BMLF1) and latent EBNA1 and EBNA3a antigens in IM patients (Amyes *et al,* 2003; Precopio *et al,* 2003). However, such CD4+ve T cell-mediated responses decline rapidly during the disease and are at a low (or undetectable) level 1 year after diagnosis.

The massive CTL response observed in IM is thought to cause its characteristic symptoms through excessive cytokine release such as raised Th1-type cytokine levels [for example, IL2 and interferon (IFN)γ; Foss *et al,* 1994; Biglino *et al,* 1996]. Furthermore, recent studies have also demonstrated a correlation between the severity of IM symptoms and the level of activated T lymphocytes (Williams *et al,* 2004). Thus, signaling lymphocytic activation molecule (SLAM; CD150), SLAM-associated protein (SAP), and CD244 (2B4) were significantly up-regulated on CD4+ve and CD8+ve T cells at time of IM diagnosis. At that time, natural killer (NK) cell levels were also significantly elevated suggesting a role for NK cells in immune control of primary EBV infection. Thus, the same group showed higher NK cell numbers at IM diagnosis to correlate with significantly lower circulating EBV VL (Williams *et al,* 2005).

2.2.2 Persistent Infection

Stable levels of circulating anti-VCA, anti-MA and anti-EBNA1 IgG antibodies are detected in healthy virus carriers and low levels of anti-EA antibodies may also be present (Henle & Henle, 1979). Antibodies against gp350/220 of the MA complex are retained and neutralizing. Additionally, 21-30% of virus carriers have anti-gp350 IgA in serum, and these antibodies are found in saliva of 12-19% of virus carriers (Yao *et al,* 1991a,b).

Immune control of EBV infection is mediated primarily by CD8+ve MHC1-restricted EBV-specific CTLs against all the latent viral proteins [CTL precursor (CTLp) frequency ranges from 1:400 to 1:42,000 of the total T cell population] although the role of T cell responses to EBNA1 is still unclear (Rickinson & Moss, 1997; for an overview of immunodominant CTL epitopes and their MHC restriction, see Moss *et al,* 2001). In particular, CTL responses to the EBNA3 antigens are immunodominant (Murray *et al,* 1990, 1992; Rickinson & Moss, 1997), and cytolysis of the CD8+ve T cells is mediated by granule exocytosis mechanisms (perforin, granzyme). EBNA1 contains glycine-alaninine repeats that interfere with proteosomal proteolysis necessary for MHC1-restricted epitope presentation to CTLs (Levitskaya *et al,* 1995, 1997) and inhibit translation of EBNA1 (Yin *et al,* 2003) although recent evidence suggests that EBNA1-specific CD8+ve CTLs can be generated *in vitro* (Lee *et al,* 2004; Voo *et al,* 2004). Such EBNA1-specific CTLs could play a future role in adoptive immunotherapy against EBV-associated malignancies – all of which express EBNA1. Collectively, up to 5% of circulating CD8+ve CTLs are committed to EBV immune control (Hislop *et al,* 2002).

In addition to immunosurveillance mediated by CD8+ve T cells, CD4+ve T cells also have a role to play. Thus, EBNA1-reactive CD4+ve T cells have been detected in healthy seropositive individuals. In particular, Münz *et al* (2000) and Bickham *et al* (2001) have shown such T cells to lyse EBNA1+ve cells, and EBNA1 is now considered highly immunogenic for CD4+ve T cells (Leen *et al,* 2001; Nikiforow *et al,* 2001). In contrast to CD8+ve CTL, such CD4+ve T cells mediate their effector mechanisms via IFNγ secretion and Fas/Fas ligand (FasL) interactions rather than granule exocytosis (Nikiforow *et al,* 2003). The role of IFNγ in mediating

CTL defences against EBV is further highlighted by studies of the severe immunodeficiency X-linked lymphoproliferative disease (XLP) which results from a defect in the signalling adaptor SAP gene that signals through SLAM (and other Ig superfamily receptors including 2B4). Thus, using autologous BLCLs as stimulators, Sharifi *et al* (2004) demonstrated that EBV-specific T cell lines generated *in vitro* from XLP patients showed markedly reduced IFNγ production and cytotoxic capacity compared to healthy controls.

During persistent infection, CTLs also control lytic infection and recognize specific IE (BZLF1, BRLF1) and EA (BMLF1, BMRF1, BALF2) antigens (Bogedain *et al,* 1995; Steven *et al,* 1997).

Immunosuppression reduces EBV-specific CTL activity, and this can lead to EBV-driven proliferation of B cells that may culminate in B cell lymphoproliferative disease (BLPD). BLPD encompasses a spectrum of B cell proliferations arising in immunocompromised patients ranging from a diffuse polymorphic ('viral lymphadenitis-like') proliferation with polyclonal Ig expression to a malignant monoclonal Ig lymphoma. EBV is aetiologically associated with BLPD in most cases and the disease is characterized by rapid onset, aggressive behaviour, and high mortality despite treatment. In the organ transplant recipient, iatrogenic immunosuppression may result in BLPD which is then referred to as PTLD. EBV is associated with around 90% of PTLD.

3. Post-Transplant Lymphoproliferative Disease (PTLD)

PTLD develops in up to 10% of organ graft patients and is characterized by rapid onset, aggressive behaviour, and high mortality despite treatment. The disease encompasses a spectrum of primarily B cell proliferations (BLPD) although T and NK cell tumours have also been described (Nalesnik, 2001). Whilst EBV is aetiologically associated with PTLD in most cases, EBV-negative lesions are well recognized and constitute up to 10% of PTLD (Newstead, 2005).

3.1 Incidence And Risk Factors

The 2 major risk factors for PTLD formation are **(1)** the degree and duration of immunosuppression required for graft maintenance, and **(2)** primary EBV infection following transplantation (Thomas *et al,* 1995).

(1) Immunosuppression predisposes to the development of *de novo* cancers (Penn, 1991a,b). The degree of immunosuppression required to facilitate organ transplantation correlates with PTLD formation which in turn depends on the type of organ graft. Generally, immunosuppression is heaviest during the first year post-transplant when the risk of rejection is greatest and, thus, the risk of PTLD is high during this period (Opelz & Henderson, 1993). However, PTLD incidence at 1 year post-graft amounts to only a fifth of the 10 year cumulative incidence, and the median time to PTLD is 5 years following transplantation surgery (Opelz & Dohler, 2004). Current immunosuppressive regimes used in organ transplantation include the T cell suppressants Cy-A, azathioprine, prednisone, tacrolimus and mycophenolate mofetil (Newstead, 2005). Additionally, mab against T cell surface antigens (anti-CD3: OKT3; anti-CD25: basiliximab and daclizumab) that result in T cell depletion are in clinical use. Furthermore, anti-lymphocyte and anti-thymocyte globulin (ALG, ATG) are available for T cell depletion and graft-*versus*-host disease (GVHD) prophylaxis (Dey *et al,* 2005).

Overall, <1-33% transplant patients develop PTLD (Williams & Crawford, 2006). However, the incidence of PTLD shows marked variation in different

transplant groups with reports of between 0.2-1.6% in bone marrow (Beveridge *et al,* 1984; Shapiro *et al,* 1988), 0.4-2.5% in kidney (Birkeland, 1983; Starzl *et al,* 1984), 1.8-3.4% in heart (Nalesnik *et al,* 1988; Armitage *et al,* 1991), 1.8-7.9% in lung (Armitage *et al,* 1991; Levine *et al,* 1999), 2.3-13.7% in liver (Renard *et al,* 1991; Cox *et al,* 1995), 4.6-9.4% in heart/lung (Nalesnik *et al,* 1988; Randhawa *et al,* 1989), 7-11% in intestinal (Abu-Elmagd *et al,* 1998; Grant, 1999), and 13-33% (Abu-Elmagd *et al,* 1998; Grant, 1999) in multi-organ transplant recipients. The observed differences in incidence in the various organ transplant groups reflect the use of different immunosuppressive therapeutic regimens. Triple therapy consisting of Cy-A, azathioprine, and prednisone has been associated with an increased frequency of PTLD in kidney and heart recipients (Wilkinson *et al,* 1989) although high-dose Cy-A on its own correlates with increased PTLD incidence in heart/lung recipients (Gao *et al,* 2003). The risk of PTLD is also significantly increased in patients who have multiple allotransplants reflecting the higher cumulative dose of immunosuppressive agents required for retransplants (Swerdlow *et al,* 2000).

(2) Primary EBV infection in the seronegative organ transplant population is a major risk factor for development of EBV-associated PTLD. Compared to EBV-seropositive organ graft recipients, seronegative patients receiving a seropositive organ graft are at a 10-75 fold increased risk of PTLD (Cockfield, 2001). Furthermore, several serological studies have demonstrated that approximately 50% of organ transplant recipients who develop PTLD had a primary EBV infection within the previous 6 months (Ho *et al,* 1985, 1988; Thomas *et al,* 1995) demonstrating inherent risks of primary virus infection at a time when immune defences are suppressed. It follows that PTLD is more common in children than adults since children are more likely not to harbour the virus, and studies have shown that EBV can be transmitted with grafted bone marrow or transplanted solid organs from seropositive donors to seronegative graft recipients (Gratama *et al,* 1988; Cen *et al,* 1991). Thus, in a study by Haque *et al* in 1996, 2 EBV-seronegative heart/lung transplant recipients seroconverted shortly after transplantation and developed EBV+ve PTLD that contained the donor virus isolate. In contrast, EBV+ve PTLD from 2 previously seropositive heart/lung recipients contained the original recipient

virus isolate. The studies underline the significance of EBV transmission via the grafted organ as a risk factor for PTLD in seronegative recipients. Generally, PTLD derives from recipient or donor B cells in solid organ or bone marrow transplant recipients, respectively.

3.2 Presentation And Pathology

Clinically, PTLD presentation can be non-specific due to possible concomitant infection and graft rejection. However, a viral lymphadenitis (IM)-like picture is often observed when lesions arise within the first year following organ transplantation. The disease can also present as a tumour of the lymph node, or as an extranodal lesion. An extranodal lesion occurs in 69% of PTLD, and 51% of lesions have been found in multiple organs (Penn, 1993). Commonly, extranodal tumours involve lungs, liver, gastrointestinal tract, and, in one third of patients with disseminated disease, the grafted organ (Thomas *et al,* 1995). Such disseminated disease usually arises more than 1 year after organ grafting. Twelve % of PTLD are confined to the central nervous system (CNS) in contrast to 1-2% of lymphomas that arise in the general population (Penn & Porat, 1995).

PTLD shows marked morphological heterogeneity that can present as a mono-, oligo- or polyclonal Ig tumour. Originally, Frizzera *et al* (1981) described two histological types of PTLD in renal graft recipients: polymorphic B cell hyperplasia (PBH) and polymorphic B cell lymphoma (PBL). Histologically, PBH and PBL are both characterized by polymorphic cells, nodal effacement and invasion of normal architecture. PBH is further characterized by single-cell necrosis but lack of cellular atypia. In contrast, PBL shows extensive necrosis and cellular atypia. Subsequent classification schemes by Nalesnik *et al* (1988), Knowles *et al* (1995) and Swerdlow (1997) subdivided PTLD further based on detailed immunophenotyping and genotyping as well as morphology. Thus, PTLD phenotype is usually one of B lymphoblastoid cells (BLPD) with expression of cell activation markers and CAMs. Current World Health Organization (WHO) histopathological PTLD classification includes 'hyperplastic' (early, IM-like, reactive plasma cell hyperplastic lesions), 'polymorphic' (polyclonal or monoclonal tumours), and

'lymphomatous' or 'monomorphic' (of diffuse large B cell lymphoma, or BL, type) categories whilst a fourth group is often used to include 'other' lesions such as HL, plasmacytoma and myeloma (Nalesnik, 2001; Williams & Crawford, 2006). Although no single cytogenetic abnormality is characteristic of PTLD, several inconsistent cytogenetic abnormalities have been described. These include chromosomal trisomy, deletions, c-*myc* gene rearrangements, t8:14 translocations, or mutations in the p53, N-ras, c-*myc*, or *bcl*-6 genes which are often found in monomorphic PTLD (Gottschalk *et al,* 2005).

3.3 Seroepidemiology And Viral Load Monitoring

The serological profile of primary EBV infection in organ graft recipients often differs from that seen in healthy immunocompetent individuals. Specifically, IgM antibody responses to VCA or heterophile antigens are not always detected (Henle & Henle, 1981). In contrast, immunosuppressed virus carriers often have a 'reactivated' serological profile characterized by raised levels of IgG antibodies to VCA and EA but not to EBNA (Ho *et al,* 1985). Furthermore, in seropositive patients, suppressed EBV-specific CTL activity is associated with increased oropharyngeal virus shedding and raised numbers of circulating EBV+ve B cells (Crawford *et al,* 1981b; Yao *et al,* 1985b).

PCR analysis of EBV DNA VL in blood is used to assess PTLD risk and monitor response to PTLD treatment (Niesters *et al,* 2000; Leung *et al,* 2002; Gottschalk *et al,* 2005). In the UK, its use is recommended by the Health Protection Agency (HPA) as part of the HPA's National Standard Method's minimum testing algorithm for EBV serology *(www.hpa-standardmethods.org.uk).* However, there is as yet no consensus between laboratories as to how best to use EBV PCR as part of current management of transplant recipients. Therefore, its use as a diagnostic and monitoring tool varies between centres. Equally, interpretation depends on type of samples analyzed although plasma is generally accepted as being a suitable specimen for EBV PCR assessment. Furthermore, it is clear that a single VL assessment can not be used to predict the likelihood of PTLD since lesions may arise in patients with unremarkable VL (Straathof *et al,* 2002; Axelrod *et al,* 2003), and serial sampling is

indicated. Thus, a rapid increase in VL in serial samples obtained following transplantation may indicate increased risk of PTLD development (Gottschalk *et al,* 2005), and prompt reduction in immunosuppression may be indicated in such circumstances (Lee *et al,* 2005). However, the role of EBV VL measurements in assessing treatment response to PTLD therapy, and in predicting risk of PTLD relapse, is still unclear since recent studies have not shown a clear correlation between EBV VL and clinical course (Hopwood *et al,* 2002; Oertel *et al,* 2006).

3.4 EBV-Association And Pathogenesis

EBV is found in around 90% of PTLD. EBV DNA, mRNA and (mostly latent) viral proteins have been demonstrated in PTLD tumour cells (reviewed in Williams & Crawford, 2006), and this full latent viral gene expression strongly suggests that the virus plays a major role in EBV+ve PTLD pathogenesis. Indeed, it may be the only driving force behind outgrowth of early, hyperplastic lesions observed shortly following primary virus infection that express all EBV latent genes. Typically, PTLDs show such unrestricted latent viral gene expression (Young *et al,* 1989a; Thomas *et al,* 1990) although a more restricted phenotype reminiscent of HL (absence of EBNA2 and 3 proteins), or BL (EBNA1 only phenotype), has also been described (Cen *et al,* 1993; Timms *et al,* 2003). Equally, viral antigen expression may be variable within (and between) tumours in the same patient.

In a minority of cells, lytic infection is evident by the finding of linear EBV DNA and IE and, less commonly, EA and late (VCA, MA) viral proteins (Tanner & Alfieri, 2001). Thus, viral gene expression may be heterogeneous between PTLD lesions as well as within individual tumours. In such tumours, the role of EBV is not entirely clear although the virus may be sufficient to drive early lesions that may acquire genetic abnormalities and progress towards more malignant phenotype such as the one observed in aggressive monomorphic tumours. Furthermore, in contrast to the healthy state, EBV may infect both naïve and memory B cells to give rise to PTLD with evidence of infection of an abnormal cell. Thus, analysis of BCR Ig heavy (IgH) chain genes showed PTLD tumour cells to consist of either naïve or memory B cells as evident by the absence of somatic hypermutations in the former

but not the latter malignant cell type (Timms *et al,* 2003). Furthermore, non-functional BCR mutations were detected in PTLD tumour cells that would result in cell apoptosis of non-EBV-infected cells and immune recognition in the immunocompetent individual. Studies by Lam *et al* (1997) have also described BCR-deficient PTLD tumour cells.

PTLD cells express cell activation markers and CAMs typical of B lymphoblasts and BLCLs. Since the majority of PTLD shows unrestricted viral gene expression, the tumour is (in theory at least) susceptible to EBV-specific CTL destruction. *In vitro,* the immunosuppressants Cy-A, FK506 and OKT3 are powerful inhibitors of EBV-specific CTLs, and CTL activity often becomes undetectable in peripheral blood from organ transplant recipients receiving immunosuppressive therapy (Crawford *et al,* 1981b; Haque *et al,* 1997). Thus, immunosuppression promotes survival of EBV+ve B cells which may lead to their unchecked proliferation and, ultimately, PTLD. Studies by Patton *et al* (1990) demonstrating clonal EBV in monoclonal PTLD suggests that virus infection occurs at an early stage of tumorigenesis before expansion of the malignant clone. Expression of the viral oncogenes EBNA2 and LMP1 further supports an essential role for EBV in PTLD pathogenesis.

PTLD only develops in a minority of transplant patients and lesions are often single and clonal in nature. Equally, late onset (often single nodal or extranodal) PTLD is more often an EBV-negative lesion (Leblond *et al,* 1998; Swerdlow *et al,* 2000). Thus, genetic and/or epigenetic factors must play a role in PTLD pathogenesis in addition to EBV. The microenvironment in which PTLD arises is thought to favour EBV-driven B cell proliferation, and chronic low-grade antigen stimulation resulting from host-*versus*-graft disease in the grafted organ may cause expansion of the EBV-infected B cell pool following virus reactivation from latently infected cells. The non-neoplastic component in PTLD from solid organ graft recipients consists primarily of mature CD4+ve (helper) CD45RO+ve (memory) T cells which could act as a source of soluble growth factors that facilitate tumour growth (Thomas *et al,* 1990; Perera *et al,* 1998). The role of CD4+ve T cells is further underlined by studies in SCID mice demonstrating that these cells are required for development of

PTLD-like tumours *in vivo* from seropositive peripheral blood B lymphocytes (see section 5.4.3; Johannessen *et al,* 2000).

3.5 Treatment

In spite of current treatment, PTLD carries a high mortality of up to 60% and 80% in solid organ and bone marrow transplant recipients, respectively (Armitage *et al,* 1991; Opelz & Dohler, 2004; Svoboda *et al,* 2006). Adverse predictive factors include number of anatomical sites involved, tumour monoclonality, and primary CNS location (Leblond *et al,* 2001). Current treatment options for PTLD are summarized in Table 4.

TABLE 4
Therapy Options For PTLD

First Line Treatment: Reduction Of Tumour Mass	**1.** Reduction in immunosuppression with/without nucleoside analogues (aciclovir/ganciclovir) **2.** Combination of chemotherapy, radiotherapy, surgery, and anti-CD20 mab treatment
Promotion Of CTL Activity	**1.** Reduction in immunosuppression **2.** Adoptive T cell therapy: - Donor CTLs - Autologous CTLs - Allogeneic CTLs **3.** Cytokines
Suppression And/Or Eradication Of EBV Infection	**1.** Nucleoside analogues (aciclovir/ganciclovir) **2.** Hydroxyurea **3.** Induction of EBV lytic cycle

CTL: Cytotoxic T lymphocytes; mab: Monoclonal antibody (Adapted from Williams & Crawford, 2006)

3.5.1 Reduction Of Immunosuppression And Antivirals

Originally, PTLD treatment entailed the use of a combination of surgical removal, irradiation and chemotherapy (Hanto *et al,* 1983). In 1984, however, Starzl *et al* described the resolution of PTLD in 9 out of 12 (75%) kidney or liver recipients by partial or complete withdrawal of immunosuppression alone. Reduction of immunosuppression [alone or together with the nucleoside analogues aciclovir

(ACV) or ganciclovir (GCV) that inhibit EBV DNA polymerase and lytic replication *in vitro*] is the current mainstay of primary therapeutic intervention in PTLD although it may be accompanied by rejection of the grafted organ (Nalesnik, 1991). This potentially life-threatening complication is of less concern in renal transplantation where patients can be returned to dialysis. Presumably, reduction in immunosuppression achieves reactivation of virus-specific CD8+ve T lymphocytes. However, the effect of simultaneous use of ACV and GCV remains to be clarified since PTLD consists largely of latently infected cells (Hanto *et al,* 1982; Pirsch *et al,* 1989).

ACV and GCV are used as prophylaxis in EBV-seronegative organ graft recipients that receive an organ transplant from a seropositive donor. Thus, prophylactic use of GCV to combat EBV-driven B cell proliferation in seronegative paediatric organ graft recipients following liver transplantation has been shown to decrease PTLD incidence (McDiarmid *et al,* 1998), and similar observations have been made in heart and/or lung transplant recipients (Malouf *et al,* 2002). However, it may perhaps be counterproductive to use antivirals in PTLD patients when one considers that using valproic acid (VPA; used alongside the chemotherapeutic agent gemcitabine) to induce lytic cycle in BLCL-inoculated SCID mice inhibited growth of PTLD-like lesions *in vivo*. The effect of VPA was dependent on the presence of an intact BZLF1 gene (Feng & Kenney, 2006). In line with this is a recent study by Opelz *et al* (2007) demonstrating no prophylactic effect of antiviral treatment on the incidence of PTLD development in renal transplant recipients. In contrast, however, in their study of 44,828 recipients of cadaveric kidney transplants, Opelz *et al* showed that prophylactic administration of anti-CMV Ig (used to protect CMV seronegative recipients of seropositive organs from CMV infection) resulted in complete protection against PTLD development during the first year (period of Ig administration) post-transplant. Since most available anti-CMV Ig preparations contain antibodies against EBV proteins, such prophylactic Ig use may be directed against EBV infection although non-specific immunomodulatory effects may also have a role to play.

Whilst reduction of immunosuppression has been of most benefit in the treatment of polyclonal, polymorphic lesions, it may also result in regression of

tumours containing oligo- or monoclonal tumour cell populations (Nalesnik *et al.*, 1992). On the whole, 40-86% of paediatric, and 25-63% of adult, organ graft recipients experience remission following reduction in immunosuppression but mortality is high (up to 90%) if patients do not respond to this treatment form (Gottschalk *et al,* 2005; Taylor *et al,* 2005). Equally, relapsed PTLD is difficult to treat with reduction of immunosuppression alone.

3.5.2 Conventional Therapy

Chemotherapy, radiotherapy and surgery still have a role in PTLD management. Thus, a combination of these treatment forms may be used alongside reduction in immunosuppression, or when tumours either fail to respond to such an approach or relapse occurs (McCarthy *et al,* 1997; Koffman *et al,* 2000; Bollard *et al*, 2003). Inclusion of low-dose chemotherapy to minimize its inherent toxicity may then be appropriate (Gross *et al,* 2005). Equally, a combination of conventional therapeutic options may be employed when reduction in immunosuppression may result in loss of a life-saving organ graft such as a heart (Webber *et al,* 2006). Thus, radiotherapy and surgical resection have been used successfully in patients with localized PTLD lesions (Newstead, 2005: Foroncewicz *et al*, 2006).

3.5.3 Cytokines

The immunomodulatory effects of cytokines have been used against PTLD. For example, Shapiro *et al* (1988) successfully used recombinant IFNα (a CTL and NK cell stimulant) with intravenous (iv) Ig to treat a monoclonal and a polyclonal EBV-positive PTLD lesion in 2 bone marrow recipients, respectively. Furthermore, Davis *et al* (1998, 2001) showed that 8 of 14 (57%) PTLD patients responded to IFNα although 4 (29%) of them developed graft rejection. Whilst IFNα treatment has considerable side effects (including flu-like illness), this is not the case when anti-IL6 antibodies have been employed in PTLD management with a view to neutralizing the B cell growth-promoting effects of IL6. Using such murine anti-IL6 mab, Haddad *et al* (2001) obtained partial or complete PTLD regression in 8 of 12

(67%) solid organ transplant recipients (that were refractory to reduction in immunosuppression) at up to 27 months' follow-up without serious side effects.

3.5.4 Adoptive Immunotherapy

Increasingly, novel PTLD treatment strategy has focused on development of adoptive immunotherapy with a view to providing rapid, targeted treatment that is well tolerated. Such an approach entails the use of either adoptive **(1)** humoral or **(2)** cellular immunotherapy.

(1) Adoptive humoral immunotherapy centres on the use of mabs directed against surface markers of B cells. Thus, Fischer *et al* (1991) and Benkerrou *et al* (1993, 1998) used a combination of anti-CD21 and anti-CD24 mabs to treat PTLD in bone marrow and solid organ recipients. Whilst oligoclonal lesions responded well to therapy, monoclonal tumours were resistant to this treatment form. However, these murine mabs are no longer available commercially. More recently, the anti-CD20 mab 'rituximab' has been licensed for PTLD treatment (Cook *et al,* 1999). One mechanism of action of rituximab is activation of antibody-directed cell cytotoxicity (ADCC; van der Kolk *et al,* 2002). Whilst this humanized mouse mab (with murine antibody variable regions) has shown great promise with up to 100% response rate in some studies, these studies have used rituximab in therapeutic protocols that also include reduction in immunosuppression and/or conventional treatment approaches (for example, chemotherapy; Milpied *et al*, 2000; Berney *et al*, 2002; Gianni *et al,* 2003; Gottschalk *et al*, 2005; Oertel *et al*, 2005). In contrast, in a (prospective) phase 2 trial to examine the safety and efficacy of rituximab in PTLD following solid organ transplantation, Choquet *et al* (2006) treated 43 patients that did not respond to reduction in immunosuppression with 4 weekly mab injections. At day 80, 37 (86%) patients were alive with a response rate of 44% including 12 cases of complete response. At day 360, 56% of patients were alive and the response rate was maintained in 68% of patients. The overall survival rate at 1 year was 67%. Based on their results, the group suggested a role for rituximab in a therapeutic approach that combined different modalities (for example, reduction in immunosuppression).

Further support for such a strategy derives from a retrospective study by Elstrom *et al* (2006) who examined the clinical course of 35 PTLD patients (34 solid organ graft and 1 bone marrow recipients) that failed to respond to reduction in immunosuppression and received further therapy using rituximab. Patients that failed rituximab treatment received chemotherapy. Overall, 22 patients underwent rituximab treatment whilst 23 patients received further chemotherapy with an overall response rate of 68% and 74%, respectively. Whilst rituximab and chemotherapy were both effective, rituximab was well tolerated but chemotherapy was associated with considerable toxicity resulting in death of 6 (26%) patients. The study result suggested that rituximab is a suitable choice for management of PTLD patients who do not respond fully to reduction in immunosuppression alone. Chemotherapy may be reserved for patients who fail rituximab, need rapid response to treatment, or develop EBV-ve PTLD.

Despite the overall encouraging results obtained in different studies evaluating rituximab in PTLD therapy, tumour relapse can occur (Savoldo *et al,* 2005). The emergence of CD20-negative escape tumour variants has also been observed in NHL out with the transplant setting rendering such lesions refractory to rituximab (Davis *et al,* 1999).

(2) Adoptive cellular immunotherapy focuses on the use of lymphoid cells. Our detailed understanding of immune control of EBV infection has led to development of novel immunotherapeutic approaches to PTLD treatment based on tumour expression of viral antigens that can be targeted by T lymphocytes. Such novel strategies aim to restore EBV-specific T cell immune defences, and to mediate PTLD regression without the side effects that accompany other approaches. Initial results by Riddell *et al* (1992) demonstrated the potential effectiveness of adoptive immunotherapy when they prevented CMV-induced pneumonitis in 3 bone marrow transplant recipients using CMV-specific T cells from the seropositive donors.

Adoptive cellular immunotherapy has been shown to be very effective in preventing and treating PTLD (Rooney *et al,* 1995, 1998a; Straathof *et al,* 2002; Haque *et al,* 1998, 2002, 2007). Similarly, such an approach using autologous or allogeneic EBV-specific CTLs has been shown to mediate regression of other EBV-

associated malignancies such as HL (Rooney *et al,* 1998b; Lucas *et al,* 2004), and NPC (Straathof *et al,* 2005). Generation of CTLs relies on stimulation (and expansion) of the circulating EBV-infected memory donor B cell pool *in vitro* using either BLCL, or virus gene-transfected dendritic cells (DCs), as antigen presenters (Gottschalk *et al,* 2003; Wilkie *et al,* 2004).

In 1994, Papadopoulos *et al* described the infusion of unirradiated donor leukocytes to treat EBV-associated PTLD in 5 recipients of T-cell depleted allogeneic bone marrow transplants. Whilst 3 patients experienced long-term remissions, they developed GVHD. The remaining 2 patients succumbed to respiratory failure of unknown causes. Furthermore, Nalesnik *et al* (1997) demonstrated regression of EBV+ve PTLD in 4 solid organ graft recipients following treatment with autologous PBLs which had been depleted of monocytes and stimulated *in vitro* with IL2 for 10-11 days prior to their infusion (lymphokine-activated killer cells, LAK cells). Whilst 2 patients developed controllable graft rejection, 3 patients remained disease-free for up to 16 months post-infusion, and 1 patient died of unrelated pneumonia. 3 graft recipients with EBV-ve PTLD failed to respond to this treatment form. The group has also shown LAK cells to be effective in a SCID mouse model of PTLD (Randhawa *et al,* 1998).

EBV-specific CTLs have been expanded *in vitro* for use in PTLD patients. In 1995, Rooney *et al* reported the use of neo^R-marked autologous EBV-specific CD4+ve/CD8+ve polyclonal CTL lines produced *ex vivo* from donor leukocytes to prevent PTLD in 10 bone marrow recipients without GVHD. It was possible to regenerate marker gene neo^R+ve CTLs from peripheral blood of recipients *in vitro* for up to 18 months after infusion (Heslop *et al,* 1996; Bollard *et al,* 2004). The group also demonstrated curative effects of CTL infusions in 2 bone marrow recipients with established PTLD (Rooney *et al,* 1998a). These initial studies also uncovered evidence of CTL selection of tumour escape (EBNA-3b deletion) mutants in a third PTLD patient who succumbed to the disease despite CTL therapy (Gottschalk *et al,* 2001) raising the possibility of such treatment resistance. An overview of studies employing CTL immunotherapy against EBV-associated PTLD is shown in Table 5.

TABLE 5
Trials Employing EBV-Specific CTLs To Prevent/Treat PTLD

Study	Transplant Type	No of Patients	Study Design	Immuno-therapy	Results
Rooney *et al*, 1995, 1998a, 2002*	BMT	56	Prophylaxis	BMD-CTL	No PTLD; 12% incidence in a historical control group
Gustafsson *et al*, 2000	BMT	6	Prophylaxis	BMD-CTL	High pre-infusion EBV VL; 5/6 no PTLD; 1/6 PTLD
Rooney *et al*, 1995, 1998a	BMT	2	Treatment	BMD-CTL	2/2 CR
Gottschalk *et al*, 2001	BMT	1	Treatment	BMD-CTL	NR; EBV escape mutation
Haque *et al*, 1998	SOT	3	Pilot	Auto-CTL	3/3 decreased VL and increased EBV-specific CTLp
Comoli *et al*, 2002	SOT	7	Prophylaxis	Auto-CTL	High pre-infusion VL; 5/7 decreased VL; 7/7 increased EBV-specific CTLp; no PTLD
Khanna *et al*, 1999	SOT	1	Treatment	Auto-CTL	Initial CR followed by fatal secondary PTLD; Primary EBV infection post-transplant
Sherritt *et al*, 2003	SOT	1	Treatment	Auto-CTL	CR; CTLp to latent EBV antigens
Savoldo *et al*, 2006	SOT	12/2	Prophylaxis/Treatment	Auto-CTL	Prophylaxis: 12/12 no PTLD, high EBV VL post-infusion; Treatment: 1/2 CR, 1/2 PR
Haque *et al*, 2002	BMT/SOT	1/7	Treatment	Allo-CTL	3/8 CR; 2/8 NR; 1/8 PR; 2/8 died of unrelated causes
Gandhi *et al*, 2007	SOT	3	Treatment	Allo-CTL	2/3 CR; 1/3 died of unrelated causes
Haque *et al*, 2007	BMT/SOT	2/31	Treatment	Allo-CTL	14/33 CR; 3/33 PR; 16/33 NR; Good MHC match and CD4+ve T cells were important

Allo: Allogeneic; Auto: Autologous; BMD: Bone marrow donor; BMT: Bone marrow transplant; CR: Complete remission; CTL: Cytotoxic T Lymphocytes; CTLp: CTL precursors; EBV: Epstein-Barr virus; MHC: Major histocompatibility complex; NR: No remission; PR: Partial remission; SOT: Solid organ transplant; VL: Viral load; *: Straathof *et al,* 2002. (Adapted from Burns & Crawford, 2004)

The situation for CTL therapy is somewhat more complex in solid organ transplant patients since donors of such organs are often not available, or suitable, to donate T cells for *in vitro* expansion. In contrast, the use of polyclonal autologous patient-derived CTLs has proven to be of some benefit in prevention (Haque *et al*, 1998; Comoli *et al*, 2002) and treatment (Khanna *et al*, 1999; Sherritt *et al*, 2003) of PTLD. In a pilot dose escalation study in solid organ graft recipients, *ex vivo*-expanded autologous EBV-specific CTLs were infused into 3 adult seropositive recipients (2 liver and 1 kidney; Haque *et al*, 1998). Peripheral blood CTLp frequency (as measured by limiting dilution analysis) increased above pre-infusion levels and remained high for up to 3 months post-infusion concomitant with a significant fall in EBV DNA VL during that period as measured by PCR. Similar observations were made by Comoli *et al* (2002) in 7 solid organ transplant recipients, and PTLD did not develop in either study. In further studies by Khanna *et al* (1999) and Sherritt *et al* (2003) on 2 solid organ transplant recipients suffering from PTLD demonstrated the effectiveness of autologous CTLs in mediating tumour regression. Despite an immunosuppressive drug regime, it has been possible to generate such CTLs from seronegative organ graft recipients that experienced a primary EBV infection post-transplant (Khanna *et al*, 1999).

The use of autologous CTLs remains a challenge since *in vitro* expansion of the cells is labour intensive, costly, and takes up to 12 weeks. The last point is particularly poignant since such a delay means that specific therapy may come too late for PTLD sufferers. In order to circumvent the technical difficulties of using autologous T lymphocytes, Haque *et al* set up and characterized a frozen tissue bank of around 100 EBV-specific CTLs expanded *in vitro* from healthy blood donors (Wilkie *et al*, 2004). Initial studies using CTLs from this tissue bank on a 'best MHC match' basis demonstrated PTLD regression in a liver/intestine transplant recipient (Haque *et al*, 2001). Using the same approach in a phase I/II clinical trial, Haque *et al* (2002) infused allogeneic CTLs into 7 solid organ (2 liver, 3 liver/small bowel, 2 kidney) and 1 bone marrow transplant patients with EBV+ve PTLD. Of the 5 patients that completed the treatment course of 1-6 (10^6 CTL per kg) iv infusions of partly MHC-matched allogeneic EBV-specific CTLs, 3 individuals experienced complete remission whilst 2 had no clinical response. The responders showed no

evidence of disease for up to 28 months after completion of the CTL treatment course. Organ graft function improved in responders with no evidence of GVHD or other side effects. Of the 3 patients that did not complete the CTL course, 1 patient showed partial response whilst 2 patients died rapidly of causes unrelated to CTL infusion.

A direct role for infused CTLs in mediating EBV+ve tumour destruction has been obtained in a study demonstrating complete regression of a primary cerebral EBV+ve B cell lymphoma in a child with primary immunodeficiency and, thus, no functional EBV-specific CTLs of her own (Wynn *et al,* 2005). The infused allogeneic CTLs were able to access CNS which is in line with previous studies showing that B and T lymphocytes can access the brain (Hickey *et al,* 1991; Anthony *et al,* 2003). Furthermore, Gandhi *et al* (2007) have recently shown homing of infused allogeneic CTLs generated *in vitro* from a healthy male blood donor to pulmonary PTLD arising in a female lung transplant recipient. The PTLD was of recipient origin. Using fluorescent *in situ* hybridisation and immunostaining, the group demonstrated XY (male) chromosomes in CD8+ve T cells within the tumour mass.

Recently, Haque *et al* (2007) reported the overall results at 6 months post-transplant of the first phase II multi-centre clinical trial using allogeneic CTLs against EBV+ve PTLD. Using their EBV-specific CTL bank, allogeneic CTLs were selected based on **(1)** a 'best MHC-match', and **(2)** the results of EBV-specific cytotoxicity *in vitro* as measured by ^{51}Cr-release assays. At the time of receiving CTL lines, PTLD patients had already failed a regime of conventional PTLD treatment (see Table 4 above). Overall, 33 PTLD patients received weekly CTL ($2x10^6$ per kg) infusions for 4 weeks and were monitored for between 6 months and 2 years with no adverse effects of CTL infusions observed. At 6 months, 14 patients had experienced complete remission of disease, and a further 3 patients were in partial remission. 16 patients showed no response to immunotherapy. Thus, 17 (52%) of patients treated with CTLs showed complete or partial remission 6 months after receiving the last CTL dose. There was a significant trend towards a better therapeutic response with higher numbers of CD4+ve T cells in the transferred CTL populations. Equally, a significant correlation was found between the level of MHC

matching and therapeutic success. Using such a well-characterized CTL tissue bank on a 'best MHC match' basis circumvents lengthy and labour-intensive *in vitro* expansion of autologous CTLs for individual patients and offers instead a ready source of effective PTLD therapy in a poor prognosis patient group.

In light of the above studies, adoptive immunotherapy using CTLs targeted against virus-derived antigens on a 'best MHC match' basis appears to be effective, safe, rapid, and potentially applicable to other systems where a suitable tumour-specific target antigen is known. Thus, any tumour-specific antigen can potentially be targeted in this manner. Furthermore, genetically engineering CTLs to express TCRs that specifically recognize antigens on the surface of malignant cells using an antibody construct (or single variable chain antibody fragment, scFv) circumvents MHC restrictions. The use of scFv to recognize target antigens on a tumour cell surface has shown great promise (see General Discussion). However, it is important to study such new treatment strategy *in vitro* and *in vivo* prior to introduction into clinical practice.

3.5.5 Testing Of Novel PTLD Treatment

PTLD biopsy material available for research is limited, and the few established biopsy-derived cell lines available differ phenotypically from the tumour cell type and are, therefore, not an accurate *in vitro* model for the disease (Cen *et al,* 1993). Consequently, PTLD has been modelled in various animals including severe combined immunodeficient (SCID) mice which offer valuable insight into PTLD development. Equally, SCID mice can be used to trial new PTLD prophylaxis and treatment such as novel adoptive immunotherapy.

4. Use Of Animals In Research

In order to answer a scientific question of paramount importance, animals can be employed provided a suitable *in vivo* model is available and no *in vitro* systems can be used [for alternative model systems, see the 'Fund for the Replacement of Animals in Medical Experiments' (FRAME) website: *www.frame.org.uk*]. Furthermore, it must be ensured that the most appropriate animal model, animal procedures, and animal numbers are used in order to obtain meaningful results whilst guarding animal welfare.

In the UK, use of animals in research is strictly controlled by the Home Office 'Animals (Scientific Procedures) Act 1986' (for further information, see the website: *www.homeoffice.gov.uk/animalsinsp/*). This entails that all research work involving animals must have met with the approval of local Ethical Review Committees as well as being specifically licensed ('Project Licence'; PPL) by the Home Office. Furthermore, all staff carrying out animal procedures must be specifically licensed ('Personal Licence'; PIL) by the Home Office. The Act is enforced by Home Office Inspectors with additional support from Named Veterinary Surgeons who oversee animal welfare. As part of any *in vivo* experimental work, constant efforts are made to **(1) r**educe the number of animals used (**R**eduction), **(2) r**efine the experimental approach (**R**efinement), and **(3) r**eplace animals with *in vitro* models whenever possible (**R**eplacement) – the so-called '**3 Rs**' that Home Office guidance requires PIL and PPL Holders to address continuously throughout any project/licensing period.

5. Animal Models For EBV-Induced Diseases

Non-human primates have traditionally been used to model EBV-associated diseases (for an overview of animals used for this purpose, see Table 6). However, Old World species are naturally infected with related simian herpesviruses in the same lymphocryptovirus (LCV) genus as EBV and are, thus, immune to EBV infection due to cross-reacting antibodies (Gerber & Birch, 1967; Landon & Malan, 1971; Frank *et al,* 1976; Deinhardt & Deinhardt, 1979). Over 95% of adult Old World non-human primates harbour LCV whether in the wild or held in captive colonies (Landon & Malan, 1971; Jenson *et al,* 2000; Rao *et al,* 2000), and the biology of LCV infection appears to parallel closely that of EBV in humans (Wang *et al,* 2001).

In light of the above, and the observation that there was (until recently) no solid evidence to suggest that LCV infected New World non-human primates, experimentally EBV infected New World species became widely used *in vivo* models in which to study EBV infection and disease.

TABLE 6
Animal Models Used To Study EBV Biology And EBV-Associated Diseases

Animal	Model For	Comments
Non-Human New World Primates: Common Marmoset	Primary/persistent EBV infection	- Can be infected with EBV - Develop spontaneous herpesvirus-positive B cell lymphomas that can confuse results obtained - Rare - Costly
Non-Human New World Primates: Cottontop Tamarin	EBV-associated lymphoma	
Non-Human Old World Primates: Rhesus Monkey (Cynomolgus Monkey)	Primary/persistent EBV infection	- Can not be infected with EBV - Can be infected with LCV - Physiological (oral) route of infection - Costly
MHV68-Infected Balb/c Mice	Primary/persistent EBV infection	- MHV68 used to parallel EBV - Gives rise to lytic infection - Small animal model
SCID Mice	- Hu-PBL-SCID; Primary/persistent infection and EBV-associated tumours (pathogenesis/prevention/treatment) - Hu-BLCL-SCID: EBV-associated tumours (prevention/treatment)	- Accepts human xenografts - Develops PTLD-like lymphoma - Small animal model

BLCL: B lymphoblastoid cell line; EBV: Epstein-Barr virus; Hu: Human; MHV68: Murine herpesvirus 68; PBL: Peripheral blood leukocytes; LCV: Lymphocryptovirus; SCID: Severe Combined Immunodeficient

5.1 New World Non-Human Primates: Common Marmoset And Cottontop Tamarin

New World non-human primates are susceptible to EBV infection. The **(1)** common marmoset *(Callithrix jacchus)* and the **(2)** cottontop tamarin *(Saguinus oedipus oedipus)* have been used to model EBV-associated diseases.

(1) The common marmoset is a model for primary and persistent EBV infection. Following experimental intramuscular (im) or intraperitoneal (ip) infection of the animals, an IM-like lymphocytosis is observed in some animals together with anti-VCA and anti-EA antibody-like responses similar to IM (Falk *et al,* 1976; de Thè *et al,* 1980). EBV DNA is detected in lymphoid tissues (Cox *et al,* 1996). Furthermore, regular detection of salivary EBV DNA (buccal fluid) and long term detection of EBER transcripts (by RT-PCR) in PBLs indicates persistent EBV infection (Cox *et al,* 1996; Farrell *et al,* 1997). The animal has been used for vaccine studies. However, immunization of the common marmoset using the envelope gp350 antigen does not prevent EBV infection although reduced virus is detected in buccal fluid (Cox *et al,* 1998). EBV-associated lymphomas do not develop in virus-infected common marmosets.

(2) The cottontop tamarin is a model for persistent EBV infection and lymphomagenesis. The tamarin consistently develops multifocal EBV+ve large cell lymphomas following im and/or ip EBV inoculation (Shope *et al,* 1973; Cleary *et al,* 1985). Since the tumours express all the viral latent genes (Young *et al,* 1989b) and mirror PTLD, the cottontop tamarin has played an important role as a model in which to study candidate EBV vaccines. Since the original suggestion by Epstein in 1976 that EBV vaccination would not only control EBV-associated malignancies but also establish the role of EBV in oncogenicity in man, these efforts have been based on the gp350/220 envelope protein (Epstein, 1976). Although immunization of cottontop tamarins with a subunit vaccine does not afford sterile immunity since EBER transcripts continue to be

detected in lymphoid tissue of immunized animals (Niedobitek *et al,* 1994), gp350/220 vaccines provide protection against EBV-induced lymphomas (Epstein *et al,* 1985).

New World primates are endangered (but bred in captivity), rare and costly. Furthermore, recent studies have shown that New World species are naturally infected with LCV, further undermining their use to model EBV infection and disease. Thus, Cho *et al* (2001) isolated a B cell-immortalizing LCV from a B cell lymphoma arising spontaneously in a common marmoset. Additionally, PCR studies detected this marmoset LCV (mLCV) in three different marmoset colonies and a similar LCV was also found in (New World) squirrel monkeys suggesting widespread infection. Additional studies have confirmed that LCV can be found in a number of New World species (Jenson *et al,* 2002; Ehlers *et al,* 2003). The mLCV genome has been sequenced (Rivailler *et al,* 2002a,b) and is strikingly different from that of EBV as it lacks a number of EBV (and Old World rhesus LCV, rLCV) homologue genes (for example, EBERs and BARTs) suggesting that mLCV is a primitive relative of EBV, and that EBV evolved in higher order primates. The resulting biological differences between the two viruses are not yet known. The genomic sequence divergence between mLCV and EBV does explain, however, why New World species can be infected with EBV and why mLCV went undetected for so long since previous studies used EBV-derived antigens in their screening assays. Only around 40-60% of captive marmosets tested harbour mLCV (Fogg *et al,* 2005) which is in sharp contrast to rLCV and EBV which ubiquitously infect Old World rhesus macaques and humans, respectively.

5.2 Old World Non-Human Primates: Rhesus And Cynomolgus Monkeys

The best studied LCV are those detected in the **(1)** rhesus (*Macaca mulatta*) and **(2)** cynomolgus (*Macaca fascicularis*) monkeys.

(1) Rhesus monkeys are naturally immune to EBV infection which is similar to other Old World non-human primates. In an attempt to create a new model for EBV

infection, Moghaddam *et al* (1997) orally infected 2 naïve rhesus monkeys with a rLCV (see 5.1 above) naturally endemic in rhesus monkeys. The animals developed an IM-like response with T cell lymphocytosis and activated CD23+ve B cells in peripheral blood together with cross-reacting antibodies to EBV latent (EBNA2) and lytic (VCA) viral proteins. Intermittent oropharyngeal shedding of virus and outgrowth of spontaneous rLCV+ve BLCL *in vitro* confirmed persistent rLCV infection during a 1.5 year observation period. Persistent infection conferred protection against re-challenge with virus in 1 animal tested. The rLCV genome has been sequenced demonstrating a high degree of sequence homology to EBV as well as an identical repertoire of viral genes (Rivailler *et al,* 2002a,b). Based on EBNA2 homologue gene polymorphism, two different rLCV types ('type 1' and 'type 2') have been delineated suggesting similar selective pressures for human and non-human primate hosts in terms of rLCV evolution (Cho *et al,* 1999). In further studies, Moghaddam *et al* (1998) found that rLCV and EBV failed to immortalize human and rhesus B cells *in vitro*, respectively, despite conservation of the CD21 (EBV receptor) binding domain of the rhesus major membrane glycoprotein suggesting species-specific restrictions to infection occurring beyond virus binding and penetration. The rhesus model has also been used to study CTL-mediated immune control of rLCV infection (Fogg *et al,* 2005, 2006).

(2) Cynomolgus monkeys have been considered for EBV research. Whilst spontaneous lymphomas are uncommon in Old World monkeys, concomitant infection with simian immunodeficiency virus (SIV) markedly increases their occurrence (Hunt *et al,* 1983; Baskin *et al,* 1986). Thus, up to 40% of cynomolgus monkeys develop high-grade B cell lymphomas when infected with SIV but the requirement for SIV-induced immunosuppression prevents the use of the model for PTLD studies. In an effort to create a non-human primate model of PTLD, Schmidtko *et al* (2002) carried out 160 renal allograft transplants in cynomolgus monkeys over a 5 year period under an immunosuppressive regime that included Cy-A. 9 (5.6%) animals developed cynomolgus LCV-associated (cLCV; Feichtinger *et al,* 1992) B cell (predominantly polymorphic) PTLD-like lesions 28-103 days post-transplant. Of the 9 PTLD cases, 6

animals succumbed to multiorgan failure secondary to PTLD whilst the remaining 3 monkeys died of GVHD as well as acute and chronic rejection. The potential effect of PTLD treatment (for example, reduction of immunosuppression) was not investigated nor was adoptive immunotherapy considered. Similar studies in SIV-infected rLCV-infected rhesus monkeys have demonstrated outgrowth of rLCV-associated B cell lymphomas (Rivailler *et al,* 2004).

5.3 Murine Herpesvirus 68 (MHV68)

Many aspects of murine herpesvirus 68 (MHV68), a γ-herpesvirus originally isolated from the bank vole *(Clethrionomys glareolus)* in Slovakia (Blaskovic *et al,* 1980), parallel that observed during EBV infection, and MHV68 has provided insight into γ-herpesvirus infection *in vivo*.

Primary MHV68 infection occurs in the lung, and experimental intranasal infection of Balb/c mice with MHV68 results in lytic virus infection of lung alveolar epithelium. Persistent infection is established in murine B cells although lung epithelium, macrophages and DCs can also support persistent infection (reviewed in Nash *et al,* 2001; Olivadoti *et al,* 2007). An IM-like syndrome occurs 3 weeks after primary infection with a major expansion of Vβ4+ve CD8+ve T cells (Tripp *et al,* 1997) although the exact manner in which the T cell proliferation is driven remains to be elucidated (a putative MHV68-encoded sAg was proposed at the time). Whilst CD8+ve T cells control both lytic and latent *in vivo* infection (Braaten *et al,* 2005), CD4+ve T cells are important in inhibiting reactivation of replicative infection in lung epithelium.

During primary MHV68 infection, large amounts of IFNγ are produced by lymphoid tissue. In their study of mice lacking the IFNγ cell surface receptor (IFNγ R-/- mice), Dutia *et al* (1997) failed to detect any differences in virus titres in lung (or rate of clearance of lung infection) in IFNγ R-/- mice compared to wild type animals. In contrast, splenic tissue from IFNγ R-/- mice showed marked fibrotic changes accompanied by increase in latently infected B cells. Additionally, fibrosis was observed

in the lung (Ebrahimi *et al,* 2001). These changes were dependent on the presence of CD8+ve T cells and (to a certain extent) CD4+ve T lymphocytes. Further studies by Mora *et al* (2005) have demonstrated progressive deposition of interstitial collagen in lungs of MHV68-infected IFNγ R-/- mice which can be used to model idiopathic pulmonary fibrosis (IPF). IPF is a progressive, fibrotic lung disease of unknown etiology in humans that is associated with chronic lung infection with one or more herpesviruses (including EBV). Lytic MHV68 infection is associated with IPF in mice, and antiviral treatment is of benefit *in vivo* (Mora *et al,* 2007).

Vaccination studies using gp150 (EBV gp350/200 homologue) have been unable to prevent lytic or latent MHV68 infection *in vivo* although infection following vaccination does not result in an IM-like syndrome (Stewart *et al,* 1999).

MHV68+ve lymphoproliferative disease (LPD) develops in a few MHV68-infected mice. Thus, in a study of 220 persistently infected animals, 20 (9%) mice monitored for up to 3 years developed MHV68+ve LPD, and immunosuppression with Cy-A increased the incidence to 60% (Sunil-Chandra *et al,* 1994). Although the exact role of the virus in LPD outgrowth remains to be clarified, a LPD-derived MHV68+ve cell line gives rise to tumours in nude (athymic; devoid of T cells) mice (Usherwood *et al,* 1996).

5.4 Severe Combined Immunodeficient (SCID) Mouse

The SCID mouse readily accepts human xenografts due to a lack of functional B and T cells. The animal has become a valuable tool to study PTLD pathogenesis and novel treatment strategy since the discovery that EBV+ve PBL engraft in SCID mice ('hu-PBL-SCID') and give rise to EBV+ve PTLD-like tumours (Mosier *et al,* 1988).

5.4.1 Biology

The murine SCID mutation was originally described in inbred CB.17 mice by Bosma *et al* in 1983. The mutation, which is heritable as a single autosomal recessive *(SCID)* gene on mouse chromosome 16, leads to impaired function of the 'protein kinase, DNA activated, catalytic polypeptide' ('Prkdc') enzyme which is essential in repairing dsDNA breaks and in recombining the variable (V), diversity (D) and joining (J) genes of functional BCRs and TCRs (Fulop & Phillips, 1990; Bosma & Carroll, 1991). Since V(D)J gene recombination does not proceed, differentiation of mature B and T cells is severely impaired, and mice homozygous for the mutant gene (*SCID/SCID*) are profoundly deficient in functional B and T lymphocytes. Therefore, the animals are unable to mount humoral or cellular adaptive immune responses, and can not reject allogeneic or xenogeneic tissue grafts. Since the animals have little or no immunity, they readily succumb to infections if they are not kept within a specific pathogen free (SPF) environment such as the one that is afforded by individually ventilated (microisolator) cages (IVCs) and handled using aseptic technique. However, erythroid, myeloid and NK cell differentiation is normal (reviewed in Ansell & Bancroft, 1989).

In maturing lymphocytes of SCID mice, appropriate V(D)J BCR and TCR coding sequences are not joined together properly such that a non-productive antigen-receptor gene rearrangement leads to abortive lymphocyte differentiation and deletion of B and T cell clones. However, this recombinase defect is not complete and around 2-23% of 3-9 months' old ('leaky') SCID mice develop a small number of functional B and T cells with a few B cell clones secreting Ig (Bosma *et al,* 1988). Although spontaneous thymic T cell lymphomas develop in up to 15% of SCID mice (Custer *et al,* 1985), spontaneous B cell tumours have not been described.

5.4.2 Xenoreactivity

Tary-Lehmann *et al* (1994) demonstrated in a study on the human T cell repertoire in PBL-injected SCID mice that the mouse-derived human cells were in a state of anergy when harvested from mice after 30-90 days' *in vivo* growth. Cell lines established from these T cells regained their antigen-responsiveness after *in vitro* culture, and the CD4+ve T cell subset displayed reactivity only against murine MHC2 antigens. Thus, the results suggested that only xenoreactive human T cell clones survive long-term *in vivo*. Based on their observations, Tary-Lehmann *et al* (1995) proposed that GVH reactivity determined long-term human T cell survival in SCID mice. However, the impact of GVH reactivity on human PBL engraftment *in vivo* varies between different laboratories and depends, for example, on numbers of transferred cells and the health status of the SCID mouse colony (Dick, 1994; Huppes *et al,* 1994). Thus, different investigators report subclinical to lethal GVH reaction (Mosier, 1991; Murphy *et al,* 1992; Hoffmann-Fezer *et al,* 1993). Current thinking is that a GVH reaction occurs during xenograftment of SCID mice but that it is generally asymptomatic (Murphy *et al,* 1996).

5.4.3 Modelling PTLD

Studies on EBV tumorigenesis in SCID mice have generally employed 3 methods of xenograft implantation: **(1)** ip inoculation of EBV+ve human PBLs ('hu-PBL-SCID' model; reviewed in Bankert *et al,* 2001); **(2)** inoculation/implantation of patient tumour biopsy material (for example, ip implantation of PTLD biopsy material: 'hu-Bx-SCID' model); and **(3)** inoculation of human tumour cell lines [for example, subcutaneous (sc) or ip inoculation of BLCLs: 'hu-BLCL-SCID' model].

Hu-PBL-SCID Mouse Model

As part of efforts to establish a small animal model for research on human immunodeficiency virus (HIV), Mosier *et al* reported in 1988 the engraftment of human leukocytes in SCID mice that had been inoculated ip with human PBLs (hu-PBL-SCID). Transfer of PBL resulted in a functional human immune system (as evidenced by tetanus toxoid-specific human antibody responses following immunization) in mice whose peripheral blood and lymphoid tissues were populated with human leukocytes long-term. Thus, the animals were 'humanized' in terms of their immune system. Furthermore, the group described outgrowth of EBV+ve human B cell lymphomas in their hu-PBL-SCID mice. Specifically, PBLs from 80% of their EBV-seropositive donors gave rise to ip tumours when each animal was inoculated with $\geq 5x10^7$ leukocytes although subsequent studies showed seropositive donors to differ markedly in their cells' ability to give rise to ip tumours *in vivo* (Picchio *et al,* 1992). Thus, our laboratory has observed that PBLs from 64% of an EBV-seropositive donor panel gave rise to EBV+ve B cell lymphomas in the hu-PBL-SCID mouse model with a median tumour incidence of 67% (Johannessen *et al,* 2000). Tumours developed after a median time of 62 days (range: 33-102 days). The panel varied in the ability of PBLs to cause tumours in SCID mice although leukocytes from each donor gave reproducible results. Based on the results, our donor panel could be classified according to tumour incidence in SCID mice into **(1)** 'high' (71-100% of mice), **(2)** 'intermediate' (31-70%), **(3)** 'low' (1-30%), and **(4)** 'no' (0%) incidence donors (Picchio *et al.,* 1992; Johannessen *et al.,* 2000). Such classification reflects some as yet unclear qualitative differences between healthy virus carriers in terms of the ability of their EBV+ve B cells to give rise to PTLD-like tumours *in vivo*. Around 25% of the donor panel were high and no incidence donors each whereas approximately 50% of the panel were intermediate/low incidence donors.

Transfer of human PBLs ip into SCID mice triggers influx of murine neutrophils into the peritoneal cavity with concomitant production of the murine cytokines IL4, 6, 10, 12 and IFNγ (Santini *et al,* 1995). Of these growth factors, only murine IL12 has an effect on human cells and, thus, the influence of these factors on tumour development *in*

vivo must be limited. Murine IL12 is produced by peritoneal macrophages and promotes differentiation of human and murine Th1 cells and production of IFNγ. This may explain preferential survival of human Th1 cells *in vivo* (Tripp *et al,* 1993; Amadori *et al,* 1996) which may influence any observed cytokine interactions in SCID mice. Thus, conclusions based on the relative importance of a Th1 *versus* Th2 cytokine expression profile may need to be transferred with caution from the hu-PBL-SCID model to the human setting.

The experimental design for the hu-PBL-SCID mouse model has not yet been standardized between laboratories which makes study comparisons difficult because of variables such as cell numbers injected and qualitative differences between PBL donors. Equally, pre-conditioning of mice to facilitate engraftment of transferred PBLs (defined as total human Ig >1μg/mL of murine serum; Hesselton *et al,* 1993) can be employed using methods such as depletion of murine NK cells with rabbit anti-murine asialo GM1 (ASGM1) antiserum and/or x-irradiation of mice. Again, there is no consensus agreement as to the use of such techniques and they have produced variable results. An alternative to SCID mice are non-obese diabetic (NOD)/SCID mice that are also deficient in endogenous NK cell activity (Shultz *et al,* 1995), and the animals have been used for modelling PTLD *in vivo*. In contrast to hu-PBL-SCID mice, hu-PBL-NOD/SCID animals are resistant to ip outgrowth of human PTLD-like tumours unless CD8+ve T cells are depleted *in vivo* using anti-human CD8 mab (Wagar *et al,* 2000) which is a situation reminiscent of the organ transplant recipient. Transfer of autologous CD8+ve T cells into such CD8-depleted animals restores resistance to ip tumour development. In the hu-PBL-NOD/SCID model, long-term systemic human B cell, T cell, monocyte and DC homeostasis is achieved *in vivo* following transfer of human **b**one marrow CD34+ve progenitor cells into pre-conditioned (sublethally γ-irradiated) animals implanted previously with autologous human fetal **l**iver and **t**hymic tissues ('BLT mice'; Melkus *et al,* 2006). Furthermore, the human T cells can mount an MHC-restricted immune response to EBV *in vivo* following virus challenge as manifest by **(1)** expansion of CD45RA-ve, CD27+ve memory T cells *in vivo*, and **(2)** T cell IFNγ production *in vitro* in the presence of autologous BLCLs.

EBV+ve B cell tumours that arise in the hu-PBL-SCID model are immunoblastic lesions that express B cell activation markers and CAMs akin to that observed in BLCLs and PTLD (Rowe *et al,* 1991). In contrast to PTLD, however, established lesions show a paucity of human T cells. Tumours present as solitary or multifocal masses (or as leukaemic-type infiltrates) in lymphoid tissue of the murine hepatic porta and within liver parenchyma or, less frequently, in lung, mesentery, spleen or thymus. Similar to PTLD, EBV DNA is detected in tumour cells which express all (unrestricted) virus latent genes with a small number of cells expressing lytic viral proteins. The lesions, which have a normal karyotype, are mono-, oligo- or polyclonal, and Ig clonally distinct tumours can arise in mice harbouring multifocal masses.

Analysis of EBV clonality has demonstrated that PBLs from high incidence donors give rise to tumours containing multiple viral episomes, linear DNA, and immortalizing virus reflecting lytic infection *in vivo* (Picchio *et al,* 1992). Conversely, lesions from intermediate-low incidence donors (and BLCL) often contain clonal EBV, and linear DNA is infrequently found. In 1995, Rochford and Mosier further highlighted qualitative differences in tumours in hu-PBL-SCID mice. In their studies, lesions were found to consist of two B cell subsets: intermediate levels of the B cell activation marker CD23 and the plasma B cell marker CD38 on one B cell subset correlated with latent viral gene expression, whereas lytic cycle and infectious virus was found in B cell populations expressing low levels of CD23 and high levels of CD38. Based on their results, the group proposed a step-wise model of lymphomagenesis in hu-PBL-SCID mice that entailed **(1)** proliferation of latently infected B cell blasts, **(2)** their differentiation into plasma cells concomitant with lytic EBV infection, and **(3)** virus infection and recruitment of uninfected B cells leading to tumour outgrowth.

Somewhat in contrast to the above 3-step model, a study of 10 EBV-seropositive (4 high, 4 intermediate, 1 low and 1 no incidence) healthy blood donors from our laboratory aimed at addressing qualitative differences in their EBV infection failed to demonstrate a correlation between tumour formation in SCID mice and **(1)** spontaneous *in vitro* outgrowth of BLCLs from PBLs, **(2)** PBL EBV DNA VL by PCR detection, and **(3)** *in vitro* regression assay as a measure of host CTL immunity to EBV (Johannessen *et*

al, 1998). Since each assay tested gave consistent results, the study suggested that each assay measures a different aspect of EBV infection of B cells. This may reflect heterogeneity of circulating EBV-infected B cells, or different behaviour of such cells under different experimental conditions. Our results suggest, therefore, that tumour formation in the hu-PBL-SCID mouse is not a direct function of direct B cell outgrowth, EBV VL, or CTL activity. However, an interplay of all these factors may be instrumental in tumour development *in vivo.* In light of the results, it was important to delineate which factors are required for tumour formation *in vivo.*

Cell Populations Required For PTLD Development

Tumour incidence in the hu-PBL-SCID mouse model is significantly reduced when B cells are inoculated without T cells. Thus, Veronese *et al* showed in 1992 that EBV+ve B cells from seropositive PBL donors do not give rise to ip tumours in SCID mice unless CD4+ve or CD8+ve T cells are transferred together with B cells. Studies from our laboratory confirm the requirement for T cells in the inoculum for tumour development. Our results showed that tumour incidence was dramatically reduced from 76% to only 7% (representing only 1 tumour) when CD4+ve T helper cells were removed from the inoculum (Johannessen *et al,* 2000). Furthermore, removal of CD8+ve cytotoxic, CD30+ve activated, CD45RA+ve naïve, or CD45RO+ve memory T cells resulted in less, but significant reduction of tumour incidence. The results of the CD45RA- and CD45RO-depletion experiments probably reflect a reduction in numbers of inoculated CD4+ve and CD8+ve T cell subsets since CD45RA or CD45RO antigens are expressed on both T cell subsets. Our data contrast with those of Veronese *et al* (1992) who found only minor (not significant) changes in tumour incidence in hu-PBL-SCID mice inoculated with B cells together with either CD4- or CD8-depleted leukocytes when compared with PBL-injected animals.

In light of the above results, we concluded that T cell-B cell contact and/or soluble T cell growth factors promote *in vivo* B cell proliferation and tumorigenesis. Furthermore, when we treated T cells *in vitro* with the mitogen phytohaemagglutinin

(PHA) prior to transfer ip into SCID mice, PBLs from high/intermediate donors gave rise to ip tumours more rapidly *in vivo* whereas cells from low/no incidence donors were not affected (Johannessen *et al,* 2000). The results suggest that T cells from the 2 donor groups differ qualitatively in their ability to provide EBV+ve B cells with either necessary soluble growth factors or growth-promoting signals through cell-to-cell contact necessary for tumour formation in hu-PBL-SCID mice. Support for this conclusion comes from a study by Coppola *et al* (1998) who noted that PBL from atopic individuals are less likely to give rise to ip tumours in SCID mice than healthy controls. The group suggested that qualitative differences in Th1/Th2 cell subset profiles contributed to the observed inter-donor variability in tumour development *in vivo.* Further studies on such qualitative differences between T cell subsets have focused on the role of growth factors (cytokines) in tumour formation in the hu-PBL-SCID model since antibody-stimulation of the B cell CD40 costimulatory molecule (mediated via cell-to-cell contact) inhibits rather than promotes tumour development *in vivo* (Funakoshi *et al,* 1997).

Human Cytokines And The SCID Mouse

Based on results from our laboratory, we have proposed that EBV+ve B cells require T cell help in the form of soluble growth factors at an initial stage of lymphomagenesis in the hu-PBL-SCID model. Such a hypothesis explains the need for T cell subsets to be included together with EBV+ve B cells in the inoculum at the time of mouse injection. We also postulate that malignant B cells acquire the ability to produce necessary growth factors in an autocrine manner as part of the malignant process. Therefore, established tumours become independent of T cell help *in vivo* which could explain why T cells are conspicuously absent from such lesions. To test our hypothesis, we have analyzed (by RT-PCR) the human cytokine expression profile of human PBL-derived tumours obtained in the hu-PBL-SCID model. All tumours examined were found to express human IL10 and IFNγ, and the majority also expressed IL2, 4 and 6. IL5, a B cell and eosinophil growth factor, was not detected in any tumour

tested. The observed cytokine profile is similar to that seen in activated T cells (and BLCLs), and all of these cytokines can stimulate growth and/or differentiation of B cells. Furthermore, *in situ* hybridisation studies using EBER and cytokine probes on serial tumour sections have confirmed the RT-PCR results. However, in preliminary experiments in our laboratory in which either human IL4 or IFNγ were neutralized *in vivo* in hu-PBL-SCID mice using sc transferred x-irradiated hybridoma cells producing mabs to these cytokines, we did not observe a significant difference in tumour outgrowth between test and control mice. These results suggest that neither IL4 nor IFNγ on their own are essential in tumour formation *in vivo* thus highlighting overlap in function between different cytokines.

The above results suggest that in hu-PBL-SCID mice, malignant cells supply themselves with B cell growth factors in an autocrine-stimulated fashion suggesting a direct role for the tumour cells in their own cytokine production. IL6 and IL10 are both found in serum from tumour-bearing hu-PBL-SCID mice (Veronesi *et al*, 1994; Baiocchi *et al,* 1995), and IL6 confers a malignant phenotype on BLCL in T cell-deficient athymic (nude) mice (Scala *et al,* 1990). However, inhibiting IL6 *in vivo* with a view to hinder tumour development has given inconclusive results. LMP1 induces human IL10, and this cytokine is found at high levels in serum from tumour-bearing SCID mice (Nakagomi *et al,* 1994; Baiocchi *et al,* 1995). Therefore, a direct role for EBV in induction and maintenance of autocrine growth factor production *in vivo* is likely.

Hu-PBL-SCID Mouse: Model Of PTLD Formation

Based on our results obtained in the hu-PBL-SCID mouse model, we have suggested a 2-step model of PTLD formation *in vivo* (Johannessen *et al,* 2000). In our model, **(1)** initial outgrowth of EBV+ve tumorigenic B cells is promoted by T cells, and **(2)** the malignant B cells become independent of T cell help as the tumour cells establish an autocrine, cytokine-mediated stimulatory loop that maintains tumour growth *in vivo*. This model is supported by the findings that **(a)** tumour formation *in vivo* is dependent

on T cell subset-derived help as shown by cell depletion experiments; **(b)** T cells are scant in established lesions as demonstrated by immunostaining analysis; **(c)** tumours portray a cytokine gene expression profile (as shown by RT-PCR studies) that includes B cell growth factors; **(d)** the B cell growth factors are expressed by the malignant cells themselves as demonstrated by *in situ* hybridisation analysis. In line with this model are studies on primary PTLD biopsy material. Thus, Thomas *et al* (1990) and Perera *et al* (1998) have shown that PTLD tumours arising in organ transplant recipients often contain a large non-malignant component that consists mainly of CD4+ve T cells. Such CD4+ve T helper cells may supply the malignant cells with necessary growth factors and act as a 'feeder' population. Further studies in our laboratory have shown that patient-derived PTLD biopsy material rich in non-neoplastic CD4+ve helper, CD45RO+ve memory T cells give rise to biopsy-derived tumours in the SCID mouse model (hu-Bx-SCID; Perera *et al,* 1996). In line with the hu-PBL-SCID model, the biopsy-derived SCID tumours contain few T cells. Recently, we have also demonstrated (by RT-PCR analysis) human IL2, 6, 10 and IFNγ transcripts in the patient-derived PTLD biopsy material and the biopsy-derived SCID tumours (see section 1 in Results; Johannessen *et al,* 2002). Taken together, our studies in the hu-Bx-SCID mouse model are in line with our results obtained in the hu-PBL-SCID mouse model and suggest that the hu-PBL-SCID model reflects PTLD pathogenesis in the organ transplant recipient. Our proposed model of tumour formation in the hu-PBL-SCID mouse is shown in Figure 2 (Johannessen *et al,* 2000).

In line with the above model are studies by Baiocchi *et al* (1995) who detected human IL10 and its receptor in tumours from hu-PBL-SCID mice and demonstrated that human IL6 or 10 maintain fresh SCID tumour material *in vitro*. The group suggested that human IL6 and 10 may play roles in an autocrine stimulatory loop promoting tumour outgrowth in the animals.

FIGURE 2
A Model Of Tumour Development In The Hu-PBL-SCID Mouse

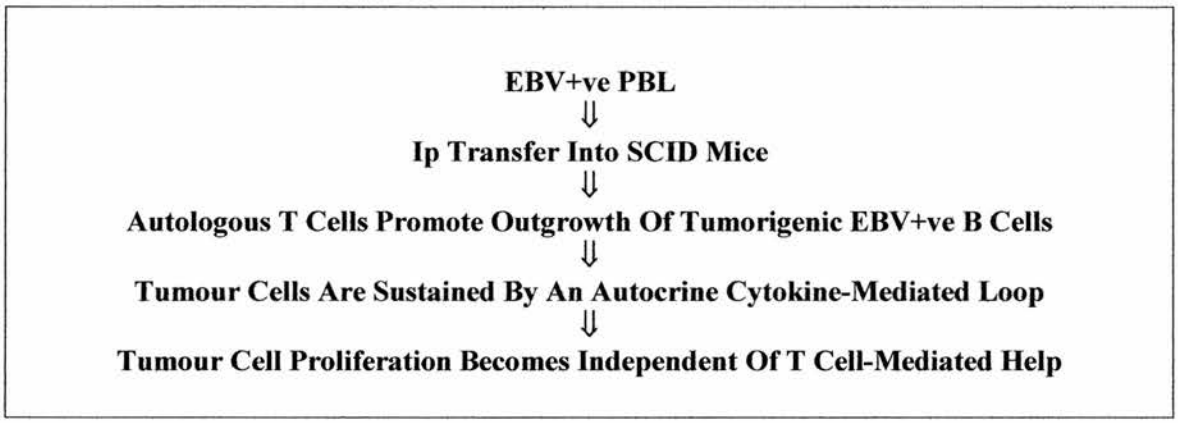

Additionally, reduction in tumour incidence has been observed in hu-PBL-SCID mice following administration of a neutralizing antibody against IL6 (Mauray *et al,* 2000), and clinical studies by Haddad *et al* (2001) have demonstrated a therapeutic effect of using neutralizing anti-IL6 antibodies in PTLD patients refractory to reduction in immunosuppression (see section 3.5.3 above). Further support comes from analysis of EBV+ve acquired immunodeficiency syndrome (AIDS)-related BLPD (ARL) showing that IL6 is expressed by ARL-derived reactive lymphocytes, and from studies of PTLD demonstrating that circulating IL6 is found at high levels in solid organ graft recipients with EBV+ve PTLD (Emilie *et al,* 1992a; Tosato *et al,* 1993). Equally, IL10 is expressed in EBV+ve ARL and high circulating IL10 levels are found in ARL patients (Emilie *et al,* 1992b). PBL from renal allograft recipients suffering acute rejection express high levels of numerous cytokines (for example, IL4, 10, IFNγ) which decline following treatment with the murine anti-human CD3 mab OKT3 (Platzer *et al,* 1994) leading to sequestration of antibody-coated T lymphocytes in liver and spleen.

In addition to the importance of T cell subsets in tumour development *in vivo,* recent studies have highlighted the role played by plasmacytoid dendritic cells (PDCs). Thus, Lim *et al* (2007) have shown that EBV+ve PBLs depleted of PDC develop tumours more rapidly in NOD/SCID mice than PBL-injected control mice. Thus, EBV-activated PDC produced IFNα and stimulated NK cells and IFNγ-producing CD3+ve T

cells. PDC-stimulation of CD3+ve T cells was mediated by cell-to-cell contact, partly through toll-like receptor (TLR)-9 signalling.

Cytokine gene polymorphism and individual differences in cytokine production can influence susceptibility to certain human diseases such as cerebral malaria (McGuire *et al,* 1994). Therefore, it is conceivable that inter-donor variability in tumour development observed in the hu-PBL-SCID model may relate to cytokine gene polymorphism involving any of the B cell growth factors expressed by the malignant cells (for example, IL4, 6, 10, or IFNγ). Based on their results, Helminen *et al* (1999, 2001) suggested that IL10 gene promoter polymorphism correlates with susceptibility to primary EBV infection, and that low IL10 production resulting from such mechanisms renders individuals more susceptible to primary EBV infection. Therefore, IL10 gene polymorphism could perhaps increase PTLD risk in seronegative organ graft recipients by increasing their risk of primary EBV infection post-transplant. Recent studies by Lee *et al* (2006) show that using genotyping to detect the adenosine/adenosine (A/A) IFNγ cytokine gene polymorphism at base +874 added predictive value to EBV VL PCR measurements in paediatric liver transplant recipients. Thus, cytokine genotyping (together with EBV VL) was helpful in identifying organ transplant patients at high risk of PTLD. These results are supported by studies in the SCID mouse demonstrating that the IFNγ A/A genotype correlates significantly with rapid and consistent tumour formation in the hu-PBL-SCID model (Dierksheide *et al,* 2005). Neutralization of transforming growth factor (TGF)β in mice injected with IFNγ A/A PBLs led to expansion of CD8+ve T cells *in vivo* and reduced tumour development suggesting that TGFβ promotes tumour outgrowth by inhibiting CTL activation in hu-PBL-SCID mice.

Novel PTLD Therapy: Hu-BLCL-SCID Mouse Model

In 1987, Reddy *et al* described the successful implantation of a human lung tumour-derived cell line in SCID mice. Since this first report of successful establishment of a human tumour in the animals, around 4,000 papers have appeared to date in the scientific literature citing their use for studies of human tumorigenesis.

SCID mice inoculated ip with PBLs from EBV-seronegative healthy donors followed by inoculation of concentrated virus preparations experience EBV infection of the transferred B cells *in vivo* and development of PTLD-like lesions (Cannon *et al*, 1990; Boyle *et al,* 1992). Therefore, it is possible to mimic EBV infection in a seronegative organ transplant recipient using a SCID mouse that has been humanized with seronegative PBL. Such modelling can be used to test the efficacy of novel measures aimed at preventing EBV infection using tumour formation as an experimental read-out.

SCID mice inoculated sc or ip with BLCL (hu-BLCL-SCID) regularly give rise to PTLD-like tumours (Rowe *et al,* 1991; Boyle *et al,* 1992). In sc-injected animals, the tumours can be visualized under the skin and directly measured. Thus, the sc hu-BLCL-SCID mouse can be used as a preclinical tool to assess novel PTLD therapy *in vivo* prior to introduction into the clinical (patient) setting. Recording changes in tumour mass over time, the effect of treatment can be assessed by serial tumour sampling and analysis of tumour material by such techniques as PCR, microarrays, immunostaining and flow cytometry.

When the hu-BLCL-SCID model has been used to address the effect of antiviral therapy on PTLD, ACV has not shown an inhibitory effect on tumour formation *in vivo* whereas GCV has been found to be effective in SCID mice (Boyle *et al,* 1992; Unpublished observations from our laboratory). Additionally, studies of adoptive CTL immunotherapy in hu-BLCL-SCID mice have provided data which support the use of EBV-specific CTL against PTLD (see section 3 in Results).

An alternative therapeutic strategy entails the use of suicide genes in EBV+ve malignant cells that renders them susceptible to pro-drug killing. In a study in 1996, Franken *et al* inoculated SCID mice with BLCL that had been transfected with a construct that included a thymidine kinase (TK) suicide gene under the control of an EBNA2-responsive promoter. In the presence of EBNA2, activation of the promoter led to TK production. In the animals, development of EBV+ve tumours resulted in EBNA2 expression and, therefore, production of TK by the tumour cells. When the animals were treated with GCV, TK-mediated phosphorylation of the pro-drug led to formation of the

active anti-viral drug and complete tumour regression. Further studies by Rogers *et al* (1996) have shown similar results when transfecting EBV+ve tumour cells with the enzyme cytosine deaminase (CyD). CyD converts the pro-drug 5-fluorocytosine (5-FC) into its active form, 5-fluorouracil. Following administration of 5-FC, CyD-transfected SCID mouse tumors regressed as a result of formation of the active anti-tumour compound.

The effectiveness of rituximab and *bcl*-2 has been studied in the hu-BLCL-SCID model. Thus, Guinness *et al* (2000) and Loomis *et al* (2003) demonstrated that combining a *bcl*-2 antisense oligonucleotide with rituximab *in vivo* was curative in 11 out of 14 (79%) tumour-bearing animals treated whereas 14 out of 14 (100%) control mice died of LPD. *Bcl*-2 or rituximab monotherapy did not achieve the therapeutic effect of combination treatment since initial monotherapy-induced delay in tumour outgrowth *in vivo* was followed by subsequent neoplastic disease. Thus, a *bcl*-2 antisense oligonucleotide potentiated the antitumor effect of rituximab suggesting that *bcl*-2 antisense oligonucleotide therapy in combination with rituximab may represent a non-toxic and effective (targeted) therapy for PTLD.

AIM

The aim of this study was to set up an established *in vivo* model of Epstein-Barr virus (EBV)-associated post-transplant lymphoproliferative disease (PTLD) in which to investigate adoptive immunotherapy for PTLD.

MATERIALS AND METHODS

1. Abbreviations And Symbols

A	Amp
ACIF	Anti-complement immunofluorescence
ACPL	Anti-complement peroxidase labelling
AP	Alkaline phosphatase
APAAP	Alkaline phosphatase anti-alkaline phosphatase
BPB	Bromophenol blue
Bq	Becquerel
BSA	Bovine serum albumin
$CaCl_2$	Calcium chloride
cDNA	Complementary DNA
CFB	Complement fixation buffer
CH_3COONa	Sodium acetate
Ci	Curie
CM	Culture medium
CO_2	Carbon dioxide
cpm	Counts per minute
Cy-A	Cyclosporin-A
DAB	Diaminobenzidine
dATP	Deoxyadenosine 5'-triphosphate
dCTP	Deoxycytidine 5'-triphosphate
DEPC	Diethylpyrocarbonate
DF	Decay factor
dGTP	Deoxyguanosine 5'-triphosphate
dH_2O	Distilled water
DMF	Dimethylformamide
DMSO	Dimethylsulphoxide
dNTPs	Deoxynucleotide 5'-triphosphates
DPX	Dibutyl-polystyrene xylene
DTT	Dithiothreitol
dTTP	Deoxythymidine 5'-triphosphate
ECACC	European Collection of Animal Cell Cultures
EDTA	Ethylene diamine-tetraacetic acid
ELISA	Enzyme-linked immunoabsorbent assay
EtBr	Ethidium bromide
FACS	Fluorescent activated cell scanning
FCS	Foetal calf serum
FITC	Fluorescein isothiocyanate
FM	Freezing medium
g	G-number/gram

HCl	Hydrochloric acid
HEPES	N-2-Hydroxyethylpiperazine-N'-2-ethanesulfonic acid
IIF	Indirect immunofluorescence
K	Kilo (10^3)
KCl	Potassium chloride
KH_2PO_4	Potassium dihydrogen orthophosphate
L	Liter
LCMV	Laboratory for Clinical & Molecular Virology
LSHTM	London School of Hygiene & Tropical Medicine
μ	Micro (10^{-6})
m	Milli (10^{-3})/meter
M	Molar (moles per liter)/Mega (10^6)
$MgCl_2$	Magnesium chloride
MMLV-RT	Moloney Murine Leukemia Virus reverse transcriptase
MRI	Magnetic resonance imaging
mRNA	Messenger RNA
n	Nano (10^{-9})
Na_2HPO_4	Disodium hydrogen orthophosphate
NaCl	Sodium chloride
$NaHCO_3$	Sodium bicarbonate
NaOH	Sodium hydroxide
NBF	Neutral buffered formalin
NHS	Normal human serum
NRS	Normal rabbit serum
OCT	Optimum tissue cutting
OD	Optical density
OPD	o-Phenylenediamine dihydrochloride
p	Pico (10^{-12})
PAP	Peroxidase anti-Peroxidase
PBS	Phosphate buffered saline
PE	Phycoerythrin
PHA	Phytohaemagglutinin
PRK	Proteinase K
PVP	Polyvinylpyrrolidine
Px	Peroxidase
RNase	Ribonuclease
rpm	Revolutions per minute
RPMI	Roswell Park Memorial Institute
SDS	Sodium dodecyl sulphate
SDW	Sterile distilled water
SSC	Standard saline citrate
TBS	Tris buffered saline
TC	Tissue culture
TE	Tris/EDTA
Tris	Tris(hydroxymethyl)aminomethane

TRITC	Tetramethylrhodamine isothiocyanate
Tween20	Polyoxethylene(20)-sorbitan monolaurate
v/v	Volume per volume
WM	Wash medium
w/v	Weight per volume

2. Suppliers

Anachem, Luton, Bedforshire, UK
Applied Biosystems, Warrington, Cheshire, UK
Arnold R Horwell, London, UK
Atta, Genetic Research Instrumentation, Dunmow, Essex, UK
Barloworld Scientific Ltd, Stone, Staffordshire, UK
BD PharMingen, Oxford, Oxfordshire, UK
Beckman Coulter, High Wycombe, Buckinghamshire, UK
Beckton-Dickinson (UK) Ltd, Oxford, Oxfordshire UK
Biometra GmbH, Goettingen, Germany
Bio-Rad Laboratories Ltd, Hemel Hempstead, Hertfordshire, UK
BOC Cryospeed, Manchester, UK
Caltag Medsystems Ltd, Towcester, Northamptonshire, UK
Capell (Precision Medical Ltd), Pickering, Yorkshire, UK
Cinna/Tel-Test Inc, Friendswood, Texas, USA
Clay Adams, Parsippany, New Jersey, USA
Clontech Laboratories Inc, Saint-Germain-en-Laye, France
Cryotechnics, Edinburgh, UK
Cymbus Bioscience, Southampton, Hampshire, UK
DakoCytomation Ltd, High Wycombe, Buckinghamshire, UK
Denley Instruments, Billinghurst, Sussex, UK
Distillers MG, Reigate, Surrey, UK
ECACC, Salisbury, Wiltshire, UK
Electrolux Domestic Appliances, Luton, Bedfordshire, UK
Eppendorf, Hamburg, Germany
Eurogentec Ltd, Southampton, Hampshire, UK
Fisher Scientific UK Ltd, Loughborough, Leicestershire, UK
Flowgen, Lichfield, Staffordshire, UK
Flow-ICN (UK), Thame, Oxfordshire, UK
FMC BioProducts, Rockland, Maine, USA
Fuji Photo Film Company, Omoya, Japan
GE Healthcare, Chalfont St Giles, Buckinghamshire, UK
Genetic Research Instrumentation, Dunmow, Essex, UK
Grant Instruments, Cambridge, Cambridgeshire, UK
GraphPad Software, Inc., San Diego, CA, USA
Greiner Bio-One Inc, Stonehouse, Gloucestershire, UK

Hanna Instruments Ltd, Leighton Buzzard, Bedfordshire, UK
Harlan Sera-Lab, Loughborough, Leicestershire, UK
Heraeus, Brentwood, Essex, UK
Hybaid Ltd, Teddington, Middlesex, UK
IBI/Eastman Kodak Company, New Haven, Connecticut, USA
International Equipment Company, Damon, Dunstable, Bedfordshire, UK
Invitrogen, Paisley, Renfrewshire, UK
ISP Europe, Tadworth, Surrey, UK
Jencons, Leighton Buzzard, Bedfordshire, UK
Johnson & Johnson Medical Inc, Arlington, Texas, USA
Jouan, Tring, Hertfordshire, UK
Leitz, Wild Leitz UK Ltd, Knowlhill, Milton Keynes, Buckinghamshire, UK
Macarthy Medical, Romford, Essex, UK
MDS Nordion, Ottawa, Ontario, Canada
Medical Air Technology Ltd, Oldham, Lancashire, UK
Millipore (UK) Ltd, Croxley Green, Hampshire, UK
Miltenyi Biotec Ltd, Bisley, Surrey, UK
Mini-Instruments Ltd, Burnham on Crouch, Essex, UK
MP Biomedicals, LLC, London, UK
Nordic Immunological Laboratories, Maidenhead, Berkshire, UK
Nordion International Inc, Ontario, Canada
Novartis Ltd, Oxford, Oxfordshire, UK
Nunc, Nalge (Europe) Ltd, Hereford, Herefordshire, UK
Ohaus Europe, Cambridge, Cambridgeshire, UK
Olympus, Gallenkamp, London, UK
Oxoid Limited, Basingstoke, Hampshire, UK
Painse and Byrne, Greenford, Middlesex, UK
Patterson Scientific, Dunstable, Bedfordshire, UK
Perkin Elmer Life Sciences, Beaconsfield, Buckinghamshire, UK
Photosol, Basildon, Essex, UK
Polybags Ltd, Lyon Way, Greenford, Middlesex, UK
Promega UK, Southampton, UK
Qiagen Ltd, Crawley, Sussex, UK
RA Lamb, London, UK
R&D Systems, Abingdon, Berkshire, UK
Roche Diagnostics Ltd, Lewes, Sussex, UK
Sandoz Ltd, Bordon, Hampshire, UK
Sanyo Gallenkamp (MSE), Loughborough, Leicestershire, UK
Sarstedt Ltd, Beaumont Leys, Leicester, UK
Scientific Industries, Bohemia, New York, USA
Scientific Laboratory Supplies (SLS), Nottingham, UK
Scottish National Blood Transfusion Centre, Edinburgh, UK
Sera Lab, Crawley Down, Sussex, UK
Serotec Ltd, Kidlington, Oxford, UK
Sharp Corporation, Abeno-Ku, Osaka, Japan

Sigma-Aldrich Ltd, Gillingham, Dorset, UK
Sigma-Genosys Ltd, Haverhill, Suffolk, UK
Skatron, Newmarket, Suffolk, UK
Starlab (UK) Ltd, Milton Keynes, Buckinghamshire, UK
StemCell Technologies, Vancouver, British Columbia, Canada
Stratagene, La Jolla, California, USA
Stuart Scientific, Barloworld Scientific Ltd, Stone, Staffordshire, UK
Thermo, Basingstoke, Hampshire, UK
Tissue Culture Services, Claydon, Buckinghamshire, UK
Ultra-Violet Products Ltd, Cambridge, Cambridgeshire, UK
Varian Ltd, Oxford, Oxfordshire, UK
Vision BioSystems (Europe) Ltd, Newcastle Upon Tyne, UK
VWR International Ltd, Poole, Dorset, UK
Wako Chemicals GmbH, Neuss, Germany
Whatman, Maidstone, Kent, UK

3. Reagents

All cell culture reagents were supplied by Invitrogen and Harlan Sera-Lab unless otherwise stated. General chemical reagents, other than those listed below, were supplied by Sigma. Tissue culture (TC) flasks, 48- and 96-well plates as well as cryovials were supplied by Nunc. All other plasticware was supplied by Barloworld Scientific, Greiner Bio-One, SLS, or Thermo.

Reagent	**Supplier**
1Kbp DNA ladder	Invitrogen
^{32}P-α-dCTP	GE Healthcare
^{32}P-γ-dATP	GE Healthcare
BPB	Sigma
BSA	Sigma
^{51}Chromium	GE Healthcare
Cy-A	Sandoz Products
DAB	Sigma
DEPC	Sigma
DMF	Sigma
DNA Polymerization Mix	GE Healthcare
DPX	R.A. Lamb
EasySep® kits	StemCell Technologies
Ethidium bromide	Invitrogen

Evans Blue	Sigma
Fast Red	Sigma
FCS	Harlan Sera-Lab
Ficoll-Hypaque	Sigma
Ficoll™ 400	GE Healthcare
Formamide	Invitrogen
ϕX174 DNA/*Hae* III markers	Promega
ϕX174 DNA/*Hinf* I dephosphorylated markers	Promega
Glycerol	Sigma
Histopaque®	Sigma
Injectable alcohol	Macarthy Medical
Levamisole	Sigma
Mayer's haemalum	Sigma
Mineral oil	Sigma
Mixed bed resin	Sigma
Naphthol ASBI phosphonic acid	Sigma
New Fuchsin Substrate System	Dako
NICK™ column	GE Healthcare
NuSieve® 3:1 agarose	FMC BioProducts
Oligonucleotides	Eurogentec
Omniscan™ (Gadodiamide)	GE Healthcare
PHA	Sigma
Preservative free heparin	Painse and Byrne
Proteinase K	Promega
PVP	Sigma
RNAzol™ B	Cinna/Tel Test Inc.
RT-PCR Kit	Stratagene
Sheared salmon sperm DNA	5'→3' Inc.
Silane	Sigma
Sodium azide	Sigma
T4 Polynucleotide kinase	Promega
Taq DNA Polymerase	Promega
Triton® X-100	Sigma
Trypan Blue	Flow
Tween20	Sigma
Ultrapure dH_2O	Sigma
X Ray Developer	Photosol
X Ray Fixer	Photosol
[^{3}H]-Thymidine	GE Healthcare

4. Consumables

4.1 General Plasticware

Item	Supplier
LP3 tubes	VWR (Falcon)
Microfuge tubes (0.5/1.5 mL)	Sarstedt
Plastic bijoux (5 mL)	Barloworld Scientific

4.2 Tissue Culture Plasticware

Item	Supplier
Cell culture flasks (50mL)	BD (Falcon)
Cryotubes	Nunc
Filter units (0.45 μm, 0.60 μm)	Millipore
Micropipette tips	Starlab
Plastic universal tubes (25 mL)	Barloworld Scientific
Polypropylene conical centrifuge tubes (50 mL)	BD (Falcon)
12x75 mm round bottom tube	BD (Falcon)
Syringes 1-60 mLs	SLS
24 wells cell culture plates (15 mm)	BD (Falcon)
96 wells flat bottom microtitre plates	BD (Falcon)
96 wells round bottom microtitre plates	BD (Falcon)

4.3 Miscellaneous Consumables

Item	Supplier
Disposable gloves	VWR
Dry ice (solid CO_2)	BOC Cryospeed
Filter mats	Skatron
Hybond™ N+ nylon membrane	GE Healthcare
Hyper-MP™ film	GE Healthcare
Layflat tubing	Polybags
3MM chromatography paper	Whatman
Parafilm	SLS
Saran wrap	SLS

5. Equipment

Equipment	Model And Supplier
Bench top centrifuge	'CR4.11', Jouan 'IEC Centra-4X', International Equipment Company 'Omnifuge 2.0RS', Heraeus 'TJ-6', Beckman Coulter 'MSE Mistral 3000E', Sanyo 'MSE Mistral 3000i', Sanyo
Cell counter	'Laboratory counter', Clay Adams
^{137}Cesium source	'Gammacell 1000 Elite', Nordion
CO_2 incubator	'CO_2-Auto-Zero', Heraeus
Cytocentrifuge	Thermo
DNA thermal cyclers	'T3', Biometra 'Omnigene', Hybaid
Electrophoresis power pack	'2197', Pharmacia Biotech '500/200', Bio-Rad Laboratories '500/2.0', Bio-Rad Laboratories
Epifluorescent microscope	Leitz Diaplan
FACScanner	'FACSCalibur', BD
Film cassettes	Genetic Research Instrumentation
Film developer	Fuji Photo Film Company
Fridges and freezers	-70°C, Abbas Ultra 85 -20°C, Electrolux +4°C, Electrolux
γ-Irradiator	'Gammacell 3000 Elan' irradiator, MDS Nordion
Geiger counter	'Mini-Monitor 900 GM Type E', Mini-Instruments
Gel scanner	'JX300', Sharp
Haemocytometer	'New improved Neubauer', BDH
Harvester	Skatron
Horizontal gel tanks	Invitrogen
Hot plate	Bibby, J Science Products
Hydrophobic marker pen	Vector Laboratories
Inverted light microscope	'S2404S', Olympus
Light microscope	Leitz
Magnetic particle separator	Invitrogen, StemCell Technologies
Magnetic stirrers	VWR

Microbiological safety cabinet	'BioMAT Class II Safety Cabinet', Medical Air Technology
Microfuge	'MicroCentaur', MSE
Micropipettes	'Gilson', Anachem
Microwave	Sharp
MRI Scanner	'Varian 7T Scanner, Magnex 115/60 Gradient', Varian
pH meter	'Digital PW9', Integra Biosciences
Pipette holder	'Pipet-Boy', Integra Biosciences
Pipette pump	'R301', Arnold R Horwell
Plastic sealer	'Hulme Martin', Genetic Research Instrumentation
Rocker	'A600', Denley
Scales	'E1500D', Ohaus Europe
Scintillation β-counter	'LS6000IC', Beckman
Scintillation γ-counter	'1480 Wizard 3" Automatic Gamma Counter', Perkin Elmer
Spectrophotometer	'GeneQuant II', GE Healthcare
Test tube heater	'SHT 1D', Stuart Scientific
UV Stratalinker	'Stratalinker™ 2400', Stratagene
UV Transilluminator	UVP Inc
Vortex	'Vortex-Genie', Scientific Industries
Waterbaths	Grant Instruments

6. Materials/Solutions

6.1 Cell Culture

Culture Medium (CM)

L-glutamine	2 mM
Penicillin	100 IU/mL
Streptomycin	100 μg/mL
Fetal calf serum	10% (or 20%) v/v

Made up in 1xRPMI 1640.

Wash Medium (WM)

Penicillin	100 IU/mL
Streptomycin	100 μg/mL
Fetal calf serum	2% v/v
7.5% $NaHCO_3$	2.7% v/v
1M Hepes buffer	2% v/v
10xRPMI 1640	10% v/v

Made up in sterile dH_2O.

Freezing Medium (FM)

Fetal calf serum	90% v/v
DMSO	10% v/v

Phytohaemagglutinin (PHA) 500 μg/mL

Made up in PBS or culture medium.

[^{3}H]-Thymidine

[methyl-^{3}H]-Thymidine	1 mCi/mL (37 MBq/mL)

^{51}Chromium

$Na_2{}^{51}CrO_4$	1 mCi/mL (37 MBq/mL)

6.2 Magnetic Resonance Imaging (MRI)

Omniscan™ (Gadodiamide) 10 nM

6.3 Immunohistochemical Techniques

Neutral Buffered Formalin (NBF)

$NaH_2PO_4xH_2O$	0.4% w/v
Na_2HPO_4 (anhydrous)	0.7% w/v
40%w/v formaldehyde	10% v/v

Made up in dH_2O, pH7.2-7.4.

Dehydration/Rehydration of Tissue Sections

Ethanol	30% v/v
	70% v/v
	90% v/v
	95% v/v
	99% v/v
	100% v/v

Made up in dH_2O.

Phosphate Buffered Saline (PBS)

NaCl	0.8% w/v
KCl	0.02% w/v
Na_2HPO_4	0.02% w/v
KH_2PO_4	0.15% w/v

Diaminobenzidine (DAB) 1% v/v

Made up in dH_2O.

Complement Fixation Buffer (CFB)

Dulbecco's A:	NaCl	0.8% w/v
	KCl	0.03% w/v
	Na_2HPO_4	0.14% w/v
	KH_2PO_4	0.03% w/v

Made up in dH_20.

Dulbecco's B:	$CaCl_2x2H_2O$	0.53% w/v

Made up in dH_20.

Dulbecco's C:	$MgCl_2x6H_2O$	0.4% w/v

Made up in dH_20.

For CFB:	Dulbecco's B	2.5% v/v
	Dulbecco's C	2.5% v/v

Made up in Dulbecco's A.

1xTris Buffered Saline (TBS)

Tris-HCl, pH7.6	0.05 M
NaCl	0.15 M

Made up in dH_2O.

Veronal Acetate Buffer

$CH_3COONax3H_2O$	0.4% w/v
NaBarbitone	0.6% w/v
0.1M HCl	1% v/v

Made up in dH_2O, pH9.2.

Levamisole 1 mM
Made up in TBS.

DEPC Water
Diethylpyrocarbonate 0.5% v/v
Made up in ddH_2O and autoclaved overnight.

10xProteinase-K (PRK) Buffer
Tris-HCl, pH7.6 0.50 M
Made up in DEPC water.

20xTris Buffered Saline (TBS)
Tris-HCl, pH7.6 1.0 M
NaCl 3.0 M
Made up in DEPC water.

1%Triton® X-100
Triton® X-100 1% v/v
Made up in DEPC water.

Substrate Buffer
Tris-HCl, pH8.2 2.5 M
Made up in DEPC water.

Proteinase-K 3 mg/mL
(from the fungus *Tritirachium album*)

6.4 Reverse-Transcriptase Polymerase Chain Reaction (RT-PCR)

10xTris-Borate-EDTA (TBE) Buffer
Tris 10.8% w/v
Boric acid 5.5% w/v
0.5M EDTA, pH8 4% v/v
Made up in dH_2O.

Loading Buffer
Glycerol 49.9% v/v
10xTBE 49.9% v/v
BPB 0.2% w/v

Ethidium Bromide (EtBr)	1% w/v
Made up in dH_2O.	
Denaturing Solution	
NaCl	1.5 M
NaOH	0.5 M
Made up in dH_2O.	
Neutralizing Solution	
NaCl	1.5 M
Tris-HCl, pH7.2	0.5 M
EDTA, pH8	0.001 M
Made up in dH_2O.	
20xStandard saline citrate (SSC)	
NaCl	3 M
Na_3citrate	0.3 M
Made up in dH_2O.	
100xDenhardt's Solution	
BSA	2% w/v
Ficoll™	2% w/v
PVP	2% w/v
Made up in dH_2O.	
10% w/v Sodium Dodecyl Suphate (SDS)	
Made up in dH_2O.	
Formamide	
Deionised in 10%w/v Mixed-bed resin.	
Sheared Salmon Sperm DNA	
10 mg/mL	1% v/v
1xTris-EDTA (TE) Buffer	
Tris-HCl, pH8	10 mM
EDTA, pH8	1 mM
Made up in dH_2O.	
RNAzol™B	200 µL per 10^6 cells or 10 mg tissue
Minigel	
NuSieve® 3:1 agarose	1% w/v
Made up in 1xTBE buffer.	

cDNA Synthesis: 'RT-PCR Kit'

Random primers	0.1 mg/mL
First-strand buffer	10x
RNase block ribonuclease inhibitor	40 U/mL
100mM dNTPs	25 mM each
MMLV-RT	50 U/mL

Taq DNA Polymerase 5 U/mL
(from the *Thermus aquaticus* bacterium strain YT1)
Enzyme storage buffer A

Glycerol	50% v/v
Tris-HCl, pH8	50 mM
NaCl	100 mM
EDTA	0.1 mM
DTT	5 mM
Triton®X-100	1% v/v

10x Thermophilic buffer

KCl	500 mM
Tris-HCl, pH9	100 mM
Triton®X-100	1% v/v
$MgCl_2$	25 mM

DNA Polymerization Mix
dATP, dCTP, dGTP, dTTP 20 mM each
Made up in water, pH7.5

Gel Electrophoresis
NuSieve® 3:1 agarose 2.5% w/v
Made up in 1xTBE buffer.

Pre-Hybridization Solution

Formamide	50% v/v
20xSSC	25% v/v
50xDenhardt's solution	10% v/v
10%w/v SDS	5% w/v
Sheared Salmon Sperm DNA	1% v/v

Made up in dH_2O.

Hybridization Solution
Prehybridization solution with ^{32}P-labelled probe and fresh 1% v/v sheared salmon sperm DNA.

T4 Polynucleotide Kinase 5 U/mL
(from a recombinant *E. coli* bacterium strain)
10x Reaction buffer
Tris-HCl, pH7.6 700 mM
$MgCl_2$ 100 mM
DTT 50 mM

Membrane Wash Solution
2xSSC/0.1% w/v SDS
1xSSC/0.1% w/v SDS

DNA Size Markers:

1Kbp DNA ladder 200µg/mL
(in 10mM Tris-HCl, pH7.5, 50 mM NaCl, 0.1 mM EDTA)

ϕX174 DNA/*Hae* III markers 1.0mg/mL
(in 10 mM Tris-HCl, pH7.5, 1 mM EDTA)

ϕX174 DNA/*Hinf* I dephosphorylated markers 50µg/mL
(in 10 mM Tris-HCl, pH7.5, 1 mM EDTA)

7. Antibodies

The antibody and serum reagents used in this study are shown in Tables A1 to A3 in Appendix 1.

8. Cell And Tissue Samples

8.1 Organ Graft Recipients

Primary biopsy material obtained from PTLD arising in organ transplant recipients was transported promptly in sterile medium from UK organ transplant centres to our laboratory for diagnostic and research purposes. The biopsy material was divided upon arrival using aseptic technique, and a small piece was teased out into a single cell

suspension in WM. Once the cells had been washed in WM, they were counted and their viability was assessed. Tumour cells were then transferred in CM ip into SCID mice.

8.2 Healthy Blood Donors

Once an informed written consent was obtained, 50-100 mL of heparinized blood was collected from healthy staff in our laboratory. Furthermore, 'buffy coats' (blood bags containing PBLs in small volume of plasma) were obtained from the Scottish National Blood Transfusion Service in Edinburgh.

8.3 Serological Analysis

EBV serostatus was determined by analysis of anti-VCA IgG antibody titer using an indirect immunofluorescence method (Henle & Henle, 1966). Test slides were prepared using standard methods. Briefly, $5x10^4$ cells of the EBV genome-positive cell line P3HR1 (Hinuma *et al,* 1967), routinely grown in our laboratory, were washed in PBS and plated out into each of 12 wells on microscope slides. Once cells had dried onto the slides at room temperature, they were fixed in acetone for 5 minutes. The slides were then dried in air again at room temperature followed by storage at -20°C. For VCA testing, slides were thawed out from storage and test samples together with known VCA-positive (KAM) and EBV-negative (WDA) control sera applied to the fixed cells. Thus, 10 μL of test sera, diluted 1:5 and 1:10 in PBS, were added separately to designated slide wells, and the slides incubated at 37°C for 1 hour. Slides were washed in PBS at room temperature followed by the addition to each well of 10 μL of FITC-conjugated rabbit anti-human IgG diluted 1:50 in PBS. The slides were incubated at room temperature for 1 hour, washed in PBS, and mounted in 1:1 PBS:glycerol. Slides were viewed under an epifluorescent microscope, and the antibody titre was determined as the higher of the two test dilutions that gave positive VCA staining. A consistent titre of <1:5 was considered to indicate an EBV-seronegative blood donor.

9. Cell Culture Techniques

Using aseptic technique, all cell culture techniques were carried out inside microbiological class 2 safety cabinets using sterile equipment and solutions.

9.1 Control Cell Lines

A viably frozen store of control cell lines was kept under liquid nitrogen in our laboratory. These cell lines were routinely grown *in vitro*, and are shown in Table A4 in Appendix 1.

9.2 Cell Culture

Cells were grown *in vitro* as suspension cultures and kept at a concentration of between $1x10^5$ and $1x10^6$ cells (depending on the nature of the culture) per mL of CM in a humidified incubator containing 5% CO_2 at 37°C. Cells were fed with CM as required (usually every 2-3 days). In order to ensure adequate humidification, sterile distilled water (SDW) was added to the outermost wells of 24, 48 and 96 wells plates, and the plates were kept in sandwich boxes containing water-filled bijoux tubes.

9.3 Cell Wash

In order to 'wash' cells, they were spun at 160 g for 7 minutes in a bench top centrifuge, resuspended in WM, and spun again. The g-number was calculated as follows:

$$\textbf{g-number} = 11.2 \times \mathbf{r} \times \mathbf{n}^2 \times 10^{-6}$$

(**r**: centrifugal radius in cm from axis to middle of tube;
n: speed in revolutions per minute, rpm)

The cell wash was was repeated as often as deemed necessary in fresh WM which was discarded after each wash cycle. Once complete, the cells were resuspended in an appropriate medium.

9.4 Viable Storage Of Cells

In order to store cells viably, $1x10^7$-$2x10^7$ cells were spun at 160 g for 7 minutes in a bench top centrifuge, resuspended in 1 mL of FM, and transferred into a 1.5 mL cryovial. The cryovials were kept at -70°C overnight, and then transferred into specialized tanks where they were stored under liquid nitrogen as frozen viable stock.

9.5 Recovery Of Frozen Cells

Following a quick thaw in a waterbath at 37°C, cells that had been stored viably frozen in a cryovial under liquid nitrogen were transferred as a thawed cell suspension into a sterile 20 mL plastic tube. Next, 9 mLs of WM were added drop-wise slowly to the suspension. Once a further 10 mLs of WM had been added more rapidly, the suspension was spun at 160 g for 7 minutes. The supernatant was discarded and the cells were washed again in fresh WM. Once complete, the cells were resuspended in 5-7 mLs of CM and placed in a 25 cm^2 TC flask for *in vitro* culture. Initially, fastidious cells were cultured in a 24-wells plate using 20% v/v FCS/CM until it was deemed safe to transfer the cells into flasks for bulk culture.

9.6 Viability Assay/Cell Counts

Cell viability was assessed using trypan blue. To this end, 10 µL of 0.5% w/v trypan blue (in PBS) was mixed with 10 µL of the cell suspension. 10 µL of the resulting mixture were placed on a haemocytometer and a cell count was performed visually on a graticule under a light microscope. Whilst live cells exclude the dye, it can access dead cells and turn them blue. Viability was expressed as the number of viable

cells out of the total number of counted cells multiplied by a factor of 100 (ie, a percentage was obtained). A viability of ≥70% was considered acceptable.

9.7 T Cell Fractionation Using Antibody-Coated Magnetic Beads

In order to select out T cell subpopulations, CD4+ve or CD8+ve T cells were positively selected from fresh or frozen cell samples using EasySep® (StemCell Technologies) kits. The manufacturer's instructions were followed and the composure of cell fractions generated was assessed by flow cytometry (see section 9.14). Briefly, cell samples were suspended in EasySep® buffer (2% v/v FCS/1mM EDTA in PBS) at a concentration of $1x10^8$ cells/mL. Next, 100µL of CD4+ve, or CD8+ve, T cell EasySep® positive selection mixture (contains tetramer complexes of bi-specific antibodies directed against the CD4, or CD8, cell surface markers and dextran) was added per 1 mL of the whole cell suspension. Having given the resulting suspension a gentle mix, it was incubated for 15 minutes at room temperature. Next, 50µl EasySep® magnetic dextran iron nanoparticles were added per 1 mL of cell suspension, and the mixuture incubated for 10 minutes at room temperature. Following a gentle mix, the final volume per sample was increased to 2.5 mLs using EasySep® buffer. Each such sample was then placed in a magnet for 5 minutes at room temperature. With the sample still in the magnet, the supernatant was poured out in one movement. The following next 3 steps were then repeated twice: **(1)** the sample was removed from the magnet and 2.5 mLs of EasySep® buffer added to the positively selected cell population followed by gentle mixing; **(2)** a further magnetic separation of 5 minutes at room temperature; **(3)** decanting of supernatant. The positively-selected cells were resuspended in CM, counted, assessed by viability assay, and used in subsequent experiments.

9.8 γ-Irradiation Of Cells

Cellular chromosomal damage to prevent cell proliferation was incurred using γ–irradiation. To this end, cell suspensions were exposed to γ-irradiation from a ^{137}Cesium source. Exposure time (ET, in minutes) was calculated as follows:

$$\mathbf{ET} = \frac{\mathbf{Y} \times 60 \text{ minutes/hour}}{4.07\text{x}10^{4} \text{ rad/hour} \times \mathbf{DF}} \times 1.10$$

(**Y**: value of the desired irradiation dose in rads;
DF: decay factor as tabulated by the manufacturer of the ^{137}Cesium source)

9.9 EBV Virus Preparation

Using standard methods, an EBV virus preparation was generated from the B95-8 EBV genome-positive marmoset cell line (Miller *et al,* 1972). Following expansion of the B95-8 cells *in vitro,* cells were left unfed for 1 week and then centrifuged at 800 g for 20 minutes. Whilst the supernatant was collected and kept (see below), the cell pellets were resuspended in 10 mLs of cold CM and subjected to 3 rounds of alternate quick freeze-thawing cycles to induce cell lysis and virus particle release. In order to pellet cell debris, samples were spun at 450 g for 20 minutes. The supernatant that was harvested in this manner was mixed with the supernatant collected previously (see above), and the combined supernatant mixture ultracentrifuged at 24,000 g at 4°C for 2 hours. The virus pellet obtained in this fashion was resuspended (concentrated x200) in cold CM and passed through a pre-wet (in PBS) sterile 0.6 μm filter. Finally, 100 μL aliquots were stored in cryovials at -70°C.

9.10 EBV Virus Preparation Immortalizing Capacity (EBV Titration)

Serial dilutions (1:10, $1:10^2$, $1:10^3$, $1:10^4$, $1:10^5$, $1:10^6$) of a concentrated EBV virus preparation generated as described above were each used to infect 10^6 PBLs obtained from EBV-seronegative healthy individuals in a total volume of 1 mL (in CM) at 37°C for 1 hour in a humidified incubator containing 5% CO_2. Cells were then washed twice in WM to remove excess virus and cells resuspended in CM. For each EBV dilution, infected PBLs were plated out in 5 replicate flat-bottom wells of a 96-wells microtiter plate. Each well contained $2x10^5$ cells in 200 μL of CM. Following 4 weeks of *in vitro* culture, cells were assessed directly under a light microscope for signs of immortalization. The transforming titer of the virus preparation was determined as the reciprocal of the virus dilution which gave rise to BLCLs in ≥3 wells. Only virus preparations with a transforming titer of $\geq 10^{-4}$ were used in subsequent studies.

9.11 Cyclosporin-A

A stock solution of 100 μg/mL Cy-A was prepared in injectable grade alcohol. For *in vitro* culture, 0.5-1 μL (50-100 ng) were used per 1 mL of CM.

9.12 Establishment Of *In Vitro* EBV-Infected BLCLs

PBLs to be infected were pelleted at 160 g for 7 minutes and resuspended in 100 μL of concentrated EBV virus preparation to which CM was added to give a final 1 mL volume. The cell/virus suspension was incubated at 37°C for 1 hour in a humidified incubator containing 5% CO_2. Cells were washed twice in WM (to remove excess virus), and resuspended at a concentration of 10^6 cells per 1 mL of CM together with Cy-A (see 9.11 above). Next, 2 mLs aliquots were plated out per well in a 24-wells plate. Following 4 weeks of *in vitro* culture, cells were assessed directly under a light microscope for signs of immortalization. BLCLs were immunophenotyped and transferred into TC flasks for bulk culture.

9.13 Establishment And Maintenance Of EBV-Specific CTLs

Using fresh, or cryopreserved, PBLs separated from buffy coats, EBV-specific CTLs were established as described previously (Wilkie *et al,* 2004). Briefly, γ-irradiated (4,000 rads) BLCLs were used to stimulate autologous PBLs *in vitro.* Initially, a cell mixture containing a 40:1 PBL:BLCL ratio was suspended at a concentration of $1x10^6$ cells per mL of 20% v/v FCS/CM in 25 cm^2 TC flasks and kept at 37°C in a humidified incubator containing 5% CO_2. The expanding T cells were restimulated 10 days later (denoted stimulation 1, or 'stim 1') with a ratio of 4:1 T cells:γ-irradiated autologous BLCL. Four days later, 20 IU/mL of recombinant IL2 (rIL2) were added to the *in vitro* cultures. From this timepoint (14 days) onwards, the T cell cultures were restimulated weekly with γ-irradiated autologous (4:1 ratio) BLCLs together with a thrice weekly dose of rIL2. At time of weekly stimulation, the T cell concentration was adjusted to $1x10^6$ cells per mL to ensure optimum growth conditions.

On occasion, aliquots of viably frozen BLCL and T cell sets at very early stimulation points were kindly donated by Ms G Wilkie (CRUK Study Group, Laboratory for Clinical & Molecular Virology, The University of Edinburgh). Following thawing of these cells, they were expanded in exactly the same manner as described above.

9.14 Flow Cytometry (Fluorescent-Activated Cell Scanning, FACS)

Flow cytometry (fluorescent-activated cell scanning, FACS) was carried out using standard methods. Briefly, FACS buffer (FB) [1% w/v bovine serum albumin (BSA), 5mM EDTA and 0.1% w/v sodium azide in PBS] was generated, and 10x concentrated CellFIX™ (BD Biosciences) was diluted 1:10 with distilled water prior to use. For each cell sample, 100 μL aliquots of a $1x10^6$ cells per mL suspension were established in FB in LP5 tubes and spun at 200 g for 5 minutes. Once resuspended in 50 μL of FB, directly-conjugated mabs shown in Table A1.2 in Appendix 1 were added to obtain a routine working dilution (as previously determined in our laboratory) for

immunostaining of each cell surface marker. For each mab, an unstained (no antibody) control and an Ig isotype-only mab control was included in every experiment. Following gentle mixing of the cell/mab mixtures, they were incubated at 4°C for 20 minutes in the dark. Next, the cell suspensions were washed twice in 1 mL of FB and spun at 200 g for 5 minutes. Cell pellets were resuspended in 200 μL of a 1:10 dilution of CellFIX™ and stored at 4°C in the dark until flow cytometric analysis. FACS acquisition (and analysis of 1,000-10,000 acquired events per sample) was performed using the 'CellQuest Software' on a FACSCalibur machine (Becton Dickinson).

9.15 ^{51}Chromium-Release Assay

A standard 4 hour ^{51}Cr-release assay was carried out as described previously (Wilkie *et al,* 2004). Briefly, target cells (autologous and mismatched BLCLs as well as NK target K562 cells) were incubated with 50 μCi of ^{51}Cr at 37°C for 1 hour in a humidified incubator containing 5% CO_2, washed twice in HBSS, resuspended in 20% v/v FCS/CM (to give a final concentration of $1x10^5$ cells/mL), and plated out in 3 replicate U-bottom wells of a 96-wells microtiter plate. Each well contained $10x10^3$ cells in 100 μL of CM. In parallel, a $2x10^6$ cells/mL effector T cell suspension was prepared in 20% v/v FCS/CM. Using 100 μL aliquots per well, $50x10^3$-$200x10^3$ T cells were added to target cell wells to generate a 5:1, 10:1 and 20:1 effector-to-target ratio in triplicate wells. In order to gauge spontaneous ^{51}Cr release by target cells, 100 μL of 20% v/v FCS/CM only were added to each target cell well in triplicate. Similarly, addition of 100 μL of 1% v/v Triton® X-100 only served to establish maximum ^{51}Cr release by target cells. Once all the cell combinations had been plated out, the cell mixtures were incubated at 37°C for 4 hours in a humidified incubator containing 5% CO_2. Following centrifugation at 300 g for 5 minutes, 100 μL of supernatant was collected from each well, transferred into scintillation tubes, loaded into racks, and ^{51}Cr release measured in a γ-counter. The % specific cell lysis was calculated as follows (results were expressed as an average of readings from triplicate wells):

$$\textbf{\% Specific Lysis} = \frac{\text{cpm } \textbf{test} \text{ release} - \text{cpm } \textbf{spontaneous} \text{ release}}{\text{cpm } \textbf{maximum} \text{ release} - \text{cpm } \textbf{spontaneous} \text{ release}} \times 100$$

(**cpm**: Counts per minute)

9.16 Proliferation Assay

Cells were grown in CM at a concentration of 10^6 cells per mL in a 24-wells plate. On the day of pulsing, cells were plated out at a concentration of $2x10^5$ cells per 200 µL per well in 3 replicate wells of a 96-wells round bottom microtiter plate. The proliferative response was assessed by pulsing the cells with 1 µCi per well of [^{3}H]-thymidine at 37°C for 4 hours in a humidified incubator containing 5% CO_2 (Taylor *et al,* 1957; Rubini *et al,* 1960). A cell harvester was used to lyse the pulsed cells in water, and the DNA-incorporated [^{3}H]-thymidine was harvested onto filter mats. The mats were immersed in scintillation solvent. The radioactivity, as a parameter of cell proliferation, was measured in a scintillation β-counter. The results were expressed as average counts per minute (cpm).

10. SCID Mice

We have a breeding colony of CB.17 SCID mice at the University of Edinburgh. The colony is kept in an SPF environment in microisolator (IVC) cages and handled in microbiological class 2 safety cabinets. The animals are fed autoclaved feed and water without antibiotics. All animal work was carried out under relevant Home Office Project and Personal Licences in accordance with the Home Office 'Animals' (Scientific Procedures) Act 1986', and monitored by Home Office Inspectors and University Named Veterinary Surgeons.

10.1 Inoculation Of Scid Mice

Cells were washed in WM and injected sc or iv in a volume of 100 μL of sterile CM into a test mouse. For ip inoculation, a volume of up to 500 μL was used per test animal.

10.2 Collection Of Murine Blood Samples

Blood samples were collected by superficial venesection as laid out in the relevant Project Licence. No more than 10% of the total blood volume (TBV) was collected in any 24 hours, and no more than 15% of the TBV was collected in any 28 days period. Samples were left to clot at 4°C for 1 hour, given a microfuge pulse, and serum collected and frozen at -20°C until testing.

10.3 Sc Tumour Measurements

Using callipers, macroscopic sc tumours were measured in 2 planes 90° on each other and tumour volume (mm^3) calculated using the formula $ab^2/2$ (tumour mass in mm^3; **a**: length; **b**: width).

10.4 Health Monitoring And Culling Procedure

Mice were observed daily for signs of sickness (for example, disinterest in their surroundings, hunched back, respiratory distress and ruffled fur). Upon showing signs of illness, or after a pre-set time limit (based on past experience), mice were culled by cervical dislocation (Schedule 1 procedure) in accordance with Home Office instructions and then submitted for necropsy. At necropsy, a macroscopic assessment was carried out and the following organs removed: lung, liver, spleen, and any tumour tissue. Each tissue sample was divided into 2 pieces which were either **(1)** fixed in neutral buffered

formalin (NBF) for histological and immunohistochemical analysis, or **(2)** preserved in RNALater™ (Qiagen) for molecular studies involving analysis of DNA and RNA.

10.5 Magnetic Resonance Imaging (MRI)

For MRI imaging, animals underwent inhalation anaesthesia as outlined in the relevant Project Licence. Once unconscious, mice were scanned using a small animal 'Varian 7T MRI Scanner' ('Magnex 115/60 gradient') housed at the University of Edinburgh. For imaging, a 'Rapid 39/59 mm Quad Coil' was used. In order to enhance image contrast, 20-30 μL of 10 nM gadolinium were iv inoculated. Scan time was gated on the animal's respiratory cycle and amounted to approximately 8.5 mins for 4 averages to give a resultant image.

11. Histopathology And Immunohistochemistry

11.1 Snap-Freezing Of Tissues

Frozen tissue blocks were prepared by placing an excised tissue piece on a cork plate, covering it with 'Optimum Tissue Cutting' (OCT) compound, snap-freezing the block in iso-pentane pre-cooled in liquid nitrogen, and transferring the frozen tissue blocks to pre-cooled cryovials for storage under liquid nitrogen. For snap-freezing of tissues for molecular analysis only, small tissue pieces were transferred into 1.5 mL cryovials that were snap-frozen in, and stored under, liquid nitrogen.

11.2 Preparation Of Cytospins

For cell sample of interest, a suspension of $5x10^5$-$10x10^5$ cells/mL was prepared in PBS, and 100 μL/sample was spun in a cytocentrifuge onto microscopy slides. The

samples were dried in air, fixed in acetone for 5 minutes, and allowed to dry in air again prior to storage at -20°C.

11.3 Preparation Of Cryo-Sections

Snap-frozen tissues were processed to 6 μm sections on polysine-coated slides, fixed in acetone for 5 minutes, dried in air at room temperature, individually wrapped in cling film (to prevent condensation upon thawing) and stored at -20°C. At time of use, slides were left to warm up at room temperature, unwrapped, and placed in a humid chamber for immunohistological analysis.

11.4 Preparation Of Paraffin Wax-Embedded Sections

Tissues fixed in NBF were paraffin wax-embedded and processed to 5 μm sections on polysine-coated slides.

11.5 Preparations For Use Of Paraffin Wax-Embedded Sections (Rehydration Of Sections)

In order to dewax paraffin wax-embedded sections, they were immersed in xylene for 5 minutes followed by 5 minutes in 100% v/v ethanol. The sections were rehydrated by sequential immersion for 3 minutes in each of 90% v/v, 70% v/v and 30% v/v ethanol which was followed by rinsing in tap water and drying in air. Sections were demarcated using a hydrophobic marker pen.

11.6 Retrieval Of Antigen

In order to ensure antigen exposure during immunostaining, slides were immersed either in a 1:10 dilution of a citrate-based (pH 6) 'Target Retrieval Solution' (DakoCytomation) at 95°C for 20 minutes, or an EDTA-based (pH 8) 'Antigen Retrieval

Solution' (DakoCytomation) at 100°C in a pressure cooker for 10 minutes. The former approach was used prior to immunostaining human cell surface markers (CD3, CD4, CD8, CD20, CD45) and EBV antigens (EBNA2, LMP1, BZLF1), whereas the latter procedure was employed prior to immunostaining cytotoxic granule molecules (perforin, granzyme B).

11.7 Section Mounting For Preservation

In order to preserve immunostained sections, they were mounted in either water- or solvent-based solutions. Thus, antibody labels that were insoluble in organic solvents were dehydrated (see section 11.9) and mounted in di-butyl-polystyrene-xylene (DPX), whereas labels insoluble in water-based solutions were mounted in either 1:1 PBS:glycerol or 'Faramount Aqueous Mounting Medium' (DakoCytomation). Lastly, sections were covered with coverslips for preservation.

11.8 Counterstaining Of Sections

Sections were counterstained by immersing them either in 0.1% w/v Evan's Blue (red cytoplasmic staining under UV-light) for 30 minutes, or Mayer's Haemalum (blue nuclear staining under light microscope) for 3 minutes at room temperature followed by rinses in tap water.

11.9 Dehydration Of Sections For Mounting In DPX

Prior to mounting antibody labels insoluble in organic solvents, sections were dehydrated by sequential immersion for 3 minutes into each of 30% v/v, 70% v/v, 90% v/v and 100% v/v ethanol followed by 3 minutes in each of acetone and xylene. Next, the sections were mounted in DPX and covered with a coverslip for preservation.

11.10 Hematoxylin And Eosin (H&E) Staining

Sections were first immersed in Mayer's Haemalum (blue nuclear staining) for 5 minutes, rinsed in tap water, and flooded with 1% w/v eosin for 15 minutes (pink cytoplasmic staining). Slides were rinsed in tap water, left to dry in air, mounted and covered with a coverslip for preservation.

11.11 Indirect Immunofluorescence (IIF) Immunostaining

Frozen test sections together with positive and negative control slides were incubated with 10 μL of primary antibody at 37°C for 1 hour in a humid chamber followed by two washes in PBS for 5 minutes each. Sections were incubated with 10 μL of either a fluorescein isothiocyanate (FITC)- or tetramethylrhodamine isothiocyanate (TRITC)-conjugated secondary antibody at room temperature for 1 hour. The slides were washed twice in PBS again and rinsed with distilled water. When an FITC-label was used, the sections were counterstained with Evan's Blue. Sections were mounted in 1:1 PBS:glycerol (or 'Faramount Aqueous Mounting Medium') and viewed under an epifluorescent microscope.

11.12 Peroxidase Anti-Peroxidase (PAP) Test

Standard methods were used (van Noorden, 1986) that involved inclusion of positive and negative control slides. Whilst paraffin wax-embedded sections were dewaxed and rehydrated, frozen sections were used directly. Antibody dilutions were made up in PBS, and incubations took place in a humid chamber.

Briefly, 10 μL of a primary murine mab were applied to sections at room temperature for 1 hour followed by two washes (for 5 minutes each) in PBS. Next, 10 μL of a secondary 1:25 rabbit anti-mouse Ig antibody/1:25 normal human serum (NHS) was applied to sections and they incubated at room temperature for 1 hour followed by further washes in PBS. Lastly, 10 μL of a 1:100 monoclonal mouse peroxidase anti-

peroxidase (PAP) complex-conjugated antibody was applied to sections at room temperature for 1 hour followed by washes in PBS. Bound antibody (PAP label) was visualized using 0.5 mg/mL of 2,3-di-aminobenzidine (DAB) in PBS for 2 minutes followed by application of 1 μL/mL of 30% w/v H_2O_2 for 3-5 minutes. Peroxidase catalyses the formation of atomic oxygen from H_2O_2, which oxidizes DAB (a chromogen) with formation of a brown end product. Following rinses in tap water, sections were counterstained in Mayer's haemalum at room temperature for 3 minutes followed by dehydration, mounting in DPX, and examination under a light microscope.

11.13 Alkaline Phosphatase Anti-Alkaline Phosphatase (APAAP) Test

Standard methods were used (van Noorden, 1986) that involved inclusion of positive and negative control slides. Whilst paraffin wax-embedded sections were dewaxed and rehydrated, frozen sections were used directly. Antibody dilutions were made up in tris buffered saline (TBS), and incubations took place in a humid chamber.

Briefly, 10 μL of a primary murine mab were applied to sections at room temperature for 1 hour followed by two washes (for 5 minutes each) in TBS. Next, 10 μL of a 1:25 secondary rabbit anti-mouse Ig antibody/1:25 NHS were applied to sections at room temperature for 1 hour followed by further washes in TBS. Lastly, 10 μL of a 1:50 monoclonal mouse alkaline phosphatase anti-alkaline phosphatase (APAAP) complex-conjugated antibody was applied to sections at room temperature for 1 hour followed by washes in TBS. Bound antibody (APAAP label) was visualized by flooding slides with filtered Solution C which was prepared as follows:

Solution A:	5 mg Fast Red TR salt/10mL veronal acetate buffer, pH9.6
Solution B:	5 mg Naphthol ASBI phosphonic acid/2 drops of DMF
Solution C:	Solutions A and B added together with 200μL of levamisole

Alkaline phosphatase (AP) hydrolizes naphthol phosphate to phenols which couple to 'Fast Red', a colourless diazonium salt (chromogen), generating a red azo dye (levamisole inhibits endogenous AP). Sections were incubated with Solution C at 37°C for 15-45 minutes whilst being monitored for the intensity of staining of control sections. Following washes in TBS, counterstaining in Mayer's haemalum for 3 minutes, and rinses in tap water, sections were mounted in an aqueous mountant.

11.14 Indirect EBNA Detection: Anti-Complement Immunofluorescence (ACIF)/ Anti-Complement Peroxidase Labelling (ACPL)

Standard methods were used (Reedman & Klein, 1973; Klein *et al,* 1976; Guohua *et al,* 1981) that involved inclusion of positive and negative control slides. Frozen sections were used directly. Antibody dilutions were made up in complement fixation buffer (CFB), and incubations took place in a humid chamber.

Indirect EBNA detection entailed immunostaining of the C3 component of complement by (anti-complement) indirect immunofluorescence (ACIF), or indirect (anti-complement) peroxidase labelling (ACPL), using the complement-fixing properties of anti-EBNA IgG antibodies. As a source of complement, the EBV negative human serum WDA (stored at -70°C) was used.

Briefly, 10 µL of either an EBNA-positive or -negative human serum diluted 1:10 in CFB containing 10% v/v complement were applied to sections at 37°C for 1 hour followed by two washes (for 5 minutes each) in CFB.

(1) ACIF: Ten µL of 10% v/v complement in CFB were applied to sections at 37°C for 30 minutes followed by washes in CFB. This step served as a complement enhancement step (Klein *et al,* 1976). Next, 10 µL of FITC-conjugated goat anti-human C3c secondary antibody diluted 1:20 in CFB was applied to sections at room temperature for 1 hour followed by washes in CFB, rinsing in distilled water, counterstaining in Evan's Blue, further PBS washes, and mounting in aqueous mountant.

(2) ACPL: Ten µL of a peroxidase (Px)-labelled rabbit anti-human C3c secondary antibody at a dilution of 1:25 in CFB was applied to sections at 37°C for 1 hour followed by washes in CFB and PBS. The Px label was developed as described above for the PAP test (see section 11.12). Sections were dehydrated and mounted in DPX.

11.15 EnVision™ And NovoLink™ Polymer Dectection Systems

Standard methods were used that involved inclusion of positive and negative control slides. Paraffin wax-embedded sections were dewaxed and rehydrated. Antibody dilutions were carried out in 'Antibody Diluent, Background Reducing' (DakoCytomation), and incubations took place in a humid chamber at room temperature. Each wash was carried out in TBS for 5 minutes. Both the **(1)** 'EnVision™' (DakoCytomation) and **(2)** 'NovoLink™ Polymer Detection System' (VisionBioSystems) approaches use polymeric labelling to increase sensitivity of the secondary detection reagent (directed against mouse and rabbit primary antibodies).

(1) EnVision™: Each section was incubated with 10 µl of primary antibody for 30 minutes followed by two washes and the application of 10 µl of the 'Rabbit/Mouse LINK' polymer reagent for 30 minutes. After further washes, sections were incubated with 10 µl of the 'AP Enzyme Enhancer' (AP-labelled amplification polymer) for 30 minutes followed by two washes. In order to visualize the AP label (red precipitate at the antigen site under the light microscope), an AP substrate working solution was prepared by mixing 100 parts of 'Permanent Red Substrate Buffer' with 1 part of 'Permanent Red Chromogen'. The AP label was developed as described above for the APAAP test (see section 11.13) followed by rinses in distilled water. Lastly, sections were counterstained with haematoxylin, rinsed in distilled water, dehydrated, mounted in DPX, and covered with coverslips for preservation.

(2) NovoLink™: Initially, in order to neutralize endogenous peroxidase, 10 µL of 'Peroxidase Block' were applied to each section for 5 minutes followed by two washes. Next, sections were incubated with 10 µL of 'Protein Block' for 5 minutes (to prevent non-specific antibody binding) followed by two washes and incubation with 10 µl of primary antibody for 30 minutes. Sections were washed again. In order to enhance binding of the polymer reagent to the primary antibody, 10 µL of 'Post Primary Block' were applied to each section for 30 minutes followed by two washes. Sections were incubated with 10 µL of the Px-labelled 'NovoLink™ Polymer' for 30 minutes followed by two washes. In order to visualize the Px label (brown precipitate at the antigen site under the light microscope), a DAB working solution (see the PAP test above; section 11.12) was prepared by adding 50 µL of 'DAB Chromogen' to 1 mL of 'NovoLink™ DAB Substrate Buffer (Polymer)' followed by rinses in distilled water. The Px label was developed as described above for the PAP test. Lastly, sections were counterstained with haematoxylin, rinsed in distilled water, dehydrated, mounted in DPX, and covered with coverslips for preservation.

11.16 Detection Of EBER1 And 2 (EBER *In Situ* Hybridization, ISH)

EBER ISH was carried out in accordance with the standard method (Howe & Steitz, 1986). Paraffin wax-embedded sections (with positive and negative control slides) were dewaxed by immersion in xylene for 3 minutes, and rehydrated by immersion in 99% v/v and 95% v/v ethanol for 3 minutes each. Sections were then left to dry in air. The 'Epstein-Barr Virus (EBER) PNA Probe/Fluorescein' and 'PNA ISH Detection Kit' from DakoCytomation were used in accordance with the manufacturer's instructions. All incubations were performed at room temperature (unless otherwise stated) in a humid chamber.

Slides were washed twice in autoclaved di-ethyl-pyrocarbonate (DEPC)-treated double distilled water for 3 minutes and each section then incubated with 20 µL of 0.1

mg/mL proteinase-K (PRK) in PRK buffer for 30 minutes followed by two 3 minutes washes in DEPC-treated water and dehydration by immersion in 95% v/v and 99% v/v ethanol for 3 minutes each. Sections were left to air dry followed by the application of 5-10 μL of a 5-carboxy-fluorescein (FITC)-labelled peptide nucleic acid (PNA) probe complimentary to EBER1 and 2 [sections were covered with pre-treated (in methanol) coverslips] at 55°C for 1.5 hours (positive and negative 'Control PNA Probe/FITC' were included in each run). Cover slips were removed and sections immersed in a pre-heated (55°C) working solution (1:60 in pure water) of 'Stringent Wash' for 25 minutes followed by a brief immersion in TBS to bring the tissue samples down to room temperature. Sections were then incubated with 10 μL of an 'Anti-FITC/AP' (AP-conjugated antibody to FITC) for 30 minutes followed by two washes in TBS and a 1 minute immersion in double-distilled water. In order to visualize bound probe (blue/black precipitate at the RNA site under light microscopy), the AP 'Substrate' containing 5-bromo-4-chloro-3-indolylphosphate (BCIP) and nitroblue tetrazolium (NBT) was applied to sections for 30-60 minutes followed by rinses in distilled water and counterstaining in hematoxylin. Following further rinses in distilled water, sections were mounted in 'Faramount Aqueous Mounting Medium' and covered with coverslips for preservation.

11.17 Viewing Slides/Photomicrography

Slides were viewed under a light microscope at a magnification of x100 and x400 (or at x1,000 under oil), and photographed when appropriate.

11.18 Cell Counts

In order to quantify labelled cells, the numbers of labelled and unlabelled (counterstained background) cells were counted in 5 high power (x1,000 under oil) fields. The results were expressed as the number of marker-positive cells out of the total counted cell population (multiplied by a factor of 100 to give % marker+ve cells).

12. Reverse-Transcriptase Polymerase Chain Reaction (RT-PCR)

RT-PCR was carried out essentially as described by Saiki *et al* (1985, 1988) and Hart *et al* (1988).

12.1 Methods Involving Ribonucleic Acids (RNA)

In order to preserve the integrity of RNA transcripts, precautions were taken throughout the following procedures. In particular, emphasis was placed on preventing contamination with RNases and gloves were worn at all times. To this end, only disposable plasticware was used, and all glassware was autoclaved prior to use. Only ultrapure (molecular biology grade) distilled water was used during the preparation of buffer solutions, all of which (except SDS) were autoclaved prior to use. RNA samples were suspended in RNase-free ultrapure sterile water.

12.2 Preparation Of Complementary Deoxyribonucleic Acid (cDNA) Template

Total RNA was extracted from PHA-treated PBMCs, Balb/c splenocytes, BLCLs, and tumour tissues. From each sample, 5 μg of RNA were used to generate complementary DNA (cDNA) by reverse transcription using reverse transcriptase (RT).

12.2.1 Extraction Of Total RNA

'RNAzol^{TM}B', which contains the RNase inhibitor guanidinium and the denaturing agent phenol, was used in accordance with the manufacturer's (Cinna/Tel Test) protocol to extract total RNA. RNAzol^{TM}B promotes the formation of

RNA/guanidinium/water complexes in an aqueous phase whilst eliminating DNA and proteins from this phase.

12.2.2 Homogenization

Vials containing snap-frozen cell pellets or tumour tissue, and stored under liquid nitrogen, were transferred onto dry ice to prevent thawing of sample. Whilst still frozen, cell pellets were solubilized in their vials in RNAzol^{TM}B (200 µL RNAzol^{TM}B per 10^6 cells) by passing the lysate a few times through a pipette tip. Frozen tumour samples were removed from vials and promptly dissected into small tissue fragments with sterile scalpel blades followed by an immediate transfer into sterile vials containing RNAzol^{TM}B (200 µL RNAzol^{TM}B per 10 mg of tissue) and homogenization using sterile plastic plungers.

12.2.3 Extraction Of RNA

Chloroform was used to extract RNA from samples by adding 200 µL per 2 mL of homogenate in their vials followed by vigorous shaking, a 5 minute incubation on ice, and 12,000 g centrifugation at 4°C for 15 minutes. The spin promotes the separation of an upper aqueous phase from a lower organic phenol/chloroform phase. Whilst RNA is contained in the upper aqueous phase, the interface and lower organic phase contains DNA and protein.

12.2.4 Precipitation Of RNA

The RNA-containing upper aqueous phase was harvested and transferred into a sterile vial containing an equal volume of isopropanol on ice. RNA precipitation was carried out in this manner for 15 minutes followed by 12,000 g centrifugation at 4°C and the formation of a visible RNA pellet.

12.2.5 Washing Of RNA

The supernatant was carefully harvested by a pipette so not to disturb the RNA pellet which was washed once with 70% v/v ethanol at 7,500 g. The resulting pellet was then resuspended carefully in pure water.

12.2.6 RNA Handling

Since RNA has its maximum absorbance at 260 nm, its concentration was determined spectrophotometrically (optical density, OD) at this wavelength. In order to assess protein contamination, further readings were taken at 280 nm. A 260/280 absorbance ratio of 1.8-2.0 indicated pure RNA. Next, the suspensions were divided into 2 aliquots. Whilst one was kept at -20°C as a working solution, the other sample was kept at -70°C as stock (suspended in 75% v/v ethanol to preserve RNA integrity).

RNA integrity was checked by running samples out on 1% w/v NuSieve® agarose gels. Under UV light, distinct bands corresponding to the 18S and 28S ribosomal RNA subunits indicated a sample containing undegraded RNA whereas sample smears suggested RNA degradation.

12.2.7 First-Strand cDNA Synthesis

cDNA synthesis was carried out using an 'RT-PCR Kit' from Stratagene in accordance with the manufacturer's protocol using reverse transcription from random primers by RT. The resulting heterogenous RNA-derived cDNA template population was subsequently used as starting material for PCR (see section 12.3).

All reagents were supplied by the manufacturer and included the following:

Random primers	0.1μg/μL
First-strand buffer	10x
RNase block ribonuclease inhibitor	40U/μL
100mM deoxynucleotide-triphosphates (dNTPs)	25mM each dNTP
Moloney Murine Leukemia Virus (MMLV)-reverse transcriptase (RT)	50U/μL

For each sample, a starting solution containing 5 μg of total RNA was made up in pure water to a final volume of 38 μL to which 3 μL (100 mg/mL) of random primers were added followed by gentle mixing. In order to denature the RNA, the sample solutions were heated at 65°C for 5 minutes followed by quenching on ice. The random primers were allowed to anneal to the cDNA templates at room temperature. Next, 5 μL of 10x first-strand buffer and 2 μL of 100 mM dNTPs were simultaneously added to the samples followed by 0.5 μL of each of a (40 U/μL) RNase block ribonuclease inhibitor and the (50 U/μL) MMLV-RT. In order to allow first-trand cDNA synthesis by the MMLV-RT, the sample solution was incubated in a waterbath at 37°C for 1 hour, and then either used directly, or stored at -20°C.

12.3 PCR

In order to amplify/generate a homogenous population of a particular target sequence of interest, PCR was carried out using sequence-specific primers.

12.3.1 Methods Involving cDNA

Precautions were taken to avoid contamination with foreign DNA. To this end, gloves were worn at all times and only sterile disposable plasticware was used. Only molecular-grade, contamination-free reagents were used including ultrapure water. Pre-amplification procedures took place in a designated clean room containing all necessary laboratory equipment including designated pipettes and aerosol-resistant pipette tips. PCR amplification was carried out in a general-purpose laboratory. cDNA samples were tested on at least 2 occasions alongside positive and negative controls. In each run, sterile distilled water (SDW) was included as a DNA template-free negative control.

12.3.2 Primer Pairs And Reaction Conditions

The sequences of the published oligonucleotide primer pairs used in this study are shown in Table A5 in Appendix 1. Primers were synthesized by Eurogentec and stored at -20˚C. Although published reaction conditions were used as reference points, all reaction conditions were optimized in our laboratory.

(1) Reaction Mixture

For each sample, 5 μL of cDNA were used as template in each reaction, and transcript amplification was carried out in a total reaction volume of 100 μL. Each reaction mixture consisted of 50 mM KCl, 10 mM Tris-HCl (pH9.0), 0.1% v/v Triton X100, and 200 μM of each of dATP, dCTP, dGTP, and dTTP as well as 2.5 U of Taq DNA polymerase (from *Thermus aquaticus* strain YT1; the IL2 and 4 primers were used with 3.5 and 2.0 units of enzyme, respectively). Additionally, 1.5 mM $MgCl_2$ was included in each reaction (the IL6 and IFNγ primers were used with 2.5 mM $MgCl_2$). The concentration of each primer was 1 μM per reaction.

Each reaction was over-laid with 2 drops of sterile mineral oil to prevent evaporation during amplification.

(2) Amplification

A thermal cycler was used for PCR amplification. Amplification of the β-actin, IL5 and 6 transcripts consisted of 40 cycles of a 1 minute long denaturing step at 94°C followed by 2 minutes of annealing/extension at 65°C. The IL2 and IFNγ transcripts were amplified using 40 cycles of 1 minute at 94°C and 2 minutes at 55°C. In order to amplify the IL4 and IL10 transcripts, a 35 cycle reaction consisted of 45 seconds at 94°, 45 seconds at 60°C (annealment), and 2 minutes at 72°C followed by a final extension step for 7 minutes. A summary of the PCR amplification cycles used is shown in Table A6 in Appendix 1.

For visualization of amplified products under UV light, 20 μL of amplified sample in 4 μL of loading buffer (6:1) were run out on 2.5% w/v NuSieve® agarose gels containing 1 μg/mL ethidium bromide (EtBr).

12.4 Gel Electrophoresis

In order to use fragment size to separate and identify amplified DNA products, they were run out on agarose gels in accordance with the protocols of Sambrook, Fritsch and Maniatis (1989). To this end, low viscosity NuSieve® 3:1 agarose (3 parts NuSieve® agarose, 1 part SeaKem® agarose) was dissolved by microwave heat treatment in 1xTBE buffer followed by cooling under running cold water and the addition of 1 μg/mL EtBr. Horizontal gels were cast in plastic gel trays incorporating plastic combs for the creation of sample wells and left to set. Once set, the gels were covered with 1xTBE buffer and the plastic combs gently removed (avoiding rupturing the wells). Next, a 1:6 v/v mixture of PCR products and loading buffer was carefully loaded into wells. Each gel included ^{32}P-end-labelled Hin*f* I-digested bacteriophage ϕX174 DNA as DNA size markers and a non-radiolabelled 1 Kbp DNA ladder. Electrophoresis of the PCR products was carried out at 60 mA, and separated product bands were visulized at 365 nm under a UV transilluminator followed by gel photographing for reference purposes.

12.5 Southern Transfer

In accordance with the method of Southern (1975), PCR products were blotted onto nylon membranes following electrophoretic separation on NuSieve® agarose gels. First, the gels were immersed in alkaline denaturing solution for 30 minutes to denature the DNA followed by neutralization at pH7.2 in neutralizing solution for 30 minutes. Next, the Southern blot proper involved inverting the gels on top of glass plates sitting on plastic trays filled with 20xSSC solution. The gels were placed on top of a single large sheet of pre-wet (in 20xSSC solution) 3MM paper, the edges of which were immersed in the 20xSSC solution of the underlying tray, and the undersurface of the gels was rid of any air bubbles. A cut-to-size piece of positively charged nylon Hybond™-N+ hybridization transfer membrane was then placed on top of the gels (avoiding the formation of air bubbles) which was followed by arranging 3 cut-to-size pieces of 3MM paper on top of the transfer membrane (the bottom sheet was pre-wet in 20xSSC solution). In order to avoid evaporation, and to guide the direct transfer of the amplified products onto the nylon membrane, the edges of the gels were sealed with cling film. To create a flow of 20xSSC solution from the underlying tray and up through the gels, a stack of dry paper towels was placed on top of the gels thus facilitating blotting of the PCR products onto the transfer membrane. Southern transfer was further aided by positioning a glass plate on top of the paper towels together with a 500 g weight, and leaving the process overnight at room temperature. Following Southern transfer, gel fragments were washed away in 2xSSC solution, and the transferred PCR DNA fragments cross-linked to membranes by 120,000 μJ UV-irradiation in an UV Stratalinker™.

12.6 Pre-Hybridization

Membranes were sealed in plastic bags containing pre-hybridization solution in preparation of gene-specific probing with ^{32}P-labelled oligonucleotide probes. In order to minimize non-specific probe binding, 100 μL of sheared salmon sperm DNA that had

been denatured by boiling in water for 5 minutes (followed by quenching on ice) was added per 10 mL of pre-hybridization solution. The transfer membranes were soaked in a waterbath at 42°C for at least 2 hours.

12.7 Radioactive Probes

Probes used in this study are shown in Table A7 in Appendix 1. Their sequences were either designed, or obtained from published papers, as indicated. Probes were all synthesized by Eurogentec, diluted in pure water to a concentration of 10 pmoles/μL (10 μM), and stored at -20°C.

Radiolabelling of probes was carried out using commercially available (Promega) T4 polynucleotide kinase with the assay buffer provided. Probes were 5' end-labelled by the enzyme by incubating 10 pmoles (1 μL) of the oligonucleotide together with 5 μL of fresh (370 MBq/mL, 10 mCi/mL) ^{32}P-labelled γ-dATP in a reaction solution containing 70 mM Tris-HCl (pH7.6), 10 mM $MgCl_2$, and 5 mM DTT in a waterbath at 37°C for 30 minutes. The probe solution was run through a pre-wet (in 1xTE buffer) NICK™ column containing Sephadex® G-50 DNA grade in distilled water to separate ^{32}P-labelled probes from unincorporated oligonucleotides. The purified radiolabelled probe was eluted off the column with 1xTE buffer and effective radiolabelling confirmed with a Geiger counter.

12.8 Hybridization Of ^{32}P-Labelled Probe

Following pre-hybridization of transfer membrane (see section 12.6), bags enclosing the membranes were opened and ^{32}P-labelled probes were added to the pre-hybridization solution together with fresh aliquots of denatured sheared salmon sperm DNA. The bags were resealed and the radiolabelled probes left to hybridize with their specific target sequences in a waterbath at 42°C overnight.

12.9 Autoradiography

Following overnight's hybridization, the hybridization solution was discarded and the membranes were rinsed to remove any probe bound to the membranes in a non-specific manner. Initially, two 10 minute rinses in 2xSSC/0.1% w/v SDS were carried out at room temperature followed by a final 15 minute rinse in 1xSSC/0.1% w/v SDS solution. Excess moisture was removed from the membranes by blotting on 3MM paper which was followed by sealing the membranes in cling film, and placing them in film cassettes to expose Hyperfilm^{TM}-MP to the membranes. In order to magnify the signal detected from bound radiolabelled probes, the cassettes contained intensifying screens and were placed at -70°C. Exposure time varied from 1 to 7 days, and the autorads were developed, annotated and kept as permanent records. A signal in a test sample lane was scored as positive if the fragment was of the expected size (when compared with DNA size markers included in each experiment) based on sequence alignment of primers with the known gene sequence. Autorads were only analyzed further if **(1)** amplifiable DNA was present as determined by β-actin cDNA amplification, and **(2)** all the positive and negative controls (as well as the template-free SDW control) indicated successful, non-contaminated RT-PCR amplification of target sequences.

12.10 Re-Probing

Transfer membranes could be re-used and re-probed with a freshly radiolabelled probe by washing them in boiling hot 0.1% w/v SDS solution for 2 hours followed by overnight autoradiography to confirm that all probe had been removed successfully. Starting with immersion in pre-hybridization solution (see section 12.6 above), the membranes were then re-probed by the usual method outlined above.

13. Clonality

In order to ascertain whether SCID tumours represented the corresponding biopsy, samples were assessed for **(1)** Ig and **(2)** EBV clonality.

(1) Ig clonality was analyzed by PCR using primers specific for a conserved region of the V segment of framework (Fr) 3 and junction (J) segments of the Ig heavy chain (IgH) gene locus (McCarthy *et al,* 1990; Stetler-Stevenson *et al,* 1990). The Fr3 PCR products were analyzed on ABI PRISM™ 310 Genetic Analyzer. Similar analysis was performed using primers derived from Fr1. Based on sequence analysis of amplification products, a TaqMan™ PCR assay specific for specific rearrangements was designed and performed using standard methodology when appropriate (Kuppers *et al,* 1995). Thus, PCR was performed with 1 μg of DNA using primers specific for a conserved region of the V segment of Fr1, or Fr3, and the J segments of the IgH gene locus. Using QIAquick 8 PCR purification kit (Qiagen), 30 μL of PCR product were purified, eluted in 60 μL of buffer, and 3 μL of purified product run on the ABI PRISM™ 310 Genetic Analyzer with 0.5 μL of the GS350 marker and 10 μL of formamide. Results were analyzed using GeneScan™ software.

(2) EBV clonality was assessed using standard Gardella gel technique (Gardella *et al,* 1984; Raab-Traub & Flynn, 1986). For each tumour sample, $10x10^6$ *Bam*HI-digested cell lysates were run on a Gardella gel (0.8% w/v agarose), Southern transferred onto a nylon membrane, and probed with a ^{32}P-labelled plasmid probe (*Eco*dhet). Following EBV infection of a target B cell, the number of reiterated 500 bp virus genome terminal direct repeats involved in generating the virus episome is characteristic of any infection event. Since progeny EBV+ve cells retain the same EBV episome, a clonal virus population can be studied using the Gardella gel technique (Hurley & Thorley-Lawson, 1988).

14. Statistical Analysis

The statistical tests used in this study were: **(1)** Fisher's exact test for comparison of proportions; **(2)** Linear regression and Logrank test for comparison of survival of 2 (or more) groups of mice, and **(3)** non-parametric tests (Kruskall test, Mann-Whitney test, Spearman's test) for analysis of association between 2 variables for comparison of 2 (or more) groups. Tumour incidence in different groups of SCID mice was compared by the Fisher's exact test (with 2-tailed p value). The time to tumour in different groups of animals was compared using the Kruskall test, Mann-Whitney test, and Spearman's test.

Statistical analysis was performed using 'GraphPad Prism' software (GraphPad Software, Inc). Significance was determined using p values as follows: $p>0.05$ and $p\leq0.05$ were considered to be non-significant and significant, respectively (Kirkwood, 1988).

Standard Error (SE) was calculated as: $SE=SD_{n-1}/\sqrt{n}$ where SD is the standard deviation and n denotes the number of samples analyzed. The value of SE was shown as error bars on graphs.

RESULTS

1. Expansion Of PTLD Biopsy Material

PTLD biopsy material is not readily available, is very difficult to expand *in vitro,* and the few PTLD-derived cell lines available do not reflect accurately the initial tumour phenotype (Cen *et al,* 1993). Furthermore, PTLD biopsy material generally contains heavy infiltrates of non-malignant T cells (Perera *et al,* 1998) which can limit its use in molecular studies. In light of these difficulties, the tumours have been modelled *in vivo*. Our initial aim was to expand PTLD biopsies in SCID mice (hu-SCID-Bx model). Using this approach, we wished to generate human PTLD-like lesions in the animals. To this end, EBV+ve PTLD biopsy material was obtained from 5 solid organ transplant recipients (denoted 'patient 1-5'; for patient details, see Table 7). We have previously reported on successful *in vivo* expansion of PTLD biopsy samples from these patients (Perera *et al,* 1996; Johannessen *et al,* 2002 – see Appendix 2).

TABLE 7
Patient Details

Pt No	Age (Years)[1]	Sex	Organ Transplant	Onset Of 1° Tumour[2] (Months)	EBV-Serostatus At Time Of 1° Tumour	Site Of 1° Tumour	Pathological Diagnosis Of 1° Tumour
1	5	M	Kidney	72	Carrier	Lymph node	Myeloma
2	9	M	Liver	34[3]	Carrier[3]	Lymph node	BLPD
3	0.1	F	Liver	16	Primary infection	Tonsil	BLPD
4	7	M	Heart	45[4]	Carrier[4]	Lymph node	HL
5	15	M	Heart	7	Primary Infection	Lymph node	BLPD

[1]: At time of transplantation; [2]: Time from organ graft to tumour; [3]: Recurrence, original lesion arose 2 months post-graft; [4]: Recurrence, original lesion arose 29 months post-organ graft; HL: Hodgkin's lymphoma; BLPD: B cell lymphoproliferative disease; M: Male; F: Female; Pt: Patient; No: Number

For each biopsy received, $25x10^6$–$50x10^6$ biopsy cells (denoted 'biopsy') were injected ip into one SCID mouse within 12 hours of patient sampling (material from

patient 2 was inoculated into two animals). All samples gave rise to EBER+ve ip tumours (denoted 'SCID tumour') in SCID mice. It was possible to passage material from patient 3 only. Thus, our tissue panel consisted of 5 sets of PTLD biopsy and SCID tumours. This panel was analyzed for **(1)** Ig and EBV clonality, **(2)** cell surface phenotype, **(3)** *in vitro* proliferation, and **(4)** cytokine expression. Since sample material was limited, a full complement of tests could not always be carried out.

1.1 Clonality

Initially, samples were assessed for **(1)** Ig and **(2)** EBV clonality to determine whether SCID tumour cells represented the corresponding malignant cells in the PTLD biopsy.

(1) Ig clonality was analyzed by PCR using primers specific for a conserved region of the variable (V) segment of either framework (Fr) 1 (patient 2) or 3 (patients 1, 3, 4 and 5) and junction (J) segments of the Ig heavy chain (IgH) gene locus. Representative results are shown in Figure 3.

Matching Ig clones were found in PTLD biopsy and SCID tumour sets from 4 out of 5 (80%) patients (number 1-3 and 5). Thus, 4 biopsies gave rise to identical lesions *in vivo* which had expanded successfully in SCID mice. Additional sequence analysis of material from patient 2 confirmed the identical Ig gene rearrangement in the biopsy and SCID tumour (Figure 3A; Johannessen *et al,* 2002). The malignant Ig clone was also detected in a PBL sample taken from patient 2 at time of PTLD. Biopsy and SCID tumour from patient 3 were oligoclonal with an identical dominant rearrangement. The passaged SCID tumours from patient 3 were clonal, one of which was identical to the dominant biopsy and SCID tumour rearrangement (Figure 3B). Conversely, the biopsy from patient 4 contained a dominant clone in a polyclonal Ig background (Figure 3C). Whilst the SCID tumour was clonal, it was not identical to the biopsy.

FIGURE 3
Analysis Of Ig Gene Rearrangements

Samples were analyzed for Ig clonality using PCR in order to ascertain whether SCID tumour cells represented the corresponding PTLD malignant cells. **Figure 3A:** Electropherogram of Fr1 PCR from patient 2. Panel 1: PTLD biopsy result; Panels 2 and 3: Two SCID tumours. VH3 rearrangement of 328bp is indicated in each panel. **Figure 3B:** Electropherogram of Fr3 PCR from patient 3. Panel 1: PTLD biopsy showing oligoclonal distribution; Panel 2: SCID tumour showing oligoclonal distribution with 3 dominant rearrangements; Panel 3: SCID tumour (passage 1) showing 1 dominant rearrangement; Panel 4: SCID tumour (passage 2) showing a single rearrangement. **Figure 3C:** Electropherogram of Fr3 PCR from patient 4. Panel 1: PTLD biopsy; Panel 2: SCID tumour. Dominant clones were detected at 109bp and 91bp, respectively, as indicated.

The symbol ⋇ denotes GeneScan™ 35O ROX-labelled size standard.

→ : 97bp; ⟶ : 100bp; ⇦ : 109bp

3A: Patient 2

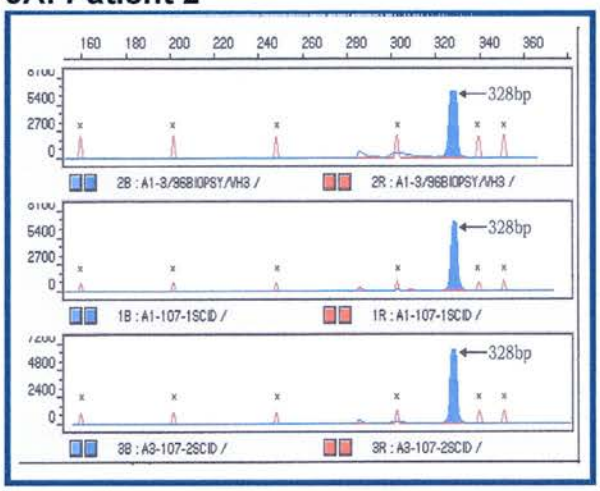

Panel 1

Panel 2

Panel 3

3B: Patient 3

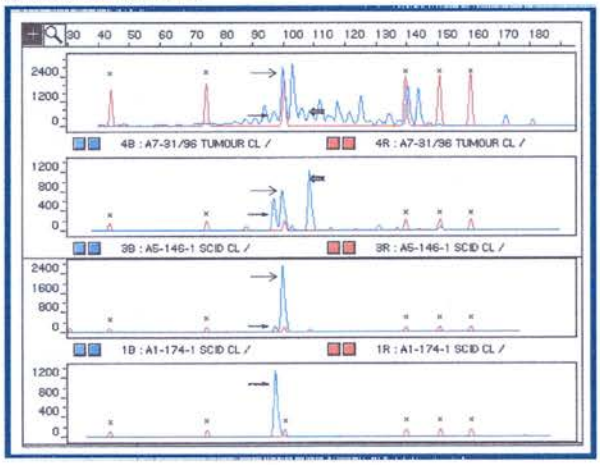

Panel 1

Panel 2

Panel 3

Panel 4

3C: Patient 4

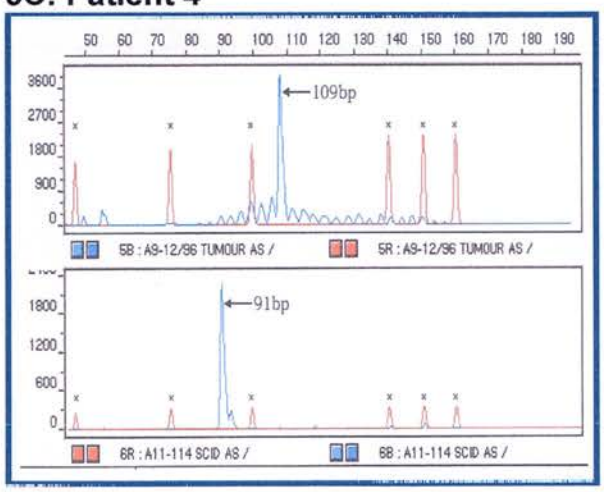

Panel 1

Panel 2

(2) EBV clonality was assessed by standard Gardella gel technique (Gardella *et al,* 1984). Biopsy and SCID tumour pairs from patients 2, 4 and 5 were analyzed. The results are shown in Figure 4.

FIGURE 4
EBV Clonality Of PTLD Biopsy And SCID Mouse Tumours

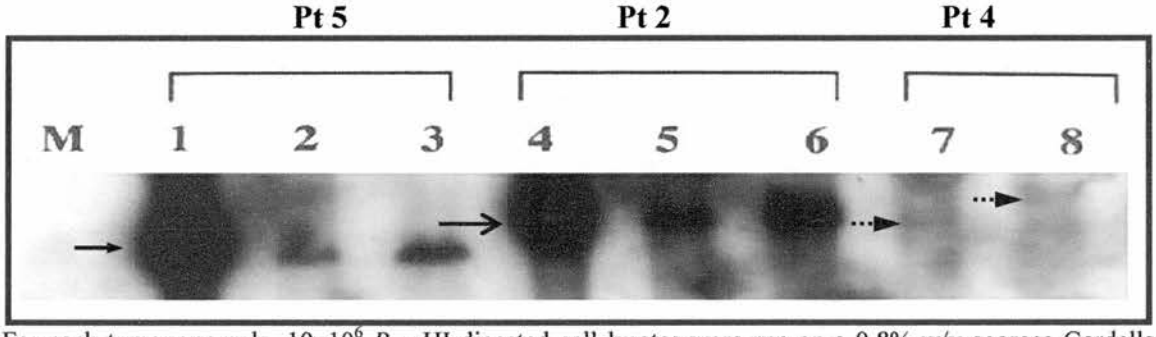

For each tumour sample, $10x10^6$ *Bam*HI-digested cell lysates were run on a 0.8% w/v agarose Gardella gel, Southern hybridized onto a nylon membrane, and probed with a radiolabelled plasmid probe (*Eco*dhet).
Lane 1: PTLD biopsy from patient 5. **Lanes 2-3:** SCID tumour (2 extracts from the same tumour material) from patient 5. **Lane 4:** PTLD biopsy from patient 2. **Lanes 5-6:** Two SCID tumours from patient 2. **Lane 7:** PTLD biopsy from patient 4. **Lane 8:** SCID tumour from patient 4. **M:** Non-radiolabelled 1Kbp DNA ladder as DNA size markers.
Pt: Patient; Clonal bands: → : Pt 5; → : Pt 2; ⇢ : Pt 4

All lesions tested contained a single band indicating virus clonality. Each PTLD biopsy and SCID tumour set from patients 2 and 5 contained identical size bands indicating that they were derived from the same infected cell in each case. Conversely, the biopsy and SCID tumour pair from patient 4 contained different EBV clones indicating that the SCID tumour arose from a non-malignant B cell in the biopsy sample.

1.2 Cell Phenotype

Next, PTLD biopsy and SCID tumour sets from patients 2-5 were immunostained to determine the cellular phenotype. Bound antibody was detected using PAP and APAAP techniques, and the proportion of specific antibody-positive cells in tumour sections was assessed using the scheme shown in Table 8.

TABLE 8
Quantification Scheme For Immunostained Tissue Sections

Score	Percentage Of Antibody-Positive Cells Out Of Total Cells Counted
-	None
OC	Occasional Cell
+/-	<5%
(+)	5-10%
1+	11-25%
2+	26-50%
3+	51-75%
4+	>75%

The results of the immunophenotyping studies are shown in Table 9.

TABLE 9
Immunophenotypic Comparison Of PTLD Biopsy And SCID Mouse Tumours

Antibody Specificity	Tumour Sample							
	Pt 2	SCID 2	Pt 3	SCID 3	Pt 4	SCID 4	Pt 5	SCID 5
TCRα/β	3+	OC	2+	-	4+	OC	3+	-
CD3	3+	OC	2+	-	4+	OC	3+	-
CD19	2+	3+	2+	2+	2+	2+	3+	3+
CD23	2+	2+	2+	2+	2+	2+	2+	3+
Polyclonal EBV Serum[1]	3+	3+	3+	3+	-	3+	3+	3+
EBNA1	3+	3+	3+	3+	-[2]	3+	3+	3+
EBNA2	2+	2+	2+	2+	-	2+	2+	2+
LMP1	1+	1+	1+	1+	1+	1+	1+	1+
BZLF1	+/-	(+)	+/-	(+)	-	(+)	+/-	(+)
EA(D)	+/-	(+)	+/-	(+)	-	(+)	+/-	(+)
VCA	+/-	(+)	+/-	(+)	-	(+)	+/-	(+)
MA	+/-	(+)	+/-	(+)	-	(+)	+/-	(+)
Mouse MHC1D[d]	NT	(+)	NT	(+)	NT	(+)	NT	(+)

NT: Not tested; TCR: T cell receptor; Pt: Patient; [1]: Polyclonal EBV+ve human serum ('JAT'; London School of Hygiene & Tropical Medicine, London); [2]: EBNA1-positive by RT-PCR

PTLD biopsy and SCID tumour pairs from all patients (number 2-5) tested expressed the B cell surface antigens CD19 and CD23 indicating an activated, B lymphoblastoid phenotype (Table 9). All biopsy material contained a substantial T cell component (26->75%) whilst all SCID tumours contained no, or only the occasional, T cell. Biopsy material from patients 2, 3 and 5 showed EBNA1 and 2 together with LMP1 suggestive of full EBV latent gene expression. All SCID tumours demonstrated similar virus gene expression profile. In biopsy lesions, low level (<5% of cells) expression of the lytic cycle antigens BZLF1, EA(D), VCA, and MA was detected. In the corresponding SCID tumours, increased (5-10%) lytic cycle antigen expression was observed. Conversely, biopsy from patient 4 showed restricted pattern of EBV gene expression with only LMP1 detected by immunostaining (although EBNA1 transcripts were detected by RT-PCR). No lytic cycle antigens were observed. The corresponding SCID tumour showed EBNA1, EBNA2 and LMP1 expression with similar lytic antigen expression [BZLF1, EA(D), VCA, MA] to other SCID tumours tested, further emphasizing differences in tumour cell type between the biopsy and SCID tumour in this case.

1.3 Expansion Of Tumour Material *In Vitro*

In vitro growth characteristics of PTLD biopsy and SCID tumour sets from patients 1 and 3 were assessed using [^{3}H]-thymidine incorporation into DNA as a measure of proliferative capacity. Representative results are shown in Figure 5.

An initial growth spurt of biopsy-derived cells was observed during the first 24 hours followed by a low proliferation rate over the ensuing 13 days. The cells subsequently died in culture. When culturing SCID tumour cells, an initial growth spurt was observed during the first 24 hours followed by a low proliferation rate over the next 6 days. A high proliferation rate was then noted on day 14 in one case, and the cells continued to grow up until day 56 when they died in culture. No permanent PTLD cell lines were established.

FIGURE 5
***In Vitro* Proliferation Of PTLD Biopsy And SCID Mouse Tumour (Patient 3)**

(Standard error, SE, is shown on each column as a vertical bar.)

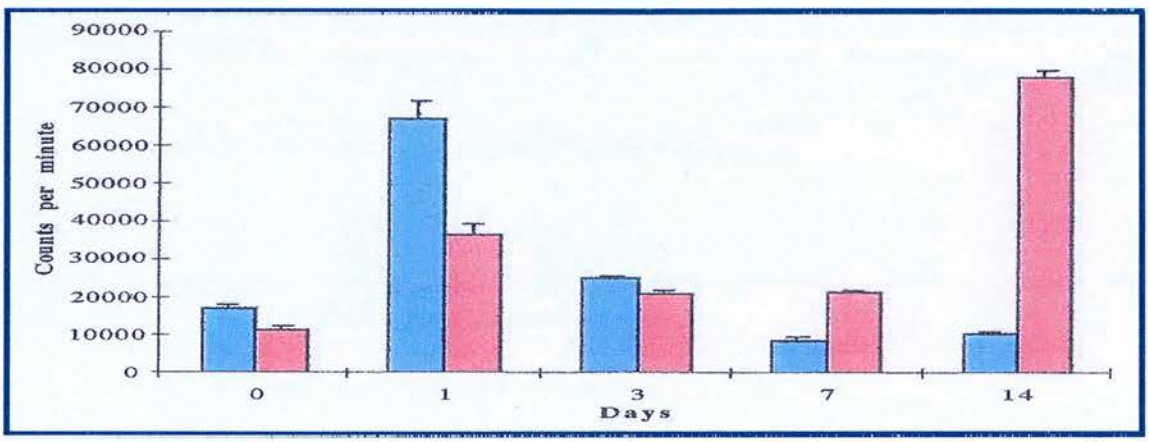

Cells were pulsed with 1μCi [^{3}H]-thymidine for 4 hours, lysed, and the DNA-incorporated [^{3}H]-thymidine was measured in a scintillation β-counter (expressed as average counts per minute).

: PTLD biopsy; : SCID tumour

1.4 Human Cytokine Gene Expression

In line with a previous report from our laboratory (Perera *et al,* 1998), extensive T cell infiltrates (≥26% of all cells; see Table 9) were apparent in all PTLD biopsy material tested. Conversely, only the occasional (or no) T cells were detected in corresponding SCID tumours. To address the possible role of T cell-derived growth factors in tumour development, the human cytokine gene expression of all lesions (from patients 1-5) were examined using RT-PCR. Representative results are shown in Figure 6.

All PTLD biopsy and SCID tumour sets demonstrated a similar cytokine profile with expression of the B cell growth factors IL2, 4, 6, 10 and IFNγ.

FIGURE 6
Human Cytokine Gene Expression: IL10

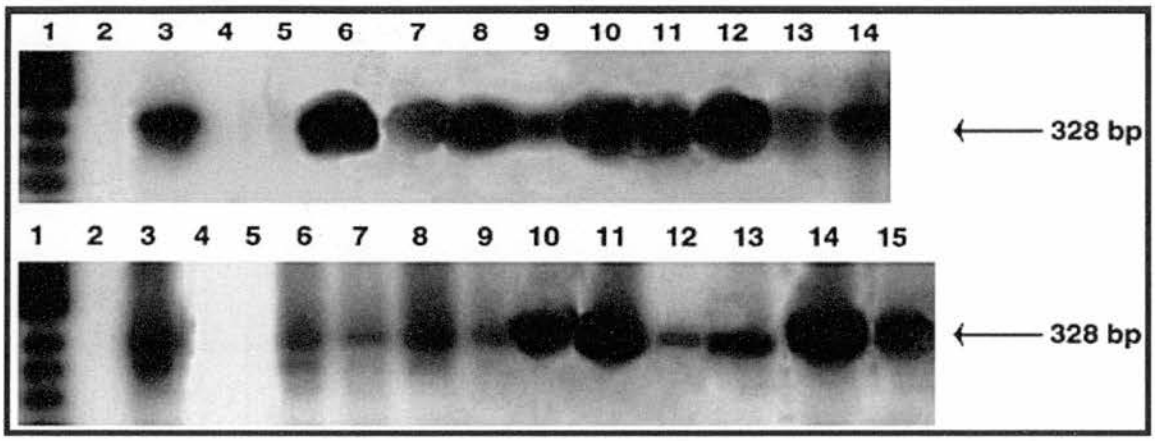

Using human IL10 primers, cDNA from 5μg of RNA was amplified in a 35 cycle RT-PCR reaction. The PCR products were run on a 2.5% w/v agarose gel, Southern transferred onto a nylon membrane, and hybridized using human IL10-specific radiolabelled oligonucleotide probe.
Top panel: PTLD biopsy results; **Lane 1**: Radiolabelled size marker; **Lane 2**: Non-radiolabelled DNA ladder; **Lane 3**: PHA-treated human PBLs; **Lane 4**: PHA-treated Balb/c murine splenocytes; **Lane 5**: Sterile distilled water; **Lanes 6-9**: Four EBV *in vitro* immortalized BLCLs; **Lanes 10-14**: PTLD biopsy material from patients 1-5, respectively. **Bottom panel**: SCID tumour results. **Lanes 1-9**: as above. **Lanes 10-15**: SCID tumours from patients 1-5, respectively. **Lanes 11-12**: Two SCID tumours derived from patient 2. Bp: Base pairs; IL: Interleukin. The size of the IL10 RT-PCR product (328bp) is indicated.

1.5 Conclusions And Discussion

We transferred PTLD biopsy material from 5 organ graft recipients successfully into SCID mice (hu-Bx-SCID model). Four (80%) of our PTLD biopsy and SCID tumour sets arose from the same malignant cell (Figures 3A,B), whereas material from one patient (number 4) that developed HL (Table 7) gave rise to a SCID lesion that did not reflect the original malignant cell (Figure 3C). Rather, the SCID tumour probably developed from a non-malignant EBV+ve 'bystander' B cell which is an observation that has been reported by others. Thus, Meggetto *et al* (1996) inoculated cell suspensions of 25 HL lymph node biopsy samples sc and ip into SCID mice. Whilst EBER transcripts were detected in Hodgkin Reed-Sternberg (HRS) cells in 8 out of 25 (32%) biopsies, 10 (40%) of these lymph node samples gave rise to EBER+ve, EBNA2+ve, LMP1+ve sc and/or ip tumours in SCID mice. Of these 10 lymph node biopsies, **(1)** 4 (40%) derived from lymph node samples containing EBER+ve HRS and EBER+ve non-

neoplastic small lymphocytes; **(2)** 5 (50%) originated from biopsies whose only EBV+ve cells were non-neoplastic small lymphocytes; and **(3)** 1 (10%) arose from a lymph node that contained EBER-ve cells only. Whilst there was a significant correlation between the detection of EBV+ve non-neoplastic lymphocytes in biopsies and SCID tumour outgrowth, no significant difference in SCID tumour formation was found between transfer of lymph node samples with and without EBER+ve HRS cells.

The biopsy from patient 4 expressed EBNA1 and LMP1 only. In contrast, biopsy material from the other patients, and all SCID tumours, expressed EBNA1, 2 and LMP1 antigens suggestive of unrestricted latency with a minor lytic [BZLF1, EA(D), VCA, and MA] component (Table 9) further underlining differences in tumour cell type between the biopsy and SCID tumour from patient 4.

It was only possible to passage SCID tumour material from one patient (number 3; see Figure 3B). Whilst the PTLD biopsy and SCID tumour from this patient were oligoclonal with an identical dominant Ig rearrangement, the passaged SCID tumours were clonal, one clone of which was identical to the dominant biopsy and SCID rearrangement. Thus, these SCID lesions may reflect clonal progression *in vivo* whereby an oligoclonal lesion (biopsy) gives rise to clonal tumours with increased malignant potential. This is in line with what is known about the natural history of PTLD in organ transplant recipients. It is generally agreed that PTLD represents a spectrum of lesions where polyclonal hyperplastic reactive (viral lymphadenitis-like) B cell proliferations may give rise in a step-wise manner to oligoclonal polymorphic and, ultimately, monoclonal monomorphic lymphomas with increasing malignant potential and resistance to therapy (Larratt *et al,* 2001).

All PTLD biopsy and SCID tumour sets demonstrated a similar cytokine profile that included the expression of the B cell growth factors IL2, 4, 6, 10 and IFNγ (Figure 6). Additional *in situ* hybridization studies in our laboratory have demonstrated that these B cell growth factors were expressed by the PTLD tumour cells themselves rather than the infiltrating T cells (Johannessen *et al,* 2000). The results obtained in the hu-SCID-Bx model support our previous model of PTLD formation (see Figure 2 in

Introduction) postulating that the malignant cells supply themselves with B cell growth factors in an autocrine cytokine-mediated manner (Johannessen *et al,* 2000).

To our knowledge, the results showed for the first time the successful expansion of a panel of PTLD biopsy material in SCID mice. Our findings contrast with an earlier report by Randhawa *et al* (1997) suggesting that such material did not generally grow *in vivo*. In their study, the group transferred 5 EBER+ve (2 polymorphic, 3 monomorphic) PTLD biopsies sc into SCID mice. Whilst all 5 mice developed sc or thymic monomorphic tumours, only 2 (40%) animals developed EBER+ve lesions (both were sc tumours). Ig gene rearrangement and EBV clonality analysis showed a clonal relationship of 1 of these 2 (50%) tumours to the corresponding biopsy sample. Randhawa *et al* concluded that human PTLD was maintained in the patient setting by host-derived growth stimuli that did not exist in the SCID mouse. Our findings do not support that conclusion (see above). Rather, our results suggest autonomous PTLD tumour development in SCID mice.

In the current study, analysis of the *in vitro* proliferation capacity of the tumour panel demonstrated that PTLD biopsy and SCID tumour cells do not survive outside the *in vivo* microenvironment (Figure 5) which is in line with previous (unpublished) results from our laboratory as well as the experience of others. Not only is it difficult to obtain adequate amount of lymphoma biopsy material for research purposes, but biopsy cells do not generally grow *in vitro,* and the occasional biopsy-derived cell line does not reflect the original tumour cell type. Thus, Cen *et al* (1993) examined EBV gene expression in 23 PTLD biopsies and demonstrated that biopsy-derived BLCL outgrowth *in vitro* reflected the selection of cell subpopulations that did not reflect the original biopsy tumour cell type.

Whilst the above sets of experiments provided an adequate quantity of SCID mouse-expanded homogenous PTLD material from 4 organ transplant recipients that was uncontaminated with infiltrating non-malignant cells, we were unable to generate PTLD biopsy-derived cell lines *in vitro* that could be used to generate further PTLD-like tumours in SCID mice. Therefore, in order to model PTLD *in vivo,* we established a SCID mouse model using *in vitro* EBV-infected BLCLs (Rowe *et al,* 1991).

2. Establishment Of A SCID Mouse Model

The aim of these experiments was to establish SCID mouse models of PTLD suitable for the testing of novel immunotherapies using inoculation of BLCLs. Thus, we inoculated BLCL cells generated from a panel of healthy EBV-seropositive blood donors either sc or ip to create hu-BLCL-SCID models in which to study **(1)** tumour regression and **(2)** tumour prevention, respectively.

2.1 Sc Hu-BLCL-SCID Model: Tumour Regression

Initially, we assessed the sc tumorigenic potential of BLCL in SCID mice. The aim was to establish an *in vivo* model in which tumour development could be visualized and measured directly providing changes in tumour volume (ie, tumour regression) over time as the read-out of the experiments. Using sc tumour development, therapeutic intervention could be instigated at the time when small sc macroscopic lesions appeared and treatment-induced tumour changes assessed.

2.1.1 Number Of BLCL Cells Required And Time To Tumour

To define the minimum cell number required for consistent BLCL-derived tumour formation *in vivo*, we inoculated groups of 3 animals (2 sites per mouse) sc with $1x10^6$, $2x10^6$ or $4x10^6$ BLCL cells derived from a panel of 10 healthy EBV seropositie donors (denoted 'donor A-J'). In parallel control experiments, PBL from 3 EBV-seronegative healthy donors were used. These did not give rise to sc tumours. The results are shown in Table 10.

TABLE 10
Tumour Development In Sc Hu-BLCL-SCID Mice

Number Of BLCL Cells Injected Sc Per Site (Donor A-J)	Number Of Tumours/ Number Of Sc Sites Injected (%)	Number Of Mice That Developed Sc Tumours In Both Flanks (%)
1 x10^6	11/20 (55)	3/10 (30)
2 x10^6	20/20 (100)	10/10 (100)
4 x10^6	20/20 (100)	10/10 (100)

Twenty out of 20 (100%) sites injected sc with either $2x10^6$ or $4x10^6$ BLCL cells showed macroscopic sc tumour outgrowth. In contrast, an inoculum of $1x10^6$ BLCL cells produced sc tumours in 11 out of 20 (55%) sites injected. In sc-inoculated mice, tumours presented as sc macroscopic circumscribed masses at the site of sc inoculation. The time to tumour development is shown in Table 11. It took a median time of 10, 5, and 5 weeks for sc tumours to develop when an inoculum of $1x10^6$, $2x10^6$ and $4x10^6$ BLCL cells was used, respectively.

TABLE 11
Time To Tumour Formation In Sc Hu-BLCL-SCID Mice

Donor	Number Of BLCL Cells Inoculated Sc Into Each Flank		
	1x10^6	**2x10^6**	**4x10^6**
	Right/Left Flank	**Right/Left Flank**	**Right/Left Flank**
A	10/9	4/7	3.5/5
B	NTD/NTD	5/5	4/6
C	7/NTD	7/6	7/7
D	9/NTD	4/5	4/6
E	11/NTD	4.5/6	4.5/5
F	15/NTD	4.5/6	4/6
G	8.5/10	4/5	3.5/4.5
H	12/13	5/6.5	4.5/5
I	NTD/NTD	7/8	5/6
J	9/NTD	4.5/7	4/4
Median Time (Weeks) To Macroscopic Sc Tumour Formation	**10**	**5**	**5**

NTD: No tumour developed

Injection of $2x10^6$ BLCL cells per sc site was the minimum requirement for consistent sc tumour outgrowth in 5 weeks. Therefore, we induced sc tumours in all our animals with this standard BLCL does.

2.2 Ip Hu-BLCL-SCID Model: Tumour Prevention

Next, we assessed the ip tumorigenic potential of BLCL in SCID mice. The aim was to establish an *in vivo* model in which the effects of novel preventative therapy on tumour development could be ascertained using presence or absence of ip tumours as the read-out of the experiments.

2.2.1 Number Of BLCL Cells Required And Time To Tumour

To define the minimum cell number required for consistent BLCL-driven ip tumour formation *in vivo*, we inoculated groups of 3 animals with $1x10^6$, $2x10^6$ or $4x10^6$ BLCL cells derived from a donor panel of 5 healthy EBV-seropositive donors (denoted 'donor K-O'). In parallel control experiments, PBL from 3 EBV-seronegative healthy donors were used. These did not give rise to ip tumours. The results are shown in Table 12.

TABLE 12
Tumour Development In Ip Hu-BLCL-SCID Mice

Number Of BLCL Cells Injected Ip (Donor K-O)	Number Of Tumours/ Number Of SCID Mice Injected (%)
$1 x10^6$	2/5 (40)
$2 x10^6$	5/5 (100)
$4 x10^6$	5/5 (100)

Five out of 5 (100%) mice injected ip with either $2x10^6$ or $4x10^6$ BLCL cells developed macroscopic ip tumours. In contrast, an inoculum of $1x10^6$ BLCL cells produced ip tumours in 2 out of 5 (40%) animals injected. In ip-injected animals, ip tumours presented as macroscopic circumscribed masses in the upper or middle abdominal cavity at the under surface of the liver at the porta hepatis or in the mesentery. At times, the lesions extended into the liver. The time to tumour development is shown in Table 13. It took a median time of 6, 6.5, and 6 weeks for ip tumours to develop when an inoculum of $1x10^6$, $2x10^6$ and $4x10^6$ BLCL cells was used, respectively.

TABLE 13
Time To Tumour Formation In Ip Hu-BLCL-SCID Mice

Donor	Number Of BLCL Cells Inoculated Ip		
	$1x10^6$	$2x10^6$	$4x10^6$
K	NTD	6.5	6
L	NTD	13	11
M	7	7	6
N	NTD	6	4
O	5	5	4
Median Time (Weeks) To Macroscopic Ip Tumour Formation	**6**	**6.5**	**6**

NTD: No tumour developed; Ip: Intraperitoneally

Injection of $2x10^6$ BLCL cells ip was the minimum requirement for consistent ip tumour outgrowth in SCID mice in 6.5 weeks. Therefore, we induced ip tumours in all our animals with this standard BLCL dose.

2.3 Factors Influencing/Predicting Tumour Development

Previously, we have examined the effect of **(1)** age of SCID mice at the time of inoculation of EBV-infected B cells, **(2)** sex of mice, **(3)** murine serum Ig (mo-s-Ig) levels, and **(4)** murine NK cell activity on PTLD-like tumour development *in vivo* and

found none of these factors to adversely influence tumour outgrowth (Johannessen, 1997; Johannessen *et al,* 2000). Therefore, they were not studied further and 4-15 weeks' old SCID mice of both sexes used in all subsequent experiments without depletion of endogenous (murine) NK cells or measurements of mo-s-Ig levels. Equally, we have previously established that EBV-infected B cells do not give rise to PTLD-like lesions *in vivo* beyond a period of 100 days after inoculation and, thus, all experiments were terminated at this time point. Whilst we have also demonstrated previously that fresh and frozen PBL stocks are equally able to give rise to ip tumours in the hu-PBL-SCID model, we used freshly *in vitro* cultured BLCL, CTL and T cell subsets in all subsequent experiments unless otherwise stated.

We have previously analyzed the usefulness of changes in mouse weight and human serum Ig (hu-s-Ig) levels in predicting tumour outgrowth in SCID mice inoculated with EBV-infected B cells, and not found these factors to be helpful in forecasting tumour formation *in vivo* (Johannessen, 1997). Therefore, changes in murine weight or hu-s-Ig were not used to predict tumour development in the animals.

2.4 Analysis Of Tissues And Tumours

The aim of these experiments was to determine the histology of BLCL-derived tumours in SCID mice and to assess the tissue distribution of tumour cells in BLCL-inoculated animals. Initially, paraffin wax-embedded tissue sections from lung, liver, spleen and any tumour tissue from a panel of 10 sc and 10 ip mice inoculated with BLCL from different donors were screened using **(1)** H&E staining, **(2)** anti-human CD45 and CD20 immunostaining, **(3)** *in situ* hybridization for EBERs, and **(4)** immunostaining for EBV latent (EBNA2, LMP1) and IE lytic (BZLF1) antigens. Tissue sections from mice injected with saline only were used as species-specific controls for all immunohistochemical analysis (for all other control tissues used, see Materials & Methods). The results of analysis of serial tissue sections were as follows:

(1) H&E: Sections were scored for distortion of normal tissue morphology and cellular infiltrations. Large immunoblastic tumour cells were only consistently detected in sc and ip tumour tissues (see Figures 7C-D).

(2) Human CD45 and CD20: Scattered or small foci of human CD45+ve, CD20+ve cells were rarely found in lung and liver, occasionally in spleen, and abundantly in sc and ip tumour tissues (see Figures 7E-H).

(3) EBERs: Scattered or small foci of EBER+ve cells were rarely found in lung and liver, occasionally in spleen, and abundantly in sc and ip tumour tissues (see Figures 8A-B).

(4) EBV Antigens: EBER+ve cells in tumour tissue were found to express the latent EBNA2 and LMP1 antigens with the occasional cell expressing the IE lytic BZLF1 lytic antigen (see Figures 8C-H).

Macroscopic sc and ip BLCL-derived lesions were EBV+ve human B immunoblastic tumours portraying full (unrestricted) latent virus gene expression with the occasional tumour cell in lytic cycle. Immunostaining of the murine pan-nucleated cell marker MHC1 on tumour sections showed no (or the very occasional) murine cell underlining further that the lesions were human in origin. Taken together, tumours in sc and ip hu-BLCL-SCID mice reflect PTLD in the organ transplant recipient.

In light of the above results as well as published reports (Rowe *et al,* 1991; Picchio *et al,* 1992; Johannessen *et al,* 2000), further macroscopic sc and ip tumours were not examined for their histological or EBV status, but were assumed to be EBV+ve, PTLD-like lesions. Furthermore, microscopic tumours were assumed only to develop in animals with macroscopic lesions.

FIGURE 7
Immunophenotyping Of SCID Mouse Tumours: Human Leukocyte Markers
(Paraffin Wax-Embedded Sections)

Figures 7A,B: Photographs of the peritoneal cavity of ip inoculated control (Figure 7A: suspension medium only) and test (Figure 7B: BLCL) SCID mice taken at necropsy. Arrow indicates ip BLCL-derived tumour in test mouse (Figure 7B). **Figures 7C** (x100)**,D** (x400): Photomicrographs of H&E staining of tumour sections showing large lymphoblastoid tumour cells with large nuclei (blue haematoxylin staining) and scant cytoplasm. **Figures 7E,F** (x400): Photomicrographs of immunostaining of the human pan-leukocyte marker CD45 on tumour sections using an alkaline phosphatase (AP) label. Figure 7E shows CD45+ve human cells (red membrane staining) counterstained with Mayer's haemalum. Figure 7F shows the conjugate control with counterstained cells only. **Figures 7G,H** (x400): Photomicrographs of immunostaining of the human pan-B cell marker CD20 on tumour sections using a peroxidase (HRP) label. Figure 7G shows CD20+ve human cells (brown membrane staining) counterstained with Mayer's haemalum. Figure 7H shows the conjugate control with counterstained cells only.

The panels show a single mouse experiment but are representative of several experiments.

7A: Necropsy (Normal)

7B: Necropsy (Ip Tumour)

7C: H&E

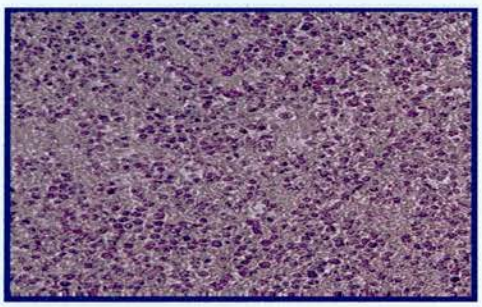

7D: H&E

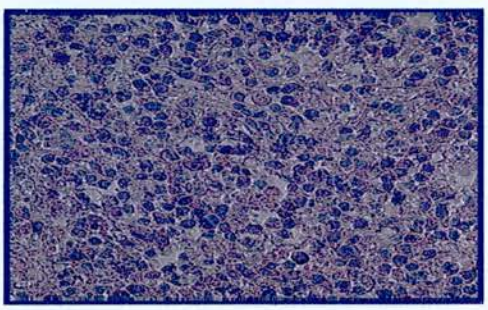

7E: CD45

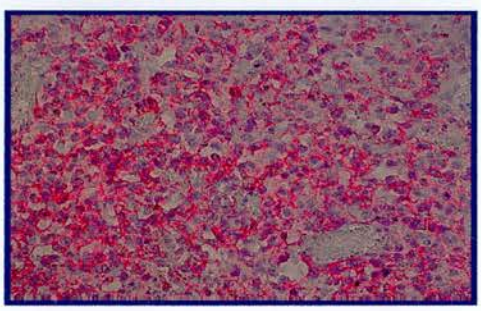

7F: CD45 Control

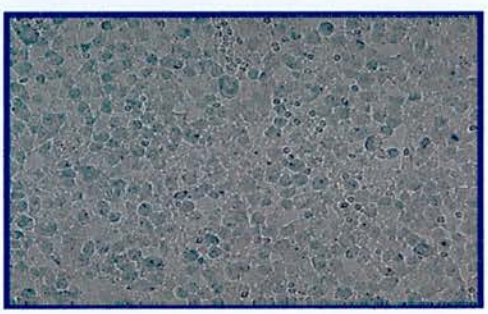

7G: CD20

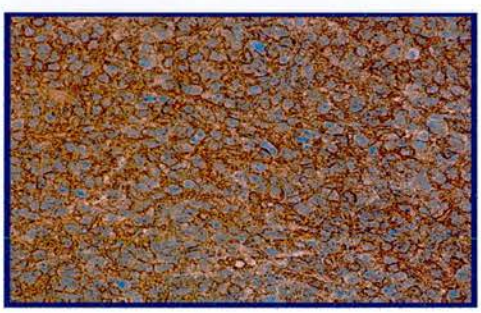

7H: CD20 Control

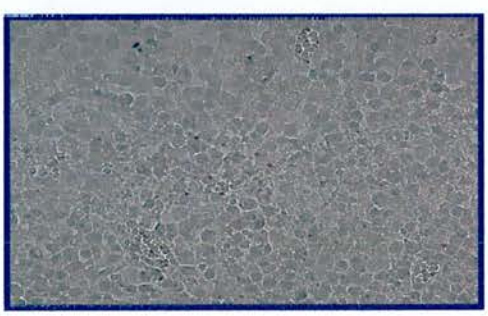

FIGURE 8
Immunophenotyping Of SCID Mouse Tumours: EBV Transcripts/Antigens
(Paraffin Wax-Embedded Sections)

Figures 8A,B (x400): Photomicrographs of *in situ* hybridization for EBERs on tumour sections using an alkaline phosphatase (AP) label. Figure 8A shows EBER+ve cells (dark blue/black nuclear staining) on a probed tumour section which was counterstained with Mayer's haemalum (blue nuclear staining). Figure 8B shows the counterstained unprobed (negative) control tumour section. **Figures 8C,D** (x400): Photomicrographs of immunostaining of EBNA2 on tumour sections using an alkaline phosphatase (AP) label. Figure 8C shows EBNA2+ve cells (red nuclear staining) counterstained with Mayer's haemalum (superimposed blue nuclear staining). Figure 8D shows the conjugate control with counterstained cells only. **Figures 8E,F** (x400): Photomicrographs of immunostaining of LMP1 on tumour sections using an alkaline phosphatase (AP) label. Figure 8E shows LMP1+ve cells (red membrane staining) counterstained with Mayer's haemalum (blue nuclear staining). Figure 8F shows the conjugate control with counterstained cells only. **Figures 8G,H** (x400): Photomicrographs of immunostaining of BZLF1 on tumour sections using an alkaline phosphatase (AP) label. Figure 8G shows BZLF1+ve cells (red cytoplasmic staining) counterstained with Mayer's haemalum (blue nuclear staining). Figure 8H shows the conjugate control with counterstained cells only.

The panels show a single mouse experiment but are representative of several experiments.

Arrows point to examples of specific transcript+ve/antibody+ve cells.

8A: EBERs

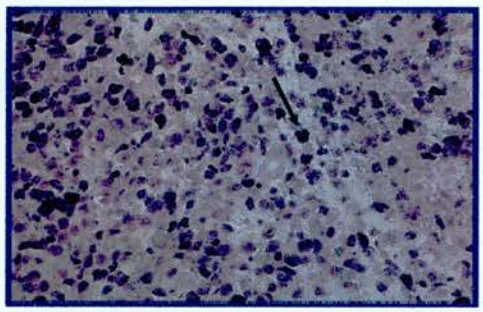

8B: EBERs Control

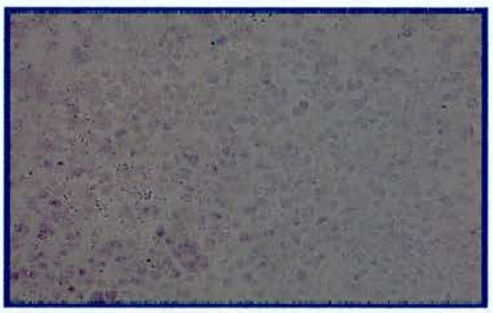

8C: EBNA2

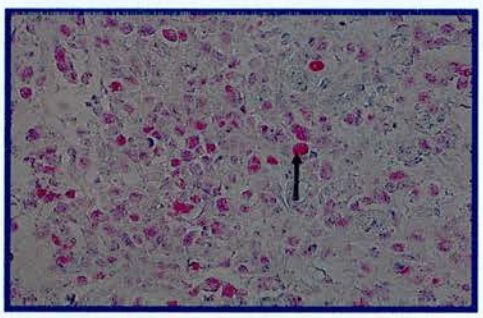

8D: EBNA2 Control

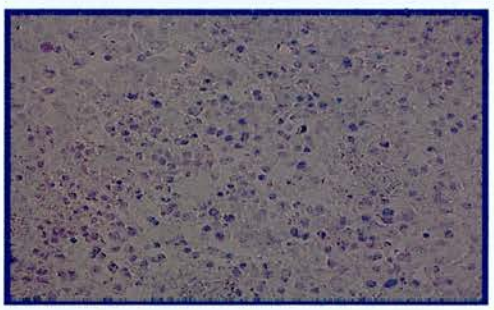

8E: LMP1

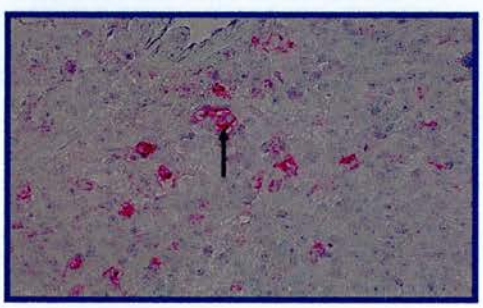

8F: LMP1 Control

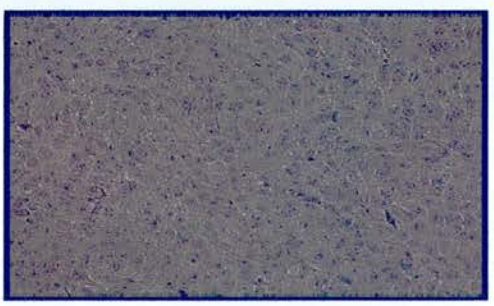

8G: BZLF1

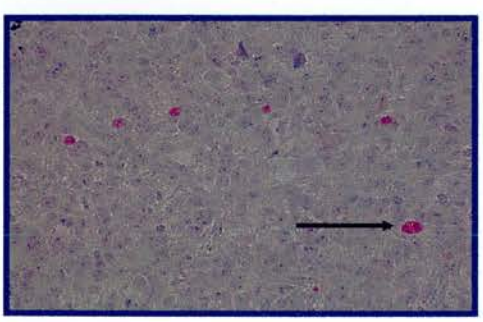

8H: BZLF1 Control

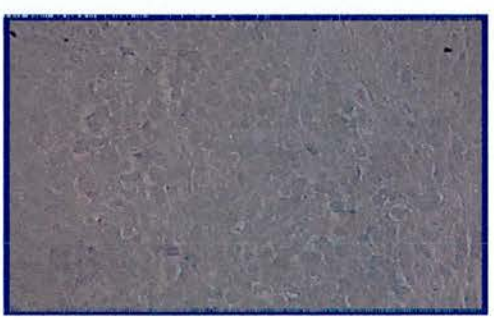

2.5 Conclusions And Discussion

Based on the standardization experiments, the following points were established regarding the sc and ip hu-BLCL-SCID mouse models:

(1) A minimum inoculum of $2x10^6$ BLCL cells consistently gives rise to macroscopic sc and ip tumours in SCID mice.

(2) BLCL-derived macroscopic sc and ip tumours in SCID mice are immunoblastic human CD45+ve, CD20+ve B cell lesions.

(3) The SCID tumours are EBER+ve and show unrestricted latent EBV gene expression with the occasional tumour cell in lytic cycle.

(4) Control mice injected with suspending medium alone, or PBLs from EBV-seronegative donors, do not develop PTLD-like tumours *in vivo*.

In light of the above, we concluded that BLCL-derived SCID tumours mirror PTLD in the organ transplant recipient and, therefore, BLCL-inoculated SCID mice can be used to model the disease. Overall, the results agree with other published data by Rowe *et al* (1991) and Lacerda *et al* (1996) who obtained consistent tumour growth following sc or ip inoculation of BLCLs into SCID mice. The lesions that developed were EBV+ve human B cell immunoblastic malignancies identical to PBL-derived SCID tumours and PTLD. Whilst sc tumours developed locally, ip lesions formed at the porta hepatis and in the mesentery.

The optimized experimental design used in subsequent experiments involved sc or ip transfer of $2x10^6$ BLCL cells that consistently give rise to sc and ip tumours, respectively, within a median time of 5-7 weeks (Tables 10-13) in experimental groups of at least 3 SCID mice. Mice were sacrificed **(1)** when any sc tumour diameter reached 18 mm (as stipulated by the Project Licence); **(2)** at the time of signs of ip tumour; **(3)** at a pre-set time limit of 100 days. Following termination, macroscopic examination at necropsy was carried out together with routine harvesting of tumour (if present), lung, liver and spleen tissue.

Donor BLCLs consistently gave rise to sc and/or ip tumours in SCID mice. In contrast, we (and others) have shown that PBLs from EBV-seropositive donors vary greatly in their ability to give rise to ip tumours in the hu-PBL-SCID model, (Picchio *et al,* 1992; Johannessen *et al,* 1998, 2000). Therefore, these two SCID models differ in terms of the ability of the EBV-infected cells to give rise to tumours *in vivo* although the specific mechanisms are not yet clear (see General Discussion).

Next, we established and characterized panels of EBV-specific CTLs *in vitro* with a view to investigating the capacity of these cells to mediate tumour regression in the sc hu-BLCL-SCID model.

3. Adoptive Immunotherapy And Hu-BLCL-SCID Mice

Initially, we established a panel of 28 healthy EBV-seropositive blood donors (denoted 'donor 1-28'). EBV serostatus was confirmed by indirect immunofluorescence anti-VCA immunostaining. Tissue typing of donor PBLs was carried out at the Anthony Nolan Research Institute (London) or the Scottish National Blood Transfusion Service (Edinburgh) using PCR-based methods. The results are shown in Table A8 in Appendix 1. Using this donor panel, we established BLCL and EBV-specific CTL sets (BLCLs only were established from donors 26-28).

3.1 Phenotype Of *In Vitro* Expanded T Cells

In order to expand EBV-specific T cells from PBLs *in vitro* from donors 1-25 and after an initial *in vitro* growth period of 10 days, weekly stimulations using x-irradiated autologous BLCLs were carried out and IL2 was added to cultures every second day (from day 14). The cell surface phenotype of the 25 T cell lines was determined using flow cytometry to delineate the relative proportion of T and NK cell subsets. The results are shown in Table A9 in Appendix 1.

Cells were harvested following 7-17 weeks (median: 10 weeks) of *in vitro* culture. At that time, 0-96% (median: 6%) were CD4+ve T cells whereas 3-97% (median: 84%) were CD8+ve T cells. Of the 19 cell lines tested, 0-20% (median: 1%) of the cells were CD56+ve NK cells. On all occasions, cultures contained <1% CD19+ve B cells.

3.2 Cytotoxic Function Of *In Vitro* Expanded T Cells

In order to assess the cytotoxic function of the T cell lines generated from PBLs from donors 1-25, we carried out a 4 hour standard ^{51}Cr-release assay. The target cells included autologous and allogeneic (MHC mismatched) BLCLs as well as the NK target K562. Tests were carried out at effector to target ratios of 20:1, 10:1, and 5:1. The

results for an effector:target ratio of 10:1 for each individual donor are shown in Table A10 in Appendix 1.

At a 10:1 effector:target ratio, T cells from the 25 donors lysed 2-91% (median: 36%) of autologous BLCL targets whereas 0-30% (median: 6%) of allogeneic BLCL targets were killed. Zero to 40% (median: 7%) of the NK cell target K562 were lysed by the T cells.

An overview of percentage (%) specific lysis is shown in Figure 9.

FIGURE 9
% Specific CTL Lysis At A 10:1 Effector:Target Ratio
(Donors 1-25)

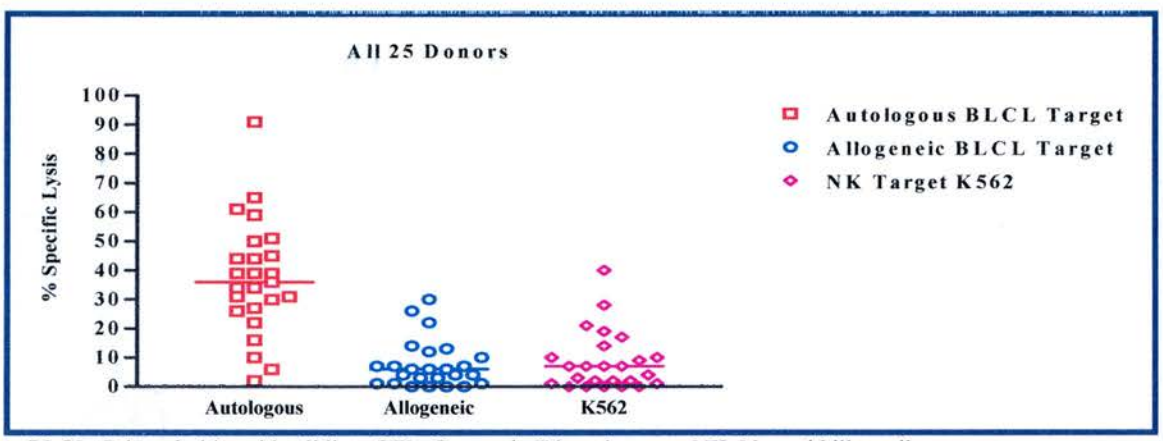

BLCL: B lymphoblastoid cell line; CTL: Cytotoxic T lymphocytes; NK: Natural killer cell
(For each column, the median is shown as a horizontal bar.)

Further analysis shows a significant difference between median % specific lysis when comparing autologous targets with either allogeneic target cells, or the NK target K562 (Mann-Whitney test: $p<0.0001$ on both occasions). We concluded that our *in vitro* expanded T cells were EBV-specific CTLs.

3.3 Sc Hu-BLCL-SCID Model: Tumour Regression

For our studies in the sc hu-BLCL-SCID mouse model, we used **(1)** unfractionated CTL populations and **(2)** T cell subset-enriched T cells.

3.3.1 Unfractionated CTL Populations

Initially, we examined the anti-tumour capacity of unfractionated CTL populations in the sc hu-BLCL-SCID model.

In Vivo Sc Tumour Regression Following Iv CTL Transfer

In order to assess the potential effectiveness of *in vitro* expanded T cell lines in mediating regression of PTLD-like tumours *in vivo*, we used autologous BLCL and CTL cell sets from 4 donors (number 1, 3-5; see Tables A8-10 in Appendix 1). For each donor, $2x10^6$ BLCL were used to induce a sc tumour in the right flank of each mouse in groups of 6-12 animals. At the first sign of macroscopic sc tumour development, direct thrice weekly tumour measurements were commenced and half of each group (3-6 mice) were injected iv with autologous CTLs whereas the other half of the animals (3-6 mice) received iv suspension medium only. Cell transfer details are shown in Table 14.

TABLE 14
CTL Cell Numbers Used *In Vivo*
(Donors 1, 3-5)

	Number Of Cells Inoculated Iv Per Mouse			
	CTLs ($x10^6$)	CD4+ve T Cells ($x10^6$)	CD8+ve T Cells ($x10^6$)	CD56+ve NK Cells ($x10^6$)
Range	4-15	0-3	4-13	0
Median	5	1	4	0

CTLs: Cytotoxic T lymphocytes; Iv: Intravenous; NK: Natural Killer

Four million to $15x10^6$ (median: $5x10^6$) autologous CTLs were inoculated iv into each mouse. Thereof, $0\text{-}3x10^6$ (median: $1x10^6$) cells were CD4+ve T cells whereas $4x10^6\text{-}13x10^6$ (median: $4x10^6$) cells were CD8+ve T cells. Less than $1x10^5$ NK cells were detected in the inocula. Individual results showing average tumour volume including regression lines are shown in Figure 10.

FIGURE 10
Sc Tumour Volume Over Time Following Iv Transfer Of 1 Dose Of Autologous CTLs (Donors 1, 3-5)
(Standard error, SE, is shown on each column as a vertical bar.)

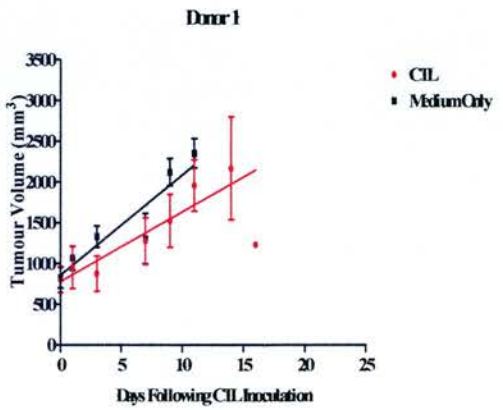

(Linear regression: p=0.25)

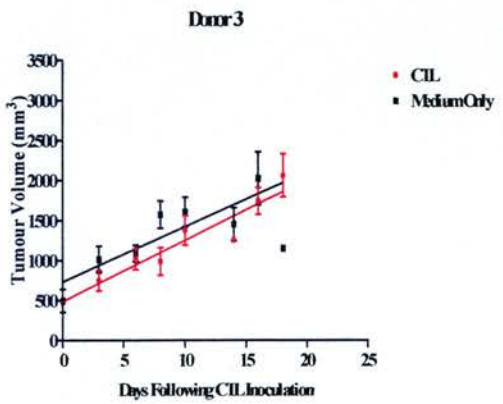

(Linear regression: p=0.66)

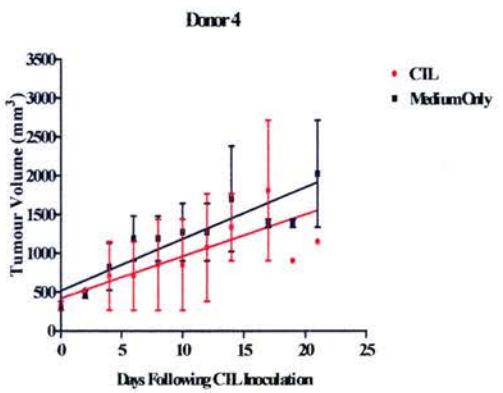

(Linear regression: p=0.63)

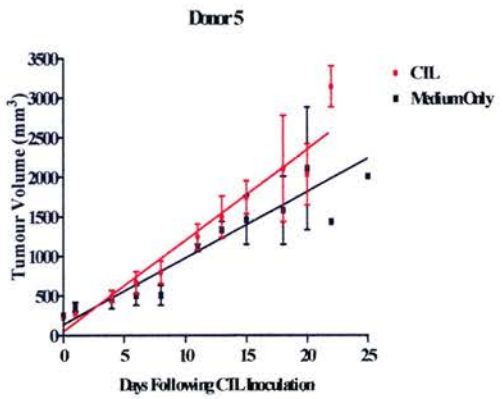

(Linear regression: p=0.03)

Regression analysis to compare the slopes of regression lines shows that for each donor the slopes were not significantly different apart from data obtained using donor 5. For this donor, $15x10^6$ CTLs (containing $3x10^6$ CD4+ve T cells) were transferred iv into each test mouse. The differences between the slopes of donor 5 regression lines were significant (Linear regression: p=0.03) suggesting that the administration of CTLs had significantly facilitated tumour progression.

The overall combined results are shown in Figure 11.

FIGURE 11
Sc Tumour Volume Over Time Following Iv Transfer Of 1 Dose Of Autologous CTLs (Donors 1, 3-5)
(Standard error, SE, is shown on each column as a vertical bar.)

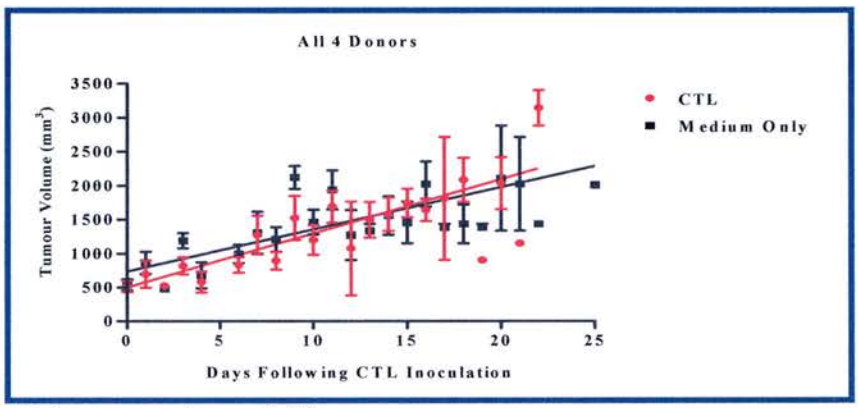

(Linear regression: p=0.12)

Regression analysis to compare the slopes of regression lines shows that for the pooled results, the slopes were not significantly different (Linear regression: p=0.12) suggesting no overall effect of administration of CTLs. Tumour growth eventually reached the maximum size permitted by our Project Licence and all animals were sacrificed.

In light of the above results, in the next set of experiments we administered 2 CTL doses iv. Thus, $2x10^6$ BLCL from 4 donors (number 1-4; see Tables A8-10 in Appendix 1) were used to induce a sc tumour in the right flank of each mouse in groups of 6-12 animals. At the first sign of macroscopic sc tumour development, direct thrice

weekly tumour measurements were commenced and half of each group (3-6 mice) were injected iv with autologous CTLs whereas the other half of the animals (3-6 mice) received iv suspension medium only. Using the same CTL lines, the second iv CTL dose followed a week later. Cell transfer details are shown in Table 15.

TABLE 15
CTL Cell Numbers Used *In Vivo*
(Donors 1-4)

	Number Of Cells Inoculated Iv Per Mouse: 1st Dose			
	CTLs ($x10^6$)	CD4+ve T Cells ($x10^6$)	CD8+ve T Cells ($x10^6$)	CD56+ve NK Cells ($x10^6$)
Range	8	0-3	6-8	0
Median	8	1	7	0
	Number Of Cells Inoculated Iv Per Mouse: 2nd Dose			
	CTLs ($x10^6$)	CD4+ve T Cells ($x10^6$)	CD8+ve T Cells ($x10^6$)	CD56+ve NK Cells ($x10^6$)
Range	4-8	0-1	3-7	0
Median	5	1	4	0

CTLs: Cytotoxic T lymphocytes; Iv: Intravenous; NK: Natural Killer

For the first dose, $8x10^6$ (median: $8x10^6$) autologous CTLs were inoculated iv into each mouse. Thereof, $0\text{-}3x10^6$ (median: $1x10^6$) cells were CD4+ve T cells whereas $6x10^6\text{-}8x10^6$ (median: $7x10^6$) cells were CD8+ve T cells. For the second dose, $4x10^6\text{-}8x10^6$ (median: $5x10^6$) autologous CTLs were inoculated iv into each mouse. Thereof, $0\text{-}1x10^6$ (median: $1x10^6$) cells were CD4+ve T cells whereas $3x10^6\text{-}7x10^6$ (median: $4x10^6$) cells were CD8+ve T cells. Less than $3x10^5$ NK cells were detected in the inocula. Individual results showing average tumour volume including regression lines are shown in Figure 12.

FIGURE 12
Sc Tumour Volume Over Time Following Iv Transfer Of 2 Doses Of Autologous CTLs (Donors 1-4)

(Standard error, SE, is shown on each column as a vertical bar.)
(Arrows indicate timing of 2nd CTL dose.)

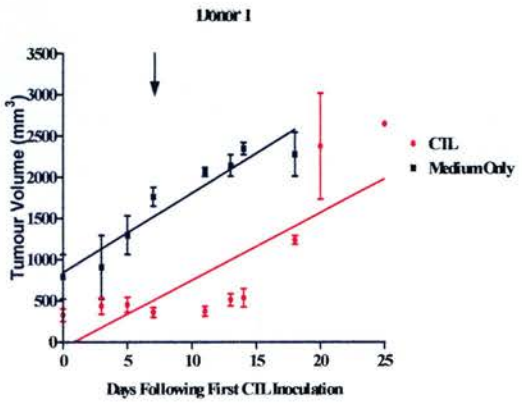

(Linear regression: p=0.57)

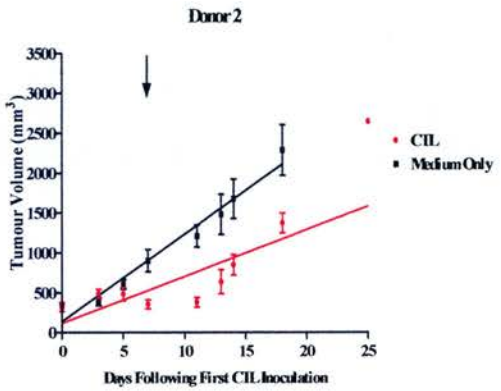

(Linear regression: p=0.0004)

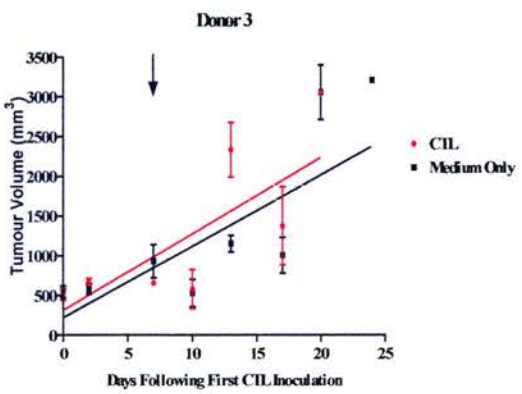

(Linear regression: p=0.84)

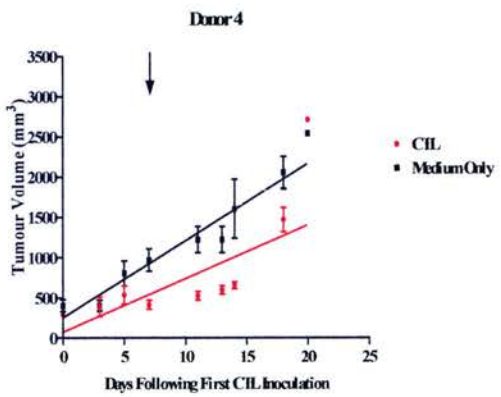

(Linear regression: p=0.08)

Regression analysis to compare the slopes of regression lines shows that for each donor the differences between the slopes were not significant apart from data obtained using donor 2. For this donor, $8x10^6$ CTLs ($1x10^6$ of which were CD4+ve T cells) were transferred iv into each test mouse on both occasions. The differences between the slopes of donor 2 regression lines were highly significant (Linear regression: p=0.0004) suggesting that the administration of 2 CTL doses significantly delayed tumour progression. The overall combined results are shown in Figure 13.

FIGURE 13
Sc Tumour Volume Over Time Following Iv Transfer Of 2 Doses Of Autologous CTLs (Donors 1-4)
(Standard error, SE, is shown on each column as a vertical bar.)
(Arrow indicates timing of 2nd CTL dose.)

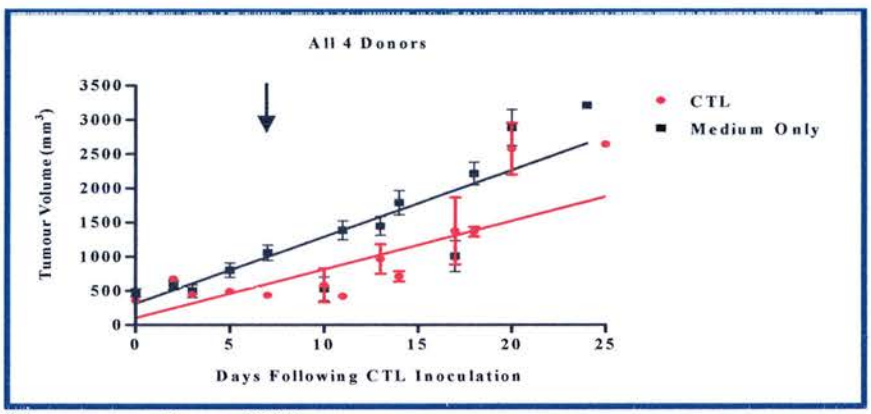

(Linear regression: p=0.01)

Regression analysis to compare the slopes of regression lines shows that for the pooled results, the slopes were significantly different (Linear regression: p=0.01) suggesting a significant delay in tumour development following the administration of 2 doses of CTLs. Tumour growth eventually reached the maximum size permitted by our Project Licence and all animals were sacrificed.

In light of the above results, we concluded that iv administration of 2 doses of $4x10^6$-$8x10^6$ autologous EBV-specific CTLs can significantly delay sc tumour growth in

SCID mice. Therefore, the use of CTL therapy at the first sign of macroscopic sc tumour development can be effective *in vivo* albeit not consistently so.

Next, we assessed the contribution of T cell subsets in mediating tumour suppression in the sc hu-BLCL-SCID mouse model. Since the above results suggested that higher CTL numbers are more effective *in vivo,* we also increased the size of our CTL inocula

3.3.2 Enriched T Cell Subsets

Next, we examined the capacity of CD4- and CD8-enriched T cell subsets to mediate tumour regression *in vivo* using our sc hu-BLCL-SCID mouse model. Due to restricted cell numbers, it was not possible to carry out cytotoxicity testing on enriched T cell subsets prior to *in vivo* studies.

First, we used donors 4, 21-22 (see Tables A8-10 in Appendix 1) to test the magnetic bead separation procedure and determine whether cell manipulation and/or cell loss during *in vitro* manipulations significantly affected *in vivo* experiments. These experiments were carried out in the ip hu-BLCL-SCID model.

Enrichment Technique

For each of the 3 donors, $2x10^6$ BLCLs were inoculated ip into each mouse in 3 groups of 3 SCID mice each. Whilst $50x10^6$ unfractionated autologous CTLs were inoculated into each animal in the first test group of 3 mice, each mouse in a second test group of 3 animals received $50x10^6$ CTLs that had been fractionated into CD4+ve and CD8+ve T cell subpopulations using magnetic beads and recombined in the original CTL subset proportions. The third (control) group received suspension medium only. The results are shown in Figure 14.

FIGURE 14
% Survival Using Unfractionated And Fractionated/Recombined CTLs (Donors 4, 21-22)
(Standard error, SE, is shown as a vertical bar.)

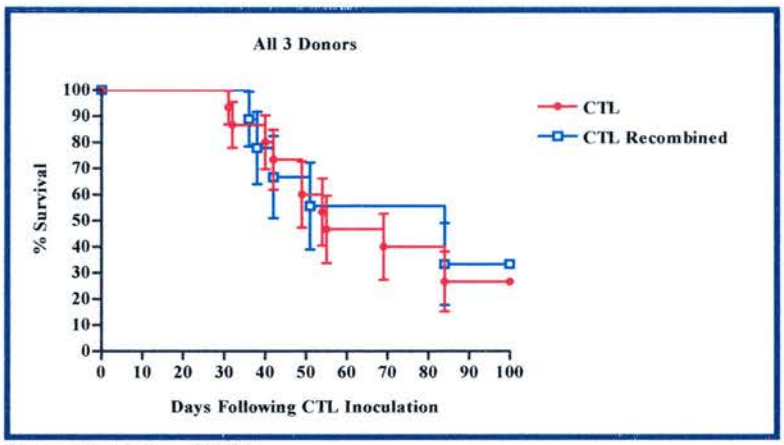

(Logrank test: p=0.71)

In the ip hu-BLCL-SCID mouse model, unfractionated CTLs and fractionated/recombined CTLs have similar effect *in vivo* (Logrank test: p=0.71). We concluded that *in vitro* manipulations *per se* do not significantly affect CTL performance in the ip hu-BLCL-SCID model. Based on these results, and the restricted availability of human leukocytes and SCID mice, we used **(1)** unfractionated CTL populations and **(2)** suspension medium only as controls in all subsequent experiments.

Enriched T Cell Subsets

Using donors 6-9 (see Tables A8-10 in Appendix 1), we enriched CD4+ve and CD8+ve T cells in our CTL samples using magnetic beads and assessed the purity of the T cell subsets obtained using flow cytometry. The individual results are shown in Table A11 in Appendix 1.

Following magnetic bead separation, 51-90% (median: 80%) of the CD4-enriched population consisted of CD4+ve T cells whereas 82-96% (median: 96%) of CD8-enriched cells were CD8+ve T cells. The CD4-/CD8-depleted subpopulations consisted of 3-62% (median: 8%) CD4+ve T cells, 4-21% (median: 5%) CD8+ve T

cells, and 9-84% (median: 80%) CD56+ve NK cells. The monocyte marker CD14 was not analyzed.

In Vivo Sc Tumour Regression Following Iv CTL Transfer

For each donor, $2x10^6$ BLCL were used to induce a sc tumour in the right flank of each mouse in groups of 3 mice each. At the first sign of macroscopic sc tumour development, direct thrice weekly tumour measurements were commenced and 3 mice were injected iv with suspension medium only whereas further groups of 3 SCID mice each were inoculated iv with autologous CTLs and T cell subsets. Cell transfer details are shown in Table 16.

TABLE 16
Cell Numbers Used *In Vivo*
(Donors 6-9)

	Number Of Cells Inoculated Iv Per Mouse			
	CTLs ($x10^6$)	**CD4-Enriched T Cells ($x10^6$)**	**CD8-Enriched T Cells ($x10^6$)**	**CD4-/CD8-Depleted T Cells ($x10^6$)**
Range	50	8-16	12-50	1-8
Median	50	10	31	8

CTLs: Cytotoxic T lymphocytes; Iv: Intravenous

Each mouse received iv either $50x10^6$ autologous EBV-specific CTLs, $8x10^6$-$16x10^6$ (median: $10x10^6$) autologous CD4-enriched T cells, $12x10^6$-$50x10^6$ (median: $31x10^6$) autologous CD8-enriched T cells, or $1x10^6$-$8x10^6$ (median: $8x10^6$) autologous CD4-/CD8-depleted T cells. Individual results showing average tumour volume including linear regression lines are shown in Figure 15. The results of regression analysis to compare the slopes of individual regression lines are shown in Table 17.

FIGURE 15
Sc Tumour Volume Over Time Following Iv Transfer Of 1 Dose Of Autologous T Cells (Donors 6-9)

(Standard error, SE, is shown on each column as a vertical bar.)

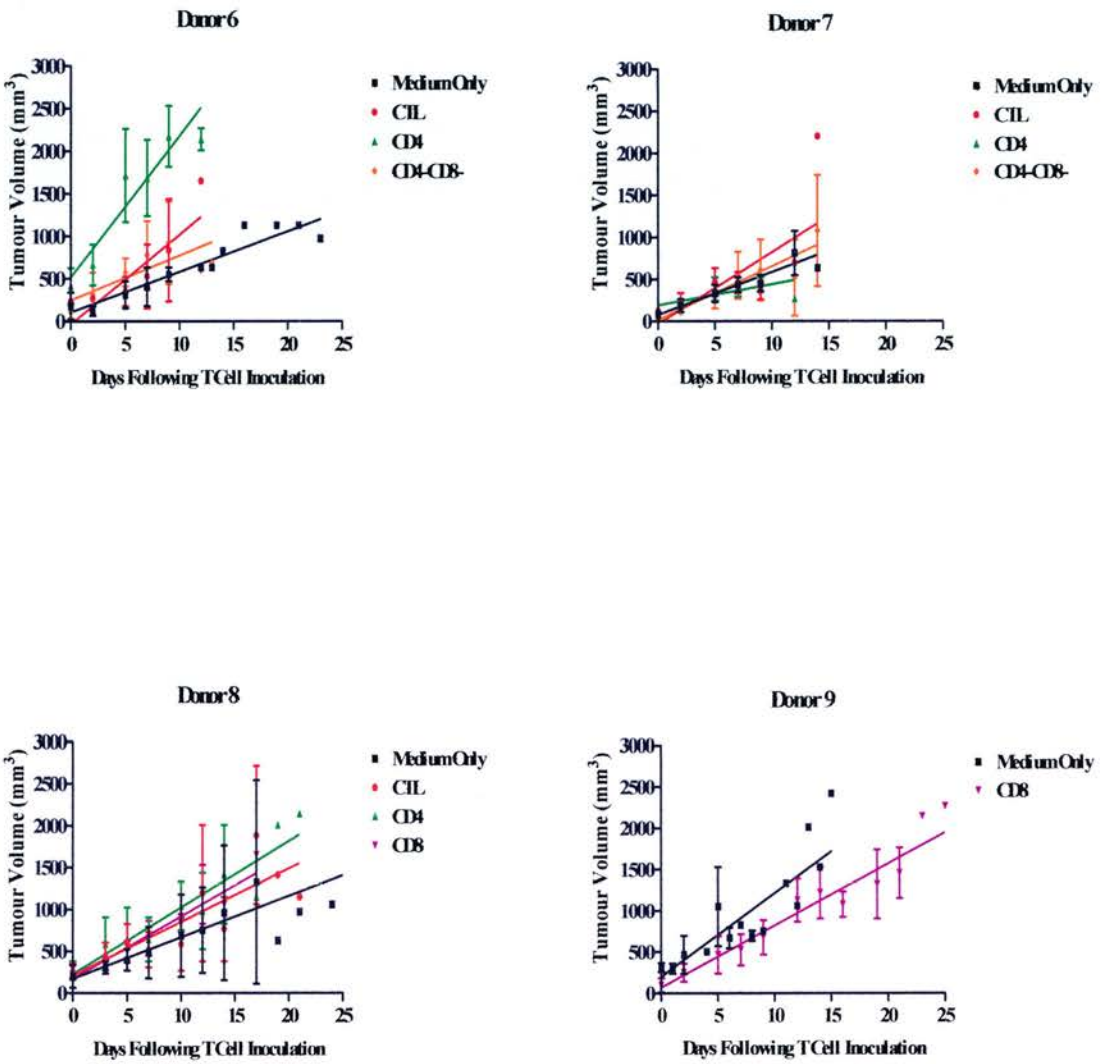

TABLE 17
Statistical Analysis (Linear Regression): Sc Tumour Volume Over Time Following Iv Transfer Of 1 Dose Of Autologous T Cells (Donors 6-9)

Regression Lines Compared		Significant Difference Between Slopes of Regression Lines?
Donor 6		
Medium and	**CTL**	No (p=0.06)
	CD4-Enriched	**Yes** (p=0.0006)
	CD4/CD8-Depleted	No (p=0.83)
CTL and	**CD4-Enriched**	No (p=0.35)
	CD4/CD8-Depleted	No (p=0.31)
CD4-Enriched and	**CD4/CD8-Depleted**	**Yes** (p=0.02)
Donor 7		
Medium and	**CTL**	No (p=0.18)
	CD4-Enriched	No (p=0.12)
	CD4/CD8-Depleted	No (p=0.61)
CTL and	**CD4-Enriched**	**Yes** (p=0.04)
	CD4/CD8-Depleted	No (p=0.55)
CD4-Enriched and	**CD4/CD8-Depleted**	No (p=0.20)
Donor 8		
Medium and	**CTL**	No (p=0.55)
	CD4-Enriched	No (p=0.24)
	CD8-Enriched	No (p=0.37)
CTL and	**CD4-Enriched**	No (p=0.53)
	CD8-Enriched	No (p=0.67)
CD4-Enriched and	**CD8-Enriched**	No (p=0.80)
Donor 9		
Medium and	**CD8-Enriched**	No (p=0.10)

CTL: Cytotoxic T lymphocytes

For donor 6, statistical analysis shows a significant difference between the slopes of regression lines for medium only and CD4-enriched T cells as well as between CD4-enriched and CD4-/CD8-depleted cells (Linear regression: p=0.0006 and p=0.02, respectively). For donor 7, similar analysis shows a significant difference between the slopes of regression lines for CTLs and CD4-enriched T cells (Linear regression: p=0.04). Thus, administration of CD4-enriched T cells facilitated tumour development when using donor 6.

In contrast, mice that received CTLs from donor 7 developed tumours significantly faster when compared to animals inoculated with CD4-enriched T cells

(Linear regression: p=0.04). For donor 7, however, there was no significant difference when either of these groups was compared with animals that received medium only indicating that neither CTLs nor CD4-enriched T cells had a significant impact on tumour development *in vivo*. Tumour growth eventually reached the maximum size permitted by our Project Licence and all animals were sacrificed.

The overall combined results for the first 10 days post-inoculation of CTLs and T cell subsets are shown in Figure 16.

FIGURE 16
Sc Tumour Volume Over Time Following Iv Transfer Of 1 Dose Of Autologous T Cells (Donors 6-9)
(Standard error, SE, is shown on each column as a vertical bar.)

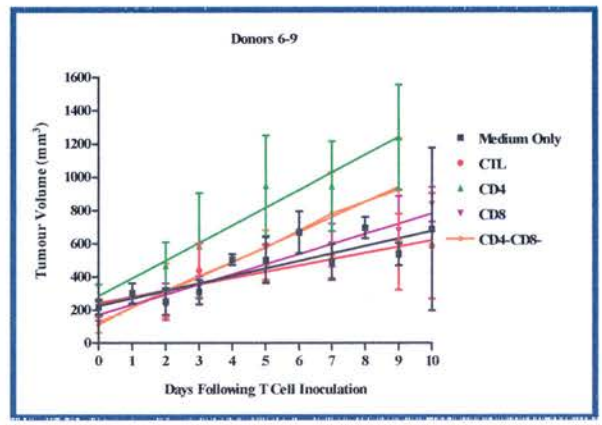

The results of regression analysis to compare the slopes of individual regression lines are shown in Table 18. Statistical analysis shows a significant difference between the slopes of regression lines for medium only and CD4-enriched T cells (Linear regression: p=0.04) suggesting that CD4-enriched T cells facilitated tumour development *in vivo*.

TABLE 18
Statistical Analysis (Linear Regression):
Sc Tumour Volume Over Time Following Iv Transfer Of
1 Dose Of Autologous T Cells
(Donors 6-9)

Regression Lines Compared		Significant Difference Between Slopes of Regression Lines?
Medium and	**CTL**	No (p=0.71)
	CD4-Enriched	**Yes** (p=0.04)
	CD8-Enriched	No (p=0.39)
CTL and	**CD4-Enriched**	No (p=0.07)
	CD8-Enriched	No (p=0.26)
CD4-Enriched and	**CD8-Enriched**	No (p=0.23)

CTL: Cytotoxic T lymphocytes

The sc hu-BLCL-SCID model proved difficult to manage because **(1)** in a group of BLCL-inoculated animals, sc tumours did not always arise at a similar timepoint making iv administration of T cells difficult. Additionally, **(2)** it was difficult to inject large T cell numbers iv without posing some risk to the animals. In order to circumvent these problems, and in line with constant efforts to refine the *in vivo* study design, we repeated the experiments in the ip hu-BLCL-SCID mouse model which circumvents these difficulties and is technically easier to manage albeit being a prevention model.

3.4 Ip Hu-BLCL-SCID Model: Tumour Prevention

The aim of these experiments was to establish whether T cell-enriched subpopulations on their own could prevent tumour development in the ip hu-BLCL-SCID model.

3.4.1 Enriched T Cell Subsets

Using 10 donors (number 6, 8-16; see Tables A8-10 in Appendix 1), we enriched CD4+ve and CD8+ve T cells in our CTL samples using magnetic beads and assessed the

purity of the T cell subsets obtained using flow cytometry. The results are shown in Table A12 in Appendix 1.

Following fractionation, 0-97% (median: 53%) of the CD4-enriched population consisted of CD4+ve T cells whereas 40-97% (median: 88%) of CD8-enriched cells were CD8+ve T cells. The CD4-/CD8-depleted subpopulations consisted of 1-49% (median: 5%) CD4+ve T cells, 14-86% (median: 20%) CD8+ve T cells, and 10-25% (median: 12%) CD56+ve NK cells. The monocyte marker CD14 was not analyzed.

In Vivo Ip Tumour Prevention Following Ip CTL Transfer

For each donor, $2x10^6$ BLCL were inoculated ip into each mouse in groups of 3 SCID mice. This was followed 1 hour later by the ip inoculation of suspension medium only into one group of 3 animals whereas further groups of 3 SCID mice each were inoculate ip with autologous T cells and T cell subsets. Cell transfer details are shown in Table 19.

TABLE 19
T Cell Numbers Used *In Vivo*
(Donors 6, 8-16)

	Number Of Cells Inoculated Ip Per Mouse			
	CTLs ($x10^6$)	CD4-Enriched T Cells ($x10^6$)	CD8-Enriched T Cells ($x10^6$)	CD4-/CD8- Depleted T Cells ($x10^6$)
Range	40-50	3-67	3-50	1-50
Median	50	7	37	16

CTLs: Cytotoxic T lymphocytes; Ip: Intraperitoneal

Each mouse received ip either $40x10^6$-$50x10^6$ (median: $50x10^6$) autologous EBV-specific CTL cells, $3x10^6$-$67x10^6$ (median: $7x10^6$) autologous CD4-enriched T cells, $3x10^6$-$50x10^6$ (median: $37x10^6$) autologous CD8-enriched T cell, or $1x10^6$-$50x10^6$ (median: $16x10^6$) autologous CD4-/CD8-depleted T cells. Animals were culled when showing signs of illness, or at a pre-determined time limit of 100 days. On each occasion, an ill mouse was found to harbour ip macroscopic tumour at necropsy.

Analysis of the proportion (%) of mice that developed ip tumours is shown in Table 20.

TABLE 20
Ip Tumour Development
(Donors 6, 8-16)

Inoculum	Medium Only	CTL	CD4+	CD8+	CD4-/CD8-
Number Of Tumours/ Number Of Mice Injected (%)	29/30 (97)	26/30 (87)	25/30 (83)	18/30* (60)	11/15* (73)

*: Statistically significant difference ($p<0.05$) when compared with mice inoculated with medium only; CTL: Cytotoxic T lymphocytes; Ip: Intraperitoneal

Tumours developed in 26 (87%), 25 (83%), 18 (60%) and 11 (73%) out of 30 mice injected with CTLs, CD4- or CD8-enriched T cells, and CD4-/CD8-depleted cells, respectively. In contrast, 29 out of 30 (97%) mice inoculated with suspension medium only formed ip tumours. Thus, significantly fewer mice inoculated with CD8-enriched T cells developed ip tumours than animals injected with suspension medium only (Fisher's exact test: 0.001). Similarly, the transfer of CD4-/CD8-depleted cells resulted in significantly fewer ip tumours than control mice (Fisher's exact test: $p=0.04$).

The time to end point (in days) for individual CTL donors is shown in Table A13 in Appendix 1, and the combined results are shown in Figure 17. Statistical analysis of the data is shown in Table A14 in Appendix 1.

FIGURE 17
Time To End Point Following Ip CTL Transfer
(Donors 6, 8-16)

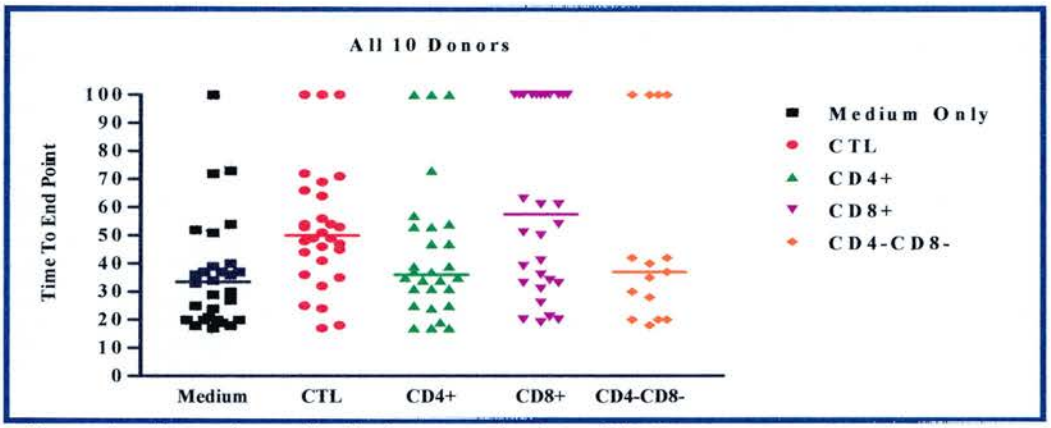

(For each column, the median is shown as a horizontal bar.)

Overall results showing proportion (%) mouse survival over time (in days) are shown in Figure 18.

FIGURE 18
% Survival Using CTLs And T Cell Subsets
(Donors 6, 8-16)
(Standard error, SE, is shown as a vertical bar.)

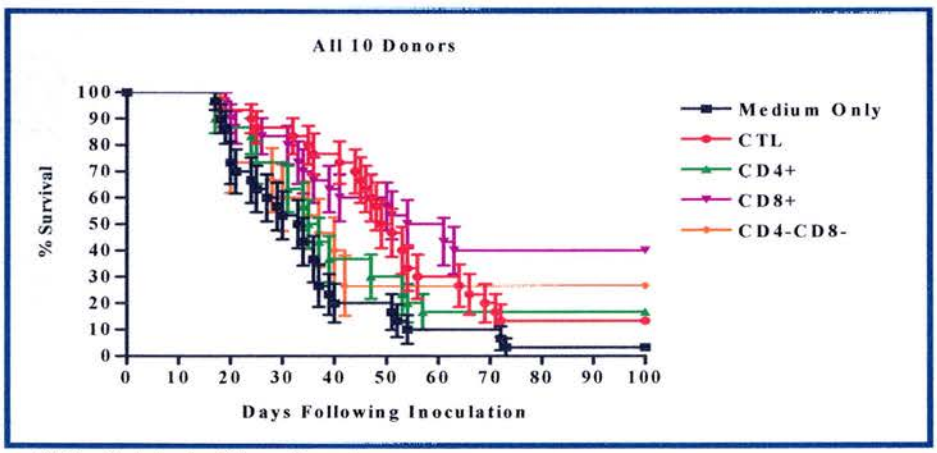

CTL: Cytotoxic T lymphocytes

Individual results together with Logrank test results are shown in Figure 19.

FIGURE 19
% Survival Using CTLs And T Cell Subsets
(Donors 6, 8-16)

(Standard error, SE, is shown as a vertical bar.)

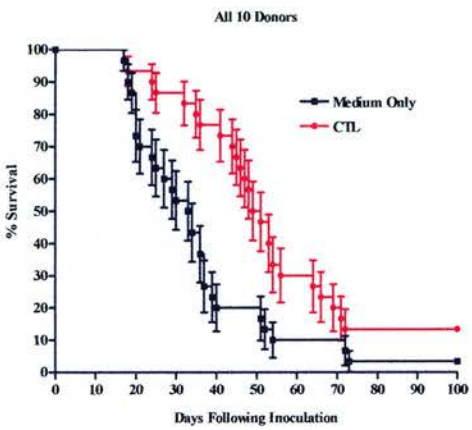

(Logrank test: p=0.003)

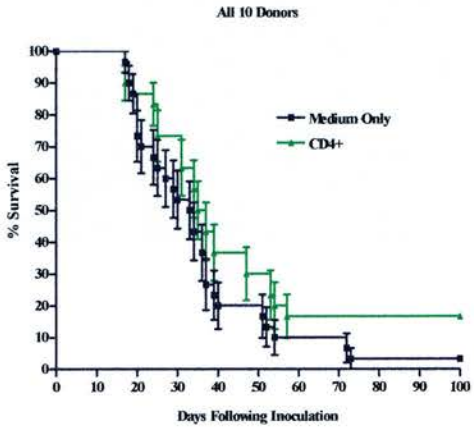

(Logrank test: p=0.101)

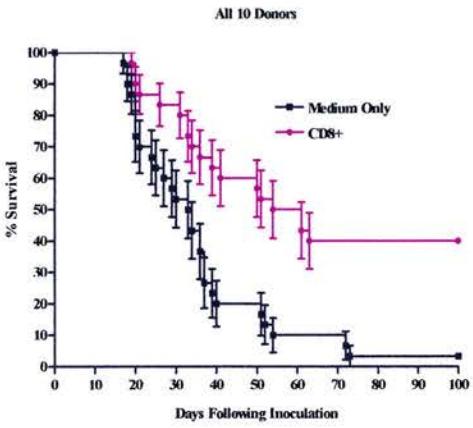

(Logrank test: p=0.0002)

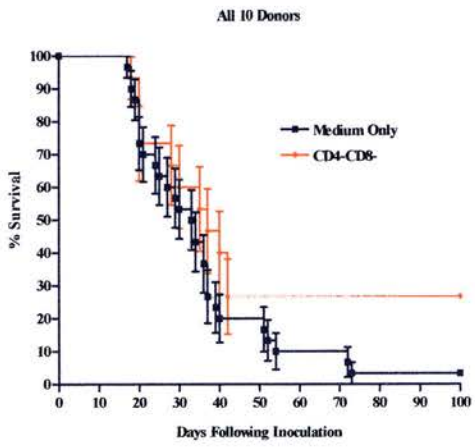

(Logrank test: p=0.09)

Overall, the median time to end point is significantly different between the groups analyzed (Kruskal-Wallis test: p=0.003). Further analysis shows that mice injected with CTLs or CD8-enriched T cells survived significantly longer than control animals (Mann-Whitney test: p=0.001 for both analysis; Logrank test: p=0.003 and p=0.0002, respectively). Conversely, the use of CD4-enriched or CD4-/CD8-depleted T cells did not significantly impact tumour development *in vivo* (Logrank test: p=0.101 and p=0.09, respectively).

Following initial CD4-enrichment, the proportion of CD4+ve cells in the transferred inoculum differed markedly between donors (see Table A12 in Appendix 1). Therefore, we re-analysed the results using data obtained when using CD4-enriched cells from the 5 donors (number 6, 8-9, 14-15) whose CD4-enriched populations contained 70-97% (median: 74%) CD4+ve cells. The results showing proportion (%) mouse survival over time (in days) together with Logrank test results are shown in Figure B1 in Appendix 1. The transfer of CD4-enriched cells from these 5 donors did not significantly impact tumour development *in vivo* (Logrank test: p=0.35) which is in line with the results above.

In light of the results, we concluded that autologous CTL and CD8-enriched T cell subsets significantly delay development of PTLD-like tumours *in vivo.* Furthermore, CD8-enriched T cells can prevent tumour formation in a significant proportion of mice (Table 20).

Role Of CTL Cytotoxicity

The role of CTL cytotoxicity (as assayed *in vitro* by ^{51}Cr-release studies) in survival of ip inoculated SCID mice was assessed by statistical testing of the data. The results of the analysis of the correlation between % specific CTL lysis of autologous BLCL targets (at a 10:1 effector:target ratio) *in vitro* (see Table A10 in Appendix 1), and the average % survival (in days) beyond control animals inoculated with medium only, is shown in Figure 20.

Statistical analysis of the data in Figure 20 shows a non-significant correlation between CTL cytotoxicity *in vitro* and % survival of CTL-inoculated SCID mice (Spearman's test: p=0.17). Since cytotoxicity assays could not be carried out on T cell subsets due to low cell numbers, it was not possible to correlate their cytotoxicity *in vitro* and survival of T cell-treated SCID mice.

FIGURE 20
% Survival As A Function Of
% Specific CTL Lysis At A 10:1 Effector:Target Ratio
(Donors 6, 8-16)

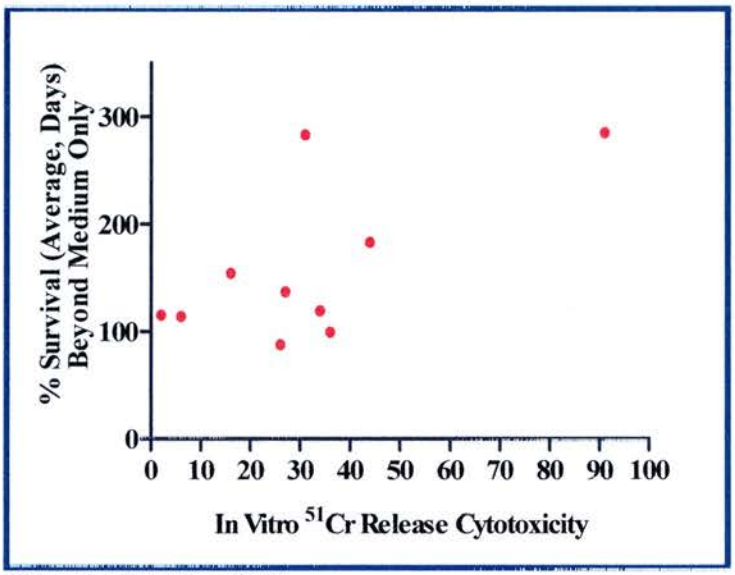

(Spearman's test: p=0.17)

3.4.2 Delayed CTL Inoculation

To study the effect of delayed ip inoculation of CTLs on tumour development in the ip hu-BLCL-SCID mouse, we ip injected $2x10^6$ BLCL from donors 4 and 21 (see Tables A8-10 in Appendix 1) into each mouse in groups of 3 animals. This was followed 3 weeks later by ip transfer into each mouse of either suspension medium only or $50x10^6$ autologous CTLs. The results are shown in Figure 21.

Delaying ip CTL inoculation for 3 weeks did not significantly improve survival (Logrank test: p=0.60). However, the impact of delaying CTL transfer needs to be

analyzed further in future studies where CTLs are administered at pre-determined time points during the initial 3 weeks post-BLCL injection.

FIGURE 21
% Survival Using Delayed CTL Ip Transfer
(Donors 4 and 21)
(Standard error, SE, is shown as a vertical bar.)

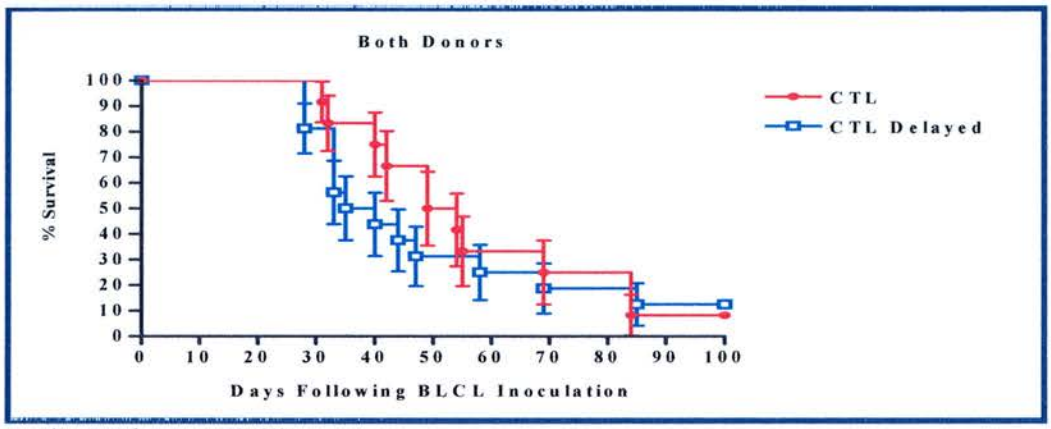

(Logrank test: p=0.60)

3.4.3 Mismatched Allogeneic CTLs

In order to assess the importance of MHC restriction on the effectiveness of transferred CTLs, we examined the ability of mismatched allogeneic CTLs to prevent ip tumour development in the ip hu-BLCL-SCID model. Thus, $2x10^6$ BLCLs from donors 27-28 (see Table A8 in Appendix 1) were ip inoculated into each SCID mouse in groups of 3 animals followed by ip injection into each mouse of either suspension medium only or $50x10^6$ mismatched allogeneic CTLs from donors 21-22 (see Tables A8-10 in Appendix 1). The results are shown in Figure 22.

Mismatched CTLs did not have a significant impact on tumour development *in vivo* (Logrank test: p=0.77). Therefore, the data suggests that tumour prevention *in vivo* is MHC restricted.

Based on our findings in the hu-BLCL-SCID model, we determined the ability of *in vitro* expanded T cell subsets to home to PTLD-like tumour tissue *in vivo.*

FIGURE 22
% Survival Using Mismatched Allogeneic CTLs
(Donors 21-22/27-28)
(Standard error, SE, is shown as a vertical bar.)

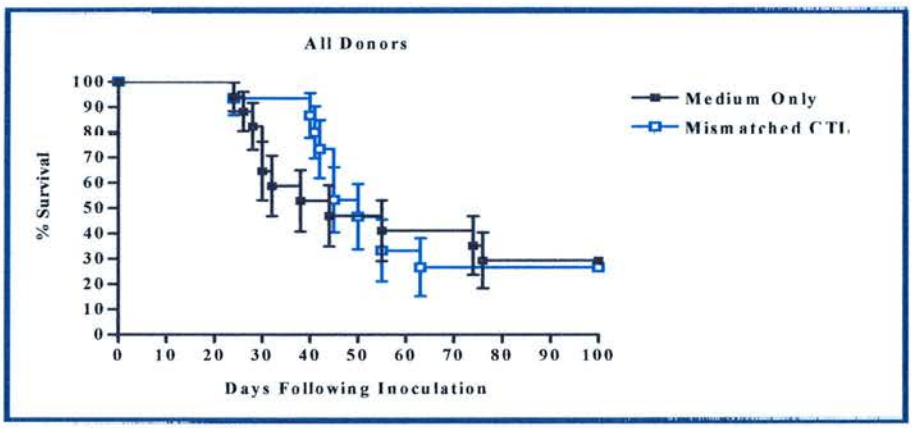

(Logrank test: p=0.77)

3.5 *In Vivo* Trafficking Of Human T Cells

Paraffin wax-embedded serial sections from lung, liver, spleen, and tumour tissue were immunostained using standard methods, and the proportion of specific antibody-positive cells was assessed using the scheme shown in Table 21.

TABLE 21
Quantification Scheme For Immunostained Tissue Sections

Score	Percentage Of Antibody-Positive Cells Out Of Total Cells Counted
-	None
(+)	<1%
1+	1-29%
2+	30-60%
3+	>60%

3.5.1 Sc Hu-BLCL-SCID-Model

Initially, we used the sc hu-BLCL-SCID model to examine human T cell trafficking *in vivo.* Using 6 donors (numbers 6, 8, 17-20; see Tables A8-10 in Appendix 1), $2x10^6$ BLCLs were sc inoculated into each SCID mouse in groups of 3 animals. At the first sign of macroscopic sc tumour outgrowth, each mouse was iv inoculated with $14x10^6$-$49x10^6$ (median: $42x10^6$) autologous CTLs. We investigated the cell surface phenotype of human leukocytes in tissues derived from 31 sc hu-BLCL-SCID (16 test and 15 control) mice harvested at each of 5 specific time points (1 animal per time point: 1 hour, or 1, 2, 7 or 14 days).

Since we only very rarely detected human CD45+ve leukocytes in lung and liver tissue, pulmonary and hepatic samples were not analyzed further. The results of the immunophenotyping studies are shown in Table 22.

TABLE 22
Immunophenotyping Of Spleen And Sc SCID Mouse Tumour Tissue (Donors 6, 8, 17-20)

Donor No	Iv Infusion	Time Post CTL Infusion	Spleen					Sc Tumour				
			CD45	CD20	CD3	CD4	CD8	CD45	CD20	CD3	CD4	CD8
6	Medium	1d	-	-	-	NT	NT	3+	3+	-	-	-
	CTL	1d	-	-	-	-	-	2+	3+	-	-	-
		7d	-	NT	-	NT	NT	1+	3+	-	-	-
8	Medium	1d	-	NT	NT	NT	NT	3+	3+	-	-	-
		7d	-	-	-	-	-	1+	1+	-	-	-
	CTL	1d	-	-	-	-	-	3+	3+	-	-	-
		7d	-	-	-	-	-	3+	3+	-	-	-
17	Medium	1hr	NT	NT	NT	NT	NT	3+	3+	-	-	-
		1d	-	-	-	NT	NT	3+	3+	NT	NT	NT
		2d	NT	NT	NT	NT	NT	3+	3+	-	-	-
		7d	NT	NT	NT	NT	NT	3+	3+	NT	NT	NT
		14d	1+	1+	-	-	-	3+	2+	-	-	-
	CTL	1hr	NT	NT	NT	NT	NT	3+	1+	-	-	-
		1d	-	-	(+)	-	(+)	3+	2+	1+	-	-
		2d	2+	2+	2+	2+	2+	3+	2+	-	-	-
		7d	NT	NT	NT	NT	NT	3+	2+	(+)	-	-
		14d	-	-	-	-	-	3+	2+	-	-	-
18	Medium	1hr	NT	NT	NT	NT	NT	3+	3+	-	-	-
		1d	NT	NT	NT	NT	NT	3+	3+	-	-	-
		2d	-	-	-	-	-	3+	2+	-	-	-
		7d	-	-	-	-	-	3+	1+	-	-	-
		14d	-	-	-	-	-	3+	1+	-	-	-
	CTL	1hr	-	-	(+)	-	-	2+	1+	-	-	-
		1d	-	-	(+)	(+)	-	3+	3+	-	-	-
		2d	-	-	-	-	-	3+	3+	(+)	-	-
		7d	(+)	(+)	-	-	-	3+	3+	-	-	-
		14d	-	-	-	-	-	3+	1+	-	-	-
19	Medium	1d	-	-	NT	-	-	3+	1+	-	-	-
	CTL	1d	-	-	-	-	-	3+	1+	-	-	-
20	Medium	1d	-	NT	NT	NT	NT	2+	1+	-	-	-
	CTL	1d	-	-	-	-	-	3+	1+	(+)	(+)	(+)

CTL: Cytotoxic T lymphocytes; d: Day; hr: hour; Iv: Intravenous; No: Number; NT: Not tested; Sc: Subcutaneous

Representative results are shown in Figure 23.

FIGURE 23
Immunophenotyping Of Sc SCID Mouse Tumour Tissue: Human Leukocyte Markers (Donors 6, 8, 17-20)
(Paraffin Wax-Embedded Sections)

Figures 23A,B (x400): Photomicrographs of immunostaining of the human pan-leukocyte marker CD45 on tumour sections using an alkaline phosphatase (AP) label. Figure 23A shows CD45-positive human cells (red membrane staining) counterstained with Mayer's haemalum. Figure 23B shows the conjugate control with counterstained cells only. **Figures 23C,D** (x400): Photomicrographs of immunostaining of the human pan-T cell CD3 marker on tumour sections using an alkaline phosphatase (AP) label. Figure 23C shows CD3-positive human cells (red membrane staining) counterstained with Mayer's haemalum. Figure 23D shows the conjugate control with counterstained cells only. **Figures 23E,F** (x400): Photomicrographs of immunostaining of the human T helper cell CD4 marker on tumour sections using an alkaline phosphatase (AP) label. Figure 23E shows CD4-positive human cells (red membrane staining) counterstained with Mayer's haemalum. Figure 23F shows the conjugate control with counterstained cells only. **Figures 23G,H** (x400): Photomicrographs of immunostaining of the human T cytotoxic CD8 marker on tumour sections using an alkaline phosphatase (AP) label. Figure 23G shows CD8-positive human cells (red membrane staining) counterstained with Mayer's haemalum. Figure 23H shows the conjugate control with counterstained cells only.

The panels represent data obtained when using cells from donor 20 (see Table 22).

Arrows point to examples of specific antibody+ve cells.

23A: CD45

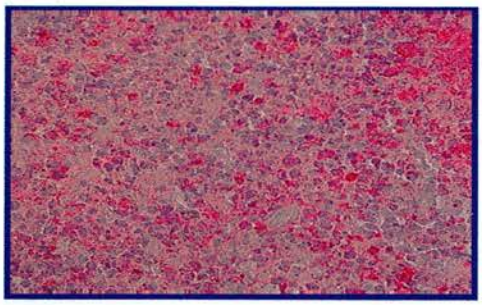

23B: CD45 Control

23C: CD3

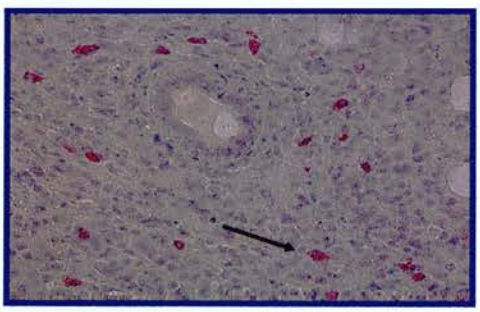

23D: CD3 Control

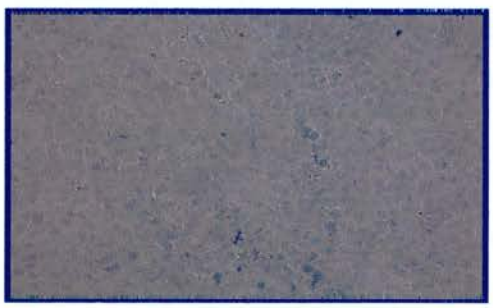

23E: CD4

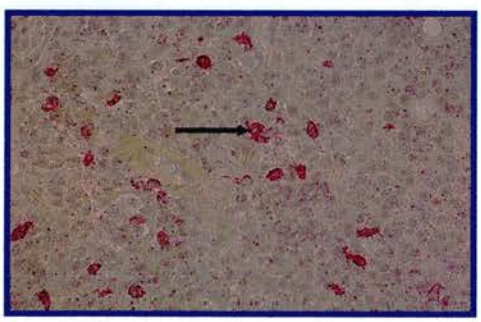

23F: CD4 Control

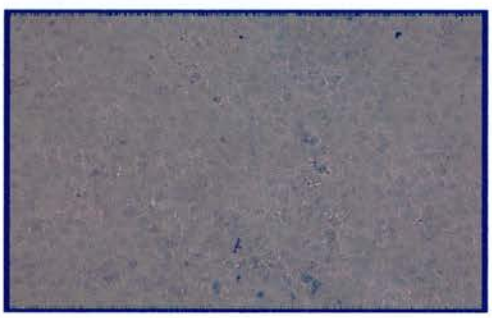

23G: CD8

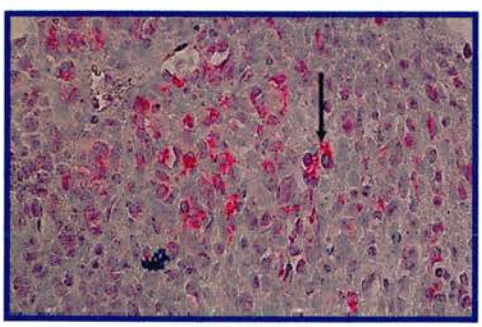

23H: CD8 Control

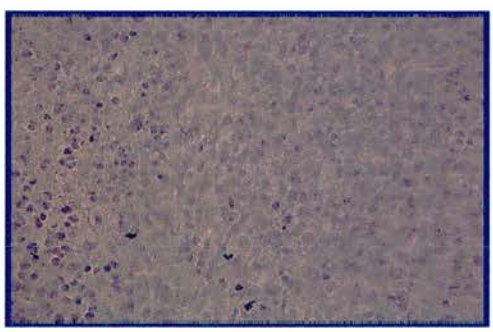

Human CD45+ve/CD20+ve B cells made up the vast majority of cells in all sc tumours that arose in control and test animals. In contrast, human B cells were only detected in splenic tissue from 1 out of 8 (13%) control animals tested (day 14). Similarly, only 2 out of 13 (15%) test animals examined had detectable human B cells in spleen (day 2 and 7).

Human T cells were not detected in control mice. CD3+ve T cells were found in splenic tissue from 4 out of 14 (29%) test mice analyzed (1 hour and day 1, 1 and 2, respectively) and in tumour tissue from 4 out of 16 (25%) test animals (day 1, 1, 2 and 7, respectively). Both tissues from 1 of these mice contained detectable CD3+ve T cells. Overall, 7 out of 16 (44%) test mice had detectable human CD3+ve T cells in either splenic and/or tumour tissue at time points up to 7 days following CTL infusion. Of these 7 test mice, samples from 2 (29%) animals contained CD4+ve T and CD8+ve T cells. Samples from further 2 (29%) test mice contained CD4+ve or CD8+ve T cells, respectively. However, tissues from the remaining 3 test animals did not immunostain with antibodies against the CD4 or CD8 surface markers. Overall, T cells comprised <1-29% of each T marker+ve tumour section. Immunostaining against NK markers was not carried out.

We concluded that human T cells can home to spleen and tumour tissue in the sc hu-BLCL-SCID mouse model. Next, we determined whether human T cells could be detected in tissues harvested at necropsy from ip hu-BLCL-SCID mice.

3.5.2 Ip Hu-BLCL-SCID Model

Serial sections of 32 paraffin wax-embedded ip tumour samples obtained in experiments described in section 3.4.1 using 10 donors (number 6, 8-16) were examined. Since human CD45+ve leukocytes were very rarely detected in lung, liver and splenic tissue, these samples were not analyzed further. The results of the immunophenotyping study are shown in Table 23.

TABLE 23
Immunophenotyping Of Ip SCID Mouse Tumour Tissue
(Donors 6, 8-16)

Donor No	Cells Inoculated Ip Into SCID Mice	CD45	CD3	CD4	CD8
6	CTL	3+	-	-	-
	CD4 Enriched	1+	-	-	-
	CD8 Enriched	NT	NT	NT	NT
	CD4/CD8 Depleted	NT	NT	NT	NT
8	CTL	1+	-	-	-
	CD4 Enriched	(+)	-	-	-
	CD8 Enriched	(+)	-	-	-
	CD4/CD8 Depleted	NT	NT	NT	NT
9	CTL	2+	1+	-	1+
	CD4 Enriched	2+	(+)	-	(+)
	CD8 Enriched	1+	-	-	-
	CD4/CD8 Depleted	3+	1+	-	1+
10	CTL	1+	-	-	-
	CD4 Enriched	3+	-	-	-
	CD8 Enriched	1+	1+	-	1+
	CD4/CD8 Depleted	2+	-	-	-
11	CTL	3+	1+	-	1+
	CD4 Enriched	3+	-	-	-
	CD8 Enriched	2+	1+	-	1+
	CD4/CD8 Depleted	3+	-	-	-
12	CTL	2+	1+	-	1+
	CD4 Enriched	2+	1+	-	1+
	CD8 Enriched	(+)	-	-	-
	CD4/CD8 Depleted	NT	NT	-	NT
13	CTL	3+	1+	-	1+
	CD4 Enriched	3+	1+	-	1+
	CD8 Enriched	NT	NT	NT	NT
	CD4/CD8 Depleted	3+	1+	-	-
14	CTL	1+	1+	-	1+
	CD4 Enriched	3+	1+	1+	1+
	CD8 Enriched	2+	1+	-	-
	CD4/CD8 Depleted	2+	1+	-	-
15	CTL	3+	-	-	-
	CD4 Enriched	2+	-	-	-
	CD8 Enriched	2+	-	-	-
	CD4/CD8 Depleted	1+	(+)	(+)	-
16	CTL	NT	NT	NT	NT
	CD4 Enriched	2+	1+	(+)	-
	CD8 Enriched	NT	NT	NT	NT
	CD4/CD8 Depleted	NT	NT	NT	NT

CTL: Cytotoxic T lymphocytes; Ip: Intraperitoneal; No: Number; NT: not tested

Human CD3+ve T cells were found in 17 out of 32 (53%) tumour samples tested. Whilst 2 out of these 17 (12%) samples contained CD4+ve T cells, 11 (65%) of the

samples had detectable CD8+ve T cells and 1 (6%) sample contained CD4+ve and CD8+ve T cells. Three (18%) samples were CD3+ve only by immunostaining. Overall, T cells comprised <1-29% of each T marker+ve tumour section. Immunostaining against NK markers was not carried out.

Taken together, we concluded that human T cells are able to home to human tumour tissue *in vivo* in sc and ip hu-BLCL-SCID mice. Therefore, we examined the possible mechanisms involved in mediating tumour rejection *in vivo.*

3.5.3 Cytotoxic Mechanisms Used By CTLs *In Vivo*

Using serial sections of the 17 paraffin wax-embedded ip tumours shown to contain CD3+ve T cells in section 3.5.2 (donors 6 and 8-16), immunostaining was used to determine whether T cells employed perforin or granzyme B cytoloytic molecules *in vivo.* Representative results are shown in Figure 24.

Six out of 17 (35%) tumour samples contained granzyme B+ve cells whereas a further 8 out 17 (47%) samples contained perforin+ve cells by immunostaining. Overall, therefore, 14 out of 17 (82%) tumour samples tested expressed one or the other cytoxic granule molecule (see Figure 24).

FIGURE 24
Immunophenotyping Of Ip SCID Mouse Tumour Tissue: Human Leukocyte Markers And Cytotoxic Granule Molecules (Donors 6, 8-16)
(Paraffin Wax-Embedded Sections)

Figures 24A,B (x400): Photomicrographs of immunostaining of the human pan-leukocyte marker CD45 on tumour sections using an alkaline phosphatase (AP) label. Figure 24A shows CD45-positive human cells (red membrane staining) counterstained with Mayer's haemalum. Figure 24B shows the conjugate control with counterstained cells only. **Figures 24C,D** (x400): Photomicrographs of immunostaining of the human pan-T cell CD3 marker on tumour sections using an alkaline phosphatase (AP) label. Figure 24C shows CD3-positive human cells (red membrane staining) counterstained with Mayer's haemalum. Figure 24D shows the conjugate control with counterstained cells only. **Figures 24E,F** (x400): Photomicrographs of immunostaining of the cytotoxic granule molecule perforin on tumour sections using a peroxidase (HRP) label. Figure 24E shows perforin-positive human cells (brown cytoplasmic staining) counterstained with Mayer's haemalum. Figure 24F shows the conjugate control with counterstained cells only. **Figures 24G,H** (x400): Photomicrographs of immunostaining of the cytotoxic granule molecule granzyme B on tumour sections using an alkaline phosphatase (AP) label. Figure 24G shows granzyme B-positive human cells (red cytoplasmic staining) counterstained with Mayer's haemalum. Figure 24H shows the conjugate control with counterstained cells only.

Arrows point to examples of specific antibody+ve cells.

24A: CD45

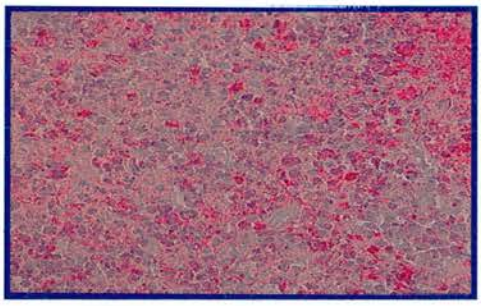

24B: CD45 Control

24C: CD3

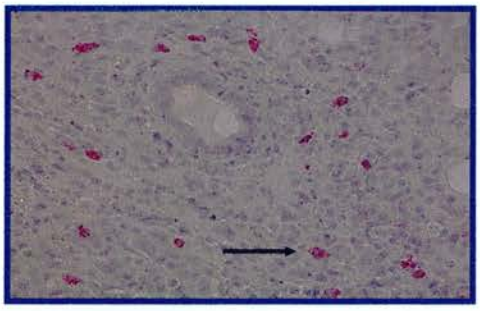

24D: CD3 Control

24E: Perforin

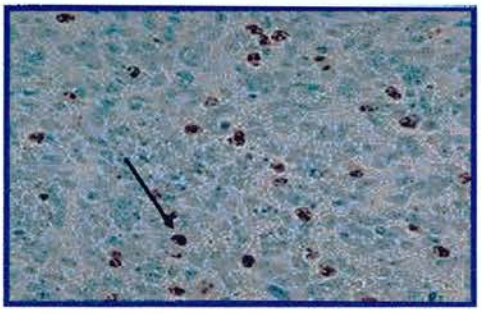

24F: Perforin Control

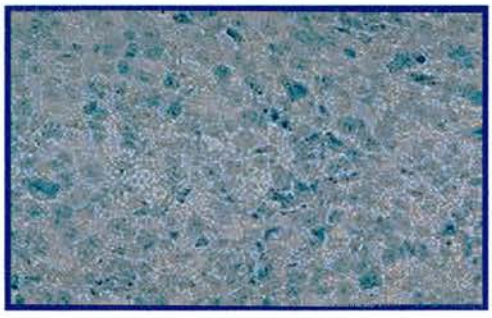

24G: Granzyme B

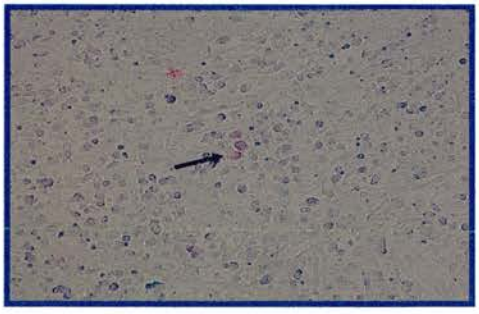

24H: Granzyme B Control

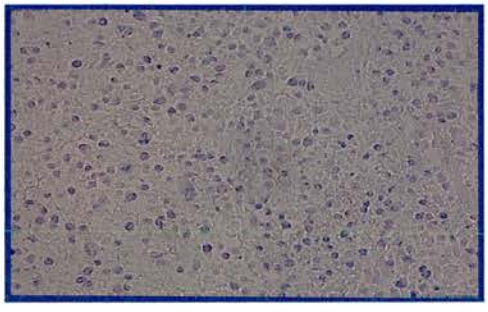

3.6 Conclusions And Discussion

The initial aim of these experiments was to examine the effect of autologous CTLs and T cell subsets on sc PTLD-like tumours in the sc hu-BLCL-SCID model in which macroscopic tumour growth can be measured directly. When 1 dose of CTLs was iv inoculated into the animals, no overall significant effect on tumour development was noted (Linear regression: p=0.12; see Figures 10-11), and lesions continued to grow in all treated animals. In contrast, Lacerda *et al* (1996) demonstrated significantly improved survival of iv CTL-treated SCID mice with established BLCL-derived sc tumours when compared to untreated control animals. Although 6 out of 10 (60%) treated mice subsequently succumbed to malignant disease, 4 (40%) animals experienced complete tumour regression.

CTLs from donor 5 facilitated sc tumour growth *in vivo* compared to untreated control animals (Linear regression: p=0.03). The cell inoculum from this donor ($15x10^6$ CTLs) contained the highest number ($3x10^6$) of transferred CD4+ve T cells of the 4 CTL lines used (from donors 1, 3-5; see Table 14) and, thus, it is plausible that these cells provided the malignant cells with growth factors that encouraged their expansion. Further support for this hypothesis comes from a similar observation in the current study when using CD4-enriched T cells from donor 6 (see Figures 15-16). Animals that received these cells developed sc tumours significantly faster than controls (Linear regression: p=0.0006) suggesting that CD4+ve T helper cells facilitated tumour formation *in vivo.* This is in line with our previous results obtained in the hu-PBL-SCID model (see Figure 2 in Introduction) highlighting key role of CD4+ve T cells in lymphomagenesis *in vivo* (Johannessen *et al,* 2000). Interestingly, CTL line 6 showed 91% lysis of autologous targets *in vitro* (see Table A10 in Appendix 1) underlining the non-correlation of *in vitro* assays with regression data obtained *in vivo* (see Figure 20 in Results). These observations are in line with results from our laboratory demonstrating non-correlation of CTL cytotoxicity as measured by ^{51}Cr-release assay and CTL treatment outcome in the PTLD patient setting (Haque *et al,* 2007). Whilst the reasons for this are not clear, it appears that the ^{51}Cr-release assay is a crude *in vitro* system for

determining CTL function *in vivo.* Clearly, the assay does not mimic the *in vivo* microenvironment in which T cells exert their cytotoxic effect and is, therefore, an artificial approach to gauging T cell function. In the clinical setting, infused T cells may prompt an inflammatory response within PTLD tumours by recruiting non-specific cytotoxic cells or activating endogenous EBV specific CTLs. When administering allogeneic CTLs on a 'best MHC match' basis to PTLD patients, such an inflammatory reaction may be similar to the graft-*versus*-leukaemia (GVL) effect that is considered to be of benefit against leukaemia following allogeneic bone marrow transplant (Bonini *et al,* 1997; Ciceri *et al,* 2007).

CD8-enriched T cells did not significantly delay sc tumour development in SCID mice (Figure 16) which is in contrast with results obtained in the ip hu-BLCL-SCID model in the current study (see below).

Administration of a CTL dose iv at time of macroscopic sc tumour formation followed a week later by a second autologous iv CTL dose significantly delayed sc tumour development in SCID mice (Linear regression: p=0.01; see Figures 12-13). Although the results agree with the observations by Lacerda *et al* (1996) cited above, they only transferred a single dose of CTLs iv.

Since the highest number of CTL cells administered in the current study was most likely to have a significant impact on sc tumour development *in vivo* (see Tables 14-16), the size of the inoculum appears to be important. Therefore, we increased the number of cells used in subsequent experiments. However, the sc hu-BLCL-SCID model proved difficult to manage because:

(1) in animals inoculated sc with BLCLs, sc tumours did not always arise at a similar timepoint making iv administration of CTL and T cell subsets problematic in terms of experimental planning,

and

(2) it proved difficult to inject large T cell inocula iv without posing some risk to the circulatory stability of the animals.

Because of continuous efforts to refine our *in vivo* study approach (see the '3 Rs' in section 4 in Introduction), we repeated the experiments in the ip hu-BLCL-SCID mouse model which circumvents these difficulties and is technically easier to manage.

In the ip hu-BLCL-SCID model, inoculating CTL lines significantly improved survival of mice injected 1 hour after ip BLCL transfer with unfractionated autologous CTLs, or CD8-enriched T cells, when compared with control animals inoculated with suspension medium only (Logrank test; p=0.003 and p=0.0002, respectively; see Figures 18-19). Furthermore, animals inoculated with CTLs, or CD8-enriched T cells, showed a significant delay in median time to tumour when compared to control mice (Mann-Whitney test: p=0.001 for both analysis; Figure 17). The importance of CD8+ve T cells is further highlighted in the current study by the observation that significantly fewer animals inoculated with CD8-enriched T cells developed ip tumours than controls (Fisher's exact test: p=0.001) and, thus, these cells not only significantly delay ip tumour development *in vivo,* but they can also prevent it altogether in a significant proportion (40%) of mice (see Table 20). These results are supported by data obtained in other laboratories. In their study, Boyle *et al* (1993) engrafted SCID mice ip with BLCL followed by simultaneous administration of autologous whole population (or CD8-enriched) CTLs. Whilst mice inoculated only with BLCL developed PTLD-like lesions on average 20 days after transfer, simultaneous administration of autologous whole population (or CD8-enriched) CTLs significantly delayed tumour formation *in vivo.* Similar results were obtained if T cell inoculation took place 7 days after BLCL transfer into mice. In contrast, mismatched CTLs failed to have an effect on tumour development. Further support for the data comes from studies by DiMaio *et al* (1995) and Buchsbaum *et al* (1996) when assessing the preventative effect of *ex vivo* expanded autologous CTLs on tumorigenic B cell lines transferred ip into SCID mice.

CD4+ve T cells can portray cytotoxic function *in vitro* and *in vivo* (Appay, 2004). Norris *et al* (2001) demonstrated perforin-mediated cytolytic function *in vitro* of group-specific antigen (*gag*)-specific CD4+ve T cell clones generated from HIV+ve PBLs. In the current project, the highest CTL killing of autologous targets *in vitro* was carried out by CTL line 6 which contained 49% CD4+ve T cells (see Figure 9 and

Tables A9-10 in Appendix 1). Similar *in vivo* data from Appay *et al* (2002) demonstrate the presence of a small subpopulation of perforin+ve, CD4+ve cytolytic T cells in healthy individuals, which is markedly expanded in patients with chronic viral infections (in particular, HIV). Additionally, CD4+ve T cells produce cytokines (mainly INFγ and TNFα) which have an anti-tumour effect whilst others are essential for priming CD8+ve CTL responses and for maintaining CTL function and proliferation (Wang, 2001). B cell tumours like PTLD express MHC2 molecules (Thomas *et al,* 1990) although most other tumour cell types do not (and therefore can not directly interact with CD4+ve T cells) suggesting the possibility of direct CD4+ve T cell-mediated cytotoxic action in PTLD. However, inoculation of CD4-enriched T cells did not have a significant impact on tumour development in the ip hu-BLCL-SCID mouse model (Figure 19). This finding also contrasts with results obtained in the hu-PBL-NOD/SCID model where treatment of mice with a depleting anti-human CD4 mab resulted in loss of both CD4+ve and CD8+ve T cells (Wagar *et al,* 2000), and data from our laboratory showing a significant trend towards better responses to allogeneic 'best MHC match' CTL treatment of PTLD patients with higher numbers of CD4+ve T cells in infused CTL lines (Haque *et al*, 2007). Further support for the importance of CD4+ve T cells comes from studies on *ex vivo* expanded biopsy-derived melanoma antigen-specific tumour infiltrating lymphocytes (TILs) showing that both CD4+ve and CD8+ve T cells are essential to obtain an effective anti-melanoma response in the patient setting (Dudley *et al,* 2002). In the hu-BLCL-SCID model, therefore, the most effective combination of CD4+ve and CD8+ve T cells still needs to be identified.

In light of the apparent discrepancy between the SCID model and the clinical setting, further analysis of the association between the number of inoculated CD4+ve T cells and survival of treated animals beyond non-treated control mice in the ip hu-BLCL-SCID model is shown in Figure 25. Similar analysis of the CD8+ve T cell population is shown in Figure 26.

FIGURE 25
% Survival As A Function Of Number Of CD4+ve T Cells Inoculated (Donors 6, 8-16)

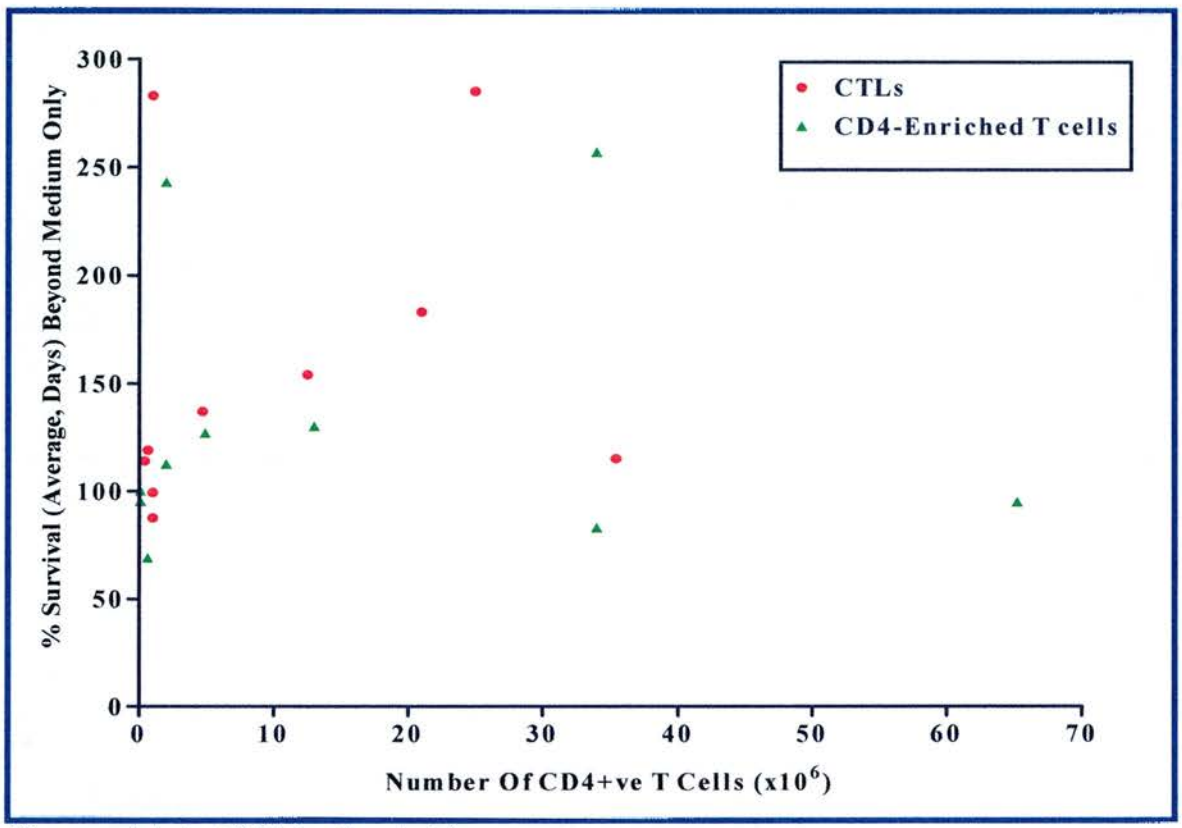

(Spearman's test: $p>0.05$ for all analysis)

Statistical analysis of the data in Figures 25-26 shows non-correlation between the number of CD4+ve, or CD8+ve, T cells (included in the CTL, CD4-enriched, or CD8-enriched T cell inoculum transferred ip into SCID mice) and the average % survival (in days) beyond control animals inoculated with medium only (Spearman's test: $p>0.05$ for all analyzes). Similar results were obtained when analysing the CD8:CD4 ratio of cells inoculated (Spearman's test: $p>0.05$ for all analyzes). Therefore, it does not appear that survival of SCID mice treated with autologous CTLs, or T cell subsets, is a direct function of the number of transferred CD4+ve or CD8+ve T cells, or their ratio.

FIGURE 26
% Survival As A Function Of Number Of CD8+ve T Cells Inoculated (Donors 6, 8-16)

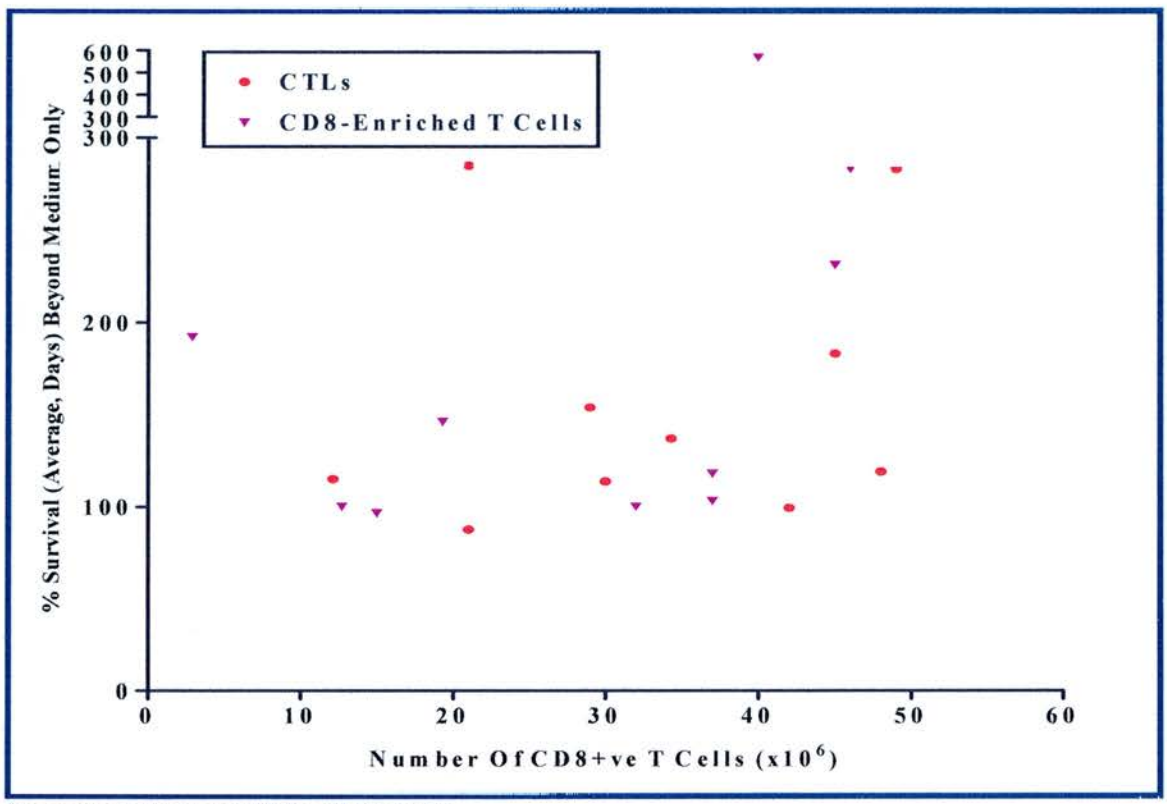

(Spearman's test: $p>0.05$ for all analysis)

In both sc and ip hu-BLCL-SCID models, human T cells were detected in T cell treated animals for up to 64 days (see Tables 22-23; Table A13 in Appendix 1). This is in line with previous (unpublished) results from our laboratory as well as observations by others underlining that T cells can home to PTLD-like tumours in SCID mice. Thus, in their study, Lacerda *et al* (1996) showed preferential homing of CD8+ve T cells to autologous tumour tissue but not to MHC-mismatched sc tumours. Similar results have been obtained in imaging studies by Koehne *et al* (2003) using radioactive labelling of human EBV-specific T cells to track the cells *in vivo.* Thus, Koehne *et al* (2003) have demonstrated selective homing of human T cells to autologous sc EBV-induced tumours in SCID mice despite subtle species-specific differences that are assumed to exist between the two species. The advent of novel *in vivo* biophotonic imaging technology

permits labelling of T cells with light-emitting reagents that can be visualized in real time by a light-sensitive photon counting-coupled device (CCD) camera connected to a dark box over a heated pad. Whilst our laboratory has only recently embarked on using this new technology, it permits analysis of homing of therapeutic T cells *in vivo.* On-going studies in our laboratory using such an approach will permit a better insight into T cell trafficking in the SCID mouse model (for further information about the imaging technology, see the website: *www.xenogen.com*).

CTLs employ 2 main cytolytic pathways: one involves cytotoxic perforin-granzyme A/B granule exocytosis, and the other entails Fas (CD95)-Fas ligand (FasL; CD178) interactions resulting in activation of the caspase enzyme cascade in target cells leading to apoptosis. Additional pathways involve the tumor necrosis factor-related apoptosis-inducing ligand (TRAIL) and its cognate receptor (De Bueger *et al,* 1992). Whilst our immunostaining data (see section 3.5) suggest that the cytotoxic molecules perforin and granzyme B are likely to be the T cell effector mechanisms in the current study (see Figure 24), we did not analyze the role of T cell-derived cytokines [for example, TNFα] or apoptotic mechanisms in mediating tumour regression/prevention.

Based on our results, we propose a scheme for T cell-mediated destruction of PTLD-like lesions in the ip hu-BLCL-SCID mice (Figure 27). In our model, transfer of autologous CTLs results in homing of CD4+ve and CD8+ve T cells to tumorigenic EBV+ve B cells in SCID mice. Upon recognition of EBV-derived peptides in an autologous MHC context, T cells are triggered to release the cytotoxic granule molecules perforin and granzyme B which results in target cell lysis. The model is supported by recent studies from our laboratory demonstrating that the main CTL effector mechanisms *in vitro* are the cytotoxic molecules perforin and granzyme B (Vanhoutte, 2006).

FIGURE 27
A Model Of CTL Function In The Ip Hu-BLCL-SCID Mouse

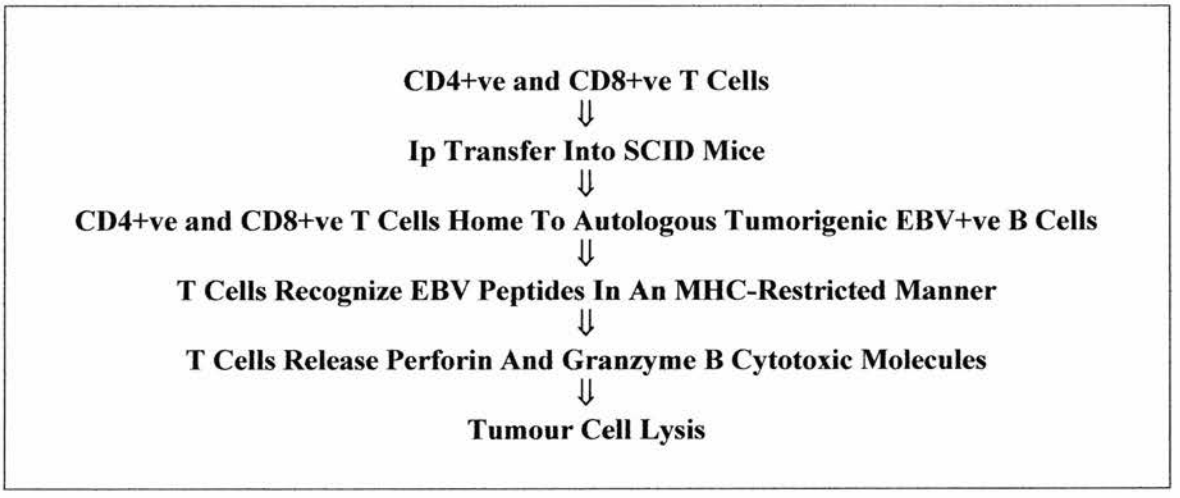

Next, we explored ways of improving the hu-BLCL-SCID model.

4. Attempts To Improve The Hu-BLCL-SCID Model

In order to improve the efficiency of the hu-BLCL-SCID model, we investigated the role of **(1)** cytokine stimulation and **(2)** MRI imaging as adjuncts to the *in vivo* model. First, we examined the effect of cytokine conditioning of CTLs *in vitro* on their capacity to prevent tumour development in the ip hu-BLCL-SCID model.

4.1 Cytokine Conditioning Of CTLs

Cytokines have the ability to enhance homing of T cells by promoting their expansion, function and survival *in vivo.* Thus, cytokines that signal through the common γ-chain (IL2, 4, 7, 15 and 21) are important for the homeostasis of CD4+ve and CD8+ve T cells (Ku *et al,* 2000; Schluns *et al,* 2000). The aim of this set of experiments was to examine the impact of *in vitro* CTL cytokine conditioning prior to *in vivo* transfer into the ip hu-BLCL-SCID model. In light of the large cell numbers required for these experiments, viably frozen CTLs were used in these experiments.

4.1.1 *In Vitro* CTL Cytokine Conditioning

CTL lines (day -1) from donors 5, 17 and 22-24 (see Tables A8-10 in Appendix 1) were placed in culture medium containing 20% v/v FCS and either human IL2 (routine CTL culture conditions), 7, 15, 21, 7 and 15, or 7 and 21, at a final concentration of 20 IU/mL (IL2) or 10 ng/mL (all other growth factors) for 24 hours (Parada *et al,* 1998; Ayyoub *et al,* 2002). The following day (day 0), the cytokine conditioned cells were washed and reconstituted in suspension medium for *in vivo* use (see below). We also assessed the EBV-specific cytotoxicity of the cell lines on day 0 using standard ^{51}Cr-release assay. The results are shown in Figure 28.

FIGURE 28
% Specific CTL Lysis At A 10:1 Effector:Target Ratio
(Donors 5, 17, 22-24)

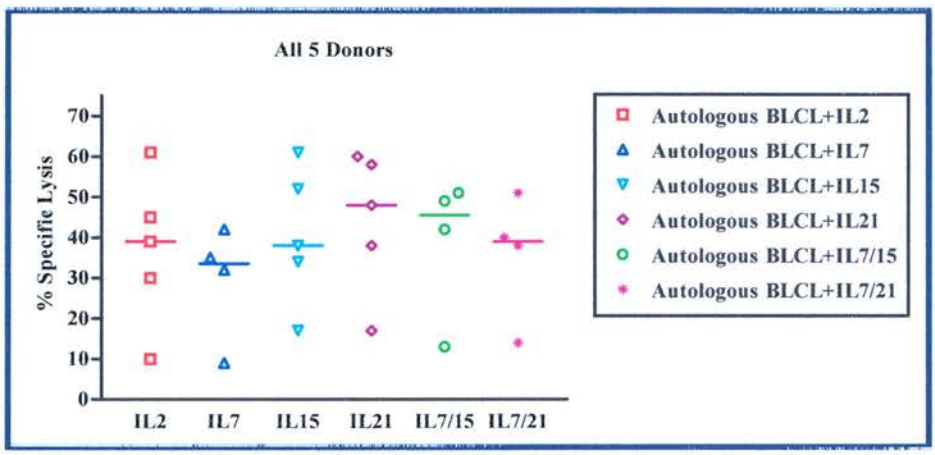

BLCL: B lymphoblastoid cell line; IL: Interleukin
(For each column, the median is shown as a horizontal bar.)

Overall, no significant difference between median % specific lysis was found when comparing autologous targets conditioned with IL2, 7, 15, 21, 7 and 15, or 7 and 21 (Kruskal-Wallis test: p=0.74). We concluded that cytokine conditioning CTLs with IL2, 7, 15, 21, 7 and 15, or 7 and 21, for 24 hours *in vitro* does not significantly influence their cytotoxic potential as measured by ^{51}Cr-release assays.

4.1.2 *In Vivo* Tumour Prevention Following Ip CTL Transfer

For each of the 5 donors, $2x10^6$ BLCL were inoculated ip into each mouse in groups of 3 SCID mice each. This was followed 1 hour later by the ip inoculation of suspension medium only into one group of 3 animals, whereas further groups of 3 SCID mice each were inoculate ip with $50x10^6$ autologous CTLs that had been conditioned for 24 hours *in vitro* with either IL2, 7, 15, 21, 7 and 15, or 7 and 21. Individual results showing proportion (%) mouse survival over time (in days) together with logrank test results is shown in Figure 29.

FIGURE 29
% Survival Using Cytokine Conditioned CTLs
(Donors 5, 17, 22-24)

(Standard error, SE, is shown on each column as a vertical bar.)

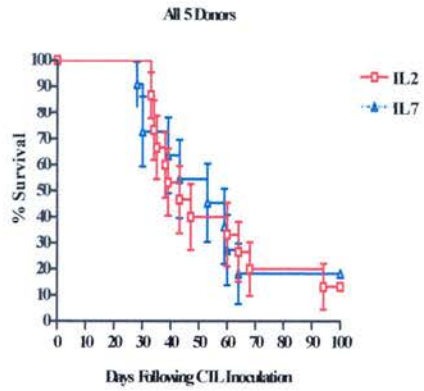

(Logrank test: p=0.96)

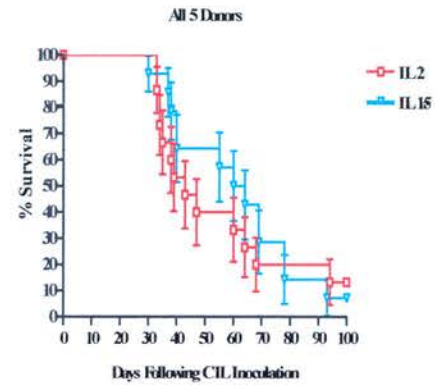

(Logrank test: p=0.67)

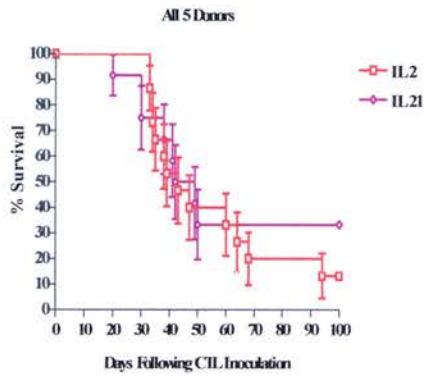

(Logrank test: p=0.52)

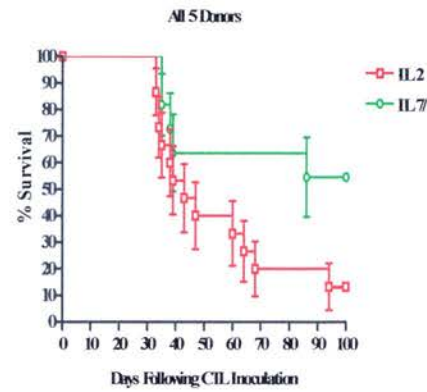

(Logrank test: p=0.04)

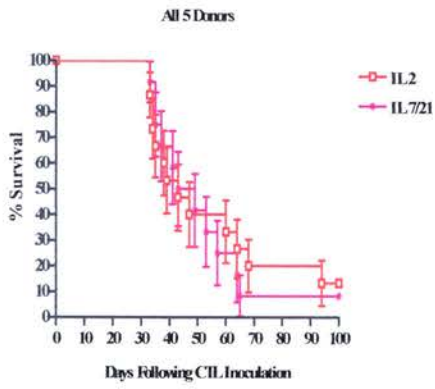

(Logrank test: p=0.75)

No significant difference was found between any survival curves apart from experiments using CTLs conditioned with a combination of IL7 and 15 when compared to cells conditioned with IL2 (Logrank test: p=0.04).

Next, we examined whether MRI imaging enabled us to monitor tumour development in the ip hu-BLCL-SCID model in a non-invasive manner.

4.2 Ip Hu-BLCL-SCID Mice And MRI Imaging: Treatment Model

The aim of these experiments was to determine whether MRI imaging could be used to assess T cell-mediated tumour regression in the ip hu-BLCL-SCID tumour model. We ip inoculated $2x10^6$ BLCL from donors 4 and 20 (see Tables A8-10 in Appendix 1) into each SCID mouse in a group of 5 animals. Two weeks later, weekly MRI scans were commenced until animals developed signs of illness and were culled. MRI imaging was carried out with either T1 or T2 weighting and with or without iv injections of the contrast medium gadolinium. Representative results of weekly scans are shown in Figure 30.

MRI imaging enabled us to detect ip tumour development. The radiological signs of tumour formation included loss of normal anatomical architecture and the blurring of organ outline together with the appearance of an ip mass at the under surface of the liver that blended into the liver contour. Gadolinium injections added contrast to the images (see Figure 30).

30A: Control

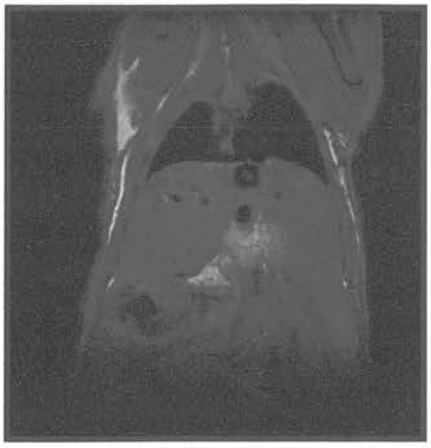

30B: At 2 Weeks

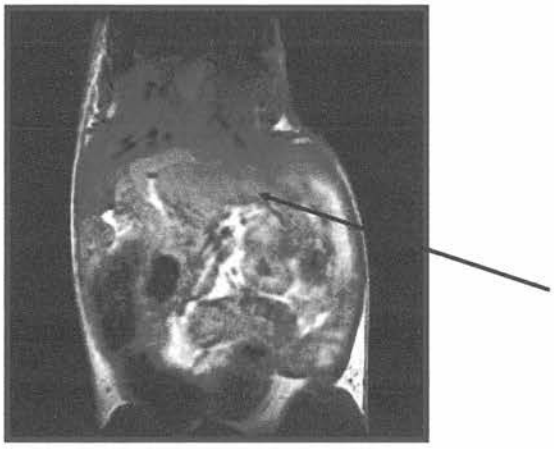

30C: At 3 Weeks

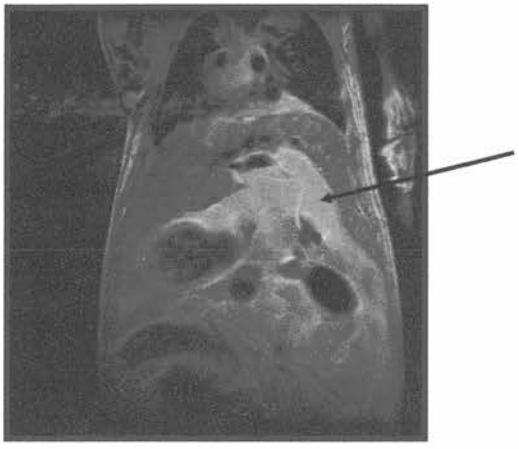

30D: At 4 Weeks

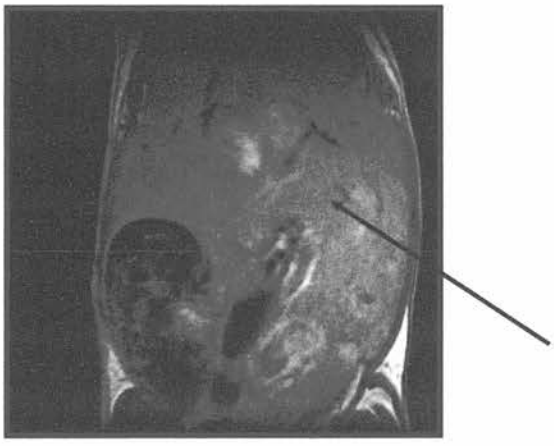

30E: At 5 Weeks

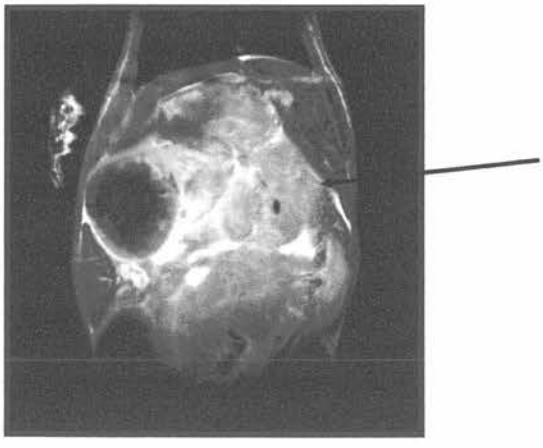

30F: At Necropsy

4.3 Conclusions And Discussion

In an effort to improve the ip hu-BLCL-SCID model:

(1) CTLs were pre-conditioned with cytokines *in vitro* prior to transfer ip into SCID mice,

and

(2) MRI imaging was carried out to assess tumour formation *in vivo* in a non-invasive, non-destructive manner.

A combination of IL7 and 15 may have enhanced the ability of CTLs to mediate tumour prevention in hu-BLCL-SCID mice although individually IL7, IL15, and IL21 did not (Figure 29). Furthermore, a combination of IL7 and IL21 did not have an impact *in vivo*. We postulate that the cytokines improved the ability of the *in vitro* conditioned T cells to home to, and mediate destruction of, human PTLD-like tumour cells *in vivo.* Cytokines that signal through the common γ-chain (for example, IL7 and 15) are known to improve T cell trafficking and function *in vivo*. In their study of ovalbumin (OVA)-specific transgenic murine CD8+ve T cells (denoted 'OT-1 cells'), Schluns *et al* (2000) demonstrated that naïve OT-1 cells transferred into lymphopenic recombination activating gene (RAG) -/-, and IL7 -/- RAG-/-, mice (both of which lack mature B and T cells) only survived and expanded in the former, but not in the latter, murine host. Furthermore, using OT-1 and IL7R -/- OT-1 cells in an immunocompetent mouse, the group showed survival and expansion of the former, but not of the latter, memory T cell population following OVA challenge *in vivo.* Similarly, using anti-IL15 blocking mabs in an immunocompetent mouse model, Ku *et al* (2000) showed that IL15 was required for survival and expansion of memory CD8+ve murine T cells *in vivo.*

Whilst *in vitro* cytokine conditioning did not significantly affect CTL cytotoxicity *in vitro* as measured by ^{51}Cr-release assay (Figure 28), additional results in the current project (see section 3 in Results), and data from clinical studies in our

laboratory (Haque *et al,* 2007), suggest that *in vitro* cytotoxicity does not correlate with CTL function *in vivo.*

We did not examine the possible role of cytokine administration in sustaining transferred T cells *in vivo* since previous studies have given conflicting results of such an approach. In their study, Baiocchi *et al* (2001) demonstrated that combined therapy with human granulocyte-macrophage colony-stimulating factor (GM-CSF) and low-dose IL2 can prevent tumour formation in the presence of human effector (CD8+ve T) cells in the hu-PBL-SCID model (Baiocchi *et al,* 1994, 2001). Furthermore, autologous and allogeneic LAK cells prolong survival of sc and ip BLCL-inoculated SCID-beige mice (that also lack endogenous NK cell activity; Randhawa *et al,* 1998). In contrast, Boyle *et al* (1993) and Rencher *et al* (1994) have shown that IL2 is not required when CTLs, or CD8-enriched T cells, are transferred into ip hu-BLCL-SCID mice. In both these studies, T cells significantly prolonged survival of treated mice compared with untreated control animals in the absence of IL2 supplementation.

Animals were imaged with an MRI scanner with a view to establishing an ip treatment model (see Figure 30). The MRI scanner consists of a magnetic cylinder in the centre of which an anaesthetized animal is placed and subjected to radiowave energy pulses. These pulses are absorbed by hydrogen ions, which resonate at a frequency particular to the tissue type. At the end of the pulse, the hydrogen ions re-align with the magnetic field and release the stored energy which is detected by sensors enabling image construction. Structures within the thoracic and abdominal cavity can be clearly seen (to within 50-100 μm resolution), but contrast dyes (such as gadolinium) may be injected to alter the local magnetic field and enhance image quality. Small animal MRI permits:

(1) imaging of internal structures in great detail,

(2) the assembly of 3 dimensional (3D) images,

and

(3) non-invasive, non-destructive longitudinal studies on the same animal.

However, the technology is very costly.

Tumours could be identified in the murine peritoneal cavity on MRI images taken as early as 2 weeks after BLCL transfer. Published data by other research teams using athymic nude mice to model liver metastasis of human colorectal disease have shown similar results. In their study, Wu *et al* (2003) implanted a highly liver-metastatic human colon cancer into the caecum of animals, whilst Cai *et al* (2005) inoculated human colon cancer cells directly into the portal vein of nude mice. Using regular MRI scans, tumour growth in the animals was analyzed in a non-invasive, non-destructive manner, and the scan images were found to correlate with macroscopic findings at necropsy.

In the current study, the radiological signs included obliteration of the normal liver contour and general signs of a space-occupying lesion in the abdomen. These signs grew more apparent with subsequent weekly scans and the iv administration of gadolinium aided interpretation of the images. However, in contrast to the metastatic colorectal cancer models described above, it was not possible in the current study to demarcate clearly the ip tumours. The main reason was that BLCL-derived tumour consistency appeared to be very similar to that of the liver itself and, therefore, it was difficult to separate the two tissues. Whilst gadolinium contrast helped highlighting the tumours, use of the agent did not result in circumscribed lesions that could be measured directly on scanned images. Thus, it is not yet possible to quantify a T cell-mediated treatment response on MRI scans.

Whilst the results are encouraging, the role of MRI imaging as an adjunct to the ip hu-BLCL-SCID model needs to be clarified further in future studies in order to establish the optimized manner in which to achieve clear visualization of BLCL-derived ip tumours *in vivo.* In light of the very costly nature of MRI imaging, the role of small animal computed tomography (CT) scanning could also be assessed although such facilities are not available to us. Thus, in a recent study, Pittet *et al* (2007) demonstrated that fused single photon emission CT (SPECT) and x-ray CT technology enabled localization and quantification of ^{111}In-oxine-labelled CTLs at tumour sites *in vivo*.

5. Tumour Prevention Using Antibodies Against Gp350

Transfer of donor EBV isolates to a recipient via a transplanted organ can be documented in EBV-seronegative recipients (Haque *et al,* 1996), but has not been observed in EBV-seropositive graft recipients. It is postulated that pre-existing neutralizing antibodies directed against the envelope gp350 antigen in EBV+ve patients may play a key role in preventing donor virus infecting recipient cells following transplantation (Haque *et al,* 2006). We hypothesized that passive immunization of EBV-seronegative organ graft recipients prior to transplant surgery, leading to circulating neutralizing antibodies directed against the envelope gp350 antigen, may prevent EBV transmission via the transplanted organ and, thereby, reduce the risk of PTLD development.

To test our hypothesis, we obtained a mouse mab against EBV envelope gp350 produced by the hybridoma cell line 72A1 from Johns Hopkins University Medical School (Baltimore, Maryland, USA). Previous studies have shown the mab to prevent EBV infection of B lymphocytes *in vitro* (Hoffman *et al,* 1980; Thorley-Lawson & Geilinger, 1980; Miller *et al,* 1982; Sairenji *et al,* 1988). Initially, we characterized the cell line and its mab. We have previously reported on the study results (Haque *et al,* 2006 – see Appendix 2).

5.1 Characterization Of 72A1 MAb

The 72A1 mab was manufactured at the Therapeutic Antibody Centre (Oxford, UK) in accordance with 'Good Manufacturing Practice' guidance (see General Discussion). As described previously, the purified 72A1 mab was found to be a mouse IgG1 containing κ and λ light chains in equal proportions (Hoffman *et al,* 1980). Since the IgG1 κ-secreting myeloma cell line P3X63Ag8 had been employed to create the 72A1 hybridoma, the purified mab was probably a mixture of active and inactive species. Thus, only a minor proportion may have had full bivalent binding to gp350. Using immortalization assays, the EBV neutralizing titer was determined to be 10^{-4}.

Next, we examined the capacity of the 72A1 mab to prevent EBV infection *in vivo* using a modified version of our ip hu-PBL-SCID model (Johannessen *et al,* 2000).

5.2 Tumour Prevention: Modified Hu-PBL-SCID Model

In order to test the ability of the 72A1 mab to hinder EBV infection *in vivo*, we used the development of PTLD-like lesions in a modified ip hu-PBL-SCID model as the experimental read-out (Cannon *et al,* 1990). In this version of the model, PBLs from an EBV-seronegative donor are inoculated into an animal followed by the administration of a concentrated EBV preparation resulting in virus infection of B cells *in vivo* and formation of PTLD-like lesions. Twenty million to $30x10^6$ PBLs from one of 4 EBV-seronegative donors were injected ip into each animal in a group of 6 SCID mice each on day 0. For each group of 6 mice, 3 test mice were also injected ip with the 72A1 mab preparation on day -1, 0 and 1, and then thrice weekly for 3 weeks. Since a minimum serum mab level of 1 μg/mL is considered to be effective for *in vivo* studies (Renner *et al,* 1994), each antibody inoculum comprised of 680 μg of the 72A1 mab as determined in our initial *in vivo* titration experiments to be adequate to maintain circulating mab above this level. Conversely, 3 control mice received ip suspension medium only at the same time points. Overall, a total of 12 mice received 72A1 mab whilst 12 animals served as controls. On day 1, all mice received 50 μL ip of a concentrated EBV preparation with an immortalizing titer of 10^{-4}. Mice were sacrificed when they showed signs of illness, or after a preset limit of 100 days. The results are shown in Table 24.

None out of 12 (0%) mice treated with the 72A1 mab developed ip tumours, whereas 8 out of 12 (67%) of control mice inoculated with medium only succumbed to malignant disease. All ip tumours were EBER+ve as determined by *in situ* hybridization. The results showed a statistically significant difference between the test and control groups (Fisher's exact test: p=0.001).

TABLE 24
72A1 MAb And Lymphomagenesis In Hu-PBL-SCID Mice

Treatment Groups	Number Of PBL Inoculated Ip Per Mouse ($x10^6$)	Number Of Tumours/ Number Of Mice (%)
Untreated (Medium Only)	20-30	8/12* (67)
Treated (72A1 mAb)	20-30	0/12* (0)

Hu: Human; Ip: Intraperitoneal; mAb: Monoclonal antibody; PBL: Peripheral blood leukocytes;
*: p=0.001

5.3 Conclusions And Discussion

Primary EBV infection following organ transplantation is a risk factor for PTLD (Cockfield, 2001). Furthermore, EBV-seronegative organ transplant recipients can acquire the virus via the grafted organ (Haque *et al,* 1996). In contrast, such virus transfer has not been observed in EBV-seropositive graft recipients. Therefore, pre-existing neutralizing antibodies directed against the envelope gp350 antigen may protect against infection with donor virus isolates, and efforts of developing EBV vaccine have focused on gp350 to elicit protective humoral immunity (Moutschen *et al,* 2007). We postulated that conferring passive virus immunity to EBV-seronegative patients about to undergo organ transplantation using the 72A1 mab could reduce the risk of primary EBV infection during the immediate post-transplant period and, thereby, reduce the risk of PTLD development.

Our initial results confirmed the *in vitro* neutralizing potential of the 72A1 mab, and we used SCID mice to assess its efficacy *in vivo.* Using PTLD-like tumour formation as the read-out of the experiments, the ip SCID model mimicked as far as possible the patient situation where a virus is transferred from a seropositive donor to a seronegative organ recipient. The 72A1 mab provided complete and significant protection against EBV-driven lymphomagenesis in the mice (p=0.001; Table 24) which

is in line with previous studies showing that administration of purified Ig pooled from EBV-seropositive donor plasma prevents outgrowth of PTLD-like lesions in hu-PBL-SCID mice inoculated with leukocytes from EBV-seropositive individuals (Abedi *et al,* 1997).

Whilst we assessed lymphomagenesis *in vivo,* the study did not examine directly whether the 72A1 mab prevents virus infection in SCID mice. It is possible that the antibody did not completely prevent EBV infection of B cells *in vivo,* and if this was the case, the 72A1 mab (of IgG isotype) may produce its effects through ADCC lysis of B cells since the target gp350 virus antigen is expressed on the surface of infected cells (Thorley-Lawson & Geilinger, 1980). Cells involved in such ADCC destruction of infected B cells may include murine NK cells and granulocytes (which exist at normal levels in SCID mice), or human NK cells and monocytes transferred in the PBL inoculum. Equally, gp350 is a component of the virus envelope and becomes accessible to the antibody upon release of virions during lytic infection which occurs in the SCID model (see section 2.4 in Results). Therefore, the 72A1 mab may neutralize infectious virus at the time of lytic infection and, thus, prevent infection and recruitment of uninfected B cells which may be one mechanism by which PTLD-like lesions arise *in vivo.*

Following successful completion of our SCID mouse experiments, inoculation of a single 10 mg dose of 72A1 mab iv into a healthy adult proceeded without any side effects [for example, human anti-mouse antibody (HAMA) production]. Peak mab serum levels (0.08–0.12 mg/mL) persisted for 52 hours following iv administration and then gradually declined, becoming undetectable after day 43. Anti-72A1 HAMA was not detected in serum samples at any stage during an 18 months observation period and the antibody was, therefore, considered to be safe.

These safety data were sufficient for ethical approval for a pilot study in which 7 children about to undergo liver transplantation were recruited (Haque *et al,* 2006). Details of the patients are shown in Table 25. Four children (denoted 'patient 1–4') received 1 mg of 72A1 mab per kg of body weight by iv infusions immediately before, and 6 hours after, organ transplant, and then every 2 days for up to 3 weeks. 72A1 mab

was detected in serum samples from all 4 infused children. Three patients (denoted 'patient 5–7') served as controls. Routine immunosuppressive treatment was administered to all 7 patients.

TABLE 25
Patient Details, 72A1 Mab Status, And Outcome Of Study

Patient No	Age At Tx (Months)	Sex	Number Of 72A1 Doses	Time (Months) Of Detection Post-Tx		
				VCA IgG	VCA IgM	EBV DNA
1	11	M	11	3	3	43
2	16	M	6	-	-	48
3	75	M	4	-	-	ND
4	18	F	7	-	-	42
5	17	M	0	3	-	40
6	10	F	0	2.5	-	ND
7	9	F	0	41	-	18

F: Female; M: Male; ND: Not detected; No: Number; Tx: Transplant; VCA: Viral capsid antigen; -: Negative (Adapted from Haque *et al,* 2006)

Three out of 4 (75%) 72A1-infused patients (number 2–4) remained EBV-seronegative during the 6 months follow-up period whereas 1 (25%) patient (number 1) developed anti-VCA IgG antibodies 12 weeks after transplant (9 weeks after the last 72A1 dose infused). Two out of 3 (67%) non-infused control patients (number 5 and 6) became seropositive at 10 and 12 weeks whereas the remaining control patient (number 7) seroconverted 41 months following liver transplantation. All EBV+ve organ graft recipients tested EBNA IgG-negative. When plasma samples were analyzed by PCR, EBV DNA was detected in 5 out of 7 (71%) patients (numbers 1, 2, 4, 5, and 7) during a post-transplant follow-up period of up to 4 years despite none of these patients having developed any symptoms of EBV disease. Conversely, 2 out of 7 (29%) patients (numbers 3 and 6) did not have detectable EBV in plasma samples, and patient 3 remained EBV DNA, EBNA IgG, and VCA IgM and IgG seronegative for 4 years after organ grafting. Retrospective analysis did not detect EBV DNA in pre-transplant PBL samples from any of the patients.

Taken together, there is some evidence that the 72A1 mab may have prevented EBV infection immediately after transplantation surgery. However, the study is small in scale and it is difficult to draw firm conclusions about the effect of the 72A1 mab on EBV infection in the children. All 7 liver transplant recipients were alive with a functioning organ graft 4 years after transplantation surgery, and none had developed PTLD.

All 4 (100%) children infused with the 72A1 antibody developed HAMA despite being on iatrogenic immunosuppressive treatment. One child (patient 4) suffered a severe reaction (hypotension, peripheral cyanosis, and vomiting) during the seventh infusion that required cessation of treatment. Patient 4 also developed *staphylococcus aureus* septicaemia. Whilst the hypersensitivity reaction required cessation of antibody infusion, the actual cause of the reaction (including an IgE-mediated response to HAMA) could not be identified.

Based on the above results, we concluded that the 72A1 mab was effective in preventing EBV-driven lymphomagenesis in SCID mice. However, the mab in its native form may not be safe in humans. Alternatives include humanizing the 72A1 mab, or producing a human mab (Breedveld, 2000).

GENERAL DISCUSSION AND FUTURE PERSPECTIVES

EBV-associated PTLD is an aggressive disease with high mortality despite current treatment. Therefore, novel therapeutic strategies are urgently needed to combat the lesions and improve patient prognosis. One such strategy involves the use of EBV-specific CTLs. In order to test the efficacy of such novel immunotherapy, PTLD can be modelled in SCID mice which are deficient in functional B and T cells and, thus, readily accept human xenografts (Bosma *et al,* 1983; Reddy *et al,* 1987; Mosier *et al,* 1988). Using either EBV-seropositive PBLs or BLCLs, the tumours that develop *in vivo* closely resemble that of BLCLs and PTLD in terms of cell surface phenotype and virus gene expression (Rowe *et al,* 1991; Johannessen *et al,* 2000; Figures 7-8 in Results), and the SCID model has become the small animal model of choice for *in vivo* studies on EBV-associated malignancies (for a review, see Mosier, 1996).

The current project was designed to set up a SCID mouse model in our laboratory suitable for investigating adoptive CTL immunotherapy for EBV+ve PTLD. In this section, **(1)** general aspects of the role of the SCID mouse in PTLD modelling, and **(2)** some future perspectives, will be addressed.

1. SCID Mice And PTLD Modelling

Following the original description of EBV+ve PTLD-like tmours in SCID mice inoculated with seropositive PBLs (Mosier *et al,* 1988), the animal became the model of choice in which to study EBV-associated neoplasia. Our laboratory has used the animals for nearly 15 years to investigate EBV pathogenesis and lymphomagenesis.

The SCID mouse is a small animal model which is relatively easy to manage and maintain. Furthermore, the animals are not endangered and can be bred in captivity with ease and at a releatively low cost. The importance of the SCID mouse is further underlined by the fact that the use of higher order mammals (for example, non-human primates) for experimental purposes is difficult in the UK due to strict Home Office

guidance and adverse public attitude towards such *in vivo* research. The humanized SCID mouse offers a valuable model in which to study human neoplasia although care must be taken when extrapolating between data obtained in the animals and a human patient. The relative advantages and disadvantages of the **(1)** hu-PBL-SCID and **(2)** hu-BLCL-SCID mouse models are shown below.

(1) Hu-PBL-SCID Mouse

The advantages of this model are summarized below:

(1) EBV+ve PBLs give rise to ip PTLD-like tumours.
(2) Model of choice for studies of PTLD pathogenesis.
(3) EBV infection of seronegative PBLs can be used to model primary infection.

However, some disadvantages exist:

(i) Healthy virus carriers vary in their ability to give rise to ip tumours.
(ii) Large PBL numbers ($\geq 50 \times 10^6$) are required for each ip inoculum.
(iii) Tumour formation takes a long time (up to 100 days).

(2) Hu-BLCL-SCID Mouse

As demonstrated in this thesis, in this model:

(1) EBV+ve B cells consistently give rise to sc or ip tumours.
(2) Direct sc tumour measurements enable assessment of treatment response.
(3) Ip tumour formation can be used as the read-out of preventative therapy.

However, some disadvantages exist:

(i) Time to sc tumour can vary between inoculated animals in a test group.

(ii) Administration of large cell inocula iv is difficult.

(iii) Imaging techniques need to be optimized.

In light of **2.i** and **2.ii** above, we developed the ip hu-BLCL-SCID model for therapy testing.

The importance of animal modelling has not diminished over the years despite efforts to offer alternative *in vitro* options (for further information, see the FRAME website: *www.frame.org.uk*), and pre-clinical data obtained in suitable animal models are vital to support testing in the clinical (patient) setting. Events in March 2006 at Northwick Park Hospital in London underline the importance of such relevant *in vivo* pre-clinical data prior to phase I clinical (safety) trials. During the Northwick Park study, 6 healthy volunteers became seriously ill within 3 hours of iv administration of a fully humanized new anti-CD28 mab (labelled 'TGN1412') to be used to modulate T cell immunity in autoimmune and inflammatory disease and leukaemia by a German firm (Mayor, 2006). The trial was approved by the Medicines and Healthcare Products Regulatory Agency (MHRA), the executive agency of the UK Department of Health that oversees and regulates clinical trials in the UK, and a local ethics committee. In a subsequent report, the MHRA did not identify any errors made in the manufacture, or administration, of TGN1412. However, whilst the mab had been tested in rabbits and monkeys prior to human use, it did not cross react with CD28-like molecules in these animals, and there was no reporting of the reagent having been studied in relevant humanized immunodeficient models.

The MHRA is the final regulator of clinical trials in the UK (for further information, see the Agency's website: *www.mhra.gov.uk*), and the regulator expects pre-clinical data to demonstrate medicinal product quality and *in vivo* safety to avoid such incidents as the one detailed above. During medicinal product development, both pre-clinical and clinical studies must be performed to quality standards and follow

quality guidelines (collectively referred to as 'GxP'). Important GxP include 'Good Clinical Practice' (GCP), 'Good Laboratory Practice' (GLP), and 'Good Manufacturing Practice' (GMP). **GCP** provides an international quality standard [as defined by the 'International Conference On Harmonization of Technical Requirements for Registration of Pharmaceuticals for Human Use' (ICH) to which the European Union (EU) is signatory; see the website: *www.ich.org*] on how clinical trials should be carried out, whereas **GLP** addresses systems of management controls to ensure product consistency and quality as defined by the 'Organization For Economic Co-Operation And Development (OECD) Principles of Corporate Governance' (see the website: *www.oecd.org*) as well as national legislation. **GMP** centres on the control and management of product manufacturing and quality control testing (for further information on GxP, see the European Medicines Evaluation Agency website: *www.emea.europa.eu*).

Taken together, pre-clinical testing of novel therapy/medicinal product in a relevant animal model is essential to gather data on its quality and safety before an application can be made to the MHRA for a clincial trial. One such new treatment strategy is genetically engineered T cells against PTLD that may offer an exciting alternative to CTLs in the near future.

2. Future PTLD Immunotherapy

Using a bank of EBV-specific CTLs generated *in vitro* from PBLs of EBV+ve healthy blood donors, our laboratory successfully infused patients suffering from EBV-driven PTLD with virus-specific CTLs on a 'best MHC match' basis (see section 3.5 in Introduction; Haque *et al,* 2002, 2007). This proof-of-principle trial showed that CTL therapy could succeed. However, a mechanism for bypassing MHC restriction would facilitate its dissemination to the clinic.

Since the TCR defines T cell recognition of antigen, a chimeric TCR (cTCR; or chimeric immune receptor, CIR) can be constructed that directs T cells against a novel antigen (Schumacher, 2002; Mansoor *et al,* 2005). In order to:

(1) broaden the application of CTLs,

and

(2) bypass MHC restriction,

cTCRs may be engineered to re-direct CTLs to EBV-derived surface antigens on infected malignant cells.

Current CTL immunotherapy for EBV-associated malignancies (for example, HL subsets, NPC) is limited by **(a)** the need for MHC-matched donors and **(b)** bias towards immunodominant antigens (the EBNA3 complex) that are not expressed by all tumours. One way of improving efficacy is to re-target CTLs to widely expressed EBV antigens such as LMP1 and LMP2 (see Table 3 in Introduction). LMP1 is a 58-63 kDa protein encoded by the BNLF1 ORF (Fennewald *et al,* 1984; Liebowitz *et al,* 1986) that consists of 6 hydrophobic transmembrane domains with both terminal sequences in the cytoplasm so that 3 reverse turn loops are exposed on the outer surface of the host plasma membrane. Similarly, LMP2a and 2b are 54 and 40 kDa proteins, respectively, that are encoded by the BARF1/BNRF1 ORF (Laux *et al,* 1988; Sample *et al,* 1989) that consist of 12 hydrophobic transmembrane domains with both terminal sequences in the cytoplasm so that 6 reverse turn loops are exposed on the outer surface of the host plasma membrane. Since both LMP1 and 2 are expressed by PTLD (and most other EBV-associated malignancies; see Table 2 in Introduction), they are an ideal choice for cTCR immunotherapy.

Using a single chain antibody variable domain fragment (scFv) as the antigen recognition molecule, cTCRs can be made to target antigens expressed on the surface of a target cell (Eshhar *et al,* 1993; Schuhmacher, 2002; see Figure 31). Antigen targetting becomes independent of MHC resctriction when such paratope recognition is employed. Chimeric TCRs have been used to re-direct T cells to non-virus infected cells. In their

study, Hwu *et al* (1993) transduced human T cells with cTCR against folate binding protein (FBP), a surface antigen present on most human ovarian carcinomas, and showed specific lysis of human ovarian carcinoma cells *in vitro.* Similar methods have been used to re-direct T cells to virus infected tumour cells. Thus, Orentas *et al* (2001) were able to use TCR sequences of an *in vitro* expanded LMP2-specific CTL clone to re-direct PBLs to autologous LMP2 peptide-pulsed cells although their approach can not entirely be considered to have circumvented MHC restriction. Since LMP1 and 2 are expressed on the surface of EBV-infected cells, these EBV antigens are candidate targets for cTCR immunotherapy.

FIGURE 31
T Cell Receptor (TCR) And Chimeric TCR (cTCR)

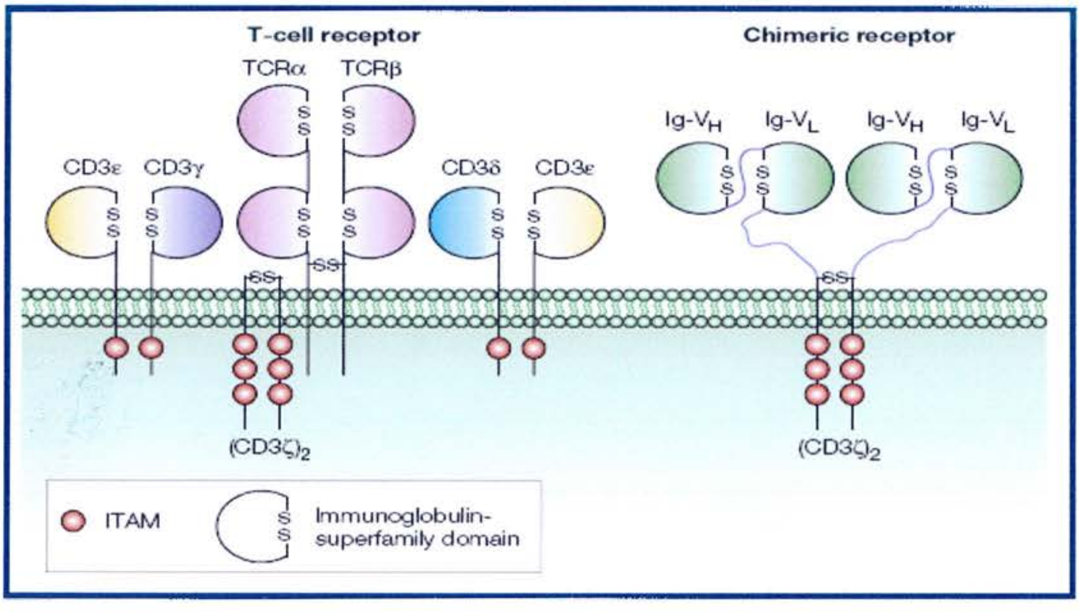

Chimeric T cell receptors (cTCRs) consist of a single-chain antibody fragment (scFv) that is coupled to additional molecular machinery to enhance function of the re-directed T cell, or 'T body'. These T bodies confer non-MHC restricted antigen recognition of target molecule. Ig-VH: Ig heavy-chain variable domain; Ig-VL: Ig light-chain variable domain; ITAM: Immunoreceptor tyrosine-based activation motif. [Reprinted from Schumacher (2002) with permission from Nature Publishing Group. *Copyright © 2002 Nature Publishing Group. All rights reserved.*]

A number of tumour cell surface antigens are poorly immunogenic, and mabs against many of them do not exist. In order to identify novel antibody targets, phage display technology employs genetically-engineered phage to 'display' human scFv antibody fragments on its surface (Dermime *et al,* 2004). Thus, a human scFv gene is fused to a phage gene coding for one of its surface coat protein molecules. As a result, the recombinant phage 'displays' a unique human antibody fragment on its surface and carries the antibody gene in its genome. Using millions of phages, an antibody phage display library contains millions of diverse antibody genes collected from the blood of healthy individuals using different donor B lymphocytes and reverse genetics. Using target protein-derived peptides, the large non-immune ('naïve') human scFv libraries are a rich source of human antibodies to virtually any target/antigen (Schumacher, 2002). Once novel antibody fragments have been identified, individual scFv fragments specific for a designated antigen can be selected and incorporated into vectors containing additional molecular machinery (for example, the lymphocyte triggering receptors TCR-ζ and FcR-γ as well as the costimulatory molecule CD28) to enhance homing, activation, cytotoxicity and survival of the transfected CTLs, to create novel cTCR CTLs, or 'T bodies'.

Using cTCR against carcinoembryonic antigen (CEA), which is expressed by gastrointestinal cancers (and other neoplasia) but rare in healthy tissue, Hawkins *et al* have transduced colorectal patient-derived T cells creating CEA-specific T bodies that recognize and lyse CEA+ve colorectal tumour cell lines *in vitro* (Sheen *et al,* 2003a,b). Similarly, CEA-specific human monocytes hindered CEA+ve tumour cell growth *in vitro* and in nude mice (Biglari *et al,* 2006). The team has used a similar approach to demonstrate:

(1) destruction of autologous CD19+ve NHL lymph node tumour biopsy cells *in vitro* by patient-derived T lymphocytes transduced with a cTCR specific for CD19 (Cheadle *et al,* 2005),

and

(2) lysis of renal cell carcinoma (RCC) cells *in vitro* by RCC patient-derived T bodies transduced with a cTCR specific against the oncofetal antigen 5T4 that is expressed by RCC (as well as other tumours) but is rarely found in healthy tissue (Griffiths *et al,* 2005).

The data have formed the basis for the group's current applications for phase I/II clinical trials using their cTCR constructs. Recent pilot studies employing cTCRs against FBP on ovarian cancer cells (Kershaw *et al,* 2006) and L1-cell adhesion molecule (CD171) overexpressed by neuroblastoma cells (Park *et al,* 2007) have shown that T bodies are well tolerated in patients. However, careful target selection and extensive pre-clinical testing in relevant animal models is vital for treatment success in the clinical setting as evidenced by a study by Lamers *et al* (2006) using cTCR against carboxy-anhydrase IX (CAIX) in RCC patients. The group demonstrated unexpected targeting of bile duct epithelial cells probably as a result of these cells expressing the same target molecule (CAIX) as the RCC cells. The ensuing hepatic toxicity necessitated cessation of treatment and the study was halted.

Recently, our laboratory has embarked on a study to identify novel LMP-derived targets in order to re-target CTLs (T bodies) against EBV-associated cancers. Once we have identified candidate phage antibody fragments, they will be used to engineer LMP-specific CTLs to generate novel T bodies (and soluble antibody fragments). These will be tested in our pre-clinical SCID mouse models of EBV-associated cancer to assess their:

(1) safety,

and

(2) efficacy against tumours *in vivo* prior to introduction into the clinical (patient) setting.

The principle remains the same for other viral and non-viral tumour antigens and, thus, the same approach is applicable to other malignancies where a tumour-specific

marker is known. Furthermore, a similar approach can be used to target virus-infected non-tumour cells. For example, the matrix 2 (M2) protein of influenza A virus is highly conserved across influenza A strains, and the ectodomain (M2e) is expressed on the surface of influenza A virus-infected cells (Pinto & Lamb, 2006). Our aim is to generate M2e-specific T bodies and investigate their efficacy against influenza A in a pre-clinical SCID mouse model (Sidwell & Smee, 2000; Ison *et al,* 2006) in order to generate translational data prior to introduction into the clinical setting.

The above projects in our laboratory will provide proof-of-principle *in vitro* and *in vivo* data supporting the use of re-directed CTLs in humans. Based on the data, we will formulate an approach to future clinical trials. Thus, it will eventually be possible to use the cTCRs to generate cells lines for use in the clinical (patient) setting.

In order to assess the **(1)** safety and **(2)** efficacy of the novel approaches to immunothereapy for EBV-associated neoplasia that are being developed and have been outlined above, *in vivo* testing in a humanized small animal model is essential prior to clinical trials. The SCID mouse is the ideal model for this purpose, and the animal provides researchers with the *in vivo* tool required to hone new therapeutic strategies before introduction into the clinical (patient) setting.

REFERENCES

Abedi, M. R., Linde, A., Christensson, B., Mackett, M., Hammarstrom, L., and Smith, C. I. (1997). Preventive effect of IgG from EBV-seropositive donors on the development of human lymphoproliferative disease in SCID mice. *International Journal of Cancer* **71**, 624–629.

Abu-Elmagd, K., Reyes, J., Todo, S., Rao, A., Lee, R., Irish, W., Furukawa, H., Bueno, J., McMichael, J., Fawzy, A. T., Murase, N., Demetris, J., Rakela, J., Fung, J. J., and Starzl, T. E. (1998). Clinical intestinal transplantation: new perspectives and immunologic considerations. *Journal of the American College of Surgeons* **186**, 512–525.

Akbar, A. N., Borthwick, N., Salmon, M., Gombert, W., Bofill, M., Shamsadeen, N., Pilling, D., Pett, S., Grundy, J. E., and Janossy, G. (1993). The significance of low bcl-2 expression by CD45RO T cells in normal individuals and patients with acute viral infections. The role of apoptosis in T cell memory. *Journal of Experimental Medicine* **178**, 427-438.

Amadori, A., Veronesi, A., Coppola, V., Indraccolo, S., Mion, M., and Chieco-Bianchi, L. (1996). The hu-PBL-scid mouse in human lymphocyte function and lymphomagenesis studies: achievements and caveats. *Seminars in Immunology* **8**, 249-254.

Amyes, E., Hatton, C., Montamat-Sicotte, D., Gudgeon, N., Rickinson, A. B., McMichael, A. J., and Callan, M. F. (2003). Characterization of the CD4+ T cell response to Epstein-Barr virus during primary and persistent infection. *Journal of Experimental Medicine* **198**, 903-911.

Ansell, J. D., and Bancroft, G. J. (1989). The biology of the scid mutation. *Immunology Today* **10**, 322-325.

Anthony, I. C., Crawford, D. H., and Bell, J. E. (2003). B lymphocytes in the normal brain: contrasts with HIV-associated lymphoid infiltrates and lymphomas. *Brain* **126**, 1058-1067.

Appay, V. (2004). The physiological role of cytotoxic CD4+ T-cells: the holy grail? *Clinical and Experimental Immunology* **138**, 10-13.

Appay, V., Zaunders, J. J., Papagno, L., Sutton, J., Jaramillo, A., Waters, A., Easterbrook, P.., Grey, P., Smith, D., McMichael, A. J., Cooper, D. A., Rowland-Jones, S. L., and Kelleher, A. D. (2002). Characterization of CD4+ CTLs Ex Vivo. *Journal of Immunology* **168**, 5954-5958.

Armitage, J. M., Kormos, R. L., Stuart, R. S., Fricker, F. J., Griffith, B. P., Nalesnik, M., Hardesty, R. L., and Dummer, J. S. (1991). Posttransplant lymphoproliferative disease in thoracic organ transplant patients: Ten years of cyclosporine-based immunosuppression. *Journal of Heart and Lung Transplantation* **10**, 877-887.

Arpin, C., Banchereau, J., and Liu, Y. J. (1997). Memory B cells are biased towards terminal differentiation: a strategy that may prevent repertoire freezing. *Journal of Experimental Medicine* **186**, 931-940.

Axelrod, D. A., Holmes, R., Thomas, S. E., and Magee, J. C. (2003). Limitations of EBV-PCR monitoring to detect EBV associated post-transplant lymphoproliferative disorder. *Pediatric Transplantation* **7**, 223-227.

Ayyoub, M., Stevanovic, S., Sahin, U., Guillaume, P., Servis, C., Rimoldi, D., Valmori, D., Romero, P., Cerottini, J. C., Rammensee, H. G., Pfreundschuh, M., Speiser, D., and Levy, F. (2002). Proteasome-assisted identification of a SSX-2-derived epitope recognized by tumor-reactive CTL infiltrating metastatic melanoma. *Journal of Immunology* **168**, 1717-1722.

Babcock, G. J., Decker, L. L., Volk, M. and Thorley-Lawson, D. A. (1998). EBV persistence in memory B cells in vivo. *Immunity* **9**, 395-404.

Babcock, G. J., Hochberg, D., and Thorley-Lawson, A. D. (2000). The expression pattern of Epstein-Barr virus latent genes in vivo is dependent upon the differentiation stage of the infected B cell. *Immunity* **13**, 497-506.

Babcock, G. J., and Thorley-Lawson, D. A. (2000). Tonsillar memory B cells, latently infected with Epstein-Barr virus, express the restricted pattern of latent genes previously found only in Epstein-Barr virus-associated tumors. *Proceedings of the National Academy of Sciences of the USA* **97**, 12250-12255.

Baer, R., Bankier, A. T., Biggin, M. D., Deininger, P. L., Farrell, P. J., Gibson, T. J., Hatfull, G., Hudson, G. S., Satchwell, S. C., Seguin, C., Tuffnell, P. S., and Barrell, B. G. (1984). DNA sequence and expression of the B95-8 Epstein-Barr virus genome. *Nature* **310**, 207-211.

Baiocchi, R. A., and Caligiuri, M. A. (1994). Low-dose interleukin 2 prevents the development of Epstein-Barr virus (EBV)-associated lymphoproliferative disease in scid/scid mice reconstituted i.p. with EBV-seropositive human peripheral blood lymphocytes. *Proceedings of the National Academy of Sciences, USA* **91**, 5577-5581.

Baiocchi, R. A., Ross, M. E., Tan, J. C., Chou, C. C., Sullivan, L., Haldar, S., Monne, M., Seiden, M. V., Narula, S. K., Sklar, J., Croce, C. M., and Caligiuri, M. A. (1995). Lymphomagenesis in the scid-hu mouse involves abundant production of human interleukin-10. *Blood* **85**, 1063-1074.

Baiocchi, R. A., Ward, J. S., Carrodeguas, L., Eisenbeis, C. F., Peng, R., Roychowdhury, S., Vourganti, S., Sekula, T., O'Brien, M., Moeschberger, M., and Caligiuri, M. A. (2001). GM-CSF and IL-2 induce specific cellular immunity and provide protection against Epstein-Barr virus lymphoproliferative disorder. *Journal of Clinical Investigation* **108**, 887-894.

Balfour, H. H. Jr, Holman, C. J., Hokanson, K. M., Lelonek, M. M., Giesbrecht, J. E., White, D. R., Schmeling, D. O., Webb, C. H., Cavert, W., Wang, D. H., and Brundage, R. C. (2005). A prospective clinical study of Epstein-Barr virus and host interactions during acute infectious mononucleosis. *Journal of Infectious Diseases* **192**, 1503-1504.

Bankert, R. B., Egilmez, N. K., and Hess, S. D. (2001). Human-SCID mouse chimeric models for the evaluation of anti-cancer therapies. *Trends in Immunology* **22**, 386-393.

Baskin, G. B., Martin, L. N., Rangan, S. R., Gormus, B. J., Murphey-Corb, M., Wolf, R. H., and Soike, K. F. (1986). Transmissible lymphoma and simian acquired immunodeficiency syndrome in rhesus monkeys. *Journal of the National Cancer Institute* **77**, 127-139.

Bechtel, D., Kurth, J., Unkel, C., and Küppers, R. (2005) Transformation of BCR-deficient germinal-center B cells by EBV supports a major role of the virus in the pathogenesis of Hodgkin and posttransplantation lymphomas. *Blood* **106**, 4345-4350.

Benkerrou, M., Durandy, A., and Fischer, A. (1993). Therapy for transplant-related lymphoproliferative diseases. *Hematology/Oncology Clinics of North America* **7**, 467-475.

Benkerrou, M., Jais, J. P., Leblond, V., Durandy, A., Sutton, L., Bordigoni, P., Garnier, J. L., Le Bidois, J., Le Deist, F., Blanche, S., and Fischer, A. (1998). Anti-B-cell monoclonal antibody treatment of severe posttransplant B-lymphoproliferative disorder: prognostic factors and long-term outcome. *Blood* **92**, 3137-3147.

Berney, T., Delis, S., Kato, T., Nishida, S., Mittal, N, K., Madariaga, J., Levi, D., Nery, J. R., Cirocco, R. E., Gelman, B., Ruiz, P., and Tzakis, A. G. (2002). Successful treatment of posttransplant lymphoproliferative disease with prolonged rituximab treatment in intestinal transplant recipients. *Transplantation* **74**, 1000-1006.

Beveridge, T., Krupp, P., and McKibbin, C. (1984). Lymphomas and lymphoproliferative lesions developing under cyclosporin therapy. *Lancet* **1i**, 788.

Bharadwaj, M., Burrows, S. R., Burrows, J. M., Moss, D. J., Catalina, M. and Khanna, R. (2001). Longitudinal dynamics of antigen-specific CD8+ cytotoxic T lymphocytes following primary Epstein-Barr virus infection. *Blood* **98**, 2588-2589.

Bickham, K., Munz, C., Tsang, M. L., Larsson, M., Fonteneau, J.-F., Bhardwaj, N., and Steinman, R. (2001). EBNA1-specific CD4+ T cells in healthy carriers of Epstein-Barr virus are primarily Th1 in function. *Journal of Clinical Investigation* **107**, 121-130.

Biggar, R., Henle, W., Fleisher, G., Bocker, J., Lennette, E. T., and Henle, G. (1978). Primary Epstein-Barr virus infections in African infants. I. Decline of maternal antibodies and time of infection. *International Journal of Cancer* **22**, 239-243.

Biglari, A., Southgate, T. D., Fairbairn, L. J, and Gilham, D. E. (2006). Human monocytes expressing a CEA-specific chimeric CD64 receptor specifically target CEA-expressing tumour cells in vitro and in vivo. *Gene Therapy* **13**, 602-610.

Biglino, A., Sinnico, A., Forno, B., Pollono, A. M., Sciandra, M., Martini, C., Pich, P., and Gioannini, P. (1996). Serum cytokine profiles in acute primary HIV-1 infection and in infectious mononucleosis. *Clinical Immunology and Immunopathology* **78**, 61-69.

Birkeland, S. A. (1983). Cancer in cadaver kidney transplant patients. *Surgery* **93**, 504-507.

Blaskovic, D., Stancekova, M., Svobodova, J., and Mistrikova, J. (1980). Isolation of five strains of herpesviruses from two species of free living small rodents. *Acta Virologica* **24**, 468.

Bogedain, C., Wolf, H., Modrow, S., Stuber, G., and Jilg, W. (1995). Specific cytotoxic T lymphocytes recognize the immediate-early transactivator Zta of Epstein-Barr virus. *Journal of Virology* **69**, 4872-4879.

Bollard, C. M., Kuehnle, I., Leen, A., Rooney, C. M., and Heslop, H. E. (2004). Adoptive immunotherapy for posttransplantation viral infections. *Biology of Blood and Marrow Transplantation* **10**, 143-155.

Bollard, C. M., Savoldo, B., Rooney, C. M., and Heslop, H. E. (2003). Adoptive T-cell therapy for EBV-associated post-transplant lymphoproliferative disease. *Acta Haematologica* **110**, 139-148.

Bonini, C., Ferrari, G., Verzeletti, S., Servida, P., Zappone, E., Ruggieri, L., Ponzoni, M., Rossini, S., Mavilio, F., Traversari, C., and Bordignon, C. (1997). FHSV-TK gene transfer into donor lymphocytes for control of allogeneic graft-versus-leukemia. *Science* **276**, 1719-1724.

Borza, C. M. and Hutt-Fletcher, L. M. (2002). Alternate replication in B cells and epithelial cells switches tropism of Epstein-Barr virus. *Nature Medicine* **8**, 594-599.

Bosma, G. C., Custer, R. P., and Bosma, M. J. (1983). A severe combined immunodeficiency mutation in the mouse. *Nature* **301**, 527-530.

Bosma, G. C., Fried, M., Custer, R. P., Carroll, A., Gibson, D. M., and Bosma, M. J. (1988). Evidence of functional lymphocytes in some (leaky) scid mice. *Journal of Experimental Medicine* **167**, 1016-1033.

Bosma, M. J., and Carroll, A. M. (1991). The scid mouse mutant: Definition, characterization, and potential uses. *Annual Review of Immunology* **9**, 323-350.

Boyle, T. J., Berend, K. R., DiMaio, M., Coles, R. E., Via, D. F., and Lyerly, H. K. (1993). Adoptive transfer of cytotoxic T lymphocytes for the treatment of transplant-associated lymphoma. *Surgery* **114**, 218-226.

Boyle, T. J., Tamburini, M., Berend, K. R., Kizilbash, A. M., Borowitz, M. J., and Lyerly, H. K. (1992). Human B-cell lymphoma in severe combined immunodeficient mice after active infection with Epstein-Barr virus. *Surgery* **112**, 378-386.

Braaten, D. C., Sparks-Thissen, R. L., Kreher, S., Speck, S. H., and Virgin, H. W. (2005). An optimized CD8+ T-cell response controls productive and latent gammaherpesvirus infection. *Journal of Virology* **79**, 2573-2583.

Brandtzaeg, P., Baekkevold, E. S., Farstad, I. N., Jahnsen, F. L., Johansen, F. E., Nilsen, E. M., and Yamanaka, T. (1999b). Regional specialization in the mucosal immune system: what happens in the microcompartments? *Immunology Today* **20**, 141-151.

Brandtzaeg, P., Farstad, I. N., and Haraldsen, G. (1999a). Regional specialization in the mucosal immune system: primed cells do not always home along the same track. *Immunology Today* **20**, 267-277.

Breedveld, F. C. (2000). Therapeutic monoclonal antibodies. *Lancet* **355**, 735–740.

Buchsbaum, R. J., Fabry, J. A., and Lieberman, J. (1996). EBV-specific cytotoxic T lymphocytes protect against human EBV-associated lymphoma in scid mice. *Immunology Letters* **52**, 145-152.

Burkitt, D. (1958). A sarcoma involving the jaws in African Children. *British Journal of Surgery* **46**, 218-223.

Burns, D. M., and Crawford, D. H. (2004). Epstein-Barr virus-specific cytotoxic T-lymphocytes for adoptive immunotherapy of post-transplant lymphoproliferative disease. *Blood Reviews* **18**, 193-209.

Cai, S.-R., Garbow, J. R., Culverhouse, R., Church, R. D., Zhang, W., Shannon, W.D., and McLeod, H. L. (2005). A mouse model for developoing treatment for secondary liver tumors. *International Journal of Oncology* **27**, 113-120.

Calame, K. L., Lin, K. I., and Tunyaplin, C. (2003). Regulatory mechanisms that determine the development and function of plasma cells. *Annual Review of Immunology* **21**, 205-230.

Caldwell, R. G., Wilson, J. B., Anderson, S. J., and Longnecker, R. (1998). Epstein-Barr virus LMP2A drives B cell development and survival in the absence of normal B cell receptor signals. *Immunity* **9**, 405-411.

Callan, M. F. (2004). The immune response to Epstein-Barr virus. *Microbes and Infection* **6**, 937-945.

Callan, M. F., Fazou, C., Yang, H., Rostron, T., Poon, K., Hatton, C., and McMichael, A. J. (2000). CD8(+) T-cell selection, function, and death in the primary immune response in vivo. *Journal of Clinical Investigation* **106**, 1251-1261.

Callan, M. F. C., Steven, N., Krausa, P., Wilson, J. D. K., Moss, P. A. H., Gillespie, G. M., Bell, J. I., Rickinson, A. B., and McMichael, A. J. (1996). Large clonal expansions of CD8+ T cells in acute infectious mononucleosis. *Nature Medicine* **2**, 906-911.

Callan, M. F. C., Tan, L., Annels, N., Ogg, G. S., Wilson, J. D., O'Callaghan, C. A., Steven, N., McMichael, A. J., Rickinson, A. B. (1998). Direct visualization of antigen-specific CD8+ T cells during the primary immune response to Epstein-Barr virus in vivo. *Journal of Experimental Medicine* **187**, 1395-1402.

Cannon, M. J., Pisa, P., Fox, R. I., and Cooper, N. R. (1990). Epstein-Barr virus induces aggressive lymphoproliferative disorders of human B cell origin in scid/hu chimeric mice. *Journal of Clinical Investigation* **85**, 1333-1337.

Casola, S., Otipoby, K. L., Alimzhanov, M., Humme, S., Uyttersprot, N., Kutok, J. L., Carroll, M. C., and Rajewsky, K. (2004). B cell receptor signal strength determines B cell fate. *Nature Immunology* **5**, 317-327.

Cen, H., Breinig, M. C., Atchison, R. W., Ho, M., and McKnight, J. L. C. (1991). Epstein-Barr virus transmission via the donor organs in solid organ transplantation: Polymerase chain reaction and restriction fragment length polymorphism analysis of IR2, IR3, and IR4. *Journal of Virology* **65**, 976-980.

Cen, H., Williams, P. A., McWilliams, H. P., Breinig, M. C., Ho, M., and McKnight, J. L. C. (1993). Evidence for restricted Epstein-Barr virus latent gene expression and anti-EBNA antibody response in solid organ transplant recipients with posttransplant lymphoproliferative disorders. *Blood* **81**, 1393-1403.

Cheadle, E. J., Gilham, D. E., Thistlethwaite, F. C., Radford, J. A., and Hawkins, R. E. (2005). Killing of non-Hodgkin lymphoma cells by autologous CD19 engineered T cells. *British Journal of Haematology* **129**, 322-332.

Chen, F., Zou, J. Z., Renzo, L. d., Winberg, G., Hu, L. F., Klein, E., Klein, G., and Ernberg, I. (1995). A subpopulation of normal B cells latently infected with Epstein-Barr virus resembles Burkitt lymphoma cells in expressing EBNA-1 but not EBNA-2 or LMP1. *Journal of Virology* **69**, 3752-3758.

Cho, Y. G., Gordadze, A. V., Ling, P. D., and Wang, F. (1999). Evolution of two types of rhesus lymphocryptovirus similar to type 1 and type 2 Epstein-Barr virus. *Journal of Virology* **73**, 9206-9212.

Cho, Y., Ramer, J., Rivailler, P., Quink, C., Garber, R.L., Beier, D.R., and Wang, F. (2001). An Epstein-Barr-related herpesvirus from marmoset lymphomas. *Proceedings of the National Academy of Sciences of the USA* **98**, 1224-1229.

Choquet, S., Leblond, V., Herbrecht, R., Socie, G., Stoppa, A.-M., Vandenberghe, P., Fischer, A., Morschhauser, F., Salles, G., Feremans, W., Vilmer, E., Peraldi, M.-N., Lang, P., Lebranchu, Y., Oksenhendler, E., Garnier, J. L., Lamy, T., Jaccard, A., Ferrant, A., Offner, F., Hermine, O., Moreau, A., Fafi-Kremer, S., Morand, P., Chatenoud, L., Berriot-Varoqueaux, N., Bergougnoux, L., and Milpied, N. (2006). Efficacy and safety of rituximab in B-cell post-transplantation lymphoproliferative disorders: results of a prospective multicenter phase 2 study. *Blood* **107**, 3053-3057.

Ciceri, F., Bonini, C., Marktel, S., Zappone, E., Servida, P., Bernardi, M., Pescarollo, A., Bondanza, A., Peccatori, J., Rossini, S., Magnani, Z., Salomoni, M., Benati, C., Ponzoni, M., Callegaro, L., Corradini, P., Bregni, M., Traversari, C., and Bordignon, C. (2007). Antitumor effects of HSV-TK-engineered donor lymphocytes after allogeneic stem-cell transplantation. *Blood* **109**, 4698-4707.

Cleary, M. L., Epstein, M. A., Finerty, S., Dorfman, R. F., Bornkamm, G. W., Kirkwood, J. K., Morgan, A. J., and Sklar, J. (1985). Individual tumors of multifocal EB virus-induced malignant lymphomas in tamarins arise from different B-cell clones. *Science* **228**, 722-724.

Cockfield, S. M. (2001). Identifying the patient at risk for post-transplant lymphoproliferative disorder. *Transplant Infectious Disease* **3**, 70-78.

Comoli, P., Labirio, M., Basso, S., Baldanti, F., Grossi, P., Furione, M., Vigano, M., Fiocchi, R., Rossi, G., Ginevri, F., Gridelli, B., Moretta, A., Montagna, D., Locatelli, F., Gerna, G., and Maccario, R. (2002). Infusion of autologous Epstein-Barr virus (EBV)-specific cytotoxic T cells for prevention of EBV-related lymphoproliferative disorder in solid organ transplant recipients with evidence of active virus replication. *Blood* **99**, 2592-2598.

Conacher, M., Callard, R., McAulay, K., Chapel, H., Webster, D., Kumararatne, D., Chandra, A., Spickett, G., Hopwood, P. A., and Crawford, D. H. (2005). Epstein-Barr Virus can establish infection in the absence of a classical memory B-cell population. *Journal of Virology* **79**, 11128-11134.

Cook, R. C., Connors, J. M., Gascoyne, R. D., Fradet, G., and Levy, R. D. (1999). Treatment of post-transplant lymphoproliferative disease with rituximab monoclonal antibody after lung transplantation. *Lancet* **354**, 1698-1699.

Coppola, V., Veronesi, A., Indraccolo, S., Calderazzo, F., Mion, M., Minuzzo, S., Esposito, G., Mauro, D., Silvestri, B., Gallo, P., Falagiani, P., Amadori, A., and Chieco-Bianchi, L. (1998). Lymphoproliferative disease in human peripheral blood mononuclear cell-injected SCID mice. IV. Differential activation of human Th1 and Th2 lymphocytes and influence of the atopic status on lymphoma development. *Journal of Immunology* **160**, 2514-2522.

Cox, C., Chang, S., Karran, L., Griffin, B., and Wedderburn, N. (1996). Persistent Epstein-Barr virus infection in the common marmoset (Callithrix jacchus). *Journal of General Virology* **77**, 1173-1180.

Cox, C., Naylor, B. A., Mackett, M., Arrand, J. R., Griffin, B. E., and Wedderburn, N. (1998). Immunization of common marmosets with Epstein-Barr virus (EBV) envelope glycoprotein gp340: effect on viral shedding following EBV challenge. *Journal of Medical Virology* **55**, 255-261.

Cox, K. L., Lawrence-Miyasaki, L. S., Garcia-Kennedy, R., Lennette, E. T., Martinez, O. M., Krams, S. M., Berquist, W. E., So, S. K. S., and Esquivel, C. O. (1995). An increased incidence of Epstein-Barr virus infection and lymphoproliferative disorder in young children on FK506 after liver transplantation. *Transplantation* **59**, 524-529.

Crawford, D. H., and Ando, I. (1986). EB virus induction is associated with B-cell maturation. *Immunology* **59**, 405-409.

Crawford, D. H., Brickell, P., Tidman, N., McConnell, I., Hoffbrand, A. V., and Janossy, G. (1981a). Increased numbers of cells with suppressor T cell phenotype in the peripheral blood of patients with infectious mononucleosis. *Clinical and Experimental Immunology* **43**, 291-297.

Crawford, D. H., and Edwards, J. M. B. (1990). 'Epstein-Barr virus.' 2nd ed. *Principles and Practice of Clinical Virology* (A. J. Zuckerman, J. E. Banatvala, and J. R. Pattison, Eds.), 103-128. John Wiley & Sons Ltd, Chichester, West Sussex, UK.

Crawford, D. H., Edwards, J. M. B., Sweny, P., Hoffbrand, A. V., and Janossy, G. (1981b). Studies on long-term T-cell-mediated immunity to Epstein-Barr virus in immunosuppressed renal allograft recipients. *International Journal of Cancer* **28**, 705-709.

Crawford, D. H., Macsween, K. F., Higgins, C. D., Thomas, R., McAulay, K., Williams, H., Harrison, N., Reid, S., Conacher, M., Douglas, J., and Swerdlow, A. J. (2006) A cohort study among university students: identification of risk factors for Epstein-Barr Virus seroconversion and infectious mononucleosis. *Clinical Infectious Diseases* **43**, 276–282.

Crawford, D. H., Thomas, J. A., Janossy, G., Sweny, P., Fernando, O. N., Moorhead, J. F., and Thompson, J. H. (1980). Epstein-Barr virus nuclear antigen positive lymphoma after cyclosporin A treatment in patient with renal allograft. *Lancet* **1**, 1355-1356.

Custer, R. P., Bosma, G. C., and Bosma, M. J. (1985). Severe combined immunodeficieny (SCID) in the mouse: Pathology, reconstitution, neoplasms. *American Journal of Pathology* **120**, 464-477.

Davis, C. L. (2001). Interferon and cytotoxic chemotherapy for the treatment of post-transplant lymphoproliferative disorder. *Transplant Infectious Disease* **3**, 108-118.

Davis, C. L., Wood, B. L., Sabath, D. E., Joseph, J. S., Stehman-Breen, C., and Broudy, V. C. (1998). Interferon-alpha treatment of posttransplant lymphoproliferative disorder in recipients of solid organ transplants. *Transplantation* **66**, 1770-1779.

Davis, T. A., Czerwinski, D. K., and Levy, R. (1999). Therapy of B-cell lymphoma with anti-CD20 antibodies can result in the loss of CD20 antigen expression. *Clinical Cancer Research* **5**, 611-615.

De Bueger, M., Bakker, A., and Goulmy, E. (1992). Existence of mature human CD4+ T cells with genuine class I restriction. *European Journal of Immunology* **22**, 875-878.

Deinhardt, F., and Deinhardt, J. (1979). 'Comparative aspects: Oncogenic animal herpesviruses.' *The Epstein-Barr Virus* (M. A. Epstein, and B. G. Achong, Eds.), 373-415. Springer-Verlag, Berlin, Germany.

Dermime, S., Gilham, D. E., Shaw, D. M., Davidson, E. J., Meziane, el-K., Armstrong, A., Hawkins, R. E., and Stern, P. L. (2004). Vaccine and antibody-directed T cell tumour immunotherapy. *Biochimica et Biophysica Acta* **1704**, 11-35.

De Thè, G., Dubouch, P., Fontaine, C., Wedderburn, N., Carter, R. L., Edwards, M. B., and Cohen, B. (1980). Natural antibodies to EBV-VCA antigens in common marmosets (Callithrix jacchus) and response after EBV inoculation. *Intervirology* **14**, 284-291.

Dey, B. R., McAfee, S., Colby, C., Cieply, K., Caron, M., Saidman, S., Preffer, F., Shaffer, J., Tarbell, N., Sackstein, R., Sachs, D., Sykes, M., and Spitzer, T. R. (2005). Anti-tumour response despite loss of donor chimaerism in patients treated with non-myeloablative conditioning and allogeneic stem cell transplantation. *British Journal of Haematology* **128**, 351-359.

Dick, J. E. (1994). Future prospects for animal models created by transplanting human haematopoietic cells into immune-deficient mice. *Research in Immunology* **145**, 380-384.

Dierksheide, J. E., Baiocchi, R. A., Ferketich, A. K., Roychowdhury, S., Pelletier, R. P., Eisenbeis, C. F., Caligiuri, M. A., and VanBuskirk, A. M. (2005). IFN-gamma gene polymorphisms associate with development of EBV+ lymphoproliferative disease in hu PBL-SCID mice. *Blood* **105**, 1558-1565.

DiMaio, J. M., Trigt, P. V., Gaynor, J. W., Davis, R. D., Coveney, E., Clary, B. M., and Lyerly, H. K. (1995). Generation of tumour-specific T lymphocytes for the treatment of posttransplant lymphoma. *Circulation* **92** (Suppl. II), II202-205.

Downey, H., and McKinlay, C. A. (1923). Acute lymphadenosis compared with acute lymphatic leukemia. *Archives of Internal Medicine* **32**, 82-112.

Dudley, M. E., Wunderlich, J. R., Yang, J. C., Hwu, P., Schwartzentruber, D. J., Topalian, S. L., Sherry, R. M., Marincola, F. M., Leitman, S. F., Seipp, C. A., Rogers-Freezer, L., Morton, K. E., Nahvi, A., Mavroukakis, S. A., White, D. E., and Rosenberg, S. A. (2002). A phase I study of nonmyeloablative chemotherapy and adoptive transfer of autologous tumor antigen-specific T lymphocytes in patients with metastatic melanoma. *Journal of Immunotherapy* **25**, 243-251.

Dutia, B. M., Clarke, C. J., Allen, D. J., and Nash, A. A. (1997). Pathological changes in the spleens of gamma interferon receptor-deficient mice infected with murine gammaherpesvirus: a role for CD8 T cells. *Journal of Virology* **71**, 4278-4283.

Ebrahimi, B., Dutia, B. M., Brownstein, D. G., and Nash, A. A. (2001). Murine gammaherpesvirus-68 infection causes multi-organ fibrosis and alters leukocyte trafficking in interferon-gamma receptor knockout mice. *American Journal of Pathology* **158**, 2117-2125.

Ehlers, B., Ochs, A., Leendertz, F., Goltz, M., Boesch, C., and Matz-Rensing, K. (2003). Novel simian homologues of Epstein-Barr virus. *Journal of Virology* **77**, 10695–10699.

Elstrom, R. L., Andreadis, C., Aqui, N. A., Ahya, V. N., Bloom, R. D., Brozena, S. C., Olthoff, K. M., Schuster, S. J., Nasta, S. D., Stadtmauer, E. A., and Tsai, D. E. (2006). Treatment of PTLD with rituximab or chemotherapy. *American Journal of Transplantation* **6**, 569-576.

Emilie, D., Coumbaras, J., Raphael, M., Devergne, O., Delecluse, H. J., Gisselbrecht, C., Michiels, J. F., Damme, J. v., Taga, T., Kishimoto, T., Crevon, M. C., and Galanaud, P. (1992a). Interleukin-6 production in high-grade B lymphomas: Correlation with the presence of malignant immunoblasts in acquired immunodeficiency syndrome and in human immunodeficiency virus-seronegative patients. *Blood* **80**, 498-504.

Emilie, D., Touitou, R., Raphael, M., Peuchmaur, M., Devergnee, O., Rea, D., Coumbraras, J., Crevon, M. C., Edelman, L., Joab, I., and Galanaud, P. (1992b). In vivo production of interleukin-10 by malignant cells in AIDS lymphomas. *European Journal of Immunology* **22**, 2937-2942.

Epstein, M. A. (1976). Epstein-Barr virus - Is it time to develop a vaccine program? (Editorial). *Journal of the National Cancer Institute* **56**, 697-700.

Epstein, M. A., Achong, B. G., and Barr, Y. M. (1964). Virus particles in cultured lymphoblasts from Burkitt's lymphoma. *Lancet* **1**, 702-703.

Epstein, M. A., and Barr, Y. M. (1964). Cultivation in vitro of human lymphoblasts from Burkitt's malignant lymphoma. *Lancet* **1**, 252-253.

Epstein, M. A., and Crawford, D. H. (2005). 'Gammaherpesviruses: Epstein-Barr virus.' 10th ed. *Topley & Wilson's Microbiology & Microbial Infections* (B. W. J. Mahy and V. Ter Meulen, Eds.), 1, 559-577. Hodder Arnold, London, UK.

Epstein, M. A., Morgan, A. J., Finerty, S., Randle, B. J., and Kirkwood, J. K. (1985). Protection of cottontop tamarins against Epstein-Barr virus-induced malignant lymphoma by a prototype subunit vaccine. *Nature* **318**, 287-289.

Eshhar, Z., Waks, T., Gross, G., and Schindler, D. G. (1993). Specific activation and targeting of cytotoxic lymphocytes through chimeric single chains consisting of antibody-binding domains and the γ or ζ subunits of the immunoglobulin and T-cell receptors. *Proceedings of the National Academy of Sciences of the USA* **90**, 720-724.

European Medicines Evaluation Agency (EMEA).
http://www.emea.europa.eu (Accessed 17 August 2007).

Fafi-Kremer, S., Morand, P., Brion, J. P., Pavese, P., Baccard, M., Germi, R., Genoulaz, O., Nicod, S., Jolivet, M., Ruigrok, R. W., Stahl, J. P. and Seigneurin, J. M. (2005). Long-term shedding of infectious Epstein-Barr virus after infectious mononucleosis. *Journal of Infectious Diseases* **191**, 985-989.

Falk, L., Deinhardt, F., Wolfe, L., Johnson, D., Hilgers, J., and deThe, G. (1976). Epstein-Barr virus: Experimental infection of Callithrix Jacchus marmosets. *International Journal of Cancer* **17**, 785-788.

Farrell, P. J., Hollyoake, M., Niedobitek, G., Agathanggelou, A., Morgan, A., and Wedderburn, N. (1997). Direct demonstration of persistent Epstein-Barr virus gene expression in peripheral blood of infected common marmosets and analysis of virus-infected tissues in vivo. *Journal of General Virology* **78**, 1417-1424.

Faulkner, G. C., Burrows, S. R., Khanna, R., Moss, D. J., Bird, A. G. and Crawford, D. H. (1999). B lymphocytes are the target cell for primary infection with Epstein-Barr virus. *Journal of Virology* **73**, 1555-1564.

Feichtinger, H., Li, S. L., Kaaya, E., Putkonen, P., Grünewald, K., Weyrer, K., Böttiger, D., Ernberg, I., Linde, A., Biberfeld, G., and Biberfeld, P. (1992). A monkey model for Epstein Barr virus-associated lymphomagenesis in human acquired immunodeficiency syndrome. *Journal of Experimental Medicine* **176**, 281-286.

Feng, W. H., and Kenney, S. C. (2006). Valproic acid enhances the efficacy of chemotherapy in EBV-positive tumors by increasing lytic viral gene expression. *Cancer Research* **66**, 8762-8769.

Fennewald, S., Santen, V. v., and Kieff, E. (1984). Nucleotide sequence of an mRNA transcribed in latent growth-transforming virus infection indicates that it may encode a membrane protein. *Journal of Virology* **51**, 411-419.

Fingeroth, J. D., Weis, J. J., Tedder, T. F., Strominger, J. L., Biro, P. A., and Fearon, D. T. (1984). Epstein-Barr virus receptor of human B lymphocytes is the C3d receptor CD2. *Proceedings of the National Academy of Sciences of the USA* **81**, 4510-4514.

Fischer, A., Blanche, S., Bidois, J. L., Bordigoni, P., Garnier, J. L., Niaudet, P., Morinet, F., Deist, F. L., Fischer, A. M., Griscelli, C., and Hirn, M. (1991). Anti-B-cell monoclonal antibodies in the treatment of severe B-cell lymphoproliferative syndrome following bone marrow and organ transplantation. *New England Journal of Medicine* **324**, 1451-1456.

Fogg, M. H., Garry, D., Awad, A., Wang, F., and Kaur, A. (2006). The BZLF1 homolog of an Epstein-Barr-related gamma-herpesvirus is a frequent target of the CTL response in persistently infected rhesus macaques. *Journal of Immunology* **176**, 3391-3401.

Fogg, M. H., Kaur, A., Cho, Y. G., and Wang, F. (2005). The CD8+ T-cell response to an Epstein-Barr virus-related gammaherpesvirus infecting rhesus macaques provides evidence for immune evasion by the EBNA-1 homologue. *Journal of Virology* **79**, 12681-12691.

Foroncewicz, B., Mucha, K., Usiekniewicz, J., Chmura, A., Kryst, P., Soldacki, D., and Paczek, L. (2006). Posttransplant lymphoproliferative disorder of the lung in a renal transplant recipient treated successfully with surgery. *Transplantation Proceedings* **38**, 173-176.

Foss, H. D., Herbst, H., Hummel, M., Araujo, I., Latza, U., Rancsò, C., Dallenbach, F., and Stein, H. (1994). Patterns of cytokine gene expression in infectious mononucleosis. *Blood* **83**, 707-712.

Fund for the Replacement of Animals in Medical Experiments (FRAME). http://www.frame.org.uk (Accessed 17 August 2007).

Frank, A., Andiman, W. A., and Miller, G. (1976). Epstein-Barr virus and nonhuman primates: natural and experimental infection. *Advances in Cancer Research* **23**, 171–201.

Franken, M., Estabrooks, A., Cavacini, L., Sherburne, B., Wang, F., and Scadden, D. T. (1996). Epstein-Barr virus-driven gene therapy for EBV-related lymphomas. *Nature Medicine* **2**, 1379-1382.

Frizzera, G., Hanto, D. W., Gajl-Peczalska, K. J., Rosai, J., McKenna, R. W., Sibley, R. K., Holahan, K. P., and Lindquist, L. L. (1981). Polymorphic diffuse B-cell hyperplasias and lymphomas in renal transplant recipients. *Cancer Research* **41**, 4262-4279.

Fulop, G. M., and Phillips, R. A. (1990). The scid mutation in mice causes a general defect in DNA repair. *Nature* **347**, 479-482.

Funakoshi, S., Taub, D. D., Asai, O., Hirano, A., Ruscetti, F. W., Longo, D. L., and Murphy, W. J. (1997). Effects of CD40 stimulation in the prevention of human EBV-lymphomagenesis. *Leukemia Lymphoma* **24**, 187-199.

Gandhi, M. K., Wilkie, G. M., Dua, U., Mollee, P. N., Grimmett, K., Williams, T., Whitaker, N., Gill, D., and Crawford, D. H. (2007). Immunity, homing and efficacy of allogeneic adoptive immunotherapy for posttransplant lymphoproliferative disorders. *American Journal of Transplantation* **7**, 1293–1299.

Gao, S. Z., Chaparro, S. V., Perlroth, M., Montoya, J. G., Miller, J. L., DiMiceli, S., Hastie, T., Oyer, P. E., and Schroeder, J. (2003). Post-transplantation lymphoproliferative disease in heart and heart-lung transplant recipients: 30-year experience at Stanford University. *Journal of Heart and Lung Transplantation* **22**, 505-514.

Gardella, T., Medveczky, P., Sairenji, T., and Mulder, C. (1984). Detection of circular and linear herpesvirus DNA molecules in mammalian cells by electrophoresis. *Journal of Virology* **50**, 248-254.

Gerber, P., and Birch, S. M. (1967). Complement-fixing antibodies in sera of human and nonhuman primates to viral antigens derived from Burkitt's lymphoma cells. *Proceedings of the Natinal Academy of Sciences of the USA* **58**, 478-484.

Gerber, P., Nonoyama, M., Lucas, S., Perlin, E., and Goldstein, L. I. (1972). Oral excretion of Epstein-Barr virus by healthy subjects and patients with infectious mononucleosis. *Lancet* **2**, 988-989.

Gianni, A. M., Magni, M., Martelli, M., Di Nicola, M., Carlo-Stella, C., Pilotti, S., Rambaldi, A., Cortelazzo, S., Patti, C., Parvis, G., Benedetti, F., Capria, S., Corradini, P., Tarella, C., and Barbui, T. (2003). Long-term remission in mantle cell lymphoma following high-dose sequential chemotherapy and in vivo rituximab-purged stem cell autografting (R-HDS regimen). *Blood* **102**, 749-755.

Gonnella, R., Angeloni, A., Calogero, A., Farina, A., Santarelli, R., Gentile, G., Arcese, W., Martino, P., Mandelli, F., Frati, L., Faggioni, A., and Ragona, G. (1997). Transcription of latent and replicative Epstein-Barr virus genes in bone marrow and peripheral blood mononuclear cells of healthy donors. *International Journal of Cancer* **70**, 524-529.

Gottschalk, S., Edwards, O. L., Sili, U., Huls, M. H., Goltsova, T., Davis, A. R., Heslop, H. E., and Rooney, C. M. (2003). Generating CTLs against the subdominant Epstein-Barr virus LMP1 antigen for the adoptive immunotherapy of EBV-associated malignancies. *Blood* **101**, 1905-1912.

Gottschalk, S., Ng, C. Y., Perez, M., Smith, C. A., Sample, C., Brenner, M. K., Heslop, H. E., and Rooney, C. M. (2001). An Epstein-Barr virus deletion mutant associated with fatal lymphoproliferative disease unresponsive to therapy with virus-specific CTLs. *Blood* **97**, 835-843.

Gottschalk, S., Rooney, C. M., Heslop, H. E. (2005). Posttransplant lymphoproliferative disorders. *Annual Review of Medicine* **56**, 29-44.

Grant, D. (1999). On behalf of the Intestinal Transplant Registry: 1997 Report of the International Registry. *Transplantation* **67**, 1061–1064.

Gratama, J. W., Oosterveer, M. A. P., Zwaan, F. E., Lepoutre, J., Klein, G., and Ernberg, I. (1988). Eradication of Epstein-Barr virus by allogeneic bone marrow transplantation: Implications for sites of viral latency. *Proceedings of the National Academy of Sciences of the USA* **85**, 8693-8696.

Griffiths, R. W., Gilham, D. E., Dangoor, A., Ramani, V., Clarke, N. W., Stern, P. L., and Hawkins, R. E. (2005). Expression of the 5T4 oncofetal antigen in renal cell carcinoma: a potential target for T-cell-based immunotherapy. *British Journal of Cancer* **93**, 670-677.

Gross, T. G., Bucuvalas, J. C., Park, J. R., Greiner, T. C., Hinrich, S. H., Kaufman, S. S., Langnas, A. N., McDonald, R. A., Ryckman, F. C., Shaw, B. W., Sudan, D. L., and Lynch, J. C. (2005). Low-dose chemotherapy for Epstein-Barr virus-positive post-transplantation lymphoproliferative disease in children after solid organ transplantation. *Journal of Clinical Oncology* **23**, 6481-6488.

Guinness, M. E., Kenney, J. L., Reiss, M., and Lacy, J. (2000). Bcl-2 antisense oligodeoxynucleotide therapy of Epstein-Barr virus-associated lymphoproliferative disease in severe combined immunodeficient mice. *Cancer Research* **60**, 5354-5358.

Guohua, P., Yi, Z., Winping, Z., and Qin, Z. (1981). Development of an anticomplement immunoenzyme test for detection of EB virus nuclear antigen (EBNA) and antibody to EBNA. *Journal of Immunological Methods* **44**, 73-78.

Gustafsson, A., Levitsky, V., Zou, J. Z., Frisan, T., Dalianis, T., Ljungman, P., Ringden, O., Winiarski, J., Ernberg, I., and Masucci, M. G. (2000). Epstein–Barr virus (EBV) load in bone marrow transplant recipients at risk to develop post-transplant lymhoproliferative disease: prophylactic infusion of EBV-specific cytotoxic T cells. *Blood* **95**:807–814.

Haddad, E., Paczesny, S., Leblond, V., Seigneurin, J.M., Stern, M., Achkar, A., Bauwens, M., Delwail, V., Debray, D., Duvoux, C., Hubert, P., de Ligny, B.H., Wijdenes, J., Durandy, A., and Fischer, A. (2001). Treatment of B-lymphoproliferative disorder with a monoclonal anti-interleukin-6 antibody in 12 patients: a multicenter phase 1-2 clinical trial. *Blood* **97**, 1590-1597.

Hanto, D. W., Frizzera, G., Gajl-Peczalska, K. J., Sakamoto, K., Purtilo, D. T., Balfour, H. H., Simmons, R. L., and Najarian, J. S. (1982). Epstein-Barr virus-induced B-cell lymphoma after renal transplantation. *New England Journal of Medicine* **306**, 913-918.

Hanto, D. W., Gajl-Peczalska, K. J., Frizzera, G., Arthur, D. C., Balfour, H. H., McClain, K., Simmons, R. L., and Najarian, J. S. (1983). Epstein-Barr virus (EBV) induced polyclonal and monoclonal B-cell lymphoproliferative diseases occurring after renal transplantation. Clinical, pathologic, and virologic findings and implications for therapy. *Annals of Surgery* **198**, 356-369.

Haque, T., Amlot, P. L., Helling, N., Thomas, J. A., Sweny, P., Rolles, K., Burroughs, A. K., Prentice, H. G., and Crawford, D. H. (1998). Reconstitution of EBV-specific T cell immunity in solid organ transplant recipients. *Journal of Immunology* **160**, 6204–6209.

Haque, T., Johannessen, I., Dombagoda, D., Sengupta, C., Burns, D. M., Bird, P., Hale, G., Mieli-Vergani, G., and Crawford, D. H. (2006). A mouse monoclonal antibody against Epstein-Barr Virus envelope glycoprotein 350 prevents infection both in vitro and in vivo. *Journal of Infectious Diseases* **194**, 584–587.

Haque, T., Taylor, C., Wilkie, G. M., Murad, P., Amlot, P. L., Beath, S., McKiernan, P. J., and Crawford, D. H. (2001). Complete regression of posttransplant lymphoproliferative disease using partially HLA-matched Epstein Barr virus-specific cytotoxic T cells. *Transplantation* **72**, 1399-1402.

Haque, T., Thomas, J. A., Falk, K. I., Parratt, R., Hunt, B. J., Yacoub, M., and Crawford, D. H. (1996). Transmission of donor Epstein-Barr virus (EBV) in transplanted organs causes lymphoproliferative disease in EBV-seronegative recipients. *Journal of General Virology* **77**, 1169-1172.

Haque, T., Thomas, J. A., Parratt, R., Hunt, B. J., Yacoub, M. H., and Crawford, D. H. (1997). A prospective study in heart and lung transplant recipients correlating persistent Epstein-Barr virus infection with clinical events. *Transplantation* **64**, 1028-1034.

Haque, T., Wilkie, G. M., Morton-Jones, M. M., Higgins, C. D., Urquhart, G., Wingate, P., Burns, D., McAulay, K., Turner, M., Bellamy, C., Amlot, P. L., Kelly, D., Macgilchrist, A., Gandhi, M. K., Swerdlow, A. J., and Crawford, D.H. (2007). Allogeneic cytotoxic T-cell therapy for EBV-positive posttransplantation lymphoproliferative disease: results of a phase 2 multicenter clinical trial. *Blood* **110**, 1123-1131.

Haque, T., Wilkie, G. M., Taylor, C., Amlot, P. L., Murad, P., Iley, A., Dombagoda, D., Britton, K. M., Swerdlow, A. J., and Crawford, D. H. (2002). Treatment of Epstein-Barr-virus-positive post-transplantation lymphoproliferative disease with partly HLA-matched allogeneic cytotoxic T cells. *Lancet* **360**, 436–442.

Hart, C., Schochetman, G., Spira, T., Lifson, A., Moore, J., Galphin, J., Sninsky, J., and Ou, C. Y. (1988). Direct detection of HIV RNA expression in seropositive subjects. *Lancet* **2**, 596-599.

He, B., Raab-Traub, N., Casali, P., and Cerutti, A. (2003). EBV-encoded latent membrane protein 1 cooperates with BAFF/BLyS and APRIL to induce T cell independent Ig heavy chain class switching. *Journal of Immunology* **171**, 5215-5224.

Health Protection Agency (HPA). 'Epstein-Barr Virus Serology.' http://www.hpa-standardmethods.org.uk (Accessed 17 August 2007)

Helminen, M. E., Kilpinen, S., Virta, M., and Hurme, M. (2001). Susceptibility to primary Epstein-Barr virus infection is associated with interleukin-10 gene promoter polymorphism. *Journal of Infectious Diseases* **184**, 777-780.

Helminen, M., Lahdenpohja, N., and Hurme, M. (1999). Polymorphism of the interleukin-10 gene is associated with susceptibility to Epstein-Barr virus infection. *Journal of Infectious Diseases* **180**, 496-499.

Henle, G., and Henle, W. (1966). Immunofluorescence in cells derived from Burkitt's lymphoma. *Journal of Bacteriology* **91**, 1248-1256.

Henle, W., and Henle, G. (1969). The relation between the Epstein-Barr virus and infectious mononucleosis, Burkitt's lymphoma and cancer of the postnasal space. *East African Medical Journal* **46**, 402-406.

Henle, W., and Henle, G. (1979). 'Seroepidemiology of the virus.' *The Epstein-Barr Virus* (M. A. Epstein, and B. G. Achong, Eds.), 61-78. Springer-Verlag, Berlin, Germany.

Henle, W., and Henle, G. (1981). Epstein-Barr virus-specific serology in immunologically compromised individuals. *Cancer Research* **41**, 4222-4225.

Herbst, H. and Niedobitek, G. (1994) Epstein-Barr virus in Hodgkin's disease. *EBV Report* **1**, 31-35.

Heslop, H. E., Ng, C. Y. C., Li, C., Smith, C. A., Loftin, S. K., Krance, R. A., Brenner, M. K., and Rooney, C. M. (1996). Long-term restoration of immunity against Epstein-Barr virus infection by adoptive transfer of gene-modified virus-specific T lymphocytes. *Nature Medicine* **2**, 551-555.

Hesselton, R. M., Koup, R. A., Cromwell, M. A., Graham, B. S., Johns, M., and Sullivan, J. L. (1993). Human peripheral blood xenografts in the scid mouse: Characterisation of immunologic reconstitution. *Journal of Infectious diseases* **168**, 630-640.

Hickey, W. F., Hsu, B. L., and Kimura, H. (1991). T-lymphocyte entry into central nervous system. *Journal of Neuroscience Research* **28**, 254-260.

Hinuma, Y., Konn, M., Yamaguchi, J., Wudarski, D. J., Blakeslee, J. R., and Grace, J. T. (1967). Immunofluorescence and herpes-type virus particles in the P3HR-1 Burkitt lymphoma cell line. *Journal of Virology* **1**, 1045-1051.

Hislop, A. D., Annels, N. E., Gudgeon, N. H., Leese, A. M., and Rickinson, A. B. (2002). Epitope-specific evolution of human CD8+ T cell responses from primary to persistent phases of Epstein–Barr virus infection. *Journal of Experimental Medicine* **195**, 893–905.

Ho, M., Jaffe, R., Miller, G., Breinig, M. K., Dummer, J. S., Makowka, L., Atchison, R. W., Karrer, F., Nalesnik, M. A., and Starzl, T. E. (1988). The frequency of Epstein-Barr virus infection and associated lymphoproliferative syndrome after transplantation and its manifestations in children. *Transplantation* **45**, 719-727.

Ho, M., Miller, G., Atchison, R. W., Breinig, M. K., Dummer, J. S., Andiman, W., Starzl, T. E., Eastman, R., Griffith, B. P., Hardesty, R. L., Bahnson, H. T., Hakala, T. R., and Rosenthal, J. T. (1985). Epstein-Barr virus infections and DNA hybridization studies in posttransplantation lymphoma and lymphoproliferative lesions: The role of primary infection. *Journal of Infectious Diseases* **152**, 876-886.

Hoagland, R. J. (1955). The transmission of infectious mononucleosis. *American Journal of the Medical Sciences* **229**, 262-272.

Hochberg, D., Middeldorp, J. M., Catalina, M., Sullivan, J. L., Luzuriaga, K., and Thorley-Lawson, D. A. (2004b). Demonstration of the Burkitt's lymphoma Epstein-Barr virus phenotype in dividing latently infected memory cells in vivo. *Proceedings of the National Academy of Sciences of the USA* **101**, 239-244.

Hochberg, D., Souza, T., Catalina, M., Sullivan, J. L., Luzuriaga, K., Thorley-Lawson, D. A. (2004a) Acute infection with Epstein–Barr virus targets and overwhelms the peripheral memory B-cell compartment with resting, latently infected cells. *Journal of Virology* **78**, 5194–5204.

Hoffman, G. J., Lazarowitz, S. G., and Hayward, D.H. (1980). Monoclonal antibody against a 250,000-Dalton glycoprotein of Epstein-Barr virus identifies a membrane antigen and a neutralizing antigen. *Proceedings of the National Academy of Sciences of the USA* **77**, 2979–2983.

Hoffmann-Fezer, G., Gall, C., Zengerle, U., Kranz, B., and Thierfelder, S. (1993). Immunohistology and immunocytology of human T-cell chimerism and graft-versus-host disease in scid mice. *Blood* **81**, 3440-3448.

Home Office.
'www.homeoffice.gov.uk/animalsinsp/ (Accessed 17 August 2007).

Hopwood, P. A., Brooks, L., Parratt, R., Hunt, B. J., Bokhari, M., Thomas, J. A., Yacoub, M., and Crawford, D. H. (2002). Persistent Epstein-Barr virus infection: unrestricted latent and lytic viral gene expression in healthy immunosuppressed transplant recipients. *Transplantation* **74**, 194-202.

Hoshino, Y., Morishima, T., Kimura, H., Nishikawa, K., Tsurumi, T., and Kuzushima, K. (1999). Antigen-driven expansion and contraction of CD8_-activated T cells in primary EBV infection. *Journal of Immunology* **163**, 5735-5740.

Howe, J. G., and Steitz, J. A. (1986). Localization of Epstein-Barr virus-encoded small RNAs by in situ hybridization. *Proceedings of the National Academy of Sciences of the USA* **83**, 9006-9010.

Hunt, R. D., Blake, B. J., Chalifoux, L. V., Sehgal, P. K., King, N. W., and Letvin, N. L. (1983). Transmission of naturally occurring lymphoma in macaque monkeys. *Proceedings of the National Academy of Sciences of the USA* **80**, 5085-5089.

Huppes, W., Fickenscher, H., 'tHart, B. A., and Fleckenstein, B. (1994). Cytokine dependence of human to mouse graft-versus-host disease. *Scandinavian Journal of Immunology* **40**, 26-36.

Hurley, E. A., and Thorley-Lawson, D. A. (1988). B cell activation and the establishment of Epstein-Barr virus latency. *Journal of Experimental Medicine* **168**, 2059-2075.

Hwu, P., Shafer, G. E., Treisman, J., Schindler, D. G., Gross, G., Cowherd, R., Rosenberg, S. A., and Eshhar, Z. (1993). Lysis of ovarian cancer cells by human lymphocytes redirected with a chimeric gene composed of an antibody variable region and the Fc receptor γ chain. *Journal of Experimental Medicine* **178**, 361-366.

Imai, S., Koizumi, S., Sugiura, M., Tokunaga, M., Uemura, Y., Yamamoto, N., Tanaka, S., Sato, E., and Osato, T. (1994). Gastric carcinoma: Monoclonal epithelial malignant cells expressing Epstein-Barr virus latent infection protein. *Proceedings of the National Academy of Sciences of the USA* **91**, 9131-9135.

International Conference on Harmonization of Technical Requirements for Registration of Pharmaceuticals for Human Use (ICH).
http://www.ich.org (Accessed 17 August 2007).

Ison, M. G., Mishin, V. P., Braciale, T. J., Hayden, F. G., and Gubareva, L. V. (2006). Comparative activities of oseltamivir and A-322278 in immunocompetent and immunocompromised murine models of influenza virus infection. *Journal of Infectious Diseases* **193**, 765-772.

Israele, V., Shirley, P., and Sixbey, J. W. (1991). Excretion of the Epstein-Barr virus from the genital tract of men. *Journal of Infectious Diseases* **163**, 1341-1343.

Janz, A., Oezel, M., Kurzeder, C., Mautner, J., Pich, D., Kost, M., Hammerschmidt, W. and Delecluse, H.J. (2000). Infectious Epstein-Barr virus lacking major glycoprotein BLLF1 (gp350/220) demonstrates the existence of additional viral ligands. *Journal of Virology* **74**, 10142-10152.

Jarrett, R. F. (2003). Risk factors for Hodgkin's lymphoma by EBV status and significance of detection of EBV genomes in serum of patients with EBV-associated Hodgkin's lymphoma. *Leukemia and Lymphoma* **44** (Suppl. 3), S27-32.

Jarrett, R. F., Stark, G. L., White, J., Angus, B., Alexander, F. E., Krajewski, A. S., Freeland, J., Taylor, G. M., Taylor, P. R.; Scotland and Newcastle Epidemiology of Hodgkin Disease Study Group. (2005). Impact of tumor Epstein-Barr virus status on presenting features and outcome in age-defined subgroups of patients with classic Hodgkin lymphoma: a population-based study. *Blood* **106**, 2444-2451.

Jenson, H. B., Ench, Y., Gao, S. J., Rice, K., Carey, D., Kennedy, R. C., Arrand, J. R., and Mackett, M. (2000). Epidemiology of herpesvirus papio infection in a large captive baboon colony: similarities to Epstein-Barr virus infection in humans. *Journal of Infectious Diseases* **181**, 1462–1466.

Jenson, H. B., Ench, Y., Zhang, Y., Gao, S. J., Arrand, J. R., and Mackett, M. (2002). Characterization of an Epstein-Barr virus-related gammaherpesvirus from common marmoset (Callithrix jacchus). *Journal of General Virology* **83**, 1621–1633.

Johannessen, I. Studies on the pathogenesis of Epstein-Barr virus (EBV)-associated B cell lymphoproliferative disease (BLPD) using an in vivo model. The University of London. *PhD Thesis* 1997.

Johannessen, I., Asghar, M., and Crawford, D.H. (2000). Essential role for T cells in human B cell lymphoproliferative disease development in SCID mice. *British Journal of Haematology* **109**, 600-610.

Johannessen, I., Haque, T., N'Jie-Jobe, J., and Crawford, D.H. (1998). Non-correlation of in vivo and in vitro parameters of Epstein-Barr virus persistence suggests heterogeneity of B cell infection. *Journal of General Virology* **79**, 1631-1636.

Johannessen, I., Perera, S.M., Gallagher, A., Hopwood, P.A., Thomas, J.A., and Crawford, D.H. (2002). Expansion in SCID mice of Epstein-Barr virus-associated post-transplantation lymphoproliferative disease biopsy material. *Journal of General Virology* **83**, 173-178.

Jones, J. F., Shurin, S., Abramowsky, C., Tubbs, R. R., Sciotto, C. G., Wahl, R., Sands, J., Gottman, D., Katz, B. Z., and Sklar, J. (1988). T-cell lymphomas containing Epstein-Barr viral DNA in patients with chronic Epstein-Barr virus infections. *New England Journal of Medicine* **318**, 733-741.

Joseph, A. M., Babcock, G. J., and Thorley-Lawson, D. A. (2000). Cells expressing the Epstein-Barr virus growth program are present in and restricted to the naïve B-cell subset of healthy tonsils. *Journal of Virology* **74**, 9964-9971.

Kershaw, M. H., Westwood, J. A., Parker, L. L., Wang, G., Eshhar, Z., Mavroukakis, S. A., White, D. E., Wunderlich, J. R., Canevari, S., Rogers-Freezer, L., Chen, C. C., Yang, J. C., Rosenberg, S. A., and Hwu, P. (2006) A phase I study on adoptive immunotherapy using gene-modified T cells for ovarian cancer. *Clinical Cancer Research* **12**, 6106-6115.

Khan, G., Miyashita, E. M., Yang, B., Babcock, G. J., and Thorley-Lawson, D. A. (1996). Is EBV persistence in vivo a model for B cell homeostasis? *Immunity* **5**, 173-179.

Khanna, R., Bell, S., Sherritt, M., Galbraith, A., Burrows, S. R., Rafter, L., Clarke, B., Slaughter, R., Falk, M. C., Douglass, J., Williams, T., Elliott, S. L., and Moss, D. J. (1999). Activation and adoptive transfer of Epstein-Barr virus-specific cytotoxic T cells in solid organ transplant patients with posttransplant lymphoproliferative disease. *Proceedings of the National Academy of Sciences of the USA* **96**, 10391-10396.

Khanna, R., and Burrows, S. R. (2000). Role of cytotoxic T lymphocytes in Epstein-Barr virus-associated diseases. *Annual Review of Microbiology* **54**, 19-48.

Kieff, E. D., and Rickinson, A. B. (2007) 'Epstein-Barr virus and its replication.' 5th ed. *Fields Virology* (D. M. Knipe and P. M. Howley, Eds.), 2, 2603-2654. Lippincott, Williams & Wilkins Publishers, Philadelphia, Pennsylvania, USA.

Kirkwood, B. R. (1988). *'Essentials of Medical Statistics.'* Blackwell Science Ltd, Oxford, UK.

Klein, G., and Dombos, L. (1973). Relationship between the sensitivity of EBV-carrying lymphoblastoid lines to superinfection and the inducibility of the resident viral genome. *International Journal of Cancer* **11**, 327-337.

Klein, G., Giovanella, B., Westman, A., Stehlin, J. S., and Mumford, D. (1975). An EBV-genome-negative cell line established from an American Burkitt lymphoma: Receptor characteristics, EBV infectibility and permanent conversion into EBV-positive sublines by in vitro infection. *Intervirology* **5**, 319-334.

Klein, G., Svedmyr, E., Jondal, M., and Persson, P. O. (1976). EBV-determined nuclear antigen (EBNA)-positive cells in the peripheral blood of infectious mononucleosis patients. *International Journal of Cancer* **17**, 21-26.

Knowles, D. M., Cesarman, E., Chadburn, A., Frizzera, G., Chen. J., Rose, E. A., and Michler, R. E. (1995). Correlative morphologic and molecular genetic analysis demonstrates three distinct categories of posttransplantation lymphoproliferative disorders. *Blood* **85**, 552-565.

Koehne, G., Doubrovin, M., Doubrovina, E., Zanzonico, P., Gallardo, H. F., Ivanova, A., Balatoni, J., Teruya-Feldstein, J., Heller, G., May, C., Ponomarev, V., Ruan, S., Finn, R., Blasberg, R. G., Bornmann, W., Riviere, I., Sadelain, M., O'Reilly, R. J., Larson S. M., and Gelovani Tjuvajev, J. G. (2003). Serial in vivo imaging of the targeted migration of human HSV-TK-transduced antigen-specific lymphocytes. *Nature Biotechnology* **21**, 405-413.

Koffman, B. H., Kennedy, A. S., Heyman, M., Colonna, J., and Howell, C. (2000). Use of radiation therapy in posttransplant lymphoproliferative disorder (PTLD) after liver transplantation. *International Journal of Cancer* **90**, 104-109.

Ku, C. C., Murakami, M., Sakamoto, A., Kappler, J., and Marrack, P. (2000). Control of homeostasis of CD8+ memory T cells by opposing cytokines. *Science* **288**, 675-678.

Kuppers, R., Hansmann, M.-L., and Rajewsky, K. (1995). 'Micromanipulation and PCR analysis of single cells from tissue sections.' *Handbook of Experimental Immunology* (D. M. Weir, C. Blackwell, L. A. Herzenberg, Eds.), 206, 1-4. Blackwell Scientific Publishers, Cambridge, Massachusetts, USA.

Lacerda, J. F., Ladanyi, M., Louie, D. C., Fernandez, J. M., Papadopoulos, E. B., and O'Reilly, R. J. (1996). Human Epstein-Barr virus (EBV)-specific cytotoxic T lymphocytes home preferentially to and induce selective regressions of autologous EBV-induced B cell lymphoproliferations in xenografted C.B-17 SCID/SCID mice. *Journal of Experimental Medicine* **183**, 1215-1228.

Laichalk, L. L., and Thorley-Lawson, D. A. (2005). Terminal differentiation into plasma cells initiates the replicative cycle of Epstein-Barr virus in vivo. *Journal of Virology* **79**, 1296-1307.

Lam, K. P., Kuhn, R., and Rajewsky, K. (1997). In vivo ablation of surface immunoglobulin on mature B cells by inducible gene targeting results in rapid cell death. *Cell* **90**, 1073-1083.

Lamers, C. H., Sleijfer, S., Vulto, A. G., Kruit, W. H., Kliffen, M., Debets, R., Gratama, J. W., Stoter, G., and Oosterwijk, E. (2006) Treatment of metastatic renal cell carcinoma with autologous T-lymphocytes genetically retargeted against carbonic anhydrase IX: first clinical experience. *Journal of Clinical Oncology* **24**, e20-22.

Landon, J. C., and Malan, L. B. (1971). Seroepidemiologic studies of Epstein-Barr virus antibody in monkeys. *Journal of the National Cancer Institute* **46**, 881–884.

Lang, D. J., Garruto, R. M., and Gajdusek, D. C. (1977). Early acquisition of cytomegalovirus and Epstein-Barr virus antibody in several isolated Melanesian populations. *American Journal of Epidemiology* **105**, 480-487.

Larratt, L. M., Hamilton, M., Coupland, R., and Preiksaitis, J. K. (2001). Recurrent Epstein-Barr virus associated disease in a cardiac transplant patient: evolution from plasmacytic hyperplasia to diffuse large cell lymphoma. *Transplant Infectious Disease* **3**, 119-123.

Laux, G., Perricaudet, M., and Farrell, P. J. (1988). A spliced Epstein-Barr virus gene expressed in immortalized lymphocytes is created by circularization of the linear viral genome. *EMBO Journal* **7**, 769-774.

Leblond V, Davi F, Charlotte F, Dorent, R., Bitker, M. O., Sutton, L., Gandjbakhch, I., Binet, J. L., and Raphael, M. (1998). Posttransplant lymphoproliferative disorders not associated with Epstein-Barr virus: a distinct entity? *Journal of Clinical Oncology* **16**, 2052-2059.

Leblond, V., Dhedin, N., Mamzer Bruneel, M. F., Choquet, S., Hermine, O., Porcher, R., Nguyen Quoc, S., Davi, F., Charlotte, F., Dorent, R., Barrou, B., Vernant, J. P., Raphael, M., and Levy, V. (2001). Identification of prognostic factors in 61 patients with posttransplantation lymphoproliferative disorders. *Journal of Clinical Oncology* **19**, 772-778.

Lee, E. S., Locker, J., Nalesnik, M., Reyes, J., Jaffe, R., Alashari, M., Nour, B., Tzakis, A., and Dickman, P. S. (1995). The association of Epstein-Barr virus with smooth-muscle tumors occurring after organ transplantation. *New England Journal of Medicine* **332**, 19-25.

Lee, S. P., Brooks, J. M., Al-Jarrah, H., Thomas, W. A., Haigh, T. A., Taylor, G. S., Humme, S., Schepers, A., Hammerschmidt, W., Yates, J. L., Rickinson, A. B., and Blake, N. W. (2004). CD8 T cell recognition of endogenously expressed Epstein-Barr virus nuclear antigen 1. *Journal of Experimental Medicine* **199**, 1409-1420.

Lee, T. C., Savoldo, B., Barshes, N. R., Rooney, C. M., Heslop, H. E., Gee, A. P., Caldwell, Y., Scott, J. D., and Goss, J. A. (2006). Use of cytokine polymorphisms and Epstein-Barr virus viral load to predict development of post-transplant lymphoproliferative disorder in paediatric liver transplant recipients. *Clinical Transplantation* **20**, 389-393.

Lee, T. C., Savoldo, B., Rooney, C. M., Heslop, H. E., Gee, A. P., Caldwell, Y., Barshes, N. R., Scott, J. D., Bristow, L. J., O'Mahony, C. A., and Goss, J. A. (2005). Quantitative EBV viral loads and immunosuppression alterations can decrease PTLD incidence in pediatric liver transplant recipients. *American Journal of Transplantation* **5**, 2222-2228.

Leen, A., Meij, P., Redchenko, I., Middeldorp, J., Bloemena, E., Rickinson, A., and Blake, N. (2001). Differential immunogenicity of Epstein-Barr virus latent-cycle proteins for human CD4(+) T-helper 1 responses. *Journal of Virology* **75**, 8649-8659.

Leung, E., Shenton, B. K., Jackson, G., Gould, F. K., Yap, C., and Talbot, D. (2002). Use of real-time PCR to measure Epstein-Barr virus genomes in whole blood. *Journal of Immunological Methods* **270**, 259-267.

Levine, S. M., Angel, L., Anzueto, A., Susanto, I., Peters, J. I., Sako, E. Y., and Bryan, C. L. (1999). A low incidence of posttransplant lymphoproliferative disorder in 109 lung transplant recipients. *Chest* **116**, 1273–1277.

Levitskaya, J., Coram, M., Levitsky, V., Imreh, S., Steigerwald-Mullen, P. M., Klein, G., Kurilla, M. G., and Masucci, M. G. (1995). Inhibition of antigen processing by the internal repeat region of the Epstein-Barr virus nuclear antigen-1. *Nature* **375**, 685-688.

Levitskaya, J., Sharipo, A., Leonchiks, A., Ciechanover, A., and Masucci, M. G. (1997). Inhibition of ubiquitin/proteasome-dependent protein degradation by the Gly-Ala repeat domain of the Epstein-Barr virus nuclear antigen 1. *Proceedings of the National Academy of Sciences of the USA* **94**, 12616-12621.

Liebowitz, D., Wang, D., and Kieff, E. (1986). Orientation and patching of the latent infection membrane protein encoded by Epstein-Barr virus. *Journal of Virology* **58**, 233-237.

Lim, W. H., Kireta, S., Russ, G. R., and Coates, P. T. H. (2007). Human plasmacytoid dendritic cells regulate immune responses to Epstein-Barr virus (EBV) infection and delay EBV-related mortality in humanized NOD-SCID mice. *Blood* **109**, 1043-1050.

Liu, Y. J., and Arpin, C. (1997). Germinal center development. *Immunological Reviews* **156**, 111-126.

Loomis, R., Carbone, R., Reiss, M., and Lacy, J. (2003). Bcl-2 antisense (G3139, Genasense) enhances the in vitro and in vivo response of Epstein-Barr virus-associated lymphoproliferative disease to rituximab. *Clinical Cancer Research* **9**, 1931-1939.

Lucas, K. G., Salzman, D., Garcia, A., and Sun, Q. (2004). Adoptive immunotherapy with allogeneic Epstein-Barr virus (EBV)-specific cytotoxic T-lymphocytes for recurrent, EBV-positive Hodgkin disease. *Cancer* **100**, 1892-1901.

Macsween, K. F., and Crawford, D. H. (2003). Epstein-Barr virus - Recent advances. *Lancet Infectious Diseases* **3**, 131-140.

Magrath, I. (1990). The pathogenesis of Burkitt's lymphoma. *Advances in Cancer Research* **55**, 133-270.

Malouf, M. A., Chhajed, P. N., Hopkins, P., Plit, M., Turner, J., and Glanville, A. R. (2002). Anti-viral prophylaxis reduces the incidence of lymphoproliferative disease in lung transplant recipients. *Journal of Heart and Lung Transplantation* **21**, 547-554.

Mancao, C., Altmann, M., Jungnickel, B., and Hammerschmidt, W. (2005) Rescue of 'crippled' germinal center B cells from apoptosis by Epstein-Barr virus. *Blood* **106**, 4339-4344.

Mansoor, W., Gilham, D. E., Thistlethwaite, F. C., and Hawkins, R. E. (2005). Engineering T cells for cancer therapy. *British Journal of Cancer* **93**, 1085-1091.

Mauray, S., Fuzzati-Armentero, M. T., Trouillet, P., Ruegg, M., Nicoloso, G., Hart, M., Aarden, L., Schapira, M., and Duchosal, M. A. (2000). Epstein-Barr virus-dependent lymphoproliferative disease: critical role of IL-6. *European Journal of Immunology* **30**, 2065-2073.

Mayor, S. (2006). Severe adverse reactions prompt call for trial design changes. *British Medical Journal* **332**, 683.

McCarthy, K., Sloane, J., and Wiedermann, L. (1990). Rapid method for distinguishing clonal from polyclonal B cell populations in surgical biopsy specimens. *Journal of Clinical Pathology* **43**, 429-432.

McCarthy, M., Ramage, J., McNair, A., Gane, E., Portmann, B., Pagliuca, A., Rela, M., Heaton, N., Mufti, G. J., and Williams, R. (1997). The clinical diversity and role of chemotherapy in lymphoproliferative disorder in liver transplant recipients. *Journal of Hepatology* **27**, 1015-1021.

McDiarmid, S. V., Jordan, S., Kim, G. S., Toyoda, M., Goss, J. A., Vargas, J. H., Martin, M. G., Bahar, R., Maxfield, A. L., Ament, M. E., Busuttil, R. W., and Lee, G. S. (1998). Prevention and preemptive therapy of postransplant lymphoproliferative disease in pediatric liver recipients. *Transplantation* **66**, 1604-1611.

McGuire, W., Hill, A. V. S., Allsopp, C. E. M., Greenwood, B. M., and Kwjatkowski, D. (1994). Variation in the TNF-α promoter region associated with susceptibility to cerebral malaria. *Nature* **371**, 508-511.

Medicines and Healthcare Products Regulatory Agency (MHRA). http://www.mhra.gov.uk (Accessed 17 August 2007).

Meggetto, F., Muller, C., Henry, S., Selves, J., Mariame, B., Brousset, P., Al Saati, T., and Delsol, G. (1996). Epstein-Barr virus (EBV)-associated lymphoproliferations in severe combined immunodeficient mice transplanted with Hodgkin's disease lymph nodes: Implication of EBV-positive bystander B lymphocytes rather than EBV-infected Reed-Sternberg cells. *Blood* **87**, 2435-2442.

Melkus, M. W., Estes, J. D., Padgett-Thomas, A., Gatlin, J., Denton, P. W., Othieno, F. A., Wege, A. K., Haase, A. T., and Garcia, J. V. (2006). Humanized mice mount specific adaptive and innate immue responses to EBV and TSST-1. *Nature Medicine* **12**, 1316-1322.

Miller, C. L., Lee, J. H., Kieff, E., and Longnecker, R. (1994). An integral membrane protein (LMP2) blocks reactivation of Epstein-Barr virus from latency following surface immunoglobulin crosslinking. *Proceedings of the National Academy of Sciences of the USA* **91**, 772-776.

Miller, G., Heston, L., and Hoffman, G. (1982). Neutralization of lymphocyte immortalization by different strains of Epstein-Barr virus with a murine monoclonal antibody. *Infection and Immunity* **37**, 1028–1031.

Miller, G., Shope, T., Lisco, H., Stitt, D., and Lipman, M. (1972). Epstein-Barr virus: Transformation, cytopathic changes, and viral antigens in squirrel monkey and marmoset leukocytes. *Proceedings of the National Academy of Sciences of the USA* **69**, 383-387.

Milpied, N., Vasseur, B., Parquet, N., Garnier, J. L., Antoine, C., Quartier, P., Carret, A. S., Bouscary, D., Faye, A., Bourbigot, B., Reguerre, Y., Stoppa, A. M., Bourquard, P., Hurault de Ligny, B., Dubief, F., Mathieu-Boue, A., and Leblond, V. (2000). Humanized anti-CD20 monoclonal antibody (Rituximab) in post transplant B-lymphoproliferative disorder: a retrospective analysis of 32 patients. *Annals of Oncology* **11** (Suppl. 1), 113-116.

Miyashita, E. M., Yang, B., Babcock, G. J., and Thorley-Lawson, D. A. (1997). Identification of the site of Epstein-Barr virus persistence in vivo as a resting B cell. *Journal of Virology* **71**, 4882-4891.

Miyashita, E. M., Yang, B., Lam, K. M. C., Crawford, D. H., and Thorley-Lawson, D. A. (1995). A novel form of Epstein-Barr virus latency in normal B cells in vivo. *Cell* **80**, 593-601.

Moghaddam, A., Koch, J., Annis, B., and Wang, F. (1998). Infection of human B lymphocytes with lymphocryptoviruses related to Epstein-Barr virus. *Journal of Virology* **72**, 3205-3212.

Moghaddam, A., Rosenzweig, M., Lee-Parritz, D., Annis, B., Johnson, R. P., and Wang, F. (1997). An animal model for acute and persistent Epstein-Barr virus infection. *Science* **276**, 2030-2033.

Mora, A. L., Torres-González, E., Rojas, M., Xu, J., Ritzenthaler, J., Speck, S. H., Roman, J., Brigham, K., and Stecenko, A. (2007). Control of virus reactivation arrests pulmonary herpesvirus-induced fibrosis in IFN-gamma receptor-deficient mice. *American Journal of Respiratory and Critical Care Medicine* **175**, 1139-1150.

Mora, A. L., Woods, C. R., Garcia, A., Xu, J., Rojas, M., Speck, S. H., Roman, J., Brigham, K. L., and Stecenko, A. A. (2005). Lung infection with gamma-herpesvirus induces progressive pulmonary fibrosis in Th2-biased mice. *American Journal of Physiology. Lung Cellular and Molecular Physiology* **289**, L711-721.

Mosier, D. E. (1991). Adoptive transfer of human lymphoid cells to severely immunodeficient mice: Models for normal human immune function, autoimmunity, lymphomagenesis, and AIDS. *Advances in Immunology* **50**, 303-325.

Mosier, D. E. (1996). Viral pathogenesis in hu-PBL-scid mice. *Seminars in Immunology* **8**, 255-262.

Mosier, D. E., Gulizia, R. J., Baird, S. M., and Wilson, D. B. (1988). Transfer of a functional human immune system to mice with severe combined immunodeficiency. *Nature* **335**, 256-259.

Moss, D. J., Burrows, S. R., Silins, S. L., Misko, I., and Khanna, R. (2001). The immunology of Epstein-Barr virus infection. *Philosophical Transactions of the Royal Society of London. Series B, Biological Sciences* **356**, 475-488.

Moutschen, M., Leonard, P., Sokal, E. M., Smets, F., Haumont, M., Mazzu, P., Bollen, A., Denamur, F., Peeters, P., Dubin, G., and Denis, M. (2007). Phase I/II studies to evaluate safety and immunogenicity of a recombinant gp350 Epstein-Barr virus vaccine in healthy adults. *Vaccine* **25**, 4697-4705.

Münz, C., Bickham, K. L., Subklewe, M., Tsang, M. L., Chahroudi, A., Kurilla, M. G., Zhang, D., O'Donnell, M., and Steinman, R. M. (2000). Human CD4(+) T lymphocytes consistently respond to the latent Epstein-Barr virus nuclear antigen EBNA1. *Journal of Experimental Medicine* **191**, 1649-1660.

Murphy, W. J., Bennett, M., Anver, M. R., Baseler, M., and Longo, D. L. (1992). Human-mouse lymphoid chimeras: Host-vs.-graft and graft-vs.-host reactions. *European Journal of Immunology* **22**, 1421-1427.

Murphy, W. J., Taub, D. D., and Longo, D. L. (1996). The huPBL-scid mouse as a means to examine human immune function in vivo. *Seminars in Immunology* **8**, 233-241.

Murray, R. J., Kurilla, M. G., Brooks, J. M., Thomas, W. A., Rowe, M., Kieff, E., and Rickinson, A. B. (1992). Identification of target antigens for the human cytotoxic T cell response to Epstein-Barr virus (EBV): Implications for the immune control of EBV-positive malignancies. *Journal of Experimental Medicine* **176**, 157-168.

Murray, R. J., Kurilla, M. G., Griffin, H. M., Brooks, J. M., Mackett, M., Arrand, J. R., Rowe, M., Burrows, S. R., Moss, D. J., Kieff, E., Rickinson, A. B. (1990). Human cytotoxic T-cell responses against Epstein-Barr virus nuclear antigens demonstrated by using recombinant vaccinia viruses. *Proceedings of the National Academy of Sciences of the USA* **87**, 2906-2910.

Nakagomi, H., Dolcetti, R., Bejarano, M. T., Pisa, P., Kiessling, R., and Masucci, M. G. (1994). The Epstein-Barr virus latent membrane protein-1 (LMP1) induces interleukin-10 production in Burkitt lymphoma lines. *International Journal of Cancer* **57**, 240-244.

Nalesnik, M. A. (1991). Lymphoproliferative disease in organ transplant recipients. *Seminars in Immunopathology* **13**, 199-216.

Nalesnik, M. A. (2001). The diverse pathology of post-transplant lymphoproliferative disorders: the importance of a standardized approach. *Transplant Infectious Disease* **3**, 88-96.

Nalesnik, M. A., Jaffe, R., Starzl, T. E., Demetris, A. J., Porter, K., Burnham, J. A., Makowka, L., Ho, M., and Locker, J. (1988). The pathology of posttransplant lymphoproliferative disorders occurring in the setting of cyclosporine A-prednisone immunosuppression. *American Journal of Pathology* **133**, 173-192.

Nalesnik, M. A., Locker, J., Jaffe, R., Reyes, J., Cooper, M., Fung, J., and Starzl, T. E. (1992). Experience with posttransplant lymphoproliferative disorders in solid organ transplant recipients. *Clinical Transplantation* **6**, 249-252.

Nalesnik, M. A., Rao, A. S., Furukawa, H., Pham, S., Zeevi, A., Fung, J. J., Klein, G., Gritsch, H. A., Elder, E., Whiteside, T. L., and Starzl, T. E. (1997). Autologous lymphokine-activated killer cell therapy of Epstein-Barr virus-positive and -negative lymphoproliferative disorders arising in organ transplant recipients. *Transplantation* **63**, 1200-1205.

Nash, A. A., Dutia, B. M., Stewart, J. P., and Davison, A. J. (2001). Natural history of murine gamma-herpesvirus infection. *Philosophical Transactions of the Royal Society of London. Series B: Biological Sciences* **356**, 569-579.

Newstead, C. (2005). 'Cytomegalovirus and Epstein-Barr virus following solid-organ transplantation.' *Transplantation: A Companion to Specialist Surgical Practice*. (J. Forsythe, Ed.), 245-275. Elsevier Saunders Publishers, Philadelphia, Pennsylvania, USA.

Niederman, J. C., Evans, A. S., Subrahmanyan, L., and McCollum, R. W. (1970). Prevalence, incidence and persistence of EB virus antibody in young adults. *New England Journal of Medicine* **282**, 361-365.

Niedobitek, G., Agathanggelou, A., Finerty, S., Tierney, R., Watkins, P., Jones, E. L., Morgan, A., Young, L. S., and Rooney, N. (1994). Latent Epstein-Barr virus infection in cottontop tamarins: A possible model for Epstein-Barr virus infection in humans. *American Journal of Pathology* **145**, 969-978.

Niesters, H. G., van Esser, J., Fries, E., Wolthers, K. C., Cornelissen, J., and Osterhaus, A. D. (2000). Development of a real-time quantitative assay for detection of Epstein-Barr virus. *Journal of Clinical Microbiology* **38**, 712-715.

Nikiforow, S., Bottomly, K., and Miller, G. (2001). CD4+ T-cell effectors inhibit Epstein-Barr virus-induced B-cell proliferation. *Journal of Virology* **75**, 3740-3752.

Nikiforow, S., Bottomly, K., Miller, G., and Munz, C. (2003). Cytolytic CD4(+) T-cell clones reactive to EBNA1 inhibit Epstein-Barr virus-induced B-cell proliferation. *Journal of Virology* **77**, 12088-12104.

Noorden, S. v. (1986). 'Tissue preparation and immunostaining techniques for light microscopy.' *Immunocytochemistry: Modern methods and applications* (J. M. Polak, and S. v. Noorden, Eds.), 26-53. Wright, Bristol, UK.

Norris, P. J., Sumaroka, M., Brander, C., Moffett, H. F., Boswell, S. L., Nguyen, T., Sykulev, Y., Walker, B. D., and Rosenberg, E. S. (2001). Multiple effector functions mediated by human immunodeficiency virus-specific CD4+ T-cell clones. *Journal of Virology* **75**, 9771-9779.

O'Conor, G., Rappaport, H., and Smith, E. B. (1965). Childhood lymphoma resembling 'Burkitt tumor' in the United States. *Cancer* **18**, 411-417.

Organization For Economic Co-Operation And Development (OECD). http://www.oecd.org (Accessed 17 August 2007).

Oertel, S., Trappe, R. U., Zeidler, K., Babel, N., Reinke, P., Hummel, M., Jonas, S., Papp-Vary, M., Subklewe, M., Dörken, B., Riess, H., and Gärtner, B. (2006). Epstein-Barr viral load in whole blood of adults with posttransplant lymphoproliferative disorder after solid organ transplantation does not correlate with clinical course. *Annals of Hematology* **85**, 478-484.

Oertel, S. H. K., Verschuuren, E., Reinke, P., Zeidler, K., Papp-Vary, M., Babel, N., Trappe, R. U., Jonas, S., Hummel, M., Anagnostopoulos, I., Dorken, B., and Riess, H. B. (2005). Effect of Anti-CD 20 Antibody Rituximab in Patients with Post-Transplant Lymphoproliferative Disorder (PTLD). *American Journal of Transplantation* **5**, 2901-2906.

Old, L. J., Boyse, E. A., Oettgen, H. F., Harven, E. D., Geering, G., Williamson, B., and Clifford, P. (1966). Precipitating antibody in human serum to an antigen present in cultured Burkitt's lymphoma cells. *Proceedings of the National Academy of Sciences of the USA* **56**, 1699-1704.

Olivadoti, M., Toth, L. A., Weinberg, J., and Opp, M. R. (2007). Murine gammaherpesvirus 68: a model for the study of Epstein-Barr virus infections and related diseases. *Comparative Medicine* **57**, 44-50.

Opelz, G., Daniel, V., Naujokat, C., Fickenscher, H., and Döhler, B. (2007). Effect of cytomegalovirus prophylaxis with immunoglobulin or with antiviral drugs on post-transplant non-Hodgkin lymphoma: a multicentre retrospective analysis. *Lancet Oncology* **8**, 212-218.

Opelz, G., and Dohler, B. (2004). Lymphomas after solid organ transplantation: A collaborative transplant study report. *American Journal of Transplantation* **4**, 222-230.

Opelz, G., and Henderson, R. (1993). Incidence of non-Hodgkin lymphoma in kidney and heart transplant recipients. *Lancet* **342**, 1514-1516.

Orentas, R. J., Roskopf, S. J., Nolan, G. P., and Nishimura, M. I. (2001). Retroviral transduction of a T cell receptor specific for an Epstein-Barr virus-encoded peptide. *Clinical Immunology* **98**, 220-228.

Panagopoulos, D., Victoratos, P., Alexiou, M., Kollias, G., and Mosialos, G. (2004). Comparative analysis of signal transduction by CD40 and the Epstein-Barr virus oncoprotein LMP1 in vivo. *Journal of Virology* **78**, 13253-13261.

Papadopoulos, E. B., Ladanyi, M., Emanuel, D., Mackinnoon, S., Boulad, F., Carabasi, M. H., Castro-Malaspina, H., Childs, B. H., A.P, G., Small, T. N., Young, J. W., Kernan, N. A., and O'Reilly, R. J. (1994). Infusions of donor leukocytes to treat Epstein-Barr virus-associated lymphoproliferative disorders after allogeneic bone marrow transplantation. *New England Journal of Medicine* **330**, 1185-1191.

Parada, N.A., Center, D. M., Kornfeld, H., Rodriguez, W. L., Cook, J., Vallen, M., and Cruikshank, W. W. (1998). Synergistic activation of CD4+ T cells by IL-16 and IL-2. *Journal of Immunology* **160**, 2115-2120.

Park, J. R., Digiusto, D. L., Slovak, M., Wright, C., Naranjo, A., Wagner, J., Meechoovet, H. B., Bautista, C., Chang, W. C., Ostberg, J. R., and Jensen, M. C. (2007) Adoptive transfer of chimeric antigen receptor re-directed cytolytic T lymphocyte clones in patients with neuroblastoma. *Molecular Therapy* **15**, 825-833.

Pattengale, P. K., Smith, R. W., and Gerber, P. (1973). Selective transformation of B lymphocytes by EB virus. *Lancet* **2**, 93-94.

Patton, D. F., Wilkowski, C. W., Hanson, C. A., Shapiro, R., Gajl-Peczalska, K. J., Filipovich, A. H., and McClain, K. L. (1990). Epstein-Barr virus-determined clonality in posttransplant lymphoproliferative disease. *Transplantation* **49**, 1080-1084.

Pegtel, D. M., Middeldorp, J. and Thorley-Lawson, D. A. (2004). Epstein-Barr virus infection in ex vivo tonsil epithelial cell cultures of asymptomatic carriers. *Journal of Virology* **78**, 12613-12624.

Penn, I. (1991a). Cancer in the immunosuppressed organ recipient. *Transplantation Proceedings* **23**, 1771-1772.

Penn, I. (1991b). The changing pattern of posttransplant malignancies. *Transplantation Proceedings* **23**, 1101-1103.

Penn, I. (1993). Tumors after renal and cardiac transplantation. *Hematology/Oncology Clinics of North America* **7**, 431-445.

Penn, I., and Porat, G. (1995). Central nervous system lymphomas in organ allograft recipients. *Transplantation* **59**, 240-244.

Perera, S. M., Johannessen, I., Thomas, J. A., Brooks, L. A., N'Jie-Jobe, J., Crawford, D. H., Radley-Smith, R., and Phillips, M. (1996). Growth of Epstein-Barr virus-associated B-lymphoproliferative disease tissue in a severe combined immunodeficient mouse. *Blood* **88**, 1123-1125.

Perera, S. M., Thomas, J. A., Burke, M., and Crawford, D. H. (1998). Analysis of the T-cell micro-environment in Epstein-Barr virus-related post-transplantation B lymphoproliferative disease. *Journal of Pathology* **184**, 177-184.

Perry, M., and Whyte, A. (1998). Immunology of the tonsils. *Immunology Today* **19**, 414-421.

Picchio, G., Kobayashi, R., Kirven, M., Baird, S. M., Kipps, T. J., and Mosier, D. E. (1992). Heterogeneity among Epstein-Barr virus-seropositive donors in the generation of immunoblastic B-cell lymphomas in scid mice receiving human peripheral blood leukocyte grafts. *Cancer Research* **52**, 2468-2477.

Pinto, L. H., and Lamb, R. A. (2006). The M2 proton channels of influenza A and B viruses. *Journal of Biological Chemistry* **281**, 8997-9000.

Pirsch, J. D., Stratta, R. J., Sollinger, H. W., Hafez, G. R., D'Alessandro, A. M., Kalayoglu, M., and Belzer, F. O. (1989). Treatment of severe Epstein-Barr virus-induced lymphoproliferative syndrome with ganciclovir: Two cases after solid organ transplantation. *American Journal of Medicine* **86**, 241-244.

Pittet M. J., Grimm, J., Berger, C. R., Tamura, T., Wojtkiewicz, G., Nahrendorf, M., Romero, P., Swirski, F. K., and Weissleder, R. (2007) In vivo imaging of T cell delivery to tumors after adoptive transfer therapy. *Proceedings of the National Academy of Sciences of the USA* **104**, 12457-12461.

Platzer, C., Ode-Hakim, S., Reinke, P., Doecke, W. D., Ewert, R., and Volk, H. D. (1994). Quantitative PCR analysis of cytokine transcription patterns in peripheral mononuclear cells after anti-CD3 rejection therapy using two novel multispecific competitor fragments. *Transplantation* **58**, 264-268.

Pope, J. H., Horne, M. K., and Scott, W. (1968). Transformation of foetal human leukocytes in vitro by filtrates of a human leukaemic cell line containing herpes-like virus. *International Journal of Cancer* **3**, 857-866.

Prang, N. S., Hornef, M. W., Jaeger, M., Wagner, H. J., Wolf, H., and Schwarzmann, F. M. (1997). Lytic replication of Epstein-Barr virus in the peripheral blood: Analysis of viral gene expression in B lymphocytes during infectious mononucleosis and in the normal carrier state. *Blood* **89**, 1665-1677.

Precopio, M. L., Sullivan, J. L., Willard, C., Somasundaran, M., and Luzuriaga, K. (2003). Differential kinetics and specificity of EBV-specific CD4+ and CD8+ T cells during primary infection. *Journal of Immunology* **170**, 2590-2598.

Qu, L., and Rowe, D. T. (1992). Epstein-Barr virus latent gene expression in uncultured peripheral blood lymphocytes. *Journal of Virology* **66**, 3715-3724.

Raab-Traub, N. (1992) Epstein-Barr virus and nasopharyngeal carcinoma. *Seminars in Cancer Biology* **3**, 297-307.

Raab-Traub, N., and Flynn, K. (1986). The structure of the termini of the Epstein-Barr virus as a marker of clonal cellular proliferation. *Cell* **47**, 883-889.

Raab-Traub, N., Rajadurai, P., Flynn, K., and Lanier, A. P. (1991). Epstein-Barr virus infection in carcinoma of the salivary gland. *Journal of Virology* **65**, 7032-7036.

Randhawa, P. S., Pietrzak, B., Nalesnik, M. A., Demetris, A. J., and Locker, J. (1997). Subcutaneous implantation of human post-transplant lymphoproliferative disease lesions in SCID mice. *Hematological Oncology* **15**, 39-46.

Randhawa, P. S., Whiteside, T. L., Zeevi, A., Elder, E. M., Rao, A. S., Demetris, A. J., Weng, X., Valdivia, L. A., Rakela, J., and Nalesnik, M. A. (1998). Effects of immunotherapy on experimental immunodeficiency-related lymphoproliferative disease. *Transplantation* **65**, 264-268.

Randhawa, P. S., Yousem, S. A., Paradis, I. L., Dauber, J. A., Griffith, B. P., and Locker, J. (1989). The clinical spectrum, pathology, and clonal analysis of Epstein-Barr virus-associated lymphoproliferative disorders in heart-lung transplant recipients. *American Journal of Clinical Pathology* **92**, 177-185.

Rao, P., Jiang, H., and Wang, F. (2000). Cloning of the rhesus lymphocryptovirus viral capsid antigen and Epstein-Barr virus-encoded small RNA homologues and use in diagnosis of acute and persistent infections. *Journal of Clinical Microbiology* **38**, 3219–3225.

Reddy, S., Piccione, D., Takita, H., and Bankert, R.B. (1987). Human lung tumor growth established in the lung and subcutaneous tissue of mice with severe combined immunodeficiency. *Cancer Research* **47**, 2456-2460.

Reedman, B. M., and Klein, G. (1973). Cellular localization of an Epstein-Barr virus (EBV)-associated complement-fixing antigen in producer and non-producer lymphoblasoid cell lines. *International Journal of Cancer* **11**, 499-520.

Renard, T. H., Andrews, W. S., and Foster, M. E. (1991). Relationship between OKT3 administration, EBV seroconversion, and the lymphoproliferative syndrome in pediatric liver transplant recipients. *Transplantation Proceedings* **23**, 1473-1476.

Rencher, S. D., Slobod, K. S., Smith, F. S., and Hurwitz, J. L. (1994). Activity of transplanted CD8+ versus CD4+ cytotoxic T cells against Epstein-Barr virus-immortalized B cell tumors in SCID mice. *Transplantation* **58**,629-633.

Renner, C., Jung, W., Sahin, U., Denfeld, R., Pohl, C., Truemper, L., Hartmann, F., Diehl, V., Lier, R. v., and Pfreundschuh, M. (1994). Cure of xenografted human tumors by bispecific monoclonal antibodies and human T cells. *Science* **264**, 833-835.

Rickinson, A. B., and Moss, D. J. (1997). Human cytotoxic T lymphocyte responses to Epstein-Barr virus infection. *Annual Review of Immunology* **15**, 405-431.

Riddell, S. R., Watanabe, K. S., Goodrich, J. M., Li, C. R., Agha, M. E., and Greenberg, P. D. (1992). Restoration of viral immunity in immunodeficient humans by the adoptive transfer of T cell clones. *Science* **257**, 238-241.

Rivailler, P., Carville, A., Kaur, A., Rao, P., Quink, C., Kutok, J. L., Westmoreland, S., Klumpp, S., Simon, M., Aster, J. C., and Wang, F. (2004). Experimental rhesus lymphocryptovirus infection in immunosuppressed macaques: an animal model for Epstein-Barr virus pathogenesis in the immunosuppressed host. *Blood* **104**, 1482-1489.

Rivailler, P., Cho, Y. G., and Wang, F. (2002a). Complete genomic sequence of an Epstein-Barr virus-related herpesvirus naturally infecting a new world primate: a defining point in the evolution of oncogenic lymphocryptoviruses. *Journal of Virology* **76**, 12055–12068.

Rivailler, P., Jiang, H., Cho, Y. G., Quink, C., and Wang, F. (2002b). Complete nucleotide sequence of the rhesus lymphocryptovirus: genetic validation for an Epstein-Barr virus animal model. *Journal of Virology* **76**, 421–426.

Rochford, R., and Mosier, D. E. (1995). Differential Epstein-Barr virus gene expression in B-cell subsets recovered from lymphomas in scid mice after transplantation of human peripheral blood lymphocytes. *Journal of Virology* **69**, 150-155.

Rogers, R. P., Ge, J. Q., Holley-Guthrie, E., Hoganson, D. K., Comstock, K. E., Olsen, J. C., and Kenney, S. (1996). Killing Epstein-Barr virus-positive B lymphocytes by gene therapy: comparing the efficacy of cytosine deaminase and herpes simplex virus thymidine kinase. *Human Gene Therapy* **7**, 2235-2245.

Roizman, B. (1996). 'Herpesviridae.' 3rd ed. *Fields Virology* (B. N. Fields, D. M. Knipe, and P. M. Howley, Eds.), 2, 2221-2230. Lippincott-Raven Publishers, Philadelphia, Pennsylvania, USA.

Roizman, B., Carmichael, L. E., Deinhardt, F., de The, G., Nahmias, A. J., Plowright, W., Rapp, F., Sheldrick, P., Takahashi, M., and Wolf, K. (1981). Herpesviridae: Definition, Provisional Nomenclature, and Taxonomy. *Intervirology* **16**, 201-217.

Rooney, C. M., Roskrow, M. A., Suzuki, N., Ng, C. Y., Brenner, M. K., and Heslop, H. (1998b). Treatment of relapsed Hodgkin's disease using EBV-specific cytotoxic T cells. *Annals of Oncology* **9** (Suppl. 5), S129-132.

Rooney, C. M., Smith, C. A., Ng, C. Y. C., Loftin, S., Li, C., Krance, R. A., Brenner, M. K., and Heslop, H. E. (1995). Use of gene-modified virus-specific T lymphocytes to control Epstein-Barr virus-related lymphoproliferation. *Lancet* **345**, 9-12.

Rooney, C. M., Smith, C. A., Ng, C. Y., Loftin, S. K., Sixbey, J. W., Gan, Y., Srivastava, D. K., Bowman, L. C., Krance, R. A., Brenner, M. K., and Heslop, H. E. (1998a). Infusion of cytotoxic T cells for the prevention and treatment of Epstein-Barr virus-induced lymphoma in allogeneic transplant recipients. *Blood* **92**, 1549-1555.

Rowe, M., Rowe, D. T., Gregory, C. D., Young, L. S., Farrell, P. J., Rupani, H., and Rickinson, A. B. (1987). Differences in B cell growth phenotype reflect novel patterns of Epstein-Barr virus latent gene expression in Burkitt's lymphoma cells. *EMBO Journal* **6**, 2743-2751.

Rowe, M., Young, L. S., Crocker, J., Stokes, H., Henderson, S., and Rickinson, A. B. (1991). Epstein-Barr virus (EBV)-associated lymphoproliferative disease in the scid mouse model: Implications for the pathogenesis of EBV-positive lymphomas in man. *Journal of Experimental Medicine* **173**, 147-158.

Rubini, J. R., Cronkite, E. P., Bond, V. P., and Fliedner, T. M. (1960). The metabolism and fate of tritiated thymidine in man. *Journal of Clinical Investigation* **39**, 909-918.

Saiki, R. K., Gelfand, D. H., Stoffel, S., Scharf, S. J., Higuchi, R., Horn, G. T., Mullis, K. B., and Erlich, H. A. (1988). Primer-directed enzymatic amplification of DNA with a thermostable DNA polymerase. *Science* **239**, 487-491.

Saiki, R. K., Scharf, S., Faloona, F., Mullis, K. B., Horn, G. T., Erlich, H. A., and Arnheim, N. (1985). Enzymatic amplification of β-globin genomic sequences and restriction site analysis for diagnosis of sickle cell anemia. *Science* **230**, 1350-1354.

Sairenji, T., Bertoni, G., Medveczky, M. M., Medveczky, P. G., Nguyen, Q. V., and Humphreys, R. E. (1988). Inhibition of Epstein-Barr virus (EBV) release from P3HR-1 and B95-8 cell lines by monoclonal antibodies to EBV membrane antigen gp350/220. *Journal of Virology* **62**, 2614–2621.

Sambrook, J., Fritsch, E. F., and Maniatis, T. (1989). *'Molecular cloning: A laboratory manual.'* 2nd ed. Cold Spring Harbour Laboratory Press, New York, USA.

Sample, J., Liebowitz, D., and Kieff, E. (1989). Two related Epstein-Barr virus membrane proteins are encoded by separate genes. *Journal of Virology* **63**, 933-937.

Santini, S. M., Rizza, P., Logozzi, M. A., Sestili, P., Gherardi, G., Lande, R., Lapenta, C., Belardelli, F., and Fais, S. (1995). The scid mouse reaction to human peripheral blood mononuclear leukocyte engraftment. *Transplantation* **60**, 1306-1314.

Savoldo, B., Goss, J. A., Hammer, M. M., Zhang, L., Lopez, T., Gee, A. P., Lin, Y. F., Quiros-Tejeira, R. E., Reinke, P., Schubert, S,, Gottschalk, S., Finegold, M. J., Brenner, M. K., Rooney, C. M., and Heslop, H. E. (2006). Treatment of solid organ transplant recipients with autologous Epstein Barr virus-specific cytotoxic T lymphocytes (CTLs). *Blood* **108**, 2942-2949.

Savoldo, B., Rooney, C. M., Quiros-Tejeira, R. E., Caldwell, Y., Wagner, H. J., Lee, T., Finegold, M. J., Dotti, G., Heslop, H. E., and Goss, J. A. (2005). Cellular immunity to Epstein-Barr virus in liver transplant recipients treated with rituximab for post-transplant lymphoproliferative disease. *American Journal of Transplantation* **5**, 566-572.

Sawyer, R. N., Evans, A. S., Niederman, J. C., and McCollum, R. W. (1971). Prospective studies of a group of Yale university freshmen. I. Occurrence of infectious mononucleosis. *Journal of Infectious Diseases* **123**, 263-270.

Scala, G., Quinto, I., Ruocco, M. R., Arcucci, A., Mallardo, M., Caretto, P., Forni, G., and Venuta, S. (1990). Expression of an exogenous interleukin 6 gene in human Epstein Barr virus B cells confers growth advantage and in vivo tumorigenicity. *Journal of Experimental Medicine* **172**, 61-68.

Schluns, K. S., Kieper, W. C., Jameson, S. C., and Lefrancois, L. (2000). Interleukin-7 mediates the homeostasis of naïve and memory CD8 T cells in vivo. *Nature Immunology* **1**, 426-432.

Schmidtko, J., Wang, R., Wu, C. L., Mauiyyedi, S., Harris, N. L., Della Pelle, P., Brousaides, N., Zagachin, L., Ferry, J. A., Wang, F., Kawai, T., Sachs, D. H., Cosimi, B. A., and Colvin, R.B. (2002). Posttransplant lymphoproliferative disorder associated with an Epstein-Barr-related virus in cynomolgus monkeys. *Transplantation* **73**, 1431-1419.

Schumacher, T. N. M. (2002). T-cell-receptor gene therapy. *Nature Reviews: Immunology* **2**, 512-519.

Shannon-Lowe, C.D., Neuhierl, B., Baldwin, G., Rickinson, A.B. and Delecluse, H.-J. (2006). Resting B cells as a transfer vehicle for Epstein-Barr virus infection of epithelial cells. *Proceedings of the National Academy of Sciences of the USA* **103**, 7065-7070.

Shapiro, R. S., McClain, K., Frizzera, G., Gajl-Peczalska, K. J., Kersey, J. H., Blazar, B. R., Arthur, D. C., Patton, D. F., Greenberg, J. S., Burke, B., Ramsay, N. K. C., McGlave, P., and Filipovich, A. H. (1988). Epstein-Barr virus associated B cell lymphoproliferative disorders following bone marrow transplantation. *Blood* **71**, 1234-1243.

Sharifi, R., Sinclair, J. C., Gilmour, K. C., Arkwright, P. D., Kinnon, C., Thrasher, A. J., and Gaspar, H. B. (2004). SAP mediates specific cytotoxic T-cell functions in X-linked lymphoproliferative disease. *Blood* **103**, 3821-3827.

Sheen, A. J., Irlam, J., Kirillova, N., Guest, R. D., Sherlock, D. J., Hawkins, R. E., and Gilham, D. E. (2003a). Gene therapy of patient-derived T lymphocytes to target and eradicate colorectal hepatic metastases. *Diseases of the Colon and Rectum* **46**, 793-804.

Sheen, A. J., Sherlock, D. J., Irlam, J., Hawkins, R. E., Gilham, D. E. (2003b). T lymphocytes isolated from patients with advanced colorectal cancer are suitable for gene immunotherapy approaches. *British Journal of Cancer* **88**, 1119-1127.

Sherritt, M. A., Bharadwaj, M., Burrows, J. M., Morrison, L. E., Elliott, S. L., Davis, J. E., Kear, L. M., Slaughter, R. E., Bell, S. C., Galbraith, A. J., Khanna, R., and Moss, D. J. (2003). Reconstitution of the latent T-lymphocyte response to Epstein-Barr virus is coincident with long-term recovery from posttransplant lymphoma after adoptive immunotherapy. *Transplantation* **75**, 1556-1560.

Shope, T., Dechairo, D., and Miller, G. (1973). Malignant lymphoma in cottontop marmosets after inoculation with Epstein-Barr virus. *Proceedings of the National Academy of Sciences of the USA* **70**, 2487-2491.

Shultz, L. D., Schweitzer, P. A., Christianson, S. W., Gott, B., Schweitzer, I. B., Tennent, B., McKenna, S., Mobraaten, L., Rajan, T. V., Greiner, D. L., and Leiter, E. H. (1995). Multiple defects in innate and adaptive immunological function in NOD/LtSz-scid mice. *Journal of Immunology* **154**, 180-191.

Sidwell, R. W., and Smee, D. F. (2000). In vitro and in vivo assay systems for study of influenza virus inhibitors. *Antiviral Research* **48**, 1-16.

Sinclair, J., and Sissons, J. G. P. (1994). Human cytomegalovirus: Pathogenesis and models of latency. *Seminars in Virology* **5**, 249-258.

Sixbey, J. W. (2000) Epstein-Barr virus DNA loss from tumour cells and the geography of Burkitt's lymphoma. *EBV Report* **7**, 37-40.

Sixbey, J. W., Lemon, S. M., and Pagano, J. S. (1986). A second site for Epstein-Barr virus shedding: The uterine cervix. *Lancet* **2**, 1122-1124.

Sixbey, J. W., Nedrud, J. G., Raab-Traub, N., Hanes, R. A., and Pagano, J. S. (1984). Epstein-Barr virus replication in oropharyngeal epithelial cells. *New England Journal of Medicine* **310**, 1225-1230.

Sixbey, J. W., Shirley, P., Chesney, P. J., Buntin, D. M., and Resnick, L. (1989). Detection of a second widespread strain of Epstein-Barr virus. *Lancet* **2**, 761-765.

Sixbey, J. W., Vesterinen, E. H., Nedrud, J. G., Raab-Traub, N., Walton, L. A., and Pagano, J. S. (1983). Replication of Epstein-Barr virus in human epithelial cells infected in vitro. *Nature* **306**, 480-483.

Southern, E. M. (1975). Detection of specific sequences among DNA fragments separated by gel electrophoresis. *Journal of Molecular Biology* **98**, 503-517.

Speck, P., Haan, K. M. and Longnecker, R. (2000). Epstein-Barr virus entry into cells. *Virology* **277**, 1-5.

Starzl, T. E., Nalesnik, M. A., Porter, K. A., Ho, M., Iwatsuki, S., Griffith, B. P., Rosenthal, J. T., Hakala, T. R., Shaw, B. W., Hardesty, R. L., Atchison, R. W., Jaffe, R., and Bahnson, H. T. (1984). Reversibility of lymphomas and lymphoproliferative lesions developing under cyclosporin-steroid therapy. *Lancet* **1**, 583-587.

Stetler-Stevenson, M., Crush-Stanton, S., and Cossman, J. (1990). Involvement of the bcl-2 gene in Hodgkin's disease. *Journal of the National Cancer Institute* **82**, 855-858.

Steven, N. M., Annels, N. E., Kumar, A., Leese, A. M., Kurilla, M. G., and Rickinson, A. B. (1997). Immediate early and early lytic cycle proteins are frequent targets of the Epstein-Barr virus-induced cytotoxic T cell response. *Journal of Experimental Medicine* **185**, 1605-1617.

Stewart, J. P., Micali, N., Usherwood, E. J., Bonina, L., and Nash, A. A. (1999). Murine gamma-herpesvirus 68 glycoprotein 150 protects against virus-induced mononucleosis: a model system for gamma-herpesvirus vaccination. *Vaccine* **17**, 152-157.

Straathof, K. C., Bollard, C. M., Popat, U., Huls, M. H., Lopez, T., Morriss, M. C., Gresik, M. V., Gee, A. P., Russell, H. V., Brenner, M. K., Rooney, C. M., and Heslop, H. E. (2005). Treatment of nasopharyngeal carcinoma with Epstein-Barr virus-specific T lymphocytes. *Blood* **105**, 1898-1904.

Straathof, K. C. M., Savoldo, B., Heslop, H. E., and Rooney, C. M. (2002). Immunotherapy for Post-Transplant Lymphoproliferative Disease. *British Journal of Haematology* **118**, 728-740.

Su, I.-J. (1996) Epstein-Barr virus and T-cell lymphoma. *EBV Report* **3**, 1-6.

Sunil-Chandra, N. P., Arno, J., Fazakerley, J., and Nash, A. A. (1994). Lymphoproliferative disease in mice infected with murine gammaherpesvirus 68. *American Journal of Pathology* **145**, 818-826.

Sutkowski, N., Palkama, T., Ciurli, C., Sekaly, R. P., Thorley-Lawson, D. A., and Huber, B. T. (1996). An Epstein-Barr virus-associated superantigen. *Journal of Experimental Medicine* **184**, 971-980.

Svoboda, J., Kotloff, R., and Tsai, D. E. (2006). Management of patients with post-transplant lymphoproliferative disorder: the role of rituximab. *Transplant International* **19**, 259-269.

Swerdlow, A. J., Higgins, C. D., Hunt, B. J., Thomas, J. A., Burke, M. M., Crawford, D. H., and Yacoub, M. H. (2000). Risk of lymphoid neoplasia after cardiothoracic transplantation. A cohort study of the relation to Epstein-Barr virus. *Transplantation* **69**, 897-904.

Swerdlow, S. H. (1997). Classification of the posttransplant lymphoproliferative disorders: from the past to the present. *Seminars in Diagnostic Pathology* **14**, 2-7.

Takada, K. (2000) Epstein-Barr virus and gastric carcinoma. *Journal of Clinical Pathology* **53**, 255-261.

Tanner, J. E., and Alfieri, C. (2001). The Epstein-Barr virus and post-transplant lymphoproliferative disease: interplay of immunosuppression, EBV, and the immune system in disease pathogenesis. *Transplant Infectious Diseases* **3**, 60-69.

Tary-Lehmann, M., Lehmann, P. V., Schols, D., Roncarolo, M. G., and Saxon, A. (1994). Anti-scid mouse reactivity shapes the human CD4+ T cell repertoire in hu-PBL-scid chimeras. *Journal of Experimental Medicine* **180**, 1817-1827.

Tary-Lehmann, M., Saxon, A., and Lehmann, P. V. (1995). The human immune system in hu-PBL-scid mice. *Immunology Today* **16**, 529-533.

Taylor, A. L., Marcus, R., and Bradley, J. A. (2005). Post-transplant lymphoproliferative disorders (PTLD) after solid organ transplantation. *Critical Reviews in Oncology/Hematology* **56**, 155-167.

Taylor, J. H., Woods, P. S., and Hughes, W. L. (1957). The organization and duplication of chromosomes as revealed by autoradiographic studies using tritium-labeled thymidine. *Proceedings of the National Academy of Sciences of the USA* **43**, 122-128.

Thomas, J. A., Crawford, D. H., and Burke, M. (1995). Clinicopathologic implications of Epstein-Barr virus related B cell lymphoma in immunocompromised patients. *Journal of Clinical Pathology* **48**, 287-290.

Thomas, J. A., Hotchin, N. A., Allday, M. J., Amlot, P., Rose, M., Yacoub, M., and Crawford, D. H. (1990). Immunohistology of Epstein-Barr virus-associated antigens in B cell disorders from immunocompromised individuals. *Transplantation* **49**, 944-953.

Thomas, R., Macsween, K. F., McAulay, K., Clutterbuck, D., Anderson, R., Reid, S., Higgins, C. D., Swerdlow, A. J., Harrison, N., Williams, H., and Crawford, D. H. (2006). Evidence of shared Epstein-Barr viral isolates between sexual partners, and low level EBV in genital secretions. *Journal of Medical Virology* **78**, 1204–1209.

Thorley-Lawson, D. A. (2001). Epstein-Barr virus: exploiting the immune system. *Nature Reviews: Immunology* **1**, 75-82.

Thorley-Lawson, D. A. (2005). EBV the prototypical human tumor virus—just how bad is it? *Journal of Allergy and Clinical Immunology* **116**, 251-261.

Thorley-Lawson, D. A., and Babcock, G. J. (1999). A model for persistent infection with Epstein-Barr virus: the stealth virus of human B cells. *Life Sciences* **65**, 1433-1453.

Thorley-Lawson, D. A., and Geilinger, K. (1980). Monoclonal antibodies against the major glycoprotein (gp350/220) of Epstein-Barr virus neutralize infectivity. *Proceedings of the National Academy of Sciences of the USA* **77**, 5307–5311.

Thorley-Lawson, D. A., and Gross, A. (2004). Persistence of the Epstein-Barr virus and the origins of associated lymphomas. *New England Journal of Medicine* **350**, 1328-1337.

Tierney, R. J., Steven, N., Young, L. S., and Rickinson, A. B. (1994). Epstein-Barr virus latency in blood mononuclear cells: Analysis of viral gene transcription during primary infection and in the carrier state. *Journal of Virology* **68**, 7374-7385.

Timms, J. M., Bell, A., Flavell, J. R., Murray, P. G., Rickinson, A. B., Traverse-Glehen, A., Berger, F., and Delecluse, H. J. (2003). Target cells of Epstein-Barr-virus (EBV)-positive post-transplant lymphoproliferative disease: similarities to EBV-positive Hodgkin's lymphoma. *Lancet* **361**, 217-223.

Tomkinson, B. E., Wagner, D. K., Nelson, D. L., and Sullivan, J. L. (1987). Activated lymphocytes during acute Epstein-Barr virus infection. *Journal of Immunology* **139**, 3802-3807.

Tosato, G., and Blaese, R. M. (1985). Epstein-Barr virus infection and immunoregulation in man. *Advances in Immunology* **37**, 99-149.

Tosato, G., Blaese, R. M., and Yarchoan, R. (1985). Relationship between immunoglobulin production and immortalization by Epstein-Barr virus. *Journal of Immunology* **135**, 959-964.

Tosato, G., Jones, K., Breinig, M. K., McWilliams, H. P., and McKnight, J. L. C. (1993). Interleukin-6 production in posttransplant lymphoproliferative disease. *Journal of Clinical Investigation* **91**, 2806-2814.

Tripp, C. S., Wolf, S. F., and Unanue, E. R. (1993). Interleukin 12 and tumor necrosis factor α are costimulators of interferon γ production by natural killer cells in severe combined immunodeficiency mice with listeriosis, and interleukin 10 is a physiologic antagonist. *Proceedings of the National Academy of Sciences of the USA* **90**, 3725-3729.

Tripp, R. A., Hamilton-Easton, A. M., Cardin, R. D., Nguyen, P., Behm, F. G., Woodland, D. L., Doherty, P. C., and Blackman, M. A. (1997). Pathogenesis of an infectious mononucleosis-like disease induced by a murine γ-herpesvirus: Role for a viral superantigen? *Journal of Experimental Medicine* **185**, 1641-1650.

Tugizov, S. M., Berline, J. W. and Palefsky, J. M. (2003). Epstein-Barr virus infection of polarized tongue and nasopharyngeal epithelial cells. *Nature Medicine* **9**, 307-314.

UHP-PHLS (University Health Physicians and the Public Health Laboratory Service Laboratories). (1971). Infectious mononucleosis and its relationship to EB vrus antibody. *British Medical Journal* **4**, 643-646.

Usherwood, E. J., Stewart, J. P., and Nash, A. A. (1996). Characterisation of tumor cell lines derived from murine gammaherpesvirus-68-infected mice. *Journal of Virology* **70**, 6516-6518.

van der Kolk, L. E., de Haas, M., Grillo-López, A. J., Baars, J. W., and van Oers, M. H. (2002). Analysis of CD20-dependent cellular cytotoxicity by G-CSF-stimulated neutrophils. *Leukemia* **16**, 693-699.

Vanhoutte, V. The characterisation of ex vivo generated Epstein-Barr virus-specific cytotoxic T-cell lines. The University of Edinburgh. *PhD Thesis* 2006.

Veronese, M. L., Veronesi, A., D'Andrea, E., Mistro, A. R. D., Indraccolo, S., Mazza, M. R., Mion, M., Zamarchi, R., Menin, C., Panozzo, M., Amadori, A., and Chieco-Bianchi, L. (1992). Lymphoproliferative disease in human peripheral blood mononuclear cell-injected scid mice. I. T lymphocyte requirement for B cell tumor generation. *Journal of Experimental Medicine* **176**, 1763-1767.

Veronesi, A., Coppola, V., Veronese, M. L., Menin, C., Bruni, L., D'Andrea, E., Mion, M., Amadori, A., and Chieco-Bianchi, L. (1994). Lymphoproliferative disease in human peripheral-blood-mononuclear-cell-injected scid mice. II. Role of host and donor factors in tumor generation. *International Journal of Cancer* **59**, 676-683.

Vetsika, E. K., and Callan, M. (2004). Infectious mononucleosis and Epstein-Barr virus. *Expert Reviews in Molecular Medicine* **6**, 1-16.

Voo, K. S., Fu, T., Wang, H. Y., Tellam, J., Heslop, H. E., Brenner, M. K., Rooney, C. M., and Wang, R. F. (2004). Evidence for the presentation of major histocompatibility complex class I-restricted Epstein-Barr virus nuclear antigen 1 peptides to CD8+ T lymphocytes. *Journal of Experimental Medicine* **199**, 459-470.

Wagar, E. J., Cromwell, M. A., Shultz, L. D., Woda, B. A., Sullivan, J. L., Hesselton, R. M., and Greinier, D. L. (2000). Regulation of human cell engraftment and development of EBV-related lymphoproliferative disorders in hu-PBL-SCID mice. *Journal of Immunology* **165**, 518-527.

Wang, F., Rivailler, P., Rao, P., and Cho, Y. (2001). Simian homologues of Epstein-Barr virus. *Philosophical Transactions of the Royal Society of London. Series B, Biological Sciences* **356**, 489–497.

Wang, R. F. (2001). The role of MHC class II-restricted tumor antigens and CD4+ T cells in antitumor immunity. *Trends in Immunology* **22**, 269-276.

Wang, X. and Hutt-Fletcher, L. M. (1998). Epstein-Barr virus lacking glycoprotein gp42 can bind to B cells but is not able to infect. *Journal of Virology* **72**, 158-163.

Webber, S A., Naftel, D. C., Fricker, F. J., Olesnevich, P., Blume, E. D., Addonizio, L., Kirklin, J. K., and Canter, C. E. (2006). Lymphoproliferative disorders after paediatric heart transplantation: a multi-institutional study. *Lancet* **367**, 233-239.

Weiss, L. M., Movahed, L. A., Warnke, R. A., and Sklar, J. (1989). Detection of Epstein-Barr viral genomes in Reed-Sternberg cells of Hodgkin's disease. *New England Journal of Medicine* **320**, 502-506.

Wilkie, G. M., Taylor, C., Jones, M. M., Burns, D. M., Turner, M., Kilpatrick, D., Amlot, P. L., Crawford, D. H., and Haque, T. (2004). Establishment and characterization of a bank of cytotoxic T lymphocytes for immunotherapy of Epstein-Barr virus-associated diseases. *Journal of Immunotherapy* **27**, 309-316.

Wilkinson, A. H., Smith, J. L., Hunsicker, L. G., Tobacman, J., Kapelanski, D. P., Johnson, M., Wright, F. H., Behrendt, D. M., and Corry, R. J. (1989). Increased frequency of posttransplant lymphomas in patients treated with cyclosporine, azathioprine, and prednisone. *Transplantation* **47**, 293-296.

Williams, H., and Crawford, D. H. (2006). Epstein-Barr virus: the impact of scientific advances on clinical practice. *Blood* **107**, 862-869.

Williams, H., Macsween, K., McAulay, K., Higgins, C., Harrison, N., Swerdlow, A., Britton, K., and Crawford, D. (2004). Analysis of immune activation and clinical events in acute infectious mononucleosis. *Journal of Infectious Diseases* **190**, 63-71.

Williams, H., McAulay, K., Macsween, K. F., Gallacher, N. J., Higgins, C. D., Harrison, N., Swerdlow, A. J., and Crawford, D.H. (2005). The immune response to primary EBV infection: a role for natural killer cells. *British Journal of Haematology* **129**, 266–274.

Wu, M., Mazurchuk, R., Chandhary, N. D., Spernyak, J., Veith, J., Pera, P., Greco, W., Hoffman, R. M., Kobayashi, T., and Bernacki, R. J. (2003). High-resolution magnetic resonance imaging of the efficacy of the cytosine analogue 1-[2-C-cyano-2-deoxy-β-D-arabino-pentofuranosyl]-N4-palmitoyl cytosine (CS-682) in a liver-metastasis athymic nude mouse model. *Cancer Research* **63**, 2477-2482.

Wynn, R. F., Arkwright, P. D., Haque, T., Gharib, M. I., Wilkie, G., Morton-Jones, M., and Crawford, D. H. (2005). Treatment of Epstein-Barr-virus-associated primary CNS B cell lymphoma with allogeneic T-cell immunotherapy and stem-cell transplantation. *Lancet Oncology* **6**, 344-346.

Xenogen, Inc.
http://www.xenogen.com (Accessed 17 August 2007).

Yamamura, M., Uyemura, K., Deans, R. J., Weinberg, K., Rea, T. H., Bloom, B. R., and Modlin, R. L. (1991). Defining protective responses to pathogens: Cytokine profiles in leprosy lesions. *Science* **254**, 277-279.

Yamamura, M., Wang, X. H., Ohmen, J. D., Uyemura, K., Rea, T. H., Bloom, B. R., and Modlin, R. L. (1992). Cytokine patterns of immunologically mediated tissue damage. *Journal of Immunology* **149**, 1470-1475.

Yao, Q. Y., Rickinson, A. B., and Epstein, M. A. (1985a). A re-examination of the Epstein-Barr virus carrier state in healthy seropositive individuals. *International Journal of Cancer* **35**, 35-42.

Yao, Q. Y., Rickinson, A. B., Gaston, J. S. H., and Epstein, M. A. (1985b). In vitro analysis of the Epstein-Barr virus:host balance in long-term renal allograft recipients. *International Journal of Cancer* **35**, 43-49.

Yao, Q. Y., Rowe, M., Martin, B., Young, L. S., and Rickinson, A. B. (1991a). The Epstein-Barr virus carrier state: Dominance of a single growth-transforming isolate in the blood and in the oropharynx of healthy virus carriers. *Journal of General Virology* **72**, 1579-1590.

Yao, Q. Y., Rowe, M., Morgan, A. J., Sam, C. K., Prasad, U., Dang, H., Zeng, Y., and Rickinson, A. B. (1991b). Salivary and serum IgA antibodies to the Epstein-Barr virus glycoprotein gp340: Incidence and potential for virus neutralization. *International Journal of Cancer* **48**, 45-50.

Yao, Q. Y., Tierney, R. J., Croom-Carter, D., Cooper, G. M., Ellis, C. J., Rowe, M., and Rickinson, A. B. (1996a). Isolation of intertypic recombinants of Epstein-Barr virus from T-cell-immunocompromised individuals. *Journal of Virology* **70**, 4895-4903.

Yao, Q. Y., Tierney, R. J., Croom-Carter, D., Dukers, D., Cooper, G. M., Ellis, C. J., Rowe, M., and Rickinson, A. B. (1996b). Frequency of multiple Epstein-Barr virus infections in T-cell-immunocompromised individuals. *Journal of Virology* **70**, 4884-4894.

Yin, Y., Manoury, B., and Fahraeus, R. (2003). Self-inhibition of synthesis and antigen presentation by Epstein-Barr virus-encoded EBNA1. *Science* **301**, 1371-1374.

Young, L. S., Alfieri, C., Hennessy, K., Evans, H., O'Hara, C., Anderson, K. C., Ritz, J., Shapiro, R. S., Rickinson, A. B., Kieff, E., and Cohen, J. I. (1989a). Expression of Epstein-Barr virus transformation-associated genes in tissues of patients with EBV lymphoproliferative disease. *New England Journal of Medicine* **321**, 1080-1085.

Young, L. S., Finerty, S., Brooks, L., Scullion, F., Rickinson, A. B., and Morgan, A. J. (1989b). Epstein-Barr virus gene expression in malignant lymphomas induced by experimental virus infection of cottontop tamarins. *Journal of Virology* **63**, 1967-1974.

Young, L. S. and Rickinson A. B. (2004). Epstein-Barr virus: 40 years on. *Nature Reviews: Cancer* **4**, 757-768.

APPENDIX 1: ADDITIONAL MATERIAL

TABLE A1
Primary Antibodies

A1.1 Immunohistochemistry

Antibody/Clone (Isotype)		Antigen(s)	Dilution	Source
Human Polyclonal Antibodies To EBV Antigens	JAT serum (IgG)	EBNA1-6	1:10	LSHTM
	WDA serum (IgG)	EBV-Negative	1:10	LCMV
Murine Monoclonal Antibodies To Human Leukocyte Antigens And Cytotoxic Granule Molecules	PS1 (IgG)	CD3	1:100	Vision BioSystems
	4B12 (IgG)	CD4	1:20	Vision BioSystems
	1A5 (IgG)	CD8	1:20	Vision BioSystems
	L26 (IgG)	CD20	1:50	DakoCytomation
	2B11+PD7/26 (IgG)	CD45	1:50	DakoCytomation
	11F1 (IgG)	Granzyme B	1:40	Vision BioSystems
	5B10 (IgG)	Perforin	1:20	Vision BioSystems
Murine Monoclonal Antibodies To EBV Antigens	PE2 (IgG)	EBNA2	1:25	DakoCytomation
	CS.1-4 (IgG)	LMP1	1:100	DakoCytomation
	BZ.1 (IgG)	BZLF1	1:20	DakoCytomation
Murine Monoclonal Antibodies To Murine MHC1	D1 (IgG)	MHC1D[d]	1:50	Serotec

CD: Cluster Designation; Ig: Immunoglobulin; LCMV: Laboratory for Clinical & Molecular Virology; LSHTM: London School of Hygiene & Tropical Medicine; MHC: Major Histocompatibility Complex

Additional primary antibodies used for study presented in **Table 9** of Results (Johannessen *et al,* 2002):

Anti-CD19 (HD37, DakoCytomation)
Anti-CD23 (MHM6, DakoCytomation)
Anti-EA(D) (110f-1, Biogenesis)
Anti-EBNA1 (OT1X; Kindly donated by Prof JM Middeldorp, Amsterdam Free University Hospital, the Netherlands)
Anti-MA (Serotec)
Anti-TCR α/β (BFT1, T Cell Science)
Anti-VCA (Serotec)

A1.2 Flow Cytometry

Antibody/Clone (Isotype)		Antigen(s)	Fluorochrome	Source
Murine Monoclonal Antibodies To Human Leukocyte Antigens	UCHT1 (IgG_1, κ)	CD3	FITC, PE	BD Pharmingen
	RPA-T4 (IgG_1, κ)	CD4	FITC, PE	BD Pharmingen
	RPA-T8 (IgG_1, κ)	CD8	FITC, PE	BD Pharmingen
	HIB19 (IgG_1, κ)	CD19	FITC, PE	BD Pharmingen
	HI30 (IgG_1, κ)	CD45	FITC	BD Pharmingen
	B159 (IgG_1, κ)	CD56	FITC, PE	BD Pharmingen
Murine Isotype Controls	MOPC-21 (IgG_1, κ)	-*	FITC, PE	BD Pharmingen

CD: Cluster Designation; FITC: Fluorescein isothiocyanate; Ig: Immunoglobulin; PE: Phycoerythrin;
*: Mouse myeloma protein (details of antigen specificity are not available from the manufacturer)

TABLE A2
Secondary/Tertiary Antibodies

Antibody	Dilution	Source
FITC-conjugated goat anti-human C3 IgG	1:10	Capell
Monoclonal mouse anti-FITC IgG	1:10	DakoCytomation
Mouse monoclonal AP-anti-AP complexes (APAAP) IgG	1:25	DakoCytomation
Mouse monoclonal Px-anti-Px complexes (PAP) IgG	1:100	DakoCytomation
Polyclonal AP-conjugated rabbit anti-mouse IgG,A,M	1:20	DakoCytomation
Polyclonal FITC-conjugated rabbit anti-human IgG	1:50	DakoCytomation
Polyclonal FITC-conjugated rabbit anti-mouse IgG,A,M	1:50	DakoCytomation
Polyclonal Px-conjugated goat anti-human IgG	1:10000	Sigma
Polyclonal Px-conjugated goat anti-rabbit IgG	1:10000	Nordic
Polyclonal Px-conjugated goat anti-rat IgG	1:4000	Sigma
Polyclonal Px-conjugated rabbit anti-human C3c	1:25	DakoCytomation
Polyclonal rabbit anti-mouse IgG,A,M	1:25/1:100/1:1000	DakoCytomation
Polyclonal TRITC-conjugated rabbit anti-mouse IgG,A,M	1:20	DakoCytomation

AP: Alkaline phosphatase; FITC: Fluorescein isothiocyanate; Px: Peroxidase (horseradish); TRITC: Tetramethylrhodamine isothiocyanate

TABLE A3
Serum Reagents

Serum	Dilution	Source
Normal Balb/c mouse serum	1:40	LCMV
Normal human serum (heat-treated)	1:25	LCMV
Normal rabbit serum	1:100	Dako

LCMV: Laboratory for Clinical & Molecular Virology

TABLE A4
Control Cell Lines

Cell Line	Cell Type	EBV Status	Reference
B95-8	Marmoset BLCL	+	Miller *et al,* 1972
Namalwa	BL	+	Klein & Dombos, 1973
P3HR1	BL	+	Hinuma *et al,* 1967
Ramos	BL	-	Klein *et al,* 1975

BL: Burkitt's lymphoma; BLCL: B lymphoblastoid cell line

Additional cell/tissue controls included:

Human CD4+ve T cells (Laboratory for Clinical & Molecular Virology)
Human CD8+ve T cells (Laboratory for Clinical & Molecular Virology)
Immunocompetent murine Balb/c splenocytes (Laboratory for Clinical & Molecular Virology)

TABLE A5
Primers Used For RT-PCR Reactions
(β-Actin; Human IL2, 4, 5, 6, 10, And IFNγ)

Human gene/ Primers	Primer sequences (5'→3')	Product size (Bp)
β-actin[1]		
5':	5' GTG GGG CGC CCC AGG CAC CA 3'	540
3':	5' CTC CTT AAT GTC ACG CAC GAT TTC 3'	
IL2[1]		
5':	5' ACT CAC CAG GAT GCT CAC AT 3'	266
3':	5' AGG TAA TCC ATC TGT TCA GA 3'	
IL4[1]		
5':	5' CTT CCC CCT CTG TTC TTC CT 3'	317
3':	5' TTC CTG TCG AGC CGT TTC AG 3'	
IL4[2]		
5':	5' CGG CAA CTT TGA CCA CGG ACA CAA GTG CGA TA 3'	344
3':	5' ACG TAC TCT GGT TGG CTT CCT TCA CAG GAC AG 3'	
IL5[1]		
5':	5' ATG AGG ATG CTT CTG CAT TTG 3'	405
3':	5' TCA ACT TTC TAT TAT CCA CTC GGT GTT CAT TAC 3'	
IL6[1]		
5':	5' ATG TAG CCG CCC CAC ACA GA 3'	190
3':	5' CAT CCA TCT TTT TCA GCC AT 3'	
IL10[2]		
5':	5' AAG CTG AGA ACC AAG ACC CAG ACA TCA AGG CG 3'	328
3':	5' AGC TAT CCC AGA GCC CCA GAT CCG ATT TTG G 3'	
IFNγ[1]		
5':	5' AGT TAT ATC TTG GCT TTT CA 3'	356
3':	5' ACC GAA TAA TTA GTC AGC TT 3'	

[1]:Yamamura *et al,* 1991, 1992; [2]:Clontech Laboratories, Inc., USA; Bp: Base pairs

TABLE A6
RT-PCR Reaction Conditions
(β-Actin; Human IL2, 4, 5, 6, 10, And IFNγ)

Human gene	[$MgCl_2$] (mM)	[Taq][1] (U)	Ann.T[2] (°C)	Cycle number	[Primers] (μM)[3]
β-Actin[4]	1.5	2.5	65	40	1
IL2[4]	1.5	3.5	55	40	1
IL4[5]	1.5	2.0	60	35	0.2
IL5[4]	1.5	2.5	65	40	1
IL6[4]	2.5	2.5	65	40	1
IL10[5]	1.5	2.5	60	35	1
IFNγ[4]	2.5	2.5	55	40	1

[1]: Taq DNA Polymerase; [2]: Annealing temperature (= Annealing/Extension temperature as regards primers from Yamamura *et al,* 1991, 1992); [3]: Refers to the concentration of each primer; [4]: Yamamura *et al,* 1991, 1992; [5]: Clontech Laboratories, Inc., USA; mM: 10^{-3} M; μM: 10^{-6} M; U:Units

TABLE A7
Probes Used For RT-PCR Reactions
(β-Actin; Human IL2, 4, 5, 6, 10, And IFNγ)

Human Gene	Probe Sequence (5'→3')
β-Actin[1]	5' GGA TAG CAA CGT ACA TGG CT 3'
IL2[1]	5' CCC TGG GTC TTA AGT GAA AG 3'
IL4[1]	5' GTC TGT TAC GGT CAA CTC GG 3'
IL5[2]	5' GCC AAT GAG ACT CTG AGG ATT CCT G 3'
IL6[2]	5' TCT TGT TAC ATG TCT CCT TTC TCA G 3'
IL10[2]	5' CAG GTG AAG AAT GCC TTT AAT AAG CTC CAA GAG AAA GGC ATC TAC AAA GCC ATG AGT GAG TTT GAC ATC 3'
IFNγ[1]	5' GCT ACA TCT GAA TGA CCT GC 3'

[1]: Designed by IJ; [2]: Yamamura *et al,* 1991, 1992

TABLE A8
MHC Profile Of A Panel Of Healthy EBV-Seropositive Blood Donors (Donors 1-28)

Donor No	A		B		C		DR	
	Allele 1	Allele 2	Allele 1	Allele 2	Allele 1	Allele 2	Allele 1	Allele 2
1	**02**	32	**44**	**44**	05	16	**04**	07
2	**02**	**02**	08	**44**	05	07	03	13
3	01	**02**	08	**44**	05	07	**04**	15
4	**02**	31	35	51	NT	NT	07	17
5	01	03	07	07	NT	NT	**04**	15
6	03	31	27	45	01	06	NT	NT
7	**02**	03	40	**44**	03	05	NT	NT
8	24	68	14	15	03	08	NT	NT
9	23	23	**44**	49	04	07	NT	NT
10	**02**	29	**44**	**44**	NT	NT	01	07
11	**02**	32	07	14	NT	NT	07	15
12	01	31	08	**44**	NT	NT	07	17
13	01	03	07	14	07	08	NT	NT
14	01	**02**	35	73	04	15	NT	NT
15	03	68	40	**44**	03	08	NT	NT
16	01	29	07	08	07	07	NT	NT
17	**02**	68	50	60	NT	NT	**04**	17
18	23	25	**44**	45	NT	NT	**04**	12
19	01	32	08	35	NT	NT	01	17
20	**02**	**02**	37	**44**	NT	NT	01	07
21	01	**02**	07	57	NT	NT	07	09
22	**02**	11	27	**44**	NT	NT	01	14
23	03	03	51	60	NT	NT	**04**	15
24	11	32	27	62	NT	NT	01	11
25	01	**02**	08	57	NT	NT	01	07
26	**02**	03	35	**44**	NT	NT	15	15
27	24	31	49	60	NT	NT	**04**	17
28	03	74	53	72	NT	NT	11	15

MHC: Major Histocompatibility Complex; No: Number; NT: Not tested; **Bold** type: Common UK MHC A or B allele

TABLE A9
Cell Surface Phenotype Of A Panel Of T Cell Lines (Donors 1-25)

Donor No	Period Of *In Vitro* Growth (Weeks)	% CD4+/CD45+ T Cells	% CD8+/CD45+ T Cells	% CD56+/CD45+ NK Cells
1	9	34	78	1
2	7	11	88	4
3	17	3	93	0
4	10	0	97	0
5	8	17	83	0
6	9	49	42	12
7	8	6	64	NT
8	10	37	68	4
9	11	12	86	4
10	8	2	84	NT
11	8	1	74	NT
12	12	15	68	0
13	10	1	96	NT
14	10	25	58	20
15	11	71	24	3
16	11	2	97	0
17	11	96	3	NT
18	12	12	81	4
19	11	4	93	0
20	12	4	96	8
21	8	3	96	1
22	8	4	69	1
23	9	33	89	5
24	8	4	87	NT
25	7	1	97	1

CTL: Cytotoxic T lymphocytes; No: Number; NT: Not tested; PBL: Peripheral blood leukocytes

TABLE A10
% Specific T Cell Lysis At A 10:1 Effector:Target Ratio
(Donors 1-25)

Donor No	% Specific Lysis		
	Autologous BLCL	Allogeneic BLCL	K562
1	59	26	7
2	22	7	0
3	39	1	7
4	50	6	0
5	30	3	2
6	91	6	2
7	31	1	1
8	44	14	7
9	27	3	9
10	36	13	17
11	6*	0	19
12	26	1	7
13	34	30	3
14	16	12	28
15	2*	0	1
16	31	10	4
17	65	4	21
18	39	7	14
19	44	6	10
20	51	22	40
21	39	4	0
22	34	4	0
23	10	0	2
24	45	0	0
25	61	7	10

*: Cytotoxicity was assessed following *in vivo* transfer of CTLs; BLCL: B lymphoblastoid cell line; CTL: Cytotoxic T lymphocytes; No: Number

TABLE A11
Cell Surface Phenotype Of CTL And Enriched T Cell Subsets (Donors 6-9)

Donor No	Sample	Period Of *In Vitro* Growth (Weeks)	% T Cells CD4/CD45	% T Cells CD8/CD45	% NK Cells CD56/CD45
6	CD4-Enriched	8	71	6	NT
	CD8-Enriched		2	95	NT
	CD4/CD8-Depleted		3	5	84
7	CD4-Enriched	8	51	50	NT
	CD8-Enriched		1	96	NT
	CD4/CD8-Depleted		8	4	80
8	CD4-Enriched	10	88	17	1
	CD8-Enriched		20	96	1
	CD4/CD8-Depleted		62	21	9
9	CD4-Enriched	10	90	NT	NT
	CD8-Enriched		5	82	15
	CD4/CD8-Depleted		NT	NT	NT

*: Percentage of CD45+ve leukocytes; CTL: Cytotoxic T lymphocytes; No: Number; NT: not tested

TABLE A12
Cell Surface Phenotype Of CTL And Enriched T Cell Subsets (Donors 6, 8-16)

Donor No	Sample	Period of *In Vitro* Growth (Weeks)	% T Cells CD4/CD45	% T Cells CD8/CD45	% NK Cells CD56/CD45
6	CD4-Enriched	9	70	10	NT
	CD8-Enriched		10	80	NT
	CD4/CD8-Depleted		NT	NT	NT
8	CD4-Enriched	15	74	71	NT
	CD8-Enriched		35	89	NT
	CD4/CD8-Depleted		NT	NT	NT
9	CD4-Enriched	11	71	26	4
	CD8-Enriched		2	96	4
	CD4/CD8-Depleted		49	20	12
10	CD4-Enriched	8	0	48	NT
	CD8-Enriched		1	87	NT
	CD4/CD8-Depleted		2	86	NT
11	CD4-Enriched	8	2	24	NT
	CD8-Enriched		1	87	NT
	CD4/CD8-Depleted		NT	83	NT
12	CD4-Enriched	12	2	14	0
	CD8-Enriched		0	40	0
	CD4/CD8-Depleted		NT	NT	NT
13	CD4-Enriched	10	21	96	10
	CD8-Enriched		3	97	9
	CD4/CD8-Depleted		3	14	12
14	CD4-Enriched	10	85	8	5
	CD8-Enriched		6	93	24
	CD4/CD8-Depleted		6	18	10
15	CD4-Enriched	11	97	2	2
	CD8-Enriched		20	67	19
	CD4/CD8-Depleted		7	14	25
16	CD4-Enriched	11	36	42	10
	CD8-Enriched		0	92	2
	CD4/CD8-Depleted		1	35	13

*: Percentage of CD45+ve leukocytes; CTL: Cytotoxic T lymphocytes; No: Number; NT: not tested

TABLE A13
Time To End Point
(Donors 6, 8-16)

Donor No	Days To Ip Tumour Development				
	Medium Only	CTL	CD4+	CD8+	CD4-/8-
	Range (Median)	Range (Median)	Range (Median)	Range (Median)	Range (Median)
6	17-18 (18)	45-53 (53)	17-100 (19)	100 (100)	(NT)
8	36-40 (37)	66-72 (69)	47-53 (47)	61-100 (100)	(NT)
9	19-20 (20)	24-32 (25)	25 (25)	19-41 (26)	20 (20)
10	33-73 (54)	49-56 (54)	53-100 (54)	50-61 (54)	(NT)
11	34-39 (36)	36-47 (41)	31-39 (39)	34-39 (36)	(NT)
12	25-72 (34)	46-54 (49)	31-100 (31)	31-100 (33)	(NT)
13	27-100 (29)	51-71 (64)	34-37 (37)	100 (100)	28-40 (37)
14	37-51 (37)	44-100 (48)	34-35 (35)	33-63 (51)	30-100 (35)
15	20-21 (20)	17-35 (18)	17-24 (17)	20-21 (20)	18-42 (42)
16	24-52 (30)	100 (100)	57-100 (100)	100 (100)	100 (100)

CTL: Cytotoxic T lymphocytes; No: Number; (NT): Not tested (inasmuch as a complete data set is not available)

TABLE A14
Statistical Analysis (Mann-Whitney Test):
Time To End Point Following Ip Transfer Of Autologous T Cell Subets
(Donors 6, 8-16)

Groups Compared		Significant Difference Between The Groups?
Medium and	**CTL**	**Yes** (p=0.001)
	CD4-Enriched	No (p=0.19)
	CD8-Enriched	**Yes** (p=0.001)
	CD4/CD8-Depleted	No (p=0.26)
CTL and	**CD4-Enriched**	**Yes** (p=0.04)
	CD8-Enriched	No (p=0.56)
	CD4/CD8-Depleted	No (p=0.14)
CD4-Enriched and	**CD8-Enriched**	**Yes** (p=0.03)
	CD4/CD8-Depleted	No (p=0.91)
CD8-Enriched and	**CD4/CD8-Depleted**	No (p=0.16)

CTL: Cytotoxic T lymphocytes

FIGURE B1
% Survival Using CD4-Enriched T Cell Subsets
(Donors 6, 8-9, 14-15)
(Standard error, SE, is shown as a vertical bar.)

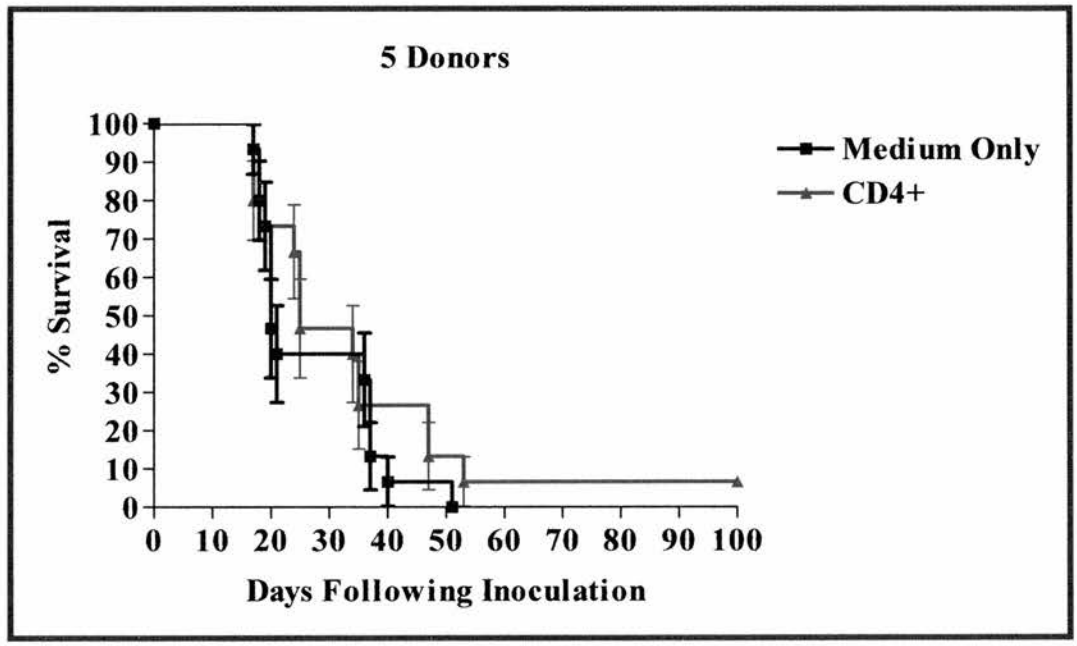

(Logrank test: p= 0.35)

APPENDIX 2: PUBLICATIONS

(Reprinted By Permission Of The Publishers.)

(1) **Johannessen, I.**, Perera, S.M., Gallagher, A., Hopwood, P.A., Thomas, J.A., and Crawford, D.H. (2002). Expansion in SCID mice of Epstein-Barr virus-associated post-transplantation lymphoproliferative disease biopsy material. *Journal of General Virology* **83**, 173-178. *(Copyright © 2002 Society for General Microbiology. All rights reserved.)*

(2) Haque, T., **Johannessen, I.**, Dombagoda, D., Sengupta, C., Burns, D. M., Bird, P., Hale, G., Mieli-Vergani, G., and Crawford, D. H. (2006). A mouse monoclonal antibody against Epstein-Barr Virus envelope glycoprotein 350 prevents infection both in vitro and in vivo. *Journal of Infectious Diseases* **194**, 584–587. *(Copyright © 2006 University of Chicago Press. All rights reserved.)*

Journal of General Virology (2002), **83**, 173–178. Printed in Great Britain SHORT COMMUNICATION

Expansion in scid mice of Epstein–Barr virus-associated post-transplantation lymphoproliferative disease biopsy material

Ingolfur Johannessen,[1] Sunimali M. Perera,[2] Alice Gallagher,[3] Paul A. Hopwood,[1] J. Alero Thomas[2] and Dorothy H. Crawford[1]

[1] Laboratory for Clinical and Molecular Virology, University of Edinburgh, Summerhall, Edinburgh EH9 1QH, UK

[2] Department of Infectious and Tropical Diseases, London School of Hygiene & Tropical Medicine, Keppel Street, London WC1E 7HT, UK

[3] Leukaemia Research Fund Virus Centre, University of Glasgow, Bearsden, Glasgow G61 1QH, UK

Post-transplant lymphoproliferative disease (PTLD) biopsy material is rarely available in adequate quantity for research. Therefore, the present study was designed to expand biopsy material in scid mice. Epstein–Barr virus (EBV)+ve PTLD samples from five transplant patients were established in scid mice. PCR analysis of immunoglobulin gene rearrangements demonstrated that four of the five biopsies (80%) gave rise to scid tumours which represented the original tumour cell clones. Immunophenotyping showed that these four biopsies (and all scid tumours) expressed all EBV latent genes and a B lymphoblast phenotype; ≥26% T cells were found in the biopsy material whereas scid tumours showed a paucity of T lymphocytes. RT–PCR analysis revealed expression of IL-2, -4, -6, -10 and IFN-γ in all tumour material, suggesting key roles for these factors in tumour growth. The results show that EBV+ve PTLD material can be expanded in scid mice giving rise to quantities of homogeneous malignant tissue sufficient for research studies.

Post-transplant lymphoproliferative disease (PTLD) develops in up to 10% of solid organ transplant recipients and carries up to 70% mortality despite treatment (Armitage *et al.*, 1991; Opelz & Henderson, 1993). The majority of PTLD cases are associated with Epstein–Barr virus (EBV). Main risk factors are primary EBV infection in previously seronegative organ recipients, and high-level immunosuppressive drug therapy (Ho *et al.*, 1985; Thomas *et al.*, 1990). Typically, tumour cells display an activated B lymphoblastic phenotype and express all EBV latent genes [six EBV nuclear antigens (EBNAs); three latent membrane proteins (LMPs)] and two EBV-encoded small non-polyadenylated RNAs (EBERs), although more restricted viral gene expression has been described (Cen *et al.*, 1993; Oudejans *et al.*, 1995). A minority of cells support lytic virus infection. PTLDs range from diffuse polymorphic lesions with polyclonal immunoglobulin (Ig) gene expression to malignant monoclonal lymphomas. The latter generally consist of large immunoblasts but include Hodgkin's disease (HD) and plasmacytoma (reviewed in Crawford, 2001).

Author for correspondence: Dorothy Crawford.
Fax +44 131 650 3711. e-mail d.crawford@ed.ac.uk

PTLD biopsy material is scant and does not generally grow *in vitro*. The few cell lines available do not reflect initial tumour phenotype (Cen *et al.*, 1993; Itoh *et al.*, 1993). Additionally, biopsies generally contain heavy infiltrates of non-malignant T cells (Perera *et al.*, 1998) which can limit their use in molecular studies. The aim of this study was to expand original PTLD biopsies in scid mice, which readily accept human xenografts due to lack of functional B and T cells (Bosma *et al.*, 1983; Johannessen & Crawford, 1999).

PTLD biopsies were obtained from five solid organ graft patients (designated 'patient 1–5'; for patient details, see Table 1). For each biopsy, 25×10^6–50×10^6 cells (denoted 'biopsy') were injected intraperitoneally (i.p.) into a scid mouse within 12 h of biopsy (sample from patient 2 was inoculated into two animals). Tumours (denoted 'scid tumour') formed in all mice. It was possible to passage material from patient 3. Patients 3 and 5 experienced primary EBV infection following transplantation whereas patients 1, 2 and 4 were persistently infected. All five biopsies gave rise to i.p. tumours in scid mice. EBER *in situ* hybridization was performed on all sample material using standard methods (Howe & Steitz, 1986). Similar to biopsies, all scid tumours were EBER+ve [for an assessment of the relative proportion of EBV+ve cells in the sample material, see '(2) Cell phenotype' below].

Our tissue panel of five sets of biopsy and scid tumours was analysed for (1) Ig and EBV clonality, (2) cell surface phenotype, (3) *in vitro* proliferation and (4) cytokine expression. Sample material was limited, and a full complement of tests could not always be carried out.

(1) Clonality. In order to ascertain whether scid tumours represented the corresponding biopsy, samples were assessed for Ig and EBV clonality. Ig clonality was analysed by PCR

Table 1. Patient details

HD, Hodgkin's disease; BLPD, B cell lymphoproliferative disease; M, male; F, female.

Patient no.	Age* (years)	Sex	Transplanted organ	Onset of 1° tumour (months)†	EBV-serostatus at time of 1° tumour	Site of 1° tumour	Pathological diagnosis of 1° tumour
1	5	M	Kidney	72	Carrier	Lymph node	Myeloma
2	9	M	Liver	34‡	Carrier‡	Lymph node	BLPD
3	0·1	F	Liver	16	Primary infection	Tonsil	BLPD
4	7	M	Heart	45§	Carrier§	Lymph node	HD
5	15	M	Heart	7	Primary infection	Lymph node	BLPD

* At time of transplantation.
† Time from graft to tumour.
‡ Recurrence; original lesion arose 2 months post-graft.
§ Recurrence; original lesion arose 29 months post-graft.

using primers specific for a conserved region of the variable (V) segment of framework (Fr) 3 and junction (J) segments of the Ig heavy chain (IgH) gene locus (McCarthy *et al.*, 1990; Stetler-Stevenson *et al.*, 1990). Fr3 PCR products were analysed on an ABI PRISM 310 Genetic Analyser. Primers derived from Fr1 were used to analyse samples from patient 2. Based on sequence analysis of the amplification products, a TaqMan PCR assay specific for the rearrangement in this case was designed and performed using standard methodology (Kuppers *et al.*, 1995). PCR analysis showed that biopsy and scid tumours from patients 1, 2 and 5 consisted of monoclonal material (for patient 2, see Fig. 1A; data not shown for patients 1 and 5). Matching clones were found in each sample set demonstrating that each tumour pair was identical. Sequence analysis of material from patient 2 confirmed the identical clonal nature of biopsy and scid lesions. TaqMan PCR analysis confirmed these results and further detected the malignant clone in a peripheral blood leukocyte sample taken from patient 2 at time of PTLD. Biopsy and scid tumour from patient 3 were oligoclonal with an identical dominant rearrangement (Fig. 1B). Passaged scid tumours were clonal, one of which was identical to the dominant biopsy and scid rearrangement. Biopsy from patient 4 contained a dominant clone in a polyclonal background (Fig. 1C). The scid tumour was clonal, but did not reflect the biopsy. EBV clonality was assessed using the standard Gardella gel technique (Gardella *et al.*, 1984; Raab-Traub & Flynn, 1986). The number of reiterated 500 bp EBV genome terminal direct repeats involved in forming the virus episome following infection of a target B cell is characteristic of any infection event. Progeny EBV + ve cells retain the same episome thus giving rise to an EBV clonal population which can be studied using the Gardella gel technique (Hurley & Thorley-Lawson, 1988). Material from cases 2, 4 and 5 was analysed with this assay. All lesions contained a single band indicating virus clonality (data not shown). Each set of samples from patients 2 and 5 contained bands of identical size, indicating a common infection event in each case, whereas material from patient 4 contained different EBV clones, suggesting that the scid tumour arose from a latently infected, non-malignant B cell.

(2) Cell phenotype. Primary antibodies against human and EBV antigens were applied to tumour sections (see Table 2). Bound antibody was detected as previously described (Reedman & Klein, 1973; Van Noorden, 1986). Immunophenotyping studies on biopsy and scid tumours from patients 2, 3, 4 and 5 demonstrated that all lesions expressed B cell surface antigens CD19 and CD23, indicating an activated, lymphoblastoid phenotype (Table 2). Biopsies from patients 2, 3 and 5 showed full EBV latent gene expression (EBNA-1,-2/LMP-1). Similarly, all scid tumours demonstrated full latent gene expression. In biopsies, low level ($< 5\%$ of cells) expression of lytic cycle antigens BZLF1, early antigen [EA(D)], viral capsid antigen (VCA) and membrane antigen (MA) was detected. Increased lytic cycle antigen expression (5–10%) was observed in corresponding scid tumours. The patient 4 biopsy showed a restricted pattern of EBV gene expression typical of HD (Deacon *et al.*, 1993): only LMP-1 was visualized by immunostaining, although EBNA-1 transcripts were detected by RT–PCR (data not shown). No lytic cycle antigens were expressed. Conversely, patient 4 scid tumour showed full EBV latent gene expression with lytic antigen expression similar to other scid tumours tested, further emphasizing differences in tumour cell type of the biopsy and scid lesion in this case.

(3) *In vitro* proliferation. In order to determine *in vitro* growth characteristics of biopsy and scid tumours, lesions from patients 1 and 3 were teased out into single cell suspensions and placed in culture. The proliferative response was assessed by [^{3}H]thymidine incorporation using standard methods (data not shown; Taylor *et al.*, 1957; Rubini *et al.*, 1960). Whilst scid-derived material grew continuously *in vitro* for up to 56 days

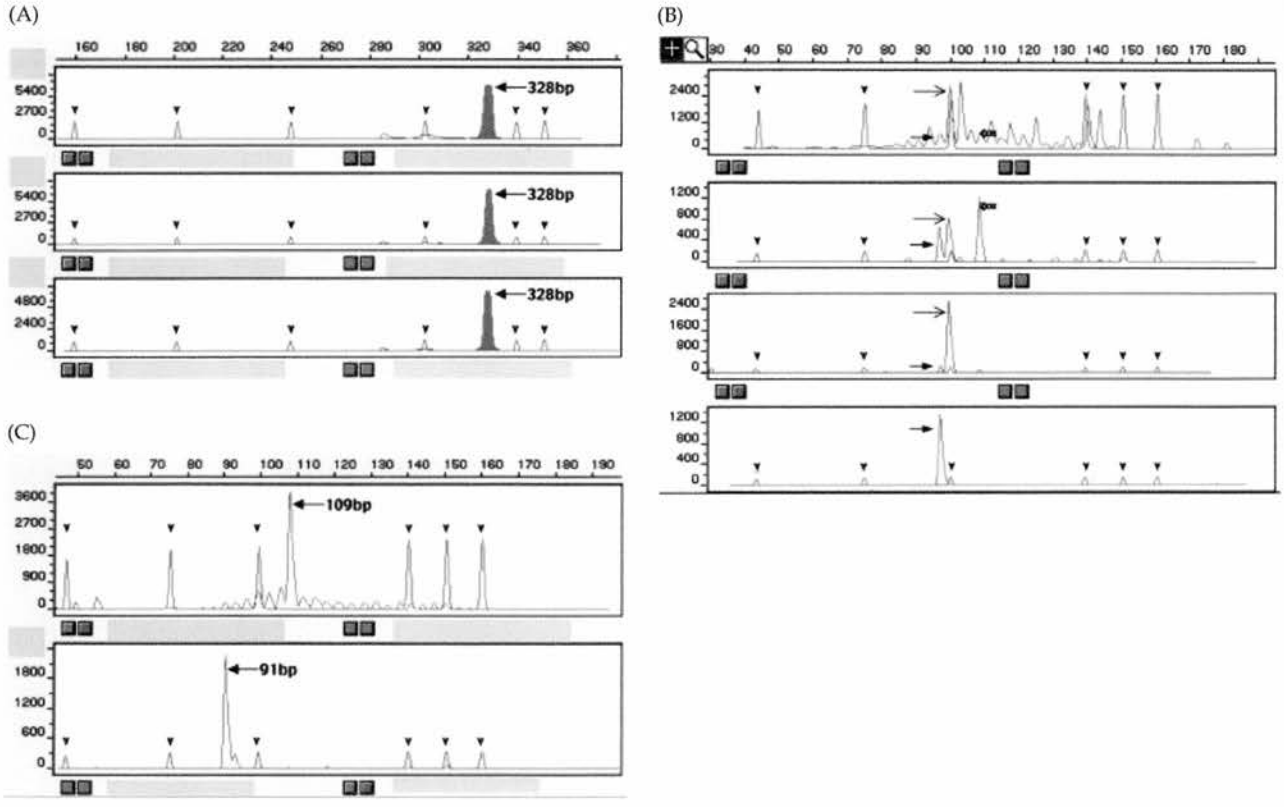

Fig. 1. Analysis of immunoglobulin gene rearrangements. All samples were analysed for Ig clonality in order to ascertain whether scid tumours represented the corresponding biopsy. PCR was performed with 1 μg of DNA using primers specific for a conserved region of the V segment of Fr1 or Fr3 and J segments of IgH gene locus. PCR product (30 μl) was purified using a QIAquick 8 PCR purification kit (Qiagen), eluted in 60 μl of buffer, and 3 μl of purified product run on an ABI PRISM 310 Genetic Analyser with 0·5 μl of GS350 marker and 10 μl of formamide. Results were analysed using GeneScan software. (A) Electropherogram of Fr1 PCR from patient 2. Top panel: biopsy result. Middle and bottom panels: results from two scid tumours derived from biopsy. VH3 rearrangement of 328 bp is indicated in each panel. (B) Electropherogram of Fr3 PCR products from patient 3. Top panel: biopsy result showing oligoclonal distribution. Second panel from top: scid tumour showing oligoclonal distribution with three dominant rearrangments. Third panel from top: scid tumour (passage 1) showing one dominant rearrangement. Bottom panel: scid tumour (passage 2) showing a single rearrangement. (C) Electropherogram of Fr3 PCR products from patient 4. Top panel: biopsy result. Bottom panel: scid tumour result. Dominant clones were detected at 109 and 91 bp, respectively, as indicated. The arrowheads (▼) indicate GeneScan 350 ROX labelled size standard. ⟶, 97 bp; →, 100 bp; ⇦, 109 bp.

(when the experiment was terminated), the biopsies failed to expand, which is in agreement with the experience of others (Itoh *et al.*, 1993; unpublished observations from our laboratory). This is unexpected since the majority of PTLD express all EBV growth-promoting latent viral genes. However, this phenomenon may be due to lack of necessary growth factors *in vitro* resulting in programmed cell death.

(4) Cytokine expression. Extensive T cell infiltrates ($\geqslant$ 26% of all cells; see Table 2) were apparent in all biopsies as previously described (Perera *et al.*, 1998). Conversely, only occasional T cells were identified in corresponding scid tumours. To address the possible role of T cell-derived factors in tumour growth, human cytokine gene expression of all material from patients 1–5 was analysed by RT–PCR (Fig. 2). Analysis of human cytokine mRNAs [interleukin (IL)-2, -4, -6, -10 and interferon (IFN)-γ] was carried out using published conditions (Yamamura *et al.*, 1991, 1992). Primers for IL-10 did not cross-amplify EBV-encoded viral IL-10. Biopsy and scid lesions demonstrated a similar cytokine profile with expression of the B cell growth factors IL-2, -4, -6, -10 and IFN-γ suggesting a key role in tumour growth. *In situ* hybridization studies in our laboratory have demonstrated that these growth factors are expressed by PTLD cells themselves (unpublished observations). The results suggest that T cells may contribute growth factors in the original malignancy whilst lack of T cells in scid tumours indicates that tumour cells supply themselves with necessary factors in an autocrine fashion supporting autonomous growth. This is in line with our previously proposed model of PTLD pathogenesis (Johannessen *et al.*, 2000).

The results demonstrate that biopsies from four out of five (80%) patients (numbers 1, 2, 3 and 5) were successfully

Table 2. Immunophenotypic comparison of biopsy and scid tumours

±, < 5% (of total cells counted); (+), 5–10%; 1+, 11–25%; 2+, 26–50%; 3+, 51–75%; 4+, > 75%; OC, occasional positive cell; NT, not tested; TCR, T cell receptor; Pt, patient. Antibody reagents: anti-TCR α/β (BFT1, T Cell Science), anti-CD3 (UCHT, Dako), anti-CD19 (HD37, Dako), anti-CD23 (MHM6, Dako), polyclonal EBV + ve human serum (London School of Hygiene & Tropical Medicine), anti-EBNA1 (OT1X; donated by J. Middeldorp, The Netherlands), anti-EBNA2 (PE2, Dako), anti-LMP1 (CS1–4, Dako), anti-BZLF1 (Dako), anti-EA(D) (110f-1, Biogenesis), anti-VCA (Serotec), anti-MA (Serotec), anti-mouse MHC1D^d (Serotec).

	Sample							
Antibody specificity	Pt 2	scid 2	Pt 3	scid 3	Pt 4	scid 4	Pt 5	scid 5
TCR α/β	3+	OC	2+	–	4+	OC	3+	–
CD3	3+	OC	2+	–	4+	OC	3+	–
CD19	2+	3+	2+	2+	2+	2+	3+	3+
CD23	2+	2+	2+	2+	2+	2+	2+	3+
Polyclonal serum	3+	3+	3+	3+	–	3+	3+	3+
EBNA1	3+	3+	3+	3+	–*	3+	3+	3+
EBNA2	2+	2+	2+	2+	–	2+	2+	2+
LMP1	1+	1+	1+	1+	1+	1+	1+	1+
BZLF1	±	(+)	±	(+)	–	(+)	±	(+)
EA(D)	±	(+)	±	(+)	–	(+)	±	(+)
VCA	±	(+)	±	(+)	–	(+)	±	(+)
MA	±	(+)	±	(+)	–	(+)	±	(+)
Mouse MHC1D^d	NT	(+)	NT	(+)	NT	(+)	NT	(+)

* EBNA1 + ve on RT–PCR.

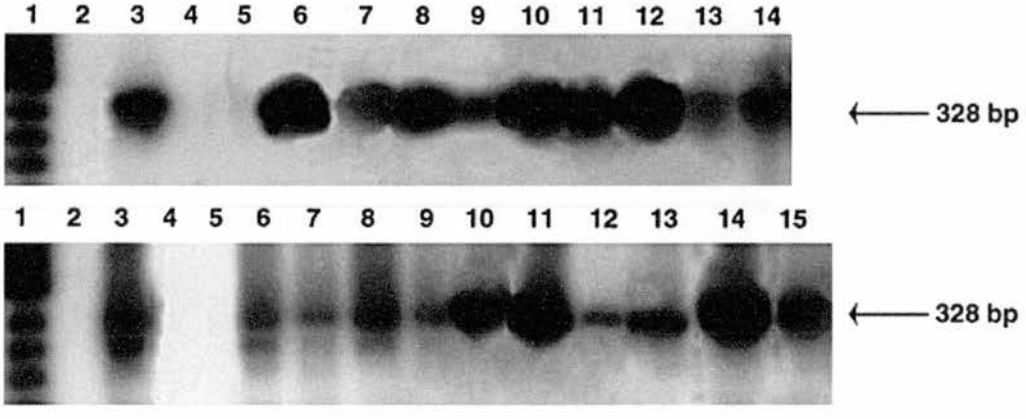

Fig. 2. Human cytokine gene expression: interleukin-10. Cytokine gene expression was analysed to determine the possible role of B cell growth factors in tumour formation. Representative results of the amplification of human cytokine gene transcripts in tumour material: IL-10. cDNA from 5 µg of RNA was amplified in a 35 cycle RT–PCR reaction using human IL10 primers. PCR product (20 µl) was run on a 2·5% (w/v) NuSieve agarose gel, Southern transferred onto a nylon membrane, and hybridized using human IL10-specific ^{32}P-labelled oligonucleotide probe. Top panel: biopsy results. Lane 1, *Hin*fI-digested ϕX174 DNA radiolabelled marker; lane 2, 1 kbp non-radiolabelled DNA ladder; lane 3, phytohaemagglutinin (PHA)-treated human peripheral blood leukocytes; lane 4, PHA-treated BALB/c murine splenocytes; lane 5, sterile distilled water; lanes 6–9, four EBV *in vitro* immortalized B cell lymphoblastoid cell lines; lanes 10–14, biopsy material from patients 1–5, respectively. Bottom panel: scid tumour results. Lanes 1–9, as above; lanes 10–15, scid tumours from patients 1–5, respectively (lanes 11 and 12 represent two scid tumours derived from patient 2). The size of the IL10 RT–PCR product (328 bp) is indicated.

expanded in scid mice (we have previously reported on *in vivo* outgrowth of PTLD biopsy from patient 5; see Perera *et al.*, 1996). Conversely, scid tumour from patient 4 probably represents a non-malignant EBV + ve B cell in the HD biopsy. This finding has been reported by others (Meggetto *et al.*, 1996).

To our knowledge, this is the first report demonstrating outgrowth of a panel of PTLD biopsies in scid mice and contrasts with an earlier study by Randhawa *et al.* (1997) suggesting that biopsies did not grow *in vivo*. Analysis of passaged scid tumours from patient 3 showed progression from oligoclonal to monoclonal tumour (Fig. 1B), thus providing possible insight into PTLD clonal progression.

Our study provides an adequate quantity of homogeneous PTLD material from four graft recipients which is uncontaminated with infiltrating non-malignant cells, thus providing opportunity for further molecular studies on PTLD pathogenesis.

The authors wish to thank Dr L. A. Brooks (London School of Hygiene & Tropical Medicine, London, UK) and Professor R. F. Jarrett (LRF Virus Centre, University of Glasgow, Glasgow, UK) for their valuable assistance and suggestions, and Mrs K. A. McAulay (University of Edinburgh, Edinburgh, UK) for technical help.

The authors also wish to thank Dr P. L. Amlot (Royal Free Hospital School of Medicine, London, UK) and Dr M. Burke (Harefield Hospital, Harefield, UK) for providing tumour material as well as Dr G. J. Bancroft, Mr J. P. Kelly, and Mr A. R. Turner (London School of Hygiene & Tropical Medicine) for supplying and maintaining the scid mice.

I.J. was supported by the British Council, a British ORS Award, a NATO Science Award, and awards from the Icelandic Jonsdottir & Kristjansson and Magnusdottir & Bjarnason Funds. This work was supported by the Medical Research Council, the United Kingdom Children Cancer Study Group and the Leukaemia Research Fund.

References

Armitage, J. M., Kormos, R. L., Stuart, R. S., Fricker, F. J., Griffith, B. P., Nalesnik, M., Hardesty, R. L. & Dummer, J. S. (1991). Posttransplant lymphoproliferative disease in thoracic organ transplant patients: ten years of cyclosporine-based immunosuppression. *Journal of Heart and Lung Transplantation* **10**, 877–886.

Bosma, G. C., Custer, R. P. & Bosma, M. J. (1983). A severe combined immunodeficiency mutation in the mouse. *Nature* **301**, 527–530.

Cen, H., Williams, P. A., McWilliams, H. P., Breinig, M. C., Ho, M. & McKnight, J. L. C. (1993). Evidence for restricted Epstein–Barr virus latent gene expression and anti-EBNA antibody response in solid organ transplant recipients with posttransplant lymphoproliferative disorders. *Blood* **81**, 1393–1403.

Crawford, D. H. (2001). Biology and disease associations of Epstein–Barr virus. *Philosophical Transactions of the Royal Society of London B Biological Sciences* **356**, 461–473.

Deacon, E. M., Pallesen, G., Niedobitek, G., Crocker, J., Brooks, L., Rickinson, A. B. & Young, L. S. (1993). Epstein–Barr virus and Hodgkin's disease: transcriptional analysis of virus latency in the malignant cells. *Journal of Experimental Medicine* **177**, 339–349.

Gardella, T., Medveczky, P., Sairenji, T. & Mulder, C. (1984). Detection of circular and linear herpesvirus DNA molecules in mammalian cells by electrophoresis. *Journal of Virology* **50**, 248–254.

Ho, M., Miller, G., Atchison, R. W., Breinig, M. K., Dummer, J. S., Andiman, W., Starzl, T. E., Eastman, R., Griffith, B. P. & Hardesty, R. L. (1985). Epstein–Barr virus infections and DNA hybridization studies in posttransplantation lymphoma and lymphoproliferative lesions: the role of primary infection. *Journal of Infectious Diseases* **152**, 876–886.

Howe, J. G. & Steitz, J. A. (1986). Localization of Epstein–Barr virus-encoded small RNAs by in situ hybridization. *Proceedings of the National Academy of Sciences, USA* **83**, 9006–9010.

Hurley, E. A. & Thorley-Lawson, D. A. (1988). B cell activation and the establishment of Epstein–Barr virus latency. *Journal of Experimental Medicine* **168**, 2059–2075.

Itoh, T., Shiota, M., Takanashi, M., Hojo, I., Satoh, H., Matsuzawa, A., Moriyama, T., Watanabe, T., Hirai, K. & Mori, S. (1993). Engraftment of human non-Hodgkin lymphomas in mice with severe combined immunodeficiency. *Cancer* **72**, 2686–2694.

Johannessen, I. & Crawford, D. H. (1999). *In vivo* models for Epstein–Barr virus (EBV)-associated B cell lymphoproliferative disease (BLPD). *Reviews in Medical Virology* **9**, 263–277.

Johannessen, I., Asghar, M. & Crawford, D. H. (2000). Essential role for T cells in human B cell lymphoproliferative disease development in SCID mice. *British Journal of Haematology* **109**, 600–610.

Kuppers, R., Hansmann, M.-L. & Rajewsky, K. (1995). Micromanipulation and PCR analysis of single cells from tissue sections. In *Handbook of Experimental Immunology*, pp. 206, 1–4. Edited by D. M. Weir, C. Blackwell & L. A. Herzenberg. Cambridge, MA: Blackwell Scientific.

McCarthy, K., Sloane, J. & Wiedermann, L. (1990). Rapid method for distinguishing clonal from polyclonal B cell populations in surgical biopsy specimens. *Journal of Clinical Pathology* **43**, 429–432.

Meggetto, F., Muller, C., Henry, S., Selves, J., Mariame, B., Brousset, P., Saati, T. A. & Delsol, G. (1996). Epstein–Barr virus (EBV)-associated lymphoproliferations in severe combined immunodeficient mice transplanted with Hodgkin's disease lymph nodes: implication of EBV+ve bystander B lymphocytes rather than EBV-infected Reed–Sternberg cells. *Blood* **87**, 2435–2442.

Opelz, G. & Henderson, R. (1993). Incidence of non-Hodgkin lymphoma in kidney and heart transplant recipients. *Lancet* **342**, 1514–1516.

Oudejans, J. J., Jiwa, M., van den Brule, A. J., Grasser, F. A., Horstman, A., Vos, W., Kluin, P. M., van der Valk, P., Walboomers, J. M. & Meijer, C. J. (1995). Detection of heterogeneous Epstein–Barr virus gene expression patterns within individual post-transplantation lymphoproliferative disorders. *American Journal of Pathology* **147**, 923–933.

Perera, S. M., Johannessen, I., Thomas, J. A., Brooks, L. A., Jobe, J. N., Crawford, D. H., Radley-Smith, R. & Phillips, M. (1996). Growth of Epstein–Barr virus-associated B-lymphoproliferative disease tissue in a severe combined immunodeficient mouse. *Blood* **88**, 1123–1125.

Perera, S. M., Thomas, J. A., Burke, M. & Crawford, D. H. (1998). Analysis of the T-cell micro-environment in Epstein–Barr virus-related post-transplantation B lymphoproliferative disease. *Journal of Pathology* **184**, 177–184.

Raab-Traub, N. & Flynn, K. (1986). The structure of the termini of the Epstein–Barr virus as a marker of clonal cellular proliferation. *Cell* **47**, 883–889.

Randhawa, P. S., Pietrzak, B., Nalesnik, M. A., Demetris, A. J. & Locker, J. (1997). Subcutaneous implantation of human post-transplant lymphoproliferative disease lesions in scid mice. *Hematological Oncology* **15**, 39–46.

Reedman, B. M. & Klein, G. (1973). Cellular localization of an Epstein–Barr virus (EBV)-associated complement-fixing antigen in producer and non-producer lymphoblastoid cell lines. *International Journal of Cancer* **11**, 499–520.

Rubini, J. R., Cronkite, E. P., Bond, V. P. & Fliedner, T. M. (1960). The metabolism and fate of tritiated thymidine in man. *Journal of Clinical Investigation* **39**, 909–918.

Stetler-Stevenson, M., Crush-Stanton, S. & Cossman, J. (1990). Involvement of the bcl-2 gene in Hodgkin's disease. *Journal of the National Cancer Institute* **82**, 855–858.

Taylor, J. H., Woods, P. S. & Hughes, W. L. (1957). The organization and duplication of chromosomes as revealed by autoradiographic studies using tritium-labeled thymidine. *Proceedings of the National Academy of Sciences, USA* **43**, 122–128.

Thomas, J. A., Hotchin, N. A., Allday, M. J., Amlot, P., Rose, M., Yacoub, M. & Crawford, D. H. (1990). Immunohistology of Epstein–Barr virus-associated antigens in B cell disorders from immunocompromised individuals. *Transplantation* **49**, 944–953.

Van Noorden, S. (1986). Tissue preparation and immunostaining techniques for light microscopy. In *Immunocytochemistry: Modern Methods and Applications*, pp. 26–53. Edited by J. M. Polak & S. Van Noorden. Bristol: Wright.

Yamamura, M., Uyemura, K., Deans, R. J., Weinberg, K., Rea, T. H., Bloom, B. R. & Modlin, R. L. (1991). Defining protective responses to pathogens: cytokine profiles in leprosy lesions. *Science* **254**, 277–279.

Yamamura, M., Wang, X. H., Ohmen, J. D., Uyemura, K., Rea, T. H., Bloom, B. R. & Modlin, R. L. (1992). Cytokine patterns of immunologically mediated tissue damage. *Journal of Immunology* **149**, 1470–1475.

Received 22 August 2001; Accepted 1 October 2001

A Mouse Monoclonal Antibody against Epstein-Barr Virus Envelope Glycoprotein 350 Prevents Infection Both In Vitro and In Vivo

Tanzina Haque,[1,a] Ingolfur Johannessen,[1] Dilani Dombagoda,[1] Chandrya Sengupta,[2] David M. Burns,[1] Pru Bird,[3] Geoff Hale,[3] Giorgina Mieli-Vergani,[2] and Dorothy H. Crawford[1]

[1]Molecular and Clinical Virology, University of Edinburgh, Summerhall, Edinburgh, [2]Institute of Liver Studies, King's College London School of Medicine, King's College Hospital, London, and [3]Sir William Dunn School of Pathology, University of Oxford, Oxford, United Kingdom

A mouse monoclonal antibody (MAb) against Epstein-Barr virus (EBV) envelope glycoprotein 350, 72A1, inhibited EBV infection of B lymphocytes in vitro. When severe combined immunodeficient mice were injected with EBV-seronegative donors' peripheral-blood mononuclear cells and challenged with EBV, 72A1 MAb prevented development of EBV-positive tumors: none of the test mice (0/12) developed EBV-positive tumors. In contrast, 67% (8/12) of control mice developed EBV-positive tumors ($P = .001$). Purified 72A1 MAb was infused into 1 healthy adult and 4 EBV-seronegative children after liver transplant. No adverse reactions were seen in the adult or in 3 of the transplant recipients. The remaining patient developed a hypersensitivity reaction, thus underlining the need to humanize the MAb.

Epstein-Barr virus (EBV), a human herpesvirus, is associated with development of posttransplant lymphoproliferative disease (PTLD), particularly after primary EBV infection in previously seronegative transplant recipients. An EBV-seronegative recipient can acquire EBV from a seropositive organ donor, and primary EBV infection thus acquired is a risk factor for PTLD [1]. This transfer of donor virus via the graft has not been observed in EBV-seropositive recipients. Because latent EBV in donor B lymphocytes has to undergo lytic replication and then infect recipient B lymphocytes, it is hypothesized that preexisting neutralizing antibodies directed against envelope gp350 in EBV-seropositive patients may be important in preventing the infection of recipient cells by donor EBV isolates during the immediate posttransplant period. If this is the case, then active or passive immunization of EBV-seronegative recipients before transplant that results in production of neutralizing anti-gp350 antibodies could prevent EBV transmission via the graft and thereby reduce the risk of PTLD development.

A mouse monoclonal antibody (MAb) against EBV gp350 produced by the hybridoma cell line 72A1 has previously been shown to prevent EBV infection of B lymphocytes in vitro [2–5]. The present study was undertaken to characterize the effect of 72A1 anti-gp350 MAb in SCID mice, an in vivo preclinical model for PTLD [6, 7]. We also aimed to assess the in vivo safety of 72A1 MAb and the effects on acquisition of EBV during the immediate posttransplant period and the subsequent development of PTLD in EBV-seronegative liver transplant recipients whose organ donors were EBV seropositive.

Subjects, materials, and methods. The 72A1 cell line was obtained from Johns Hopkins University Medical School, after a transfer agreement was signed. The antibody was manufactured in accordance with European Union good manufacturing practice guidelines at the Therapeutic Antibody Centre, Oxford. A master cell bank was made and tested for potential contaminants. Cells were cultured in a hollow fiber fermentor, and 72A1 MAb was purified by chromatography on protein A, with elution at pH 3.2, followed by cation exchange on S-Sepharose at pH 4. The purified antibody was a mouse IgG1 containing κ and λ light chains in approximately equal proportions. The hybridoma had been created using P3X63Ag8, a myeloma line that secretes mouse IgG1 κ [2]. It is likely that the purified antibody was a mixture of active and inactive species, with only a minor proportion having full bivalent binding to gp350.

To determine the EBV-neutralizing titer of 72A1, 2×10^6 peripheral-blood mononuclear cells (PBMCs) from an EBV-seronegative donor were incubated at 37°C for 1 h with 10-fold serial dilutions of concentrated EBV preparations and, for each virus dilution, with 10-fold serial dilutions of 72A1 MAb (starting concentration, 1 mg/mL). Cells (2×10^5 per well) were cultured on microtiter plates and were observed for 4 weeks for signs of outgrowth of EBV-immortalized lymphoblastoid cell lines (LCL). Control plates were set up with PBMCs infected with EBV but without 72A1 MAb. The dilution of antibody that prevented LCL formation in >50% of wells was taken as the neutralizing titer of that particular batch of 72A1 MAb [8].

Received 14 October 2005; accepted 10 April 2006; electronically published 25 July 2006.
Potential conflicts of interest: none reported.
Financial support: Association for International Cancer Research (grant 99-026); Chief Scientist Office of the Scottish Executive (grant CZB/4/126).

[a] Present affiliation: Department of Virology, Royal Free Hospital, London.
Reprints or correspondence: Dr. Tanzina Haque, Dept. of Virology, Royal Free Hospital, London NW3 2QG, United Kingdom (t.haque@medsch.ucl.ac.uk).

The Journal of Infectious Diseases 2006; 194:584–7

0022-1899/2006/19405-0008$15.00

Table 1. Effect of passive immunoprophylaxis with 72A1 monoclonal antibody (MAb) on Epstein-Barr virus (EBV)–driven lymphomagenesis in SCID mice inoculated with peripheral-blood mononuclear cells (PBMCs) from EBV-seronegative donors.

Treatment group	Intraperitoneally injected PBMCs, no.	No. of mice with tumors/total no. of mice (%)
Untreated (PBS)	2×10^7–3×10^7	8/12[a] (67)
Treated (72A1 MAb)	2×10^7–3×10^7	0/12[a] (0)

[a] $P = .001$.

An in-house EIA was set up to capture 72A1 MAb in plasma by coating the plates with goat anti-mouse IgG (Dako) and using peroxidase-conjugated rabbit anti-mouse IgG as a detection antibody. Similarly, an in-house EIA for detection of anti-72A1 human anti-mouse antibody (HAMA) was set up using 72A1 as a capture antibody and biotin-labeled 72A1 as a detection antibody. The HAMA assay was not isotype specific and could not differentiate between IgM and IgG.

PBMCs from 4 EBV-seronegative donors were injected intraperitoneally (ip) into SCID mice. For each donor, 2×10^7–3×10^7 PBMCs were inoculated into each mouse in a group of 6 SCID mice. For each such group of 6 mice, 3 test mice were injected with 72A1MAb ip the day before injection of PBMCs, on the day of PBMC injection, the day after (day 1), and then 3 times weekly for 3 weeks [9], whereas 3 control mice were injected according to the same schedule with PBS only. A total of 12 mice received 72A1, and 12 acted as controls. On day 1, all mice received 50 μL ip of a concentrated EBV preparation (immortalizing titer, 10^{-4}). Mice were monitored regularly and culled when they showed signs of illness or after a preset limit of 100 days. Assessment of tumor development was performed by necropsy, and EBV association was determined by routine staining for EBV nuclear antigen and small RNAs [10, 11]. Fisher's exact test was used to analyze the in vivo data.

Infusion of 72A1 into an adult volunteer was approved by the Medicine and Clinical Oncology Research Ethics Sub-committee, Edinburgh. A pilot study on EBV-seronegative pediatric liver transplant recipients at King's College Hospital, London, was approved by the Local Research Ethics Committee. Informed written consent was obtained from guardians.

Results. The purified 72A1 MAb was shown to be IgG1, as previously reported [2]. Exclusion of the presence of any human DNA and mouse xenotropic and ectotropic viruses in the hybridoma cell line was performed by the Forensic Laboratory, Lothian and Borders Police, Edinburgh (human DNA), and Q-One Biotech, Glasgow (mouse viruses). In vitro neutralizing assays showed that 72A1 MAb at a dilution of 1:100 (10 μg/mL) inhibited EBV immortalization of B lymphocytes by concentrated, 10^{-1} and 10^{-2} virus dilutions in all (100%) culture wells. Even at a dilution of 1:10,000 (100 ng/mL), 72A1 inhibited LCL outgrowth in >50% of wells when the EBV preparation was used at a 10^{-4} dilution (the virus immortalizing titer).

To test the efficacy of the 72A1 MAb preparation in preventing EBV infection in vivo, we used the development of PTLD-like lesions in SCID mice as a readout [9]. SCID mice were inoculated with PBMCs from 4 EBV-seronegative donors and then infected with EBV. On the basis of initial titration experiments to identify the 72A1 MAb half-life in SCID mice and to maintain circulating antibody levels >1 μg/mL (data not shown), test mice received 680 μg of 72A1 ip before PBMC inoculation and then 3 times weekly for 3 weeks, whereas the control mice received PBS only. After 100 days, the results showed that none (0%) of the total of 12 mice that received the antibody preparation developed ip tumors, whereas 8 (67%) out of the 12 control mice developed EBV-positive PTLD-like lesions ip (table 1). The outcome showed a statistically significant difference between the 2 groups ($P = .001$).

To assess the half-life and identify any adverse effects of 72A1 MAb on humans, an EBV-seropositive adult volunteer was injected intravenously (iv) with a single 10-mg dose of antibody. No adverse reactions occurred during or after the infusion. Peak 72A1 MAb levels persisted in serum samples (0.08–0.12 μg/mL) for 52 h after infusion, after which they gradually declined, becoming undetectable after day 43. Anti-72A1 HAMA was not detected in serum samples when tested up to 18 months after infusion. Purified 72A1 was considered safe for use, and 7 EBV-seronegative children undergoing liver transplantation from EBV-seropositive donors were enrolled (table 2). Four children (denoted "patients 1–4") received 1 mg of 72A1 MAb/kg of body weight by iv infusions immediately before and 6 h after transplant, then every 2 days for up to 3 weeks, whereas 3 patients ("patients 5–7") served as controls. All patients were receiving routine posttransplant immunosuppressive therapy.

Three (75%) of the 4 MAb-infused patients (patients 2–4)

Table 2. Demographic data, monoclonal antibody 72A1 infusion status, and outcome in the Epstein-Barr virus (EBV)–seronegative transplant recipients enrolled in the study.

Patient	Age at transplant, months	Sex	Doses of 72A1	Time of detection after transplant, months		
				IgG VCA	IgM VCA	EBV DNA
1	11	M	11	3	3	43
2	16	M	6	–	–	48
3	75	M	4	–	–	ND
4	18	F	7	–	–	42
5	17	M	0	3	–	40
6	10	F	0	2.5	–	ND
7	9	F	0	41	–	18

NOTE. ND, not detected; VCA, viral capsid antigen; –, seronegative.

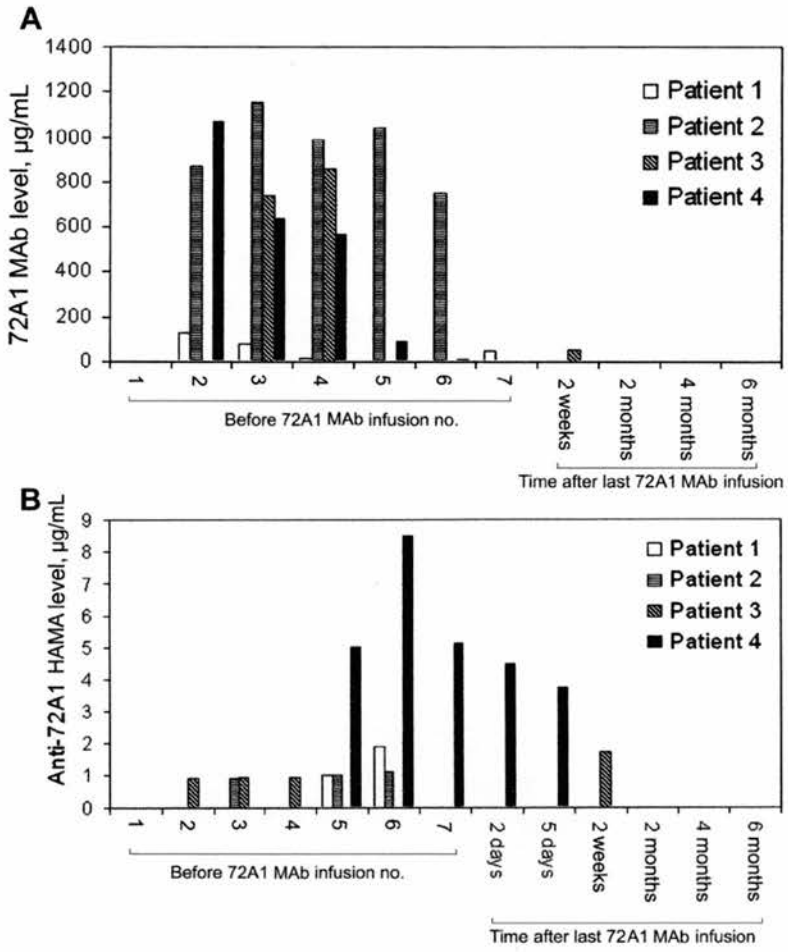

Figure 1. *A,* Levels of 72A1 monoclonal antibody (MAb). *B,* Levels of anti-72A1 human anti-mouse antibody (HAMA) in serum samples from patients infused with 72A1 MAb, as determined by EIA. *X*-axes indicate the points at which antibody levels were measured, both before each 72A1 MAb infusion and at different time points after the last infusion.

remained EBV seronegative during the 6-month follow-up period [12] (table 2). Patient 1 (1 [25%] of 4 infused) became IgG anti–viral capsid antigen (VCA) seropositive 12 weeks after transplant (9 weeks after the last MAb dose). Two (67%) of the 3 noninfused control patients (patients 5 and 6) became seropositive at 10 and 12 weeks. The remaining control patient (patient 7) seroconverted at 41 months after transplant. All seroconverted patients were seronegative for IgG to Epstein-Barr nuclear antigen (EBNA). Long-term follow-up showed that EBV DNA was detected by polymerase chain reaction 1.5–4 years after transplant in plasma from patients 1, 2, 4, 5, and 7 (performed at the Health Protection Agency Virology Laboratory, King's College Hospital, London) (table 2), although none of these patients developed any features of EBV disease. Patient 3 remained EBV DNA, EBNA IgG, and VCA IgM and IgG seronegative for 4 years after transplant. EBV DNA was not detected in pretransplant PBMC samples from any patient when retrospective analysis was performed.

72A1 MAb was detected in serum samples from all the infused children. However, the levels were lower in the child who seroconverted at 3 months (patient 1) than in those (patients 2–4) who remained EBV seronegative at 6 months after infusions (figure 1*A*). All children had detectable anti-72A1 HAMA in serum samples (figure 1*B*). Three of the 4 infused children (patients 1–3) tolerated the infusions well, with no reactions attributable to the antibody. Patient 4 (an 18-month-old girl) had a severe reaction (peripheral cyanosis, hypotension, and vomiting) during the seventh infusion, requiring cessation of treatment. The patient also had *Staphylococcus aureus* septicemia. From day 7 onward, anti-72A1 HAMA levels in patient 4 serum samples were higher (maximum, 8.5 µg/mL) than those in samples from the other infused children (figure 1*B*). Total serum IgE levels measured in samples obtained before 72A1 infusion and samples obtained up to 18 days after 72A1 infusion from this patient were within normal range (measurements were performed at the Scottish National Blood

Transfusion Services, Edinburgh), ruling out an IgE-mediated response to HAMA. No 72A1 MAb or anti-72A1 HAMA was detected in the noninfused control patients. Four years after the transplant, all the children (infused and control) were alive with a functioning graft, and none had developed PTLD.

Discussion. EBV infects B lymphocytes via the attachment of envelope gp350 to cell surface CD21/CR2 receptors, and antibodies to gp350 are neutralizing. For this reason, research into a vaccine to prevent EBV-associated diseases has focused on gp350 to elicit a protective antibody response [13]. Thus, we have argued that it may be possible to provide short-term protection to individuals at high risk for EBV disease, such as EBV-seronegative transplant recipients, by passive infusion of anti-gp350. To this end, the present study aimed to characterize the anti-gp350 mouse MAb 72A1 and assess its potential to protect against acquiring EBV from the graft during the immediate posttransplant period, thus reducing the risk for PTLD. Initial results confirmed that, as reported elsewhere [2–5], 72A1 MAb neutralizes EBV infection of B lymphocytes in vitro, and we therefore proceeded with in vivo studies. The development of PTLD-like tumors in SCID mice after injection of PBMCs from EBV-seropositive donors can be prevented with purified immunoglobulin pooled from plasma from seropositive donors [14], suggesting that neutralizing antibody plays a role in protection against tumors. With a similar SCID mouse model, using development of PTLD-like lesions as a readout [9], we attempted to mimic the situation of EBV transfer from an EBV-seropositive donor to seronegative transplant recipients by injecting PBMCs from an EBV-seronegative donor followed by concentrated EBV. The results show that 72A1 provides complete and significant protection from EBV-driven PTLD-like lesions (table 1). Although further studies will assess whether EBV infection can be completely prevented by the antibody, the results suggest that neutralization of gp350 in vivo prevented EBV-driven lymphoproliferation.

Injection of a single large dose of 72A1 MAb into a healthy adult induced no adverse reactions and no HAMA production, and we, therefore, performed a pilot study on 4 liver transplant recipients. One of 4 infused and 2 of 3 control children seroconverted during the 6-month observation period (table 2). Although it is difficult to draw conclusions from this small group, it appears that 72A1 MAb provided short-term protection against acquiring EBV during the early posttransplant period. Detection of EBV DNA in plasma from 3 of 4 infused children (patients 1, 2, and 4) 1.5–4 years later indicated that they had acquired EBV infection without any features of EBV-related disease.

Although they were on iatrogenic immunosuppression, all 4 children who received the antibody developed HAMA, and one (patient 4) developed a hypersensitivity reaction, although the actual cause of the reaction could not be identified. Thus, in vivo use of 72A1 MAb in its native form may not be safe. Further clinical studies would require either humanizing the MAb or producing a human MAb [15].

Acknowledgments

We thank Sarah L. Watson, for technical assistance, and Marc Turner at Scottish National Blood Transfusion Services, for his advice.

References

1. Haque T, Thomas JA, Falk K, et al. Transmission of donor Epstein-Barr virus in transplanted organ causes lymphoproliferative diseases in recipient. J Gen Virol **1996**; 77:1169–72.
2. Hoffman GJ, Lazarowitz SG, Hayward DH. Monoclonal antibody against a 250,000-Dalton glycoprotein of Epstein-Barr virus identifies a membrane antigen and a neutralizing antigen. Proc Natl Acad Sci USA **1980**; 77:2979–83.
3. Thorley-Lawson DA, Geilinger K. Monoclonal antibodies against the major glycoprotein (gp350/220) of Epstein-Barr virus neutralize infectivity. Proc Natl Acad Sci USA **1980**; 77:5307–11.
4. Miller G, Heston L, Hoffman G. Neutralization of lymphocyte immortalization by different strains of Epstein-Barr virus with a murine monoclonal antibody. Infect Immun **1982**; 37:1028–31.
5. Sairenji T, Bertoni G, Medveczky MM, Medveczky PG, Nguyen QV, Humphreys RE. Inhibition of Epstein-Barr virus (EBV) release from P3HR-1 and B95-8 cell lines by monoclonal antibodies to EBV membrane antigen gp350/220. J Virol **1988**; 62:2614–21.
6. Mosier DE, Gulizia RJ, Baird SM, Wilson DB. Transfer of a functional human immune system to mice with severe combined immunodeficiency. Nature **1988**; 335:256–9.
7. Johannessen I, Crawford DH. In vivo models for Epstein-Barr virus-associated B cell lymphoproliferative disease. Rev Med Virol **1999**; 9: 263–77.
8. Wison AD, Morgan AJ. Indirect measurements of Epstein-Barr virus neutralizing antibodies by ELISA. J Virol Methods **1998**; 73:11–9.
9. Cannon MJ, Pisa P, Fox RI, Cooper NR. Epstein-Barr virus induces aggressive lymphoproliferative disorders of human B cell origin in scid/hu chimeric mice. J Clin Invest **1990**; 85:1333–7.
10. Reedman BM, Klein G. Cellular localization of an Epstein-Barr virus (EBV)-associated complement-fixing antigen in producer and non-producer lymphoblastoid cell lines. Int J Cancer **1973**; 11:499–520.
11. Howe JG, Steitz JA. Localization of Epstein-Barr virus-encoded small RNAs by in situ hybridization. Proc Natl Acad Sci USA **1986**; 83:9006–10.
12. Henle G, Henle W. Immunofluorescence in cells derived from Burkitt's lymphoma. J Bacteriol **1966**; 91:1248–56.
13. Epstein MA, Morgan AJ, Finerty S, Randle BJ, Kirkwood JK. Protection of cottontop tamarins against Epstein-Barr virus-induced malignant lymphoma by a prototype subunit vaccine. Nature **1985**; 318:287–9.
14. Abedi MR, Linde A, Christensson B, Mackett M, Hammarstrom L, Smith CI. Preventive effect of IgG from EBV-seropositive donors on the development of human lymphoproliferative disease in SCID mice. Int J Cancer **1997**; 71:624–9.
15. Breedveld FC. Therapeutic monoclonal antibodies. Lancet **2000**; 355: 735–40.